SIMULTANEOUS DETERMINATION OF BISMUTH AND TELLURIUM USING TUNGSTEN COIL ATOM TRAP WITH INDUCTIVELY COUPLED PLASMA MASS SPECTROMETRY

A THESIS SUBMITTED TO
THE GRADUATE SCHOOL OF NATURAL AND APPLIED SCIENCES
OF
MIDDLE EAST TECHNICAL UNIVERSITY

BY

SELİN BORA

IN PARTIAL FULFILLMENT OF THE REQUIREMENTS
FOR
THE DEGREE OF DOCTOR OF PHILOSOPHY
IN
CHEMISTRY

JANUARY 2016

Approval of the Thesis;

SIMULTANEOUS DETERMINATION OF BISMUTH AND TELLURIUM USING TUNGSTEN ATOM TRAP WITH INDUCTIVELY COUPLED PLASMA MASS SPECTROMETRY

submitted by **SELİN BORA** in a partial fulfillment of the requirements for the degree of **Doctor of Philosophy in Chemistry Department, Middle East Technical University** by,

Prof. Dr. Gülbin Dural Ünver
Dean, Graduate School of **Natural and Applied Sciences** _____

Prof. Dr. Cihangir Tanyeli
Head of Department, **Chemistry** _____

Prof Dr. O. Yavuz Ataman
Supervisor, **Chemistry Department, METU** _____

Examining Committee Members:

Prof. Dr. E. Hale Göktürk
Chemistry Department, METU _____

Prof. Dr. O. Yavuz Ataman
Chemistry Department, METU _____

Assoc. Prof. Dr. Nusret Ertaş
Faculty of Pharmacy, Gazi University _____

Prof. Dr. Mürvet Volkan
Chemistry Department, METU _____

Assoc. Prof. Dr. Sezgin Bakırdere
Chemistry Department, Yıldız Technical University _____

Date: 28.01.2016

I hereby declare that all information in this document has been obtained and presented in accordance with academic rules and ethical conduct. I also declare that, as required by these rules and conduct, I have fully cited and referenced all material and results that are not original to this work.

Name, Last name: Selin Bora

Signature

ABSTRACT

SIMULTANEOUS DETERMINATION OF BISMUTH AND TELLURIUM USING TUNGSTEN COIL ATOM TRAP WITH INDUCTIVELY COUPLED PLASMA MASS SPECTROMETRY

Bora, Selin
Ph. D., Department of Chemistry
Supervisor: Prof. Dr. O. Yavuz Ataman

January 2016, 171 pages

Atom traps such as slotted quartz tube, quartz plate and tungsten coil have been used in atomic spectrometry in order to preconcentrate analyte hydrides and then detection was done by atomic absorption or fluorescence spectrometry. In this study, tungsten coil atom trap was used for the first time with plasma spectrometry. A novel method, which is called Hydride Generation Tungsten Trap Inductively Coupled Plasma Mass Spectrometry (HG-W-Trap-ICPMS), was developed in the first part of this study. Then as a second part, multi-element determination was performed by the proposed method.

This novel method was developed step by step and using only Bismuth at the beginning. HG and then W-coil as a trap was coupled to ICPMS. Flow injection system was used in both nebulization and HG parts. For HG, volatile analyte species were transported from a U-tube type gas-liquid separator (GLS) to plasma. HG system was connected directly to the inlet of torch without any spray chamber and nebulizer system. W-trap was located between the plasma torch inlet and the GLS outlet. 106 mL/min H_2 was passed through the atom trap to protect W-coil from oxidation. Both presence of H_2 and air in the system disturb the plasma seriously. In order to sustain the plasma stability 125 mL/min make-up Ar was introduced to the system through inlet of trap tube. Hydride species were collected on W-trap at an optimized temperature and then revolatilized by

heating the coil to a higher temperature. Transient signal with a halfwidth less than 0.5 s was obtained. Effect of dwell time and smoothing were also studied in this study. Dwell time was set to 10 ms for all parts and smoothing was not applied.

After HG-W-Trap-ICPMS method was developed for only Bi, multi-element study for simultaneous determination of Bi and Tellurium in their mixture was performed successfully. For comparison, studies were also done by Te alone. In addition, effect of three different coatings, which were iridium, platinum and rhodium, were evaluated for each element.

Sensitivities using nebulization, HG and HG-W-Trap were compared for Bi and Te determinations by ICPMS. When slopes of calibration plots are considered, as compared to nebulization, HG-W-Trap signals were 1255 and 106 times more sensitive for ^{209}Bi and ^{130}Te, respectively. For 1.0 min collection period, LOD values were found to be 2.7 ng/L for Bi with Ir-coated W-coil and 6.0 ng/L for Te with Pt-coated W-coil. Trapping efficiencies of Bi and Te were calculated as 40% and 15%, respectively. In simultaneous determination of these two elements slopes of the calibration graphs were found very close to that of single mass study for each element. Pt-coated W-coil was used for Bi and Te mixture study. Accuracies of the methods were checked by using the “NIST 1643e Trace Elements in Water” and “NIST 1643f Trace Elements in Water” standard reference materials.

Determination of three elements simultaneously by HG-W-Trap-ICPMS method was also feasible. Antimony and selenium were used separately as a third element besides Bi and Te. Three masses study was performed by using the Pt-coated W-coil.

Keywords: W-coil atom trap, hydride generation, ICPMS, multi-element determination, dwell time, smoothing, bismuth, tellurium, antimony, selenium.

ÖZ

TUNGSTEN SARMAL ATOM TUZAĞI VE ENDÜKTİF EŞLEŞMİŞ PLAZMA KÜTLE SPEKTROMETRİYLE BİZMUT VE TELLÜR'ÜN EŞZAMANLI TAYİNİ

Bora, Selin
Doktora, Kimya Bölümü
Tez Yöneticisi: Prof. Dr. O. Yavuz Ataman

Ocak 2016, 171 sayfa

Atomik Spektrometride oluşan analit hidrürlerinin önzenginleştirilmesi için yarıklı kuvars tüp, kuvars plaka ve tungsten sarmal gibi atom tuzakları kullanılarak atomik absorpsiyon veya floresans spektrometrisi ile tayin yapılmıştır. Bu çalışmada tungsten sarmal atom tuzağı ilk kez plazma spektrometride kullanılmıştır. Hidrür Oluşturmalı-W-Tuzak-Endüktif Eşleşmiş Plazma Kütle Spektrometri (HO-W-Tuzak-ICPMS) olarak adlandırılan yeni bir metot bu çalışmanın ilk kısmında geliştirilmiştir. İkinci kısımda ise geliştirilen metot kullanılarak çoklu element tayini yapılmıştır.

Bu yeni metot basamak basamak geliştirilmiş ve başlangıç olarak sadece Bizmut tayini yapılmıştır. HO ve sonraki aşamada tuzak olarak W-sarmalı ICPMS sistemine bağlanmıştır. Akışa enjeksiyon sistemi hem sisleştirme, hem de HO çalışmalarında kullanılmıştır. HO sisteminde uçucu analit türleri U-tüp tipi gaz sıvı ayıracından (GSA) plazmaya gönderilmiştir. HO sistemi sisleştirici ve püskürtme odacığı olmadan doğrudan plazma başlığı girişine bağlanmıştır. W-sarmal plazma girişi ile GSA çıkışı arasına yerleştirilmiştir. W-sarmalını oksitlenmekten korumak için atom tuzağından 106 mL/min akış hızıyla H_2 gazı geçirilmiştir. Sistemde H_2 gazı ve havanın varlığı plazmayı önemli şekilde etkilemektedir. Plazma kararlılığını korumak için 125 mL/min akış hızında düzenleyici Ar gazı tuzağın bulunduğu tüpün girişinden sisteme gönderilmiştir. W-tuzakta belirli sıcaklıkta toplanan türler daha sonra sarmalın daha yüksek sıcaklıklara

ısıtılmasıyla tekrar buharlaştırılmıştır. Yarı bant genişliği 0.5 s den küçük olan pik şeklinde sinyaller elde edilmiştir. Sinyal alma süresi ve düzgünleştirme etkileri de bu tez çalışmasında incelenmiştir. Çalışmanın tümünde sinyal alma süresi 10 ms olarak ayarlanırken düzgünleştirme özelliği kullanılmamıştır.

HO-W-Tuzak-ICPMS yöntemi yalnız Bi için geliştirildikten sonra karışımdaki Bi ve Te elementlerinin eşzamanlı tayini için çoklu-element çalışması başarıyla gerçekleştirilmiştir. Karşılaştırma için Te elementi tek olarak da çalışılmıştır. Bunlara ek olarak, üç farklı kaplama maddesi, iridyum, platin ve rodyum metallerinin her iki analit üzerine etkisi değerlendirilmiştir.

Bi ve Te için sisleştirme, HO ve HG-W-Tuzak sistemlerini kullanarak ICPMS ile elde edilen duyarlılık değerleri karşılaştırılmıştır. Kalibrasyon grafiklerinin eğimleri kıyaslandığında sisleştirme sistemine kıyasla HO-W-Tuzak düzeneği ^{209}Bi ve ^{130}Te için sırasıyla 1255 kat ve 106 kat daha duyarlıdır. 1.0 dakika toplama süresinde Bi için Ir-kaplı W-sarmal kullanılarak gözlenebilme sınırı 2.7 ng/L iken Te için Pt-kaplamalı W-sarmal ile 6.0 ng/L bulunmuştur. Tuzaklama verimleri Bi ve Te için sırasıyla %40 ve %15 olarak hesaplanmıştır. Bu iki elementin eşzamanlı tayininde her element için bulunan kalibrasyon grafiklerinin eğimleri tek kütle çalışmasındaki eğimlere çok yakın bulunmuştur. İki kütle çalışmasında Pt-kaplamalı W-sarmal kullanılmıştır. Geliştirilen yöntemlerin doğruluğu “NIST 1643e Trace Elements in Water” ve “NIST 1643f Trace Elements in Water” standart referans maddeleri kullanılarak kontrol edilmiştir.

Üç elementin eşzamanlı tayininin de HO-W-Tuzak-ICPMS yöntemiyle yapılabilir olduğu gösterilmiştir. Antimon ve selenyum elementleri ayrı ayrı üçüncü element olarak Bi ve Te elementlerinin yanına eklenmiştir. Üç kütle çalışmasında Pt-kaplamalı W-sarmal kullanılmıştır.

Anahtar Kelimeler: W-sarmal atom tuzağı, hidrür oluşturma, ICPMS, çoklu element tayini, sinyal alma süresi, düzgünleştirme, bizmut, tellür, antimon, selenyum.

Dedicated to my family, Mecit, Nermin and Egemen Bora and also Emre Sönmez

ACKNOWLEDGEMENTS

I would like to express my deep appreciation and respect to my supervisor Prof. Dr. O. Yavuz Ataman for his endless guidance, support, encouragement, understanding, patience and suggestions throughout this study.

I want to express my gratitude to my Thesis Committee members, Prof. Dr. E. Hale Göktürk and Prof. Dr. Nusret Ertaş for their valuable suggestions and comments to complete this thesis in best way.

I am deeply grateful to Assoc. Prof. Dr. Gülay Ertaş not only for her endless guidance, patience and but also her moral support during this tiring study. She spent long hours with me for discussions of results.

I would like to thank Assoc. Prof. Dr. Sezgin Bakırdere and Ahmet Yıldıran for being the initiator of this novel thesis study.

My special thanks to Emrah Yıldırım and Pınar Akay for sharing their experiences about hydride generation systems and also for their valuable friendship.

I would like to thank Anılcan Yılmaz, Başak Dügencili, Erhan Özdemir, Sezin Atıcı, Canan Höçük and Bilgi Er for their help whenever I need and for their friendship.

I also would like to thank C-50 lab members, Yeliz Akpınar, Nehir Utku, Dilek Ünal and Zuhal Vanlı for enjoyable conversations and friendship. Special thanks to Yeliz Akpınar for accompanying me until late hours while I was performing my experiments.

For providing technical support to solve the many problems of ICPMS and enabling my thesis to finish, I would like to express my appreciation to REDOKS Lab. Service Engineers who are Erdem Özdil, Metin Kırlı, Anıl Ulukan and Özgür Seçkin.

I would like to thank Halil Memiş for his help on Argon tanks and Eda Durkan for her moral support and deep friendship.

Regarding the preparation of glass tubes that I designed for thesis, I should also thank to Hamit Çağlar and Aziz Çağlar.

I would like to thank TÜBİTAK for awarding scholarship during my doctorate program. With this scholarship I was eager to study and search more.

I am grateful to Emre Sönmez for his understanding, patience and love during this study. He also made invaluable contributions to thesis by drawing the schematic diagrams.

Finally, my special thanks to my father, Mecit Bora, my mother, Nermin Bora and my brother, Egemen Bora, for their endless trust, patience, support and love. My father is proud of me for being a chemist.

TABLE OF CONTENTS

ABSTRACT v
ÖZ vii
ACKNOWLEDGEMENTS x
TABLE OF CONTENTS xii
LIST OF TABLES xvi
LIST OF FIGURES xix
LIST OF ABRREVIATIONS xxv
1. INTRODUCTION 1
1.1. Bismuth 1
1.2. Determination of Bismuth 2
1.3. Tellurium 7
1.4. Determination of Tellurium 9
1.5. Hydride Generation 15
1.5.1. Interferences in Hydride Generation 18
1.6. Hydride Generation Coupled to Plasma Spectrometry 20
1.7. Tungsten Coil Atom Traps 23
1.7.1. Trapping Efficiency 29
1.8. Inductively Coupled Plasma Mass Spectrometry - ICPMS 29
1.9. Multi-Element Detection Capability of ICPMS with Transient Signals 33
1.10. Aim of the Study 37
2. EXPERIMENTAL 39
2.1. Reagents 39
2.2. Instrumentation and Experimental Setups 40
2.2.1. Instruments for General Purpose 40
2.2.2. ICPMS with Nebulization System 41
2.2.3. Hydride Generation System 41
2.2.4. Hydride Generation W-trap ICPMS System 44

2.3. Procedures 46
2.3.1. ICPMS with Nebulization System 47
2.3.1.1. Isotopes Used in the Study 49
2.3.2. Hydride Generation System 51
2.3.3. Hydride Generation W-trap ICPMS System 52
3. RESULTS AND DISCUSSION 55
3.1. Determination of Bismuth by ICPMS 55
3.1.1. Calibration Plot and Analytical Performance for Bi Determination by ICPMS 55
3.1.2. Accuracy Check for Bi Determination by ICPMS 58
3.2. Determination of Bismuth by HG-ICPMS 58
3.2.1. Optimizations for Bi Determination by HG-ICPMS 60
3.2.1.1. Carrier Argon Flow Rate 60
3.2.1.2. $NaBH_4$ Flow Rate 61
3.2.1.3. Carrier Acid Flow Rate 62
3.2.1.4. Concentration of $NaBH_4$ 63
3.2.1.5. Concentration of HCl in Analyte Solution 64
3.2.2. Calibration Plot and Analytical Performance for Bi Determination by HG-ICPMS 66
3.2.3. Accuracy Check for Bi Determination by HG-ICPMS 69
3.3. Determination of Bismuth by HG-W-Trap-ICPMS 70
3.3.1. Effect of Coating for Bi Determination 70
3.3.2. Optimization for Bi Determination by HG-Ir coated-W Trap-ICPMS 72
3.3.2.1. H_2 Gas and Make-up Ar Flow Rate 72
3.3.2.2. Trapping Temperature 74
3.3.2.3. Revolatilization Temperature 77
3.3.2.4. Trapping Period 79
3.3.3. Calibration Plot and Analytical Performance for Bi Determination by HG-W-Trap-ICPMS 81
3.3.4. Accuracy Check for Bi Determination by HG-Ir coated-W Trap-ICPMS 84
3.3.5. Trapping Efficiency Calculations for Bi Determination 86
3.3.6. Dwell Time and Smoothing Studies for Bi Determination 88
3.4. Determination of Tellurium by ICPMS 90

3.4.1. Calibration Plot and Analytical Performance for Te Determination by ICPMS 91
3.4.2. Accuracy Check for Te Determination by ICPMS 93
3.5. Determination of Tellurium by HG-ICPMS.....95
3.5.1. Optimizations for Te Determination by HG-ICPMS 95
3.5.2. Calibration Plot and Analytical Performance for Te Determination by HG-ICPMS 96
3.5.3. Accuracy Check for Te Determination by HG-ICPMS 98
3.6. Determination of Tellurium by HG-W-Trap-ICPMS.....99
3.6.1. Effect of Coating for Te Determination 99
3.6.2. Optimizations for Te Determination by HG-Pt coated-W Trap-ICPMS .100
3.6.3. Calibration Plot and Analytical Performance for Te Determination by HG-Pt coated-W Trap-ICPMS.....101
3.6.4. Accuracy Check for Te Determination by HG-Pt coated-W Trap-ICPMS ... .104
3.6.5. Trapping Efficiency Calculations for Te.....105
3.7. Multi-Element Studies by HG-W-Trap-ICPMS.....107
3.7.1. Simultaneous Determination of Bi and Te in Mixture by HG-ICPMS....107
3.7.1.1. Optimizations for Simultaneous Determination of Bi and Te in Mixture by HG-ICPMS.....107
3.7.1.1.1. $NaBH_4$ Flow Rate for Simultaneous Determination of Bi and Te in Mixture.....108
3.7.1.1.2. Carrier Acid Flow Rate for Simultaneous Determination of Bi and Te in Mixture.....110
3.7.1.1.3. Concentration of $NaBH_4$ for Simultaneous Determination of Bi and Te in Mixture.....111
3.7.1.1.4. Concentration of HCl in Analyte Solution for Simultaneous Determination of Bi and Te in Mixture 113
3.7.1.2. Calibration Plots and Analytical Performances for simultaneous determination of Bi and Te in mixture by HG-ICPMS.....115
3.7.2. Simultaneous Determination of Bi and Te in Mixture by HG-Pt Coated-W Trap-ICPMS.....118
3.7.2.1. Optimizations for Simultaneous Determination of Bi and Te in Mixtureby HG-Pt Coated-W Trap-ICPMS 118
3.7.2.1.1. Trapping Temperature 118

3.7.2.1.2. Revolatilization Temperature 120
3.7.2.2. Calibration Plots and Analytical Performances for Simultaneous Determination of Bi and Te in Mixture by HG-Pt coated-W Trap-ICPMS.....122
3.7.2.3. Accuracy Check for Simultaneous Determination of Bi and Te in Mixture by HG-Pt Coated-W Trap-ICPMS 126
3.7.3. Dwell Time Studies for Two Masses 127
3.7.4. Studies on Simultaneous Determination of Three Elements in Mixture by HG-W-Trap-ICPMS 132
4. CONCLUSIONS 141
REFERENCES.....147
CURRICULUM VITAE 173

LIST OF TABLES

TABLES

Table 1.1. Various methods from literature for Bi determination.....3
Table 1.2. Different methods from literature for Te determination 10
Table 1.3. Nomenclature and some chemical properties of volatile hydrides. 16
Table 2.1. Operating Parameters of ICPMS.....48
Table 2.2. Natural abundances and stabilities of isotopes used in this study[196].....50
Table 2.3. Optimum hydride generation conditions for Bi and Te 51
Table 2.4. Optimum trapping system conditions for Bi and Te.....53
Table 3.1. Analytical figures of merit for Bi by ICPMS.....57
Table 3.2. Results of accuracy check for Bi determination by ICPMS. 58
Table 3.3. Optimum values of HG-ICPMS for Bi determination using U-Tube and Cylindrical GLSs.....65
Table 3.4. Analytical figures of merit for Bi determination by HG-ICPMS. 69
Table 3.5. Comparison of LOD results with literature for Bi determination using HG-ICPMS.....69
Table 3.6. Results of accuracy check for Bi determination by HG-ICPMS. 70
Table 3.7. Effect of different coating materials for Bi determination by HG-W-Trap-ICPMS. Concentration of Bi was 0.25 ng/mL. Flow rates of make-up Ar and H_2 were 125 and 106 mL/min, respectively.....71
Table 3.8. Optimum values for Bi determination by HG-Ir-Coated-W Trap-ICPMS system.....80
Table 3.9. Analytical figures of merit for Bi determination by HG-Uncoated-W Trap-ICPMS and HG-Ir coated-W Trap–ICPMS. 82
Table 3.10. Comparison of the results for Bi determination by HG-Ir coated-W Trap–ICPMS with literature. 84

Table 3.11. Results of accuracy check for Bi determination by HG-Ir-coated-W Trap-ICPMS. 84
Table 3.12. Analytical figures of merits for Bi determination by the four methods. 85
Table 3.13. Analytical figures of merit for Te determination by ICPMS 93
Table 3.14. Results of accuracy check for Te determination by ICPMS. 94
Table 3.15. Optimum values of HG parameters for Te determination by HG-ICPMS system. 96
Table 3.16. Analytical figures of merit for Te determination by HG-ICPMS. 97
Table 3.17. Comparison of results for Te determination by HG-ICPMS with literature. 98
Table 3.18. Results of accuracy check for Te determination by HG-ICPMS 99
Table 3.19. Effect of different coating materials for Te by HG-W-Trap-ICPMS. Concentration of Te was 0.5 ng/mL. Flow rates of make-up Ar and H_2 were 125 and 106 mL/min, respectively. 100
Table 3.20. Optimum values for Te by HG-Pt Coated-W Trap-ICPMS system 101
Table 3.21. Analytical figures of merit for Te determination by HG-Pt-coated-W Trap-ICPMS. 103
Table 3.22. Comparison of the results for Te by HG-Pt coated-W Trap–ICPMS with literature. 103
Table 3.23. Result of accuracy check for Te determination by HG-Pt coated-W Trap-ICPMS. 104
Table 3.24. Analytical figures of merits for ^{130}Te by three methods. 105
Table 3.25. Optimum values of HG parameters for simultaneous determination of Bi and Te in mixture by HG-ICPMS. 115
Table 3.26. Analytical figures of merit for simultaneous determination of ^{209}Bi and ^{130}Te in mixture by HG-ICPMS. 117
Table 3.27. Analytical figures of merits for Bi and Te in single and multi-element studies by HG-ICPMS. 117
Table 3.28. Optimum values of HG-Pt coated-W Trap-ICPMS system for simultaneous determination of Te and Bi 122
Table 3.29. Analytical figures of merit for simultaneous determination of ^{209}Bi and ^{130}Te in mixture by HG-Pt coated-W Trap-ICPMS. 125

Table 3.30. Analytical figures of merits for Bi and Te in single and multi-element studies by HG-Pt Coated-W Trap-ICPMS. 126
Table 3.31. Results of accuracy check for ^{209}Bi and ^{130}Te in Bi-Te mixture by HG-Pt coated-W Trap-ICPMS. 126
Table 3.32. Effect of dwell time on signal magnitude 132

LIST OF FIGURES

FIGURES

Figure 1.1. Schematic of Quadrupole-ICPMS.[177] 32
Figure 2.1. Schematic representation of HG-ICPMS system. 42
Figure 2.2. Schematic representation of U-Tube GLS.....43
Figure 2.3. Schematic representation of cylindrical type GLS 44
Figure 2.4. Schematic representation of glass tube for W-coil. 45
Figure 2.5. Picture of glass tube for W-coil and W-coil itself 45
Figure 2.6. Schematic representation of HG-W-Trap-ICPMS system. 46
Figure 3.1. Calibration plot for Bi determination between 0.10 ng/mL and 10 ng/mL using ICPMS. 56
Figure 3.2. Calibration plot for Bi determination between 0.10 ng/mL and 2.5 ng/mL using ICPMS. 56
Figure 3.3. Flow injection signals of Bi solutions using ICPMS and a loop of 500 µL. .57
Figure 3.4. The optimization of carrier Ar flow rate for Bi determination by HG-ICPMS. 0.25 ng/mL Bi solution in 1.0 M HCl and 0.5% (w/v) $NaBH_4$ was used. Flow rates of carrier acid solution and $NaBH_4$ were 2.0 mL/min and 1.1 mL/min, respectively. 61
Figure 3.5.The optimization of $NaBH_4$ flow rate for Bi determination by HG-ICPMS. 0.25 ng/mL Bi solution in 1.0 M HCl and 0.5% (w/v) $NaBH_4$ were used. Flow rates of sample and carrier Ar were 2.0 mL/min and 1.2 L/min, respectively. 62
Figure 3.6. The optimization of carrier acid solution flow rate for Bi determination by HG-ICPMS. For this optimization, 0.25 ng/mL Bi solution in 1.0 M HCl and 0.5% (w/v) $NaBH_4$ was used. Concentration of carrier HCl solution was 1.0 M. Flow rates of $NaBH_4$ and carrier Ar were 1.1 mL/min and 1.2 L/min, respectively. 63
Figure 3.7. The optimization of $NaBH_4$ concentration for Bi determination by HG-ICPMS. Concentration of Bi was 0.25 ng/mL in 1.0 M HCl. Flow rates of $NaBH_4$,

carrier acid solution and carrier Ar were 1.1 mL/min, 2.0 mL/min and 1.2 L/min, respectively.....64
Figure 3.8. The optimization of HCl concentration for Bi determination by HG-ICPMS. 0.5% (w/v) $NaBH_4$ were used. Flow rates of $NaBH_4$, carrier acid solution and carrier Ar were 1.1 mL/min, 2.0 mL/min and 1.2 L/min, respectively. 65
Figure 3.9. Calibration plot for Bi determination by using U-tube GLS and HG-ICPMS. 66
Figure 3.10. Calibration plot for Bi determination by using Cylindrical GLS and HG-ICPMS. 67
Figure 3.11. Flow injection signals of Bi by using U-tube GLS, HG-ICPMS and a loop of 500 µL. 68
Figure 3.12. The optimization of make-up Ar and H_2 flow rates for Bi determination by HG-Ir coated-W Trap-ICPMS. Concentration of Bi was 0.25 ng/mL in 1.0 M HCl. Trapping and releasing temperatures were 179 and 1600 ^oC, respectively. 73
Figure 3.13. The optimization of make-up Ar flow rates for Bi determination by HG-Ir coated-W Trap-ICPMS. Concentration of Bi was 0.25 ng/mL in 1.0 M HCl. Trapping and releasing temperatures were 179 and 1600 ^oC, respectively. Flow rate of H_2 was 106 mL/min. 74
Figure 3.14. Temperature vs. voltage relationship using thermocouple. 75
Figure 3.15. The optimization of trapping temperature for Bi determination by HG-Ir coated-W Trap-ICPMS. Concentration of Bi was 0.25 ng/mL in 1.0 M HCl. Releasing temperature was 1600 ^oC. Trapping period was 30 s. Flow rates of H_2 and make-up Ar were 106 mL/min and 125 mL/min, respectively. 75
Figure 3.16. XPS spectrum of Ir-coated W-coil with trapped Bi species 77
Figure 3.17. Temperature vs.voltage relationship for pyrometer using GF-AAS.....78
Figure 3.18. The optimization of revolatilization temperature for Bi determination by HG-Ir coated-W Trap-ICPMS. Concentration of Bi was 0.25 ng/mL in 1.0 M HCl. Trapping temperature was 179 ^oC. Trapping period was 30 s. Flow rates of H_2 and make-up Ar were 106 mL/min and 125 mL/min, respectively. 79
Figure 3.19. The optimization of trapping period for Bi determination by HG-Ir coated-W Trap-ICPMS. Concentration of Bi was 0.25 ng/mL in 1.0 M HCl. Trapping and

revolatilization temperatures were 179 ºC and 1600 ºC, respectively. Flow rates of H_2 and make-up Ar were 106 mL/min and 125 mL/min, respectively. 80
Figure 3.20. Calibration plot for Bi determination by HG-uncoated-W Trap-ICPMS. ..81
Figure 3.21. Calibration plot for Bi determination by HG-Ir coated-W Trap-ICPMS. ..82
Figure 3.22. Continuous signals of 0.25 ng/mL Bi before and during trapping period by HG-Ir coated–W Trap-ICPMS. Trapping temperature was 179 ºC. Trapping period was 30 s. Flow rates of H_2 and make-up Ar were 106 and 125 mL/min, respectively. 86
Figure 3.23. Transient signals of 0.25 ng/mL Bi by HG-Ir coated–W Trap-ICPMS. Releasing temperature was 1600 ºC. Flow rates of H_2 and make-up Ar were 106 and 125 mL/min, respectively.....88
Figure 3.24. Transient signals of 0.50 ng/mL Bi by HG-Pt coated–W Trap-ICPMS when dwell time is (a) 10 ms, (b) 20 ms, (c) 50 ms, (d) 100 ms and smoothing process is applied. 90
Figure 3.25. Calibration plot for Te determination by ICPMS. 91
Figure 3.26. Calibration plot for Te determination between 0.25 ng/mL and 5.0 ng/mL using ICPMS. 92
Figure 3.27. Standard addition plot of ^{128}Te for SRM study by ICPMS. 94
Figure 3.28. Calibration plot for ^{130}Te between 0.050 ng/mL and 25.0 ng/mL.by HG-ICPMS.....96
Figure 3.29. Calibration plot for ^{130}Te between 0.050 ng/mL and 2.5 ng/mL by HG-ICPMS.....97
Figure 3.30. Calibration plot of ^{130}Te between 0.025 ng/mL and 10.0 ng/mL by HG-Pt coated-W Trap-ICPMS. 102
Figure 3.31. Calibration plot of ^{130}Te between 0.025 ng/mL and 1.0 ng/mL by HG-Pt coated-W Trap-ICPMS. 102
Figure 3.32. Continuous ^{130}Te signals of two replicates of 2.5 ng/mL Te solution before and during trapping period by HG-Pt coated–W Trap-ICPMS. Trapping temperature was 179 ºC. Trapping period was 30 s. Flow rates of H_2 and make-up Ar were 106 and 125 mL/min, respectively.....106

Figure 3.33. Transient signals of 2.5 ng/mL ^{130}Te by HG-Pt coated–W Trap-ICPMS. Revolatilization temperature was 1600 ^{o}C. Flow rates of H_2 and make-up Ar were 106 and 125 mL/min, respectively. 106
Figure 3.34. The optimization of $NaBH_4$ flow rate for ^{209}Bi in mixture solution by HG system. 0.25 ng/mL Bi and 2.5 ng/mL Te solution in 4.0 M HCl and 0.5% (w/v) $NaBH_4$ was used. Flow rates of carrier Ar and HCl solution were 1.2 L/min and 2.0 mL/min, respectively. 109
Figure 3.35. The optimization of $NaBH_4$ flow rate for ^{130}Te in mixture solution by HG system. 0.25 ng/mL Bi and 2.5 ng/mL Te solution in 4.0 M HCl and 0.5% (w/v) $NaBH_4$ was used. Flow rates of carrier Ar and HCl solution were 1.2 L/min and 2.0 mL/min, respectively. 109
Figure 3.36. The optimization of carrier acid flow rate for ^{209}Bi in mixture solution by HG system. 0.25 ng/mL Bi and 2.5 ng/mL Te solution in 4.0 M HCl and 0.5% (w/v) $NaBH_4$ was used. Flow rates of carrier Ar and $NaBH_4$ solution were 1.2 L/min and 1.1 mL/min, respectively. 110
Figure 3.37. The optimization of carrier acid flow rate for ^{130}Te in mixture solution by HG system. 0.25 ng/mL Bi and 2.5 ng/mL Te solution in 4.0 M HCl and 0.5% (w/v) $NaBH_4$ was used. Flow rates of carrier Ar and $NaBH_4$ solution were 1.2 L/min and 1.1 mL/min, respectively. 111
Figure 3.38. The optimization of $NaBH_4$ concentration for ^{209}Bi in mixture by HG system. 0.25 ng/mL Bi and 2.5 ng/mL Te solution in 4.0 M HCl was used. Flow rates of carrier Ar, $NaBH_4$ and carrier acid solution were 1.2 L/min, 1.1 mL/min and 2.0 mL/min, respectively. 112
Figure 3.39. The optimization of $NaBH_4$ concentration for ^{130}Te in mixture by HG system. 0.25 ng/mL Bi and 2.5 ng/mL Te solution in 4.0 M HCl was used. Flow rates of carrier Ar, $NaBH_4$ and carrier acid solution were 1.2 L/min, 1.1 mL/min and 2.0 mL/min, respectively. 112
Figure 3.40. The optimization of HCl concentration for ^{209}Bi in mixture by HG system. 0.25 ng/mL Bi and 2.5 ng/mL Te solution and 0.5% (w/v) $NaBH_4$ was used. Flow rates of carrier Ar, $NaBH_4$ and carrier acid solution were 1.2 L/min, 1.1 mL/min and 2.0 mL/min, respectively. 113

Figure 3.41. The optimization of HCl concentration for ^{130}Te in mixture by HG system. 0.25 ng/mL Bi and 2.5 ng/mL Te solution and 0.5% (w/v) $NaBH_4$ was used. Flow rates of carrier Ar, $NaBH_4$ and carrier acid solution were 1.2 L/min, 1.1 mL/min and 2.0 mL/min, respectively. 114
Figure 3.42. Calibration plot for ^{209}Bi in mixture by HG-ICPMS system 116
Figure 3.43. Calibration plot for ^{130}Te in mixture by HG-ICPMS system. 116
Figure 3.44. The optimization of trapping temperature for ^{209}Bi in mixture by HG-Pt coated-W Trap-ICPMS. Concentrations of Bi and Te were 0.25 ng/mL and 2.5 ng/mL in 2.0 M HCl. Revolatilization temperature was 1600 ^{o}C. Trapping period was 30 s. Flow rates of H_2 and make-up Ar were 106 mL/min and 125 mL/min, respectively. 119
Figure 3.45. The optimization of trapping temperature for ^{130}Te in mixture by HG-Pt coated-W Trap-ICPMS. Concentrations of Bi and Te were 0.25 ng/mL and 2.5 ng/mL in 2.0 M HCl. Revolatilization temperature was 1600 ^{o}C. Trapping period was 30 s. Flow rates of H_2 and make-up Ar were 106 mL/min and 125 mL/min, respectively. 120
Figure 3.46. Optimization of revolatilization temperature for ^{209}Bi in mixture by HG-Pt coated-W Trap-ICPMS. Concentrations of Bi and Te were 0.25 ng/mL and 2.5 ng/mL in 2.0 M HCl. Trapping temperature was 179 ^{o}C. Trapping period was 30 s. Flow rates of H_2 and make-up Ar were 106 mL/min and 125 mL/min, respectively. 121
Figure 3.47. Optimization of revolatilization temperature for ^{130}Te in mixture by HG-Pt coated-W Trap-ICPMS. Concentrations of Bi and Te were 0.25 ng/mL and 2.5 ng/mL in 2.0 M HCl. Trapping temperature was 179 ^{o}C. Trapping period was 30 s. Flow rates of H_2 and make-up Ar were 106 mL/min and 125 mL/min, respectively. 121
Figure 3.48. Calibration plot for ^{209}Bi in Bi-Te mixture between 0.025 ng/mL and 2.5 ng/mL by HG-Pt coated-W Trap-ICPMS. 123
Figure 3.49. Calibration plot for ^{209}Bi in Bi-Te mixture between 0.025 ng/mL and 0.50 ng/mL by HG-Pt coated-W Trap-ICPMS. 123
Figure 3.50. Calibration plot for ^{130}Te in Bi-Te mixture between 0.025 ng/mL and 10.0 ng/mL by HG-Pt coated-W Trap-ICPMS. 124
Figure 3.51. Calibration plot for ^{130}Te in Bi-Te mixture between 0.025 ng/mL and 0.5 ng/mL by HG-Pt coated-W Trap-ICPMS. 124

Figure 3.52. Transient signals of 0.50 ng/mL Bi alone and in binary mixture by HG-Pt coated–W Trap-ICPMS when dwell time is 10 ms. 128
Figure 3.53. Transient signals of 0.50 ng/mL Bi alone and in binary mixture by HG-Pt coated–W Trap-ICPMS when dwell time is 20 ms. 129
Figure 3.54. Transient signals of 0.50 ng/mL Bi alone and in binary mixture by HG-Pt coated–W Trap-ICPMS when dwell time is 50 ms. 129
Figure 3.55. Transient signals of 0.50 ng/mL Bi alone and in binary mixture by HG-Pt coated–W Trap-ICPMS when dwell time is 100 ms. 130
Figure 3.56. Transient signals of 0.25 ng/mL ^{209}Bi and 1.0 ng/mL ^{130}Te in Bi-Te mixture by HG-Pt coated–W Trap-ICPMS. 133
Figure 3.57. Hydride and transient signals of blank and 2.0 ng/mL ^{121}Sb in Bi-Te-Sb mixture by HG-Pt coated–W Trap-ICPMS. 135
Figure 3.58. Hydride and transient signals of blank and 2.0 ng/mL ^{78}Se in Bi-Te-Se mixture by HG-Pt coated–W Trap-ICPMS. 135
Figure 3.59. Hydride and transient signals of blank and 1.0 ng/mL ^{130}Te in Bi-Te-Se/Sb mixture by HG-Pt coated–W Trap-ICPMS. 136
Figure 3.60. Hydride and transient signals of blank and 0.25 ng/mL ^{209}Bi in Bi-Te-Se/Sb mixture by HG-Pt coated–W Trap-ICPMS. 136
Figure 3.61. Hydride and transient signals of blank and 2.0 ng/mL ^{121}Sb in Bi-Te-Sb mixture by HG-Ir coated–W Trap-ICPMS. 137
Figure 3.62. Hydride and transient signals of blank and 2.0 ng/mL ^{78}Se in Bi-Te-Se mixture by HG-Ir coated–W Trap-ICPMS. 137
Figure 3.63. Hydride and transient signals of blank and 1.0 ng/mL ^{130}Te in Bi-Te-Se/Sb mixture by HG-Ir coated–W Trap-ICPMS. 138
Figure 3.64. Hydride and transient signals of blank and 0.25 ng/mL ^{209}Bi in Bi-Te-Se/Sb mixture by HG-Ir coated–W Trap-ICPMS. 138

LIST OF ABRREVIATIONS

AFS	Atomic fluorescence spectrometry
CF	Continuous flow
CPE	Cloud point extraction
CPS	Count per second
CRM	Certified reference material
DBD	Dielectric barrier discharge
EM	Electron multipliers
ETAAS	Electrothermal atomic absorption spectrometry
FAAS	Flame atomic absorption spectrometry
FI	Flow injection
GBME	Graphite bar micro extraction
GC-MS	Gas chromatography mass spectrometry
HF-LPME	Hollow fiber liquid phase micro extraction
HGAAS	Hydride generation atomic absorption spectrometry
HG-CL	Hydride generation chemiluminescence
HG-ICPMS	Hydride generation inductively coupled plasma mass spectrometry
HG-ICPOES	Hydride generation inductively coupled plasma optical emission spectrometry

HG-W-Trap-ICPMS	Hydride generation tungsten trap inductively coupled plasma mass spectrometry
ICPMS	Inductively coupled plasma mass spectrometry
ICPOES	Inductively coupled plasma optical emission spectrometry
ICPS	Integrated count per second
LOD	Limit of detection
LOQ	Limit of quantification
PSA	Potentiometric stripping analysis
QTA	Quartz tube atomizer
RLS	Resonance light scattering
RSD	Relative standard deviation
SF-ICPMS	Sector field inductively coupled plasma mass Spectrometry
SPE	Solid phase extraction
SQT-AT	Slotted quartz tube atom trap
SRM	Standard reference material
SV	Stripping voltammetry
TEx	Transient extension
THB	Tetrahydroborate
TOF	Time of flight
USN	Ultrasonic nebulization
XPS	X-ray photoelectron spectroscopy

CHAPTER 1

INTRODUCTION

1.1. Bismuth

Bismuth (Bi) is one of Group VA elements having atomic number of 83. It shows similar chemical properties with antimony although it has higher metallic character than other elements in Group VA. Bi has only one naturally occurring isotope with an atomic weight of 208.98. Melting and boiling points of Bi are 271 ^{o}C and 1564 ^{o}C, respectively. Its volume expands unusually about 3% after solidification process.[1] It is found rarely in the Earth's crust with 0.00002% and it is among few metallic elements which can be found in its elemental form in nature.[1,2]

The concentration of bismuth in soil is usually around 1.0 µg/g. However, in sediments concentration changes between 0.07[3] and 49.6[4] µg/g. For silicate rocks, Bi level is found to be less than 1.0 µg/g[2]. Lastly, some coal samples include more than 1.0 µg/g Bi and bismuth can be distributed to environment through fly ash by burning process.[5]

The concentration of bismuth in biological and food samples was also studied. In biological samples e.g. lichen, mussel tissue[6], plant leaves, animal liver[7] and in food samples e.g. cabbage[8], onion, peas[9], milk[10], bismuth concentration is approximately at ng/g level. Besides, in some food samples such as nuts and viscera Bi level is found to be in µg/g.[11]

Bismuth has become an industrially significant element because its physical and chemical properties have led it to be used in different areas of life. Bismuth has been used in medicine for treatment of dyspepsia, syphilis, dermatological disorders and peptic ulcer. It is used as an antibacterial agent against *helicobacter pylori*, which initiate ulcer formation by excreting acid.[12,13,14]

Apart from pharmaceutics and cosmetic products, Bi has been used in metallurgy, electrochemistry, iron casting, plastics and pigments, lubricants, cartridges[15] and in the preparation and recycling of uranium in nuclear fuels.[16]

Although Bi is not an essential element for humans, it is taken into human body through food. Absorbed Bi is transferred by human serum, delivered to cells and excreted through urine. However, number of toxic effects has been observed related to high bismuth intake in humans and animals. Among these are osteoarthropathy, hepatitis, neuropathology, encephalopathy and nephrotoxicity.[14] In one study with mice, it was found that Bi enters the nervous system and affects the motor neurons. Hence, it was suggested that Bi should be in the list of potential toxins that affect motor neurons.[17]

With an increase in the use of bismuth in different areas of life, chance of exposure becomes higher. Therefore, determination of bismuth at trace level becomes important in environmental and biological samples.

1.2. Determination of Bismuth

Up to date many analytical techniques have been used for determination of Bi in various types of samples. Starting from the ultraviolet-visible spectrophotometry (UV-VIS)[18,19,20,21,22], Flame . Absorption Spectrometry (FAAS)[23,24], Electrothermal Atomic Absorption Spectrometry (ETAAS)[12,20,25,26,27], Inductively Coupled Plasma Optical Emission Spectrometry (ICPOES)[28,29,30] and Inductively Coupled Plasma Mass Spectrometry (ICPMS)[31,32,33,34,35] have been used. In addition, *coupled techniques* such as HG-AAS[14,36], HG-AFS[37,38,39,40,41,42,43], HG-ICPOES[44,45, 46], HG-ICPMS[47,48,49,50] and HG-ETV-ICPMS[51] have been utilized to improve the sensitivity. Other known

techniques are Resonance Light Scattering (RLS)[52], Potentiometric Stripping Analysis (PSA)[53,54,55] and Stripping Voltammetry (SV).[56]

Various methods for Bi determination in different samples are listed in Table 1.1. Detection limits of the methods are given in the table to compare the sensitivities. Other details of each study are also given in the following text.

Table 1.1. Various methods from literature for Bi determination

Method	**Sample**	**LOD, ng/L**	**Reference**
Spectrophotometric	water	170	18
ETAAS	water and soil	19	26
ETAAS	water, human hair, urine, tea	8.6	57
ETAAS	water, human hair, urine	20	27
ICPOES	human serum	120	28
ICPMS	water	4.7	32
ICPMS	body fluids	9.7	31
HG-AAS	urine and medicine samples	320	14
HG-AAS	natural water	12	58
HG-AAS	-	160	59
HG-AFS	jilin ginseng	43	39
HG-AFS	milk	10	38
HG-AFS	tea leaves	200	41
HG-ICPMS	lead sample	0.5	60
HG-ICPMS	natural waters	2.0	48
HG-ICPMS	-	5.0	50
ETV-ICPMS	sea water, human hair	0.2	51
RLS	pharmaceutical products	980	61
PSA	human hair, sea water, urine, blood serum	3220	52
SV	pharmaceutical products, urine and water	200	62
SV	water, human hair	104	63

With the introduction of more sensitive techniques, the use of spectrophotometric techniques has declined. However, in one spectrophotometric study, detection limit for Bi(III) was found as 0.17 µg/L ($8.0x10^{-10}$ M)[18] which is comparable to Graphite Furnace AAS technique.[64]

For trace level bismuth determination, sensitivity of FAAS is not sufficient. Without any preconcentration, detection limits are at mg/L. When microextraction[24] or trapping[23] was applied, detection limits were improved down to µg/L levels. Therefore, if the concentration is low in the sample and the sensitivity of the analytical technique is not sufficient, pre-concentration procedures are often necessary and useful.

ETAAS is sensitive enough to study Bi and most of the other elements at trace level. *Chamsaz and coworkers*[26] obtained the LOD value down to 19 ng/L Bi in water and soil samples by using Liquid Phase Micro Extraction (LPME) technique and coating the graphite surface with palladium or tungsten.[26] In another study by ETAAS, a novel ion-imprinted polymer was used for extraction of Bi(III) ions. $Pd(NO_3)_2$ was used as a matrix modifier and detection limit was found to be 8.6 ng/L Bi.[57] *Shemirani and coworkers*[27] applied $Pd(NO_3)_2$ as a chemical modifier and detection limit was calculated as 20 ng/L when cloud point extraction (CPE) method was applied to samples.[27] Low detection limits can be obtained by ETAAS but short lifetimes of the graphite tubes is a serious problem especially for heavy matrices.[65]

Although the sensitivity of ICPOES and ICPMS is better compared to FAAS, they are expensive instruments and most laboratories do not have these facilities.[15] In a recent study, cloud point Extraction (CPE) technique was used to separate Bi from the human serum samples. The detection limit for flow injection system was found as 120 ng/L Bi by using ICPOES.[28]

ICPMS is more sensitive than ICPOES for most of the elements. In addition, multi-element determinations have been carried out using ICPMS at low µg/L levels. The detection limit was obtained as 4.7 ng/L Bi.[32] In another study with the use of direct

injection nebulization (DIN) LOD was improved to 9.7 ng/L. Thallium (Tl) was used as an internal standard in order to improve calibrations for analysis of body fluids from rats by ICPMS.[31]

Hydride Generation Atomic Absorption Spectrometry (HG-AAS) is one of the sensitive analytical techniques which also do not require costly instruments. Moreover, HGAAS provides higher analyte transport efficiency and eliminates some of the atomization interferences.[66] One example was the determination of Bi in urine and medicine samples by HG-AAS. Interference effect of some ions was controlled using masking reagents. Detection limit was reported as 320 ng/L for Bi for standards.[14] In another study, LOD was found as 12 ng/L using Solid Phase Extraction (SPE) method and HGAAS have been applied for Bi determination in natural water samples.[58] *Kratzer et al.* used dielectric barrier discharge (DBD) atomizer in their study[59] and detection limit was 1100 ng/L which is worse than the one reported using Quartz Tube Atomizer (QTA) as 160 ng/L.[59]

HG-AFS technique is comparable to HG-AAS in terms of sensitivity. In addition, it can be superior to HG-AAS due to the capability of multiement analysis. Recently, *Guo and co-workers* developed a HG-AFS method for the determination of Bi and Sb simultaneously in jilin ginseng samples. Detection limit was 43 ng/L Bi.[39] Better detection limit was obtained by another study. Detection limit was 10 ng/L for calibration solutions and 11.8-288.8 ng/g Bi were included in milk samples analyzed.[38] Another multi-channel study was done for tea leaves samples. Detection limits for Bi was 200 ng/L (8.0 ng/g).[41]

By coupling HG with ICPOES or ICPMS, detection limit values are improved approximately one order of magnitude compared to pneumatic nebulization.[50] Multi-element determination capability of these techniques makes them superior over others previously mentioned. However, finding a common set of optimum hydride formation conditions for the elements studied is not an easy task. Therefore, sensitivity is sacrificed to study more than one element at the same time. First reported HG-ICPOES study was

done by *Thompson and co-workers* in 1978.[67] Since then a number of papers have been published on the area. In a recently reported study, Bi determination by HG-ICPOES, LOD was found as 160 ng/L in milk matrix. A continuous flow system was applied to milk samples and interferences were also studied.[46] In another study, the effect of ferricyanide as oxidizing agent on hydride formation of Bi, Pb and Sn elements was investigated. On-line addition of ferricyanide improved the hydride formation of Bi. Detection limit was 200 ng/L.[44]

For trace element determination of Bi in Pb standard solution, *Park* developed a HG-ICPMS method.[60] Before reacting with $NaBH_4$, Pb in the solution should be oxidized to metastable form Pb(IV). However, no oxidizing agent is needed for Bi case. Therefore, easier hydride forming property of Bi compared to Pb helps the separation of Bi from the matrix. By this way, spectral interference of $^{208}PbH^+$ was eliminated. Presence of 1000 mg/L Pb decreased the bismuthine generation efficiency about 40%. In order to solve this problem, standard addition method was used. Detection limit was 0.5 ng/L for Bi in the presence of 1000 mg/L Pb.[60]

In another study, a FI-HG-ICPMS method was developed for the simultaneous determination of Bi, Sb and Sn after Solid Phase Extraction (SPE). Detection limit for Bi was 2.0 ng/L.[48] In an earlier study by *Heitkemper and Caruso*, nebulizer-spray chamber system was used to enable simultaneous determination of volatile hydride forming elements in the presence of other elements that could not form hydride. Detection limit for Bi was 5.0 ng/L with this method.[50]

By using HG-ETV-ICPMS system very sensitive methods can be developed. *Xiong and Hu* proposed a method by combining headspace Pd(II) coated graphite bar microextraction (GBME) with ETV-ICPMS for the determination of trace Bi, Te and Se. The hydrides were trapped on coated graphite bar and then, graphite bar was inserted directly into the graphite tube. Under optimal conditions, detection limit of Bi was 0.2 ng/L. The proposed method was applied to seawater and human hair samples.

Concentration of Bi was found as 200 and 270 ng/g in two human hair samples and 54, 59 and 115 ng/L in three seawater samples.[51]

RLS technique can be used at nanogram detection level. By using different molecular probes, Bi(III) determination was performed in pharmaceutical products. Detection limits were reported as 980 ng/L[61] and 3220 ng/L.[52]

PSA technique has been recently used for Bi determination in pharmaceutical formulations, human hair, sea water, urine and blood serum samples. Sensitivity obtained by this technique is very close to that obtained by HG-coupled to atomic or mass spectrometry techniques. Carbon-nanotube modified paste electrode was used in this study and detection limit was 6.6 ng/L (3.17×10^{-11} M).[53]

Stripping Voltammetry (SV) is another electrochemical technique for Bi determination. In another study, a highly selective and sensitive carbon paste electrode modified with multi-walled carbon nanotubes was used for preconcentration and determination of trace amounts of Bi by differential pulse anodic stripping voltammetry. The limit of detection was 200 ng/L.[62] In the study by *Guo et al.* trace bismuth determination was based on the bismuth–bromopyrogallol red (BPR) adsorption at a carbon paste electrode. The overall analysis involved a three-step procedure: accumulation, reduction, and anodic stripping. The detection limit was found to be 104 ng/L (5×10^{-10} M) with a 3 min accumulation time.[63]

In solid environmental samples, Bi has been determined using ICPOES, ICPMS, AAS, electrochemical and molecular spectrometric techniques.[2]

1.3. Tellurium

Tellurium (Te) is a Group VIA element with an atomic number of 52. Chemical and physical properties of tellurium are similar to that of selenium. Pure tellurium exists as

brittle, silver-white crystals or as a dark gray or brown powder. Melting point and boiling point of of tellurium are 450 ºC and 990 ºC, respectively.[68]

Te is known as a non-essential toxic element. It is used in metallurgy in the production of iron, bronze, steel and glass, in pharmaceutical and electronics as a semiconductor. In addition, in industry it is employed as catalyst in batteries and fuel cells and as vulcanizing agent.[69,70]

Te is distributed widely in biological, agricultural, geological and environmental samples at trace level.[71] An average concentration of 27 ng/g tellurium in soil has been estimated based on samples from Australia, China, Europe, New Zealand and North America.[72] Concentration of tellurium ranges from 18 to 33 ng/g in Japanese plants located far from the mining area.[73]

Tellurium can be accumulated in the target organs such as nervous system, kidney, lungs and gastrointestinal tract.[74] If exposure exceeds the 2 mg/kg degeneracy of the organs is induced.[75]

After the Fukushima Daiichi Nuclear Power Plant accident in 2011, a large amount of radioactive isotopes of Te was released into the environment. Among the radioactive isotopes, ^{127m}Te, beta emitter, has a potential risk on human health since it is taken into the body via crop ingestion and it has a relatively long half-life ($t_{1/2}$=109 days). Plant to soil transfer factor (TF) of Te is needed to estimate the internal radiation dose, however, there are no data on the TF of radioactive Te for Japan.[76]

Some vegetables accumulate Te and because of the close similarity in chemical properties of Te, Se and S, Te displaces these two elements and inhibit their biological activities.[77] According to some studies, tellurium's toxicity, bioavailability and environmental transport mechanism are highly dependent on its chemical form and oxidation state. Tellurite (Te^{4+}) is 10 times more toxic than tellurate (Te^{6+}), and inorganic Te species are more toxic than organic Te species.[78,79]

The Food and Nutrition Board of the U. S. National Research Council suggested the daily intake of tellurium for the average adult is to be around 0.6 mg.[80]

1.4. Determination of Tellurium

Although Te occurs at trace level in nature, its use in many technological processes results in its local enrichment and release. Therefore, trace level Te determination is important.

Determination of Te is difficult since it is present at trace levels and pre-concentration/enrichment step is often indispensable. Coprecipitation is the one of the preconcentration techniques where metal and metal hydroxides such as $Fe(OH)_3$[81], $La(OH)_3$[82], arsenic[83] and Hg collector[84] have been used as co-precipitating agents .

Another preconcentration technique is use of solid phase extraction cartridge. Dowex 1X8 and XAD resins were used by *Pedro and co-workers* in drinking water.[85] Hollow fiber liquid phase microextraction (HF-LPME) was developed for simultaneous separation of Te and Se in environmental samples in another study.[86]

Online in-situ trapping of gaseous H_2Te in a preheated graphite furnace is another method for preconcentration. This system is called in-situ trapping HG-ETAAS. High sensitivity, reproducibility, low interferences and easy operation are the advantages of this technique. Sensitivity of the system was increased by applying a iridium modifier on graphite surface.[87]

Various methods have been applied for the determination of total Te up to now such as AAS[88], ETAAS[81,85,89], ICPOES[90], ICPMS[76,91,34], HG-AAS[92], HG-ETAAS[87], HG-AFS[82,93], HG-ICPOES[67,94], HG-ICPMS[95,96] and HG-ETV-ICPMS[51]. *Luo et al.* coupled hydride generation to chemiluminescence detection to develop a simple, sensitive method without interferences.[97] In addition, Spectrophotometric[98,99] and Stripping

Voltammetry [100,101,102, 103] techniques are available. Among them HG-AAS and HG-AFS have been widely used for Te determination in literature.[104]

Various methods for total Te determination and speciation in different samples are listed in Table 1.2. Detection limits of the methods are given in the table to compare the sensitivities. Other details of each study are also given in the following text.

Table 1.2. Different methods from literature for Te determination

Method	**Sample**	**LOD, ng/L**	**Reference**
ETAAS	tap water	66 and 7.0	85
ETAAS		40	89
ICPOES	water	150	90
ICPMS	soil and plant	^{125}Te: 3.7 ^{126}Te: 1.3	76
ICPMS	geological	^{126}Te: 0.5 ^{128}Te: 0.8	91
HGAAS	lead and lead alloys	2500	104
HGAAS	garlic	30	92
HG-ETAAS	sea water and sediment SRMs	100	105
HG-AFS	milk	15	106
HG-ICPOES	-	1320	94
HG-ICPMS	water SRM	^{125}Te: 6.0 ^{126}Te: 2.0	96
ETV-ICPMS	sea water, human hair	^{125}Te: 2.6	51
Speciation			
HG-AFS	cereal	Te(IV): 0.2 ng/g Total Te: 0.8 ng/g	107
HG-AFS	milk	Total Te: 21	93
HGAAS	sea water	Te(IV): 37	108
HG-ETAAS	water	Total Te: 2.2	109
HG-CL	water	Te(IV): 2000	97
Spectrophotometry	environmental and telluride film sample	Te(IV): 80	99
SV	water	Te(IV): 1.0	100

Pedro et al. compared two pre-concentration systems for ultra-trace Te determination in tap water by ETAAS. First approach was based on the on-line pre-concentration of the analyte onto a strong anionic resin (Dowex 1X8) employed as packaging material of a micro-column inserted in the flow system. 37% efficiency was obtained with an enrichment factor of 42 by this resin for a pre-concentration time of 180 s. Second set-up was based on the co-precipitation of tellurium with $La(OH)_3$ followed by retention onto Amberlite-XAD resin. For the same sample flow rate, 3.0 mL/min, 72% efficiency was found for a pre-concentration time of 180 s and enhancement factor was 25. Iridium was used as a matrix modifier. Detection limit was found 7.0 ng/L and 66 ng/L for first and second set-up, respectively.[85] In another study, $La(OH)_3$ was used for co-precipitation of Te. Considering a sample consumption of 25 mL, an enrichment factor of 10 was obtained; detection limit was 40 ng/L for this system.[89]

For Te determination ICP-OES can be preferred by some researchers although sensitivity is not as good as ETAAS. In one study, on-line analyte preconcentration system was coupled to ICPOES associated with flow injection and ultrasonic nebulization (USN). Preconcentration was done by coprecipitation with $La(OH)_3$ followed by collection on Amberlite-XAD4 resin and elution with nitric acid. A total enhancement factor of 140-fold was obtained with preconcentration. LOD was 150 ng/L for 10 mL preconcentrated solution of 10 ng/mL Te.[90]

For mass spectrometric analysis one example is given by sector field ICPMS (SF-ICPMS). SF-ICPMS is known with extremely high sensitivity, which is approximately 2 orders of magnitude higher than that of typical quadrupole ICPMS. ^{125}Te and ^{126}Te were monitored in one study due to the interferences on other isotopes. Rhodium was used as an internal standard. Detection limits obtained in medium resolution mode were 3.7 ng/L and 1.3 ng/L for ^{125}Te and ^{126}Te, respectively.[76] The method was applied successfully to soil and plant samples without any separation and pre-concentration.[76] In another study, quadrupole ICPMS was used for the direct determination of Te in geological samples. Ethanol was used as a matrix modifier to suppress interference of Xe and increase the

sensitivity. LOD for ^{126}Te and ^{128}Te were 0.5 and 0.8 ng/L with ethanol and 3.6 and 7.0 ng/L without ethanol, respectively.[91]

One research group compared HG-AAS and ETAAS techniques by coprecipitating Te with $La(OH)_3$ followed by collection on Amberlite-XAD4 resin and then, the eluent was directed to the atomizer. Considering a sample consumption of 25 mL, an enrichment factor of 10 was obtained. Detection limit was 30 ng/L and 40 ng/L for HG-AAS and ETAAS, respectively.[92] *Mesko et al.* developed a method for Te determination in lead and lead-alloys by FI-HG-AAS. Pb interference was eliminated by using small volume samples while Bi interference was overcome using thiourea as masking/releasing agent. However, interference effect of Ag could not be minimized. LOD was 2500 ng/L and LOQ was 1.0 µg/g by using 25 mg of sample in 50 mL sample solution.[104]

Another coupled system used in literature is HG-ETAAS for determination of total Te. In one of the early studies, a sensitive method was developed for the measurement of nanogram levels of Te with the reduction of Te (VI) species to Te(IV) by boiling the sample with a dilute HCl solution. The hydrogen telluride (H_2Te) was collected on Amberlite LA-2, a liquid anion exchanger. ETAAS with palladium coated platforms was used to determine Te. LOD for this system was 100 ng/L.[105]

HG-AFS technique has also been utilized for determination of Te. Ultratrace determination of Te with Se was studied in cow milk by HG-AFS. Te could be accumulated in milk via diet of the animal and it replaces essential Se because of the chemical similarity between Se and Te. Therefore, Te content in milk becomes important. For preparation of milk samples microwave assisted sample digestion was applied. KBr was added to samples before HG step. Detection limit was 15 ng/L. Concentration of Te in milk samples ranged from 1000 to 9700 ng/L.[106]

HG-ICPOES technique is useful for multi-element determination of hydride forming elements. *Grotti and co-workers* developed a method for the simultaneous determination of eight hydride forming elements; As, Sb, Bi, Ge, Sn, Se, Hg and Te. According to this

study, optimum hydride forming parameters in the presence of all these elements were not very different from the ones valid for single element Te hydride forming parameters. Te signal decreased approximately 35% at any wavelength in the presence of Hg at even 1:1 ratio. For simultaneous detection, LOD for Te was 1320 ng/L.[94]

Better sensitivities were obtained by coupling HG to ICPMS in which a modified spray chamber was used as gas-liquid separator. LOD for ^{125}Te and ^{126}Te solutions prepared in dilute HCl solution were 6.0 and 2.0 ng/L, respectively.[96]

By using HG-ETV-ICPMS system sensitive methods can be developed. For simultaneous determination of Te, Bi and Se, microextraction (GBME) was combined with ETV-ICPMS. The hydrides were trapped on using Pd(II) coated graphite bars and then the bar was inserted directly into the graphite tube. Under optimal conditions, detection limit of ^{125}Te was 2.6 ng/L. The proposed method was applied to seawater and human hair samples. Concentration of Te in two human hair samples were found as 23 and 21 ng/g and between 37 and 47 ng/L for seawater samples.[51]

Speciation of tellurium species is important since the level of toxicity of Te species is not same. One approach is ion chromatography-ICPMS system which is applied to urine, milk powder and rice flour samples.[110] The other one is to apply HG-AFS based on ultrasound assisted extraction to cereal samples.[107] While H_2SO_4 was used as an extractant, KBr was employed to reduce Te(VI) to Te(IV). Te(VI) does not react with $NaBH_4$ to form the corresponding hydride. Therefore, two step analyses were carried in speciation study. Samples must be analyzed without pre-reduction, in order to determine Te(IV); then, the sample must be treated with KBr to achieve a quantitative reduction of Te(VI) to Te(IV) present in the sample. The results of the second analysis give the total concentration of Te(IV) and Te(VI) while the first one gives the concentration of Te(IV) only. Then, Te(VI) concentration can be calculated by the difference between the two analysis performed. Detection limits of Te(IV), Te(VI) and total Te were 0.2, 0.5 and 0.8 ng/g, respectively. According to analysis results, concentration of Te(VI) was higher than that of Te(IV) in the all the cereal samples analyzed. Total Te concentration was

found in the range of 1.00 to 19.8 ng/g.[107] Another study with HG-AFS was developed for milk samples.[93] After batch leaching of Te by sonication with aqua regia, one portion treated with KBr in microwave oven for Te (IV). Other portion was directly used for hydride generation step to determine total Te. For batch mode, detection limits for instrument and sample were 21 ng/L and 0.52 ng/g in terms of total Te. Concentration of Te(IV) ranged from 0.6 to 6.5 ng/mL while Te(VI) levels were between 0.4 to 4.0 ng/mL. Results of the study showed that in all samples free Te (IV) was the dominant species.[93] This result is in conflict with the report by *Reyes and co-workers*.[107] Therefore, depending on samples the species with the higher concentration may change.

In our group, a mercapto-modified silica microcolumn was used for selective separation and preconcentration of Te(IV) from water samples. Preconcentration and separation was followed by HGAAS analysis. LOD for Te(IV) in sea water with a preconcentration factor of 50 was 37 ng/L.[108] Another study in our group was carried out using in situ HG-ETAAS. Hydrides of Te(IV) were trapped in ruthenium or palladium coated graphite tubes. LOD values were 6.4 and 2.2 ng/L for Pd and Ru treated ETAAS systems with trapping totally 9.6 mL sample, respectively.[109]

Although it is not common, Hydride Generation-Chemiluminescence (HG-CL) methodology was developed for the determination of Te(IV). Strong chemiluminescence emission can be obtained during the reaction between hydrogen telluride (H_2Te) and luminol in basic medium. Interfering effect of foreign ions were also studied and LOD was calculated as 2000 ng/L for Te(IV).[97]

For spectrophotometric determination of Te(IV) *Suvardhan and co-workers*[99] proposed three simple, rapid and sensitive methods. The first method is based on the formation of purple colored complex by oxidizing4-bromophenylhydrazine (4-BPH) with tellurium in a basic medium and coupling with N-(1-naphthyl)ethylenediamine dihydrochloride (NEDA) as complexing agent. For the second method, oxidation of 3-methyl-2-benzothazoline hydrazine hydrochloride (MBTH) with tellurium in a basic medium was followed by coupling with chromotropic acid (CA) to yield a red-colored species. In the

last method, orange-colored complex formed by oxidation of 2,3-dimethoxystrychnidin-10-one (2,3-DMSO) by tellurium in acidic medium. Under optimized conditions, detection limits were 150 ng/L for 300 µL (4-BPH-NEDA method), 100 ng/L for 250 µL (MBTH-CA method) and 80 ng/L (2,3-DMSO method) for 100 µL volume of Te(IV) solution.[99]

All types of stripping voltammetry which are anodic[111], cathodic[100,101] and adsorptive[112] were used to determine Te. In a t study, *Zong and Nagaosa* proposed a method for the determination of Te(IV) by Cathodic Stripping Voltammetry. This method was based on the reduction of Te(IV) with Bi(III) onto pyrolytic graphite electrode, followed by a cathodic potential scan. Well-defined catalytic hydrogen wave resulted from the reduced Te. LOD for Te(IV) was found as 1.0 ng/L when deposition time was 30 s.[100]

1.5. Hydride Generation

Hydride generation (HG) has been applied for more than 100 years for the determination of arsenic in methods called as the Gutzeit test or Marsh reaction. Around 1970, combination of HG to AAS was introduced to overcome problems in the determination of arsenic and selenium with flame AAS[117]. Due to the advantages of HG, the method has been applied to all hydride forming elements namely arsenic (As), selenium (Se), and antimony (Sb), bismuth (Bi), tellurium (Te), germanium (Ge), lead (Pb), mercury (Hg), cadmium (Cd) and tin (Sn) which are mostly Group IVA, VA and VIA elements. Although they are not popular, indium (In) and thallium (Tl) can form hydrides. Nomenclature and some chemical information about volatile hydrides are given in Table 1.3. below.[113,114,115]

Table 1.3. Nomenclature and some chemical properties of volatile hydrides.

Analyte	Formula	Name	Melting Point, ºC	Boiling Point, ºC	Solubility in water (µg/mL)
As	AsH_3	Arsenic hydride, arsine	-116.3	-62.4	696
Bi	BiH_3	Bismuth hydride, bismuthine	-67	16.8	-
Ge	GeH_4	Germanium hydride, germane	-164.8	-88.1	Insoluble
Pb	PbH_4	Lead hydride, plumbane	-135	-13	-
Sb	SbH_3	Antimony hydride, stibine	-88	-18.4	4100
Se	SeH_2, H_2Se	Selenium hydride, hydrogen selenide	-65.7	-41.3	37700-68000
Sn	SnH_4	Tin hydride, stannane	-146	-52.5	-
Te	TeH_2, H_2Te	Tellurium hydride, hydrogen telluride	-51	-4	Very soluble

Hydride generation, which is a gas-phase sample introduction method, became very popular due to several advantages. It requires simple and low cost apparatus. In addition, this method provides preconcentration and separation of the analyte from the sample matrix. This property results in higher sensitivity with a suppression of interferences during atomization. Other advantage is its ability to perform speciation analysis of hydride forming elements.[116] On the other hand, although interferences are still encountered; however, it is easier to minimize the interferences as compared with graphite furnace or flame AAS.[113]

In earlier studies, metal/acid combination, mostly Zn/HCl was used to produce *nascent hydrogen* for analyte reduction to hydride.[117] Reactions are as follows:

$$Zn + 2H^+ \rightarrow Zn^{2+} + 2H \qquad [1]$$

$$A^{m+} + (m+n)H \rightarrow AH_n + mH^+ \qquad [2]$$

m and n represent the valency of analyte A in the sample solution and in hydride.

For hydride generation, the reaction is carried out in acidic medium and tetrahydroborate (BH_4^-) ion enroll as reducing agent. First application was reported by *Braman and co-workers* who determined trace mercury[118], arsenic and antimony[119] by atomic spectrometry. Related reactions are given below:

$$BH_4^- + 3\,H_2O + H^+ \rightarrow H_3BO_3 + 8H \qquad [3]$$

$$A^{m+} + (m+n)H \rightarrow AH_n + mH^+ \qquad [2]$$

Reaction mechanisms for both Zn-acid and BH_4^-/acid systems were proposed firstly by *Robbins and Caruso* in 1979 and called as ‘’nascent hydrogen’’ mechanism.[120] However, from thermodynamic point of view reactions [1] and [3] cannot generate atomic (nascent) hydrogen.[121] Moreover, the mechanism was re-designed by deuterium-labeled experiments on hydrolysis of BD_4^- and it was concluded that nascent hydrogen cannot be the intermediate causing the formation of molecular hydrogen as the final product of tetrahydroborate hydrolysis.[122]

D’Ulivo and co-workers investigated the HG mechanism by using different metal hydride formation on the basis of deuterium-labeled experiments and the properties of the borane (BH_3) complex. Isotopic compositions of metal hydrides formed with $NaBD_4$ and $NaBH_4$ were determined by Gas Chromatography-Mass Spectrometry (GC-MS). As a conclusion, they proposed a mechanism based on the direct transfer of hydrogen taking place via ‘analyte-borane complex’ (ABC) intermediates.[123] In the hydrolysis of BH_4^- in acidic medium, four different hydroboron intermediates are formed which are $H_2O\text{-}BH_3$, $H_2O\text{-}BH_2OH$, $H_2O\text{-}BH(OH)_2$ and $B(OH)_3$. Then, these hydroboron intermediates react with metal ion to form metal hydride. Reactions are given below.

$$BH_4^- + H_2O + H^+ \rightarrow H_2O\text{-}BH_3 + H_2 \qquad [a]$$

$$H_2O\text{-}BH_3 + H_2O \rightarrow H_2O\text{-}BH_2OH + H_2 \qquad [b]$$

$$H_2O\text{-}BH_2OH + H_2O \rightarrow H_2O\text{-}BH(OH)_2 + H_2 \qquad [c]$$

$$H_2O\text{-}BH(OH)_{2+} + H_2O \rightarrow B(OH)_3 + H_2 + H_2O \qquad [d]$$

$$BH_4^- + 3H_2O + H^+ \rightarrow B(OH)_3 + 4H_2 \qquad \text{Overall reaction}$$

M^{+n} + hydroboron intermediate $\rightarrow$ MH_x

M^{+n} : donor metal, MH_X : metal hydride

When pH of the medium is between 3.8 and 14, tetrahydroborate decomposition is a second order reaction with the rate constant 1.22 x 10^8 $mol^{-1}L\ min^{-1}$ at 30 °C. If pH ≤ 1, BH_4^- decomposition to boric acid (H_3BO_3) and hydrogen is complete within a few microseconds.[124,125] Mostly sodium and potassium salt of tetrahydroborate is used. It is dissolved in water and stabilized by potassium or sodium hydroxide. Optimum concentration of BH_4^- depends on the analyte element and type of hydride generator used. HG can be performed in batch, continuous flow (CF) or flow-injection (FI) modes.[113]

1.5.1. Interferences in Hydride Generation

Interferences in HG are divided into two classes: Spectral and non-spectral. Spectral interferences resulted from absorbed radiation by species other than free atoms of analyte at the specified wavelength for AAS measurement. Some non-spectral interferences occur in both liquid and gas phases resulting from mutual hydride-forming elements, transition metals and acids used for sample digestion. Interferences take place during the formation of the hydrides in solution phase, the separation of gaseous and liquid phase in GLS and atomization.[126] Non-spectral interferences are classified as liquid and gas phase interferences in HG.

Liquid phase interferences can take place either during hydride formation or its transfer from the solution due to differences in hydride-release rate. Liquid phase interferences can be divided into two basic groups: compound and matrix interferences. The reason of the compound interference is due the differences in oxidation state or chemical environment of the analyte in the sample and standards.[113] In case of matrix interference, hydride formation and release efficiencies are affected by matrix. Formed volatile species of concomitant ions transported to the atomizer by aerosols generated during HG have resulted in spectral and/or non-spectral interferences.[127]

On the other hand, *gas phase interferences* result from a volatile species either hydride or other compounds or liquid spray which is produced in hydride generator. There are two types of gas phase interferences; transport and atomization interferences. Delay or loss of the analyte hydride in the path between generator and atomizer causes transport interference.[113] Atomization interference is related with the mechanism of hydride atomization and transfer of the analyte vapor in atomizer. This type of interference causes reduction in atomization efficiency [113, 128]

The most common way of eliminating spectral interference is to select the other wavelength of the analyte. For the elimination or minimization of matrix interferences the general way is dilution of the sample or applying standard additions method. However, these approaches may not be helpful to solve the interference if the interferent concentration is high or analyte concentration is low. There are alternative ways to control matrix interferences in HG. For instance, changing the acid medium reduces the transition metal interferences drastically.[129,130] Apart from the acid type, concentration of acid and reducing agent, BH_4^- is important. Combination of high acid and low BH_4^- was found to reduce interference from transition metals.[131] Moreover, for mutual hydride forming elements using releasing agent suppressed the interfering hydride.[126] Another procedure for removal of transition element interferences is precipitation of transition metals by using precipitating agents. Cd, Co, Cu and Ni interferences were eliminated by precipitation as hydroxides[132] while iodides were used for Cu and Pb.[133] Liquid phase interferences of transition metals can be controlled by using the masking agents. Depending on the matrices different masking agents have been used. L-cysteine[134], L-histydine[135], 1,10-phenantroline[136], thiourea[137] are among the complexing agents used to mask interfering metal ions present in the range of 1-100 mg/L in sample solution. *Anderson et al.* used thiourea to reduce As species and to control interferences from transition elements on As.[138] Lastly, oxidizing strong acids convert the hydride forming element into its higher oxidation state. This situation results in low HG efficiency. As an example, thiourea has been used to eliminate the effect of HNO_3 on As and Sb signals.[139]

1.6. Hydride Generation Coupled to Plasma Spectrometry

Hydride generation combined with atomic absorption spectrometry (HGAAS) has become a well-established technique in literature since this technique does not require expensive spectrometers for detection and has lower detection limits.[15] In addition to HGAAS, HGAFS has been preferred by researchers due to its wide linear dynamic range, low noise level, high sensitivity, speed of analysis, ease of operation and low cost.[140,79,141,142]

Researchers combined HG technique also with plasma spectrometry to make multi-element determination (more than four elements is possible) with sub-part per billion levels, using HG-ICPOES and HG-ICPMS. Furthermore, plasma sources for atomization provide freedom from gas-phase interferences due to very high atomization and excitation temperatures of the plasma discharges.[143] One additional advantage of HG-plasma technique over HGAAS is wider linear range. Simultaneous determination of up to four elements has been shown however, problem for multi-element detection with this method is to find optimum hydride forming conditions.[45]

In an early study, simultaneous determination of As, Sb, Bi, Se and Te was performed with HG-ICPOES. Following the formation of hydrides, they were transported directly to the plasma by Argon carrier gas. Limit of detection values of 1000 ng/L or lower for aqueous solutions of the elements were obtained after optimizing the parameters for all elements simultaneously. Improvements in detection limits of elements compared to nebulization ICPOES was between 17 and 550 for the elements studied.[67,144]

Wolnik and co-workers have expanded the HG-ICPOES technique by using a “tandem nebulization system” which allows continuous hydride introduction simultaneously with sample aerosol introduction.[145] After this study, *Huang et al.* developed a “cyclone nebulizer-hydride generator system”. With this system, detection limits of ICPOES were improved more than 20-fold for hydride forming elements without affecting those for non-hydride forming elements.[146]

Simultaneous determination of As, Sb, Bi, Ge, Sn, Se, Te and Hg was studied by HG-ICPOES. All analytes can be reasonably determined together with other elements with satisfactory analytical performances. In this study, it was found that only Te and Hg mutually interfere even at 1:1 analyte interference ratio. Detection limits were 130, 1320, 130, 140, 610, 1620, 190 and 210 ng/L for Bi, Te, As, Sb, Ge, Sn, Se and Hg, respectively.[94]

Another HG-ICPOES study proposed a method for simultaneous determination of Bi, Sb and As by using different types of borane and acids. According to results, THB (tetrahydroborate) and HCl couple was the best among others. The reaction between THB and HCl was very fast and led to the formation of the hydrides with high efficiency. LOD's obtained by this couple were 1000, 530 and 1500 pg/g for Bi, Sb and As, respectively.[147,148]

Potassium ferricyanide, $K_3Fe(CN)_6$ was used for simultaneous generation of BiH_3, PbH_4 and SnH_4 in one of the studies by HG-ICPOES. It was used to achieve optimum signals and stability in hydride generation. Mechanism of ferricyanide in the generation of different element hydrides was discussed. Detection limits for Bi, Pb and Sn were 200, 130 and 100 ng/L, respectively. This method was used for biominerals analysis.[44]

In HG-ICPOES studies, interference effect of transition metals was also evaluated. AsH_3, SnH_4, BiH_3, SbH_3 and GeH_3 generation decreases as the concentration of Zn(II) in the matrix was increased. To remove this interference effect, L-cystine and L-cysteine was used to mask the interferent ions. Then, detection limits in the presence of 30% (w/v) $ZnSO_4$ solution were 3000, 3000, 8000, 2000, 3000, 2000 and 38000 ng/L for As, Bi, Ge, Sb, Se, Sn and Te, respectively. Sensitivity of the Te was worst among the other with a poor precision of 30% when 100 μg/L Te solution was used.[45]

First reported HG-ICPMS study was performed for the determination of As in 1983 by *Date and Gray.*[149] Following that work, many researchers have used HG-ICPMS since

ICPMS is a powerful analytical technique with better sensitivity and lower detection limits (sub-ng/mL).

Gas-liquid separator is used for HG studies to allow the formed gaseous hydrides to be separated from the liquid matrix. In one of the studies, scientists used conventional nebulizer/spray chamber system to separate the gaseous hydrides from the reaction mixture.[50] Then, gaseous reaction products as well as liquid aerosols were directed to the plasma with the argon carrier gas. With this system, researchers aimed simultaneous determination of volatile-hydride forming elements and others. As, Se, Sb, Te and Bi elements were the hydride forming analytes in this study. Detection limits obtained by HG-ICPMS were 5.0, 34, 31, 170 and 17 ng/L for ^{209}Bi, ^{130}Te, ^{121}Sb, ^{78}Se and ^{75}As, respectively. Improvements in detection limits of elements compared to nebulization and hydride generation was between 4.7 and 9 fold in this early work. Again, due to difficulty to find a set of optimum hydride formation conditions for multi-element detection, Pb could not be determined. Interference effect of Cu, Co and Ni on studied elements was investigated. It was found that 1.0 mg/L Cu suppressed the hydride signal of Bi, Te and Se ca. 80% while it caused 30% signal loss for Sb. On the other hand, the effect of Co and Ni at 1.0 mg/L level was minimum for all elements studied.[50]

Hall and co-workers compared the performances of HG-QTAAS and HG-ICPMS for determination of Bi, Te and Se in geological reference materials. As it is expected detection limits using HG-ICPMS were better than that of HG-QTAAS. Method detection limits were 10 ng/g for three elements by HG-QTAAS and they were improved to 1.0 ng/g for ^{209}Bi and ^{130}Te and 6.0 ng/g for ^{78}Se by HG-ICPMS. Furthermore, it was proven that mutual interferences in HG-QTAAS are worse especially for elements with low natural abundance such as Te. Magnitude of Te signal decreased to 50% when As was present in the solution at 300-fold excess level compared to Te concentration. Therefore, HG-ICPMS is clearly the preferred method especially for determination of Te in complex matrices.[49]

For simultaneous determination of Bi, Sb and Sn from natural waters, FI-HG-ICPMS system was developed. Solid phase extraction was applied by inserting the mini-column for cations in the injection valve of flow manifold. L-cysteine was used as an efficient pre-reducing and masking agent. Detection limits obtained after pre-concentration step were 2.0, 11 and 142 ng/L for ^{209}Bi, ^{121}Sb and ^{120}Sn, respectively.[48]

In recent study, *Chen et al.* developed a FI-HG-ICPMS method for trace element determination of six elements, which were Bi, Sb, Hg, As, Ge and Cd, in cosmetic lotion. Slurry sampling technique was applied without dissolution and mineralization. Thiourea was used as a masking agent. Since the sensitivities of the analytes in the slurry and in aqueous solutions were different, standard addition and isotope dilution methods were used. Instrument detection limits for ^{209}Bi, ^{74}Ge, ^{75}As, ^{111}Cd, ^{121}Sb and ^{201}Hg were 0.6, 0.5, 2.0, 4.0, 2.0 and 3.0 ng/L, respectively. In terms of sample, detection limits were found between 25 and 200 pg/g. [47]

1.7. Tungsten Coil Atom Traps

Traditionally, heated quartz cell was used as atomizer to decompose the forming volatile hydrides to yield free atoms. In the following years, graphite furnaces were also used extensively for this purpose. In recent years, tungsten coils or filaments have appeared as a good alternative to the previous atomizers. Tungsten coil is inexpensive and relatively chemically inert. It is obtained easily from a commercial visible tungsten lamp. W-coil requires a simple power supply.[150] Other advantages of W-coil are fast heating rate (>10 K ms^{-1}) with low power supply and low specific heat (0.133 J g^{-1} K^{-1}). It cools very fast. Therefore, it does not require any external cooling system unlike quartz cells. One drawback of W-coil is requirement of isothermal condition since it is an open atomizer.[151] It is severely affected by interferences. This problem can be solved with the use of a preliminary preconcentration step.[65]

In addition to its atomizer role, W-coils can be used as an electrothermal vaporizer[152] and a trap for in situ preconcentration of hydrides. Gas phase trapping of analyte has

become very popular due to its extremely high sensitivity. Another advantage of in situ trapping is elimination of the gas phase interferences from other hydride forming elements by choosing an optimum trapping temperature.[153] Moreover, some atomization interferences are avoided by trapping technique.[66]

Up to date, Slotted Quartz Tube Atom Trap (SQT-AT), quartz or metal traps and graphite tube have been used as atom traps to enhance the signal. SQT-AT is suitable only for AAS while others can be easily adapted to ICPOES, ICPMS and AFS techniques. Furthermore, quartz or metal traps have been used with vapor generation techniques.[150,154] Some quartz particles are placed in the inlet arm of a quartz tube atomizer and they serve as a trap. As metal traps molybdenum strip[155] and externally heated Au wire[153] have been used. Although graphite tube is still preferred in situ hydride trapping device, it is costly.[156]

The use of W-coil in analytical atomic spectrometry dates back to 1972[157] when it was used as an atomizer alternative to graphite furnace.[158,159,160,161] Role of W-coil as a trap for determination of hydride forming elements at ng/L level has continued since their introduction in 2002.[15,162]

Our research group has been working with W-coil traps since 2002; *Cankur et al.* developed a method for BiH_3 by trapping it on resistively heated W-coil and coupled to AAS. In this work, bismuthine was trapped on a W-coil previously heated to 270 ºC. Then, analyte species were re-volatilized by increasing the temperature to 1200 ºC and transported to an externally heated silica T-tube with the help of argon and hydrogen mixture. Here, there are two reasons for usage of hydrogen gas. First, H_2 prevents the oxidation of the W-coil by creating a reducing environment. Second reason is to improve the re-volatilization efficiency of Bi species from the trap. Detection limit of the method was 2.7 ng/L when 18 mL sample volume was used (for 3 min trapping) and enhancement factor was found as 150 compared to FI-HGAAS when LOD values were compared.[15] In another study, interference studies were done in detail both with and without trap for Bi determination in our research group. According to this study, trap

was useless to eliminate liquid phase interferences since liquid phase interferents took place before trap medium. However, interference effect of Au, Mn, Zn, Se, As, Na, Cu, PO_4^{3-}, SO_4^{2-} and Cl^- on Bi signal was reduced when W-trap was used. It means interferences from these elements and ions were generated in gas phase. Detection limit was 25 ng/L when 8 mL sample volume was used during 1 min. With trap system enhancement factor for LOD was found to be 19.[163]

A study by *Hou et al.* was first on the use of Iridium (Ir) coated W-coil for determination of Se by AAS. W-coil surface was coated with Ir as a permanent chemical modifier in this study. Coating permits operating at higher temperatures and life time of coils was increased. In addition, sensitivity and dynamic range of the method was improved.[158]

In another study for Bi determination, W-coil was coated with Pd, Rh, Pt or Ir. Among these chemical modifiers, Ir gave the best trapping efficiency. Then, Bi was determined by AFS following the online trapped on Ir-coated W-coil. With a 120 s trapping time (12 mL sample volume) LOD was 4.0 ng/L. Enhancement factor was found as 23 compared to LOD of HG-AFS. Results of interference study showed that gas-phase interferences minimized due to using W-coil trapping. In addition, 73% trapping efficiency was obtained.[156]

Lifetime of an individual W-coil is an important parameter in W-coil studies. Since oxidation of W-coil takes place, sensitivity of the system declines by time. In optimum conditions, W-coil is used at least 100 times. Moreover, H_2 flow rate affects the lifetime of the coil. Lower flow rates shorten the lifetime of W-coil.[163] In one study, effect of suction rate of waste in gas-liquid separator on Bi signal was also evaluated. It was noticed that increase in suction rate causes a decrease in Bi signal.[163]

Another pioneering W-coil trap study was performed by *Barbosa and his coworkers*[162] in 2002 when *Cankur and coworkers*[15] proposed their work. In the former work, Rhodium (Rh) coated W-coil was used effectively both as hydride collector and electrothermal atomizer for Se determination at ng/L level by AAS. For 60 s trapping

period at a flow rate 2.5 mL/min LOD was 50 ng/L and enrichment factor was 200 in terms of LODs. The coil lifetime was extended to at least 2000 firing at 2300 ^{o}C.[162]

In our group, gold-coated W-coil trapping HG-AAS was used for Se determination.[164] Coating solution was prepared by dissolving the pure gold wire in aqua regia. Gold coating provides convenient trapping and releasing which are very important for trap material. Without coating no Se signal was obtained. After hydrogen selenide was formed, it was collected on gold-coated W-coil at 165 ^{o}C. Temperature was increased to 675 ^{o}C for revolatilization and then analyte species were transported to T-tube where atomization takes place. For 27.0 mL sample with a collection time of 4.0 min, detection limit was 39 ng/L. Enhancement in detection limit compared to conventional hydride generation was 6.7.[164]

Souza et al. used Rh coated W-coil for the determination of Se and As in biological and water certified reference materials by ETAAS.[151] SRM-1577a, SRM-1577b bovine liver, RM-8414 bovine muscle powder, A-13 animal blood and SRM-1640 trace elements in natural water were analyzed. Hydride trapping period was 30 s and detection limits were found 35 ng/L and 110 ng/L for Se and As, respectively. Enrichment factor for Se and As was 150 and 95, respectively. In this study, Rh-coated coil used for at least 250 firing without losing its sensitivity.[151]

Tellurium hydride was trapped for the first time on Pt-coated W-coil and then flame AAS was used for atomization of tellurium species released from the coil.[165] It was observed that un-coated W-coil could hardly trap tellurium hydride whereas coating significantly improved the trapping efficiency. Many noble metal coatings such as Pd, Mo, Au, Rh, Ta, Re, Ir and Pt were investigated in this work. Signal increased significantly with Pt-coated W-coil comparing to others. LOD of 80 ng/L was obtained with 1.0 min trapping using 1.5 mL sampling volume and enrichment factor was 28 as compared to HGAAS.[165]

The use of Ir-coated W-coil for in situ trapping of stannane was studied by *Alp and Ertas*. The limit of detection for 6.0 mL sample with a collection time of 60 s was found to be 65 ng/L.[166]

Other W-coil trap studies by our research group was completed for determination of Cd[167] using cold vapor AAS and for determination of Sb[168] using AAS. *Cankur and Ataman*[167] used resistively heated W-coil as an online-trap for preconcentration and revolatilization of Cd vapor generated using $NaBH_4$. Then, analyte species directed to unheated quartz T-tube absorption cell. By using the optimum parameters, obtained LOD was 4.0 ng/L using a 4.2 mL sample volume for 2.0 min trapping period. Enhancement in detection limit was 25 as compared to FI-HGAAS. In a study for Sb determination, experimental parameters were optimized with and without trap experimental conditions.[168] LOD for the system was 16 ng/L when 36 mL sample was collected for 4.0 min. Enhancement factor in detection limit was calculated as 14 compared to no-trap experiment.[168]

In a recent study, *Chen et al.* have reported the use of on-atomizer trapping to determine Cd. In this design there was a quartz tip between the end of gas transfer line and glass cell in which W-coil was inserted. Volatile Cd species which left the GLS were directed to the quartz tip that was manually inserted into the glass cell. Before atomization step GLS and atomizer connection was disconnected by removing this tip. For 5.0 mL sample volume LOD was calculated as 3.0 ng/L. LOD with this system was improved 66-fold compared to conventional direct injection W-coil AAS.[169]

In W-coil trap studies, there are different definitions for the enhancement factor. In the first approach ratio of LOD values with and without trap of the analyte is used. This is an acceptable definition since both the slope of the calibration plot (calibration sensitivity) and repeatability of the system are considered. In second approach *enhancement factor, E,* is calculated by taking the ratio of characteristic concentration (C_o) values for the systems with and without trap. C_o is expressed as the concentration of an element which is required to produce a 1% absorption (0.0044 absorbance) signal. E

is a better way for comparison since it is independent of the conditions of the spectrometer, the intensity and noise level of the source beam.[150] However, C_o definition is applicable only for AAS measurements. For other techniques such as ICPOES and ICPMS first approach is usually used to determine enhancement factor. *Dedina* has proposed *procedure sensitivity* which is proportional to the reciprocal of the characteristic concentration.[128] Procedure sensitivity is defined as peak height absorbance per unit concentration. When it is applied to trap studies, ratio of peak height absorbance for conventional HGAAS to that for trap signal is used.[128] Peak height measurements are used for trap studies. Since overall trapping efficiency is not 100%, peak area measurements will not be meaningful for correct comparison.[150] *Ataman* proposed more than one enhancement factor definition to show the ability of the analytical system independent from sampling time and volume. These terms are helpful when sample or time is limited.[150] These definitions are the followings:

E: Enhancement factor (ratio of characteristic concentrations)
E_t: E/ minutes of sampling, unit: min^{-1}
E_v: E/milliliters of sample, unit: mL^{-1}
E_{max}: Maximum enhancement factor

Enhancement can never be infinitely increased even larger sample volumes or longer times were used for trapping. Saturation of the trap surface by analyte or interferent species put a practical limit for further enhancement. Therefore, E_{max} term is needed. It is an experimentally defined value and depends on analyte concentration and matrix composition.[150]

W-coil trap can be adapted to plasma techniques such as ICPOES and ICPMS by providing an opportunity for more sensitive system. Presently, there is no application of W-coil trap to plasma spectrometry.

1.7.1. Trapping Efficiency

In trap studies, sensitivity depends on the magnitude of trapping efficiency. 100% trapping efficiency can never been reached due to incomplete release of analyte species from the trap surface and the loss of volatile species on the surface of tube walls or vent of atomizaton device. There are two ways to calculate trapping efficiency. In one of the definitions where AFS was used, *Liu et al.* expressed trapping efficiency by rationing the peak area signal of trapped analyte (S_t) per trapping time to analyte signal obtained by conventional hydride generation (S_c) per sampling time as shown in the following formula.[156]

Trapping Efficiency, % = $[(S_t/t_{trapping}) / (S_c/t_{sampling})] \times 100$

The other definition made by *Ataman* is based on peak area measurements. To compute overall trapping efficiency, the ratio of peak area for transient signal to that obtained from conventional HGAAS signal is used.[150] Therefore, in this definition overall trap efficiency includes not only trapping but also revolatilization and transport efficiencies. When all conditions such as atomization and gas flows are same for with and without trap experiments, comparison of peak areas may give the meaningful overall trap efficiency.[150]

Dedina and Kratzer reported their approach to calculate the trapping efficiency. They used a quartz surface to trap As and Se. Gas flow compositions and flow rates were same for both conventional HGAAS and trap experiments. They reported total trapping efficiencies as 50% and 70% for As and Se, respectively[170] while 99% was reported for Bi.[171]

1.8. Inductively Coupled Plasma Mass Spectrometry - ICPMS

All types of mass spectrometers consist of three main parts which are ion source, mass analyzer and the ion detector. In order to minimize the collision of analyte ions with

other molecular ions during their transport from ion source to detector mass spectrometers are operated under low pressure.[172,173]

The role of ion source is to ionize analyte species. Many ionization techniques are employed in mass spectrometers. While some ionization techniques are very energetic and cause extensive fragmentation others are softer and only produce ions of the molecular species.[174] Inductively Coupled Plasma (ICP) is one of the ion sources. Temperature of plasma is about 10000 K. ICP source consists of a torch and load coil. Torch is made up of three quartz concentric tubes in which plasma gas and analyte aerosols pass through. Torch is surrounded by a cooled load coil. The plasma is fed by radio frequency (RF) energy applied to load coil. RF generator produces RF energy between 1.5 and 2.5 kW at 27 or 40.68 MHz typically. Flowing argon gas at atmospheric pressure is initially made electrically conductive by a Tesla spark which lead to ionization of the gas. Then, produced ions and electrons interact with the high-frequency oscillating inductive field created by RF current in the coil. They are accelerated, collide with argon atoms and ionize them. This process continues until argon ionization process is balanced and colliding species cause heating of the plasma. For thermal isolation high Ar flow is introduced from the outer quartz tube.

Sample is directed to the hot plasma as a vapor or finely divided aerosols by argon gas through different sample introduction techniques. Then, at high temperatures, desolvation, vaporization, atomization and also ionization of the sample take place rapidly.[174] Sample spends approximately 2 ms in the plasma. Ions extracted from plasma are introduced to the low pressure mass analyzer through the interface region. This region includes two metallic water cooled metal cones which are the sampler and skimmer cones. Orifices of the cones are less than 1 mm in diameter. Low pressure allows the use of focusing devices which provide the transport of ion beam with maximum efficiency to the mass analyzer.[173] The region between the sampler and skimmer cone is maintained at a moderate pressure of 1-2 Torr while pressure behind the skimmer cone is at approximately 10^{-6} Torr. Vacuum is maintained by means of turbo molecular pumps. Ions extracted from the interface region are then focused into

the mass analyzer by a series of electrostatic lenses. These lenses also prevent reaching of photons, particulates and neutral species to detector.[175]

Mass analyzer is used to separate produced ions according to their mass to charge ratio (*m/z*). Some mass analyzers use static or dynamic electric and magnetic fields alone or in combination to provide separation. They are divided into different groups, such as magnetic or pure electric, scanning or nonscanning and trapping or non-trapping analyzers.[173,174]

Quadrupole mass analyzers are used commonly in ICP instruments. It is made up of four parallel stainless steel rods which are arranged symmetrically. Quadrupole employs combination of direct current (DC) and a time-dependent alternating current (AC) of radio frequency applied on opposite pairs of these four rods. Opposite rods are connected electrically in pairs. The same magnitude but opposite sign potential is applied to two pairs. Positive ions which are accelerated over a potential of 5 to 20 V enter the analyzer region between the rods. Depending on the applied DC and AC, only ions with suitable m/z can have stable trajectories through the quadrupole. Other ions collide to rods, discharge themselves and never reach to detector. Therefore, in order to allow the selected mass to reach detector, optimum AC/DC ratio is adjusted for each pair of rods.[173, 175, 176]

Other common mass analyzer is time-of-flight (TOF). TOF analyzer separates ions according to time difference between a start signal and the pulse generated when an ion hits the detector. After their initial acceleration by an electric field ions drift in a free-field region, which is flight tube, according to their velocities. Ideally all ions with the same charge have the same kinetic energy when they leave the acceleration region. However, they have different velocities depending on their masses. The faster or lighter the ion, the shorter the time of flight to the detector. The analysis speed of TOF analyzers is very fast and a spectrum over a broad mass range can be obtained in micro-seconds. Using flight tube with a length of 1 to 2 m and acceleration voltage of at least 20 kV can improve sensitivity.[173,174]

Once ions reach to the ion detector, ion intensity is converted to current. In turn current is converted to digital signal by using analogue to digital (AD) cards. Ions strike the detector and the energy from the impact causes emission of electrons. The number of generated particles is directly related with the energy and/or the velocity of the ions.[173] There are two classes of ion detectors. In first group, detectors are made in order to count ions of a single mass at a time and called point ion detectors. Second group detectors such as photographic plates, image current detectors or array detectors, count multiple masses simultaneously and named array collectors.[174] The scheme of a quadrupole ICPMS is given in Figure 1.1.

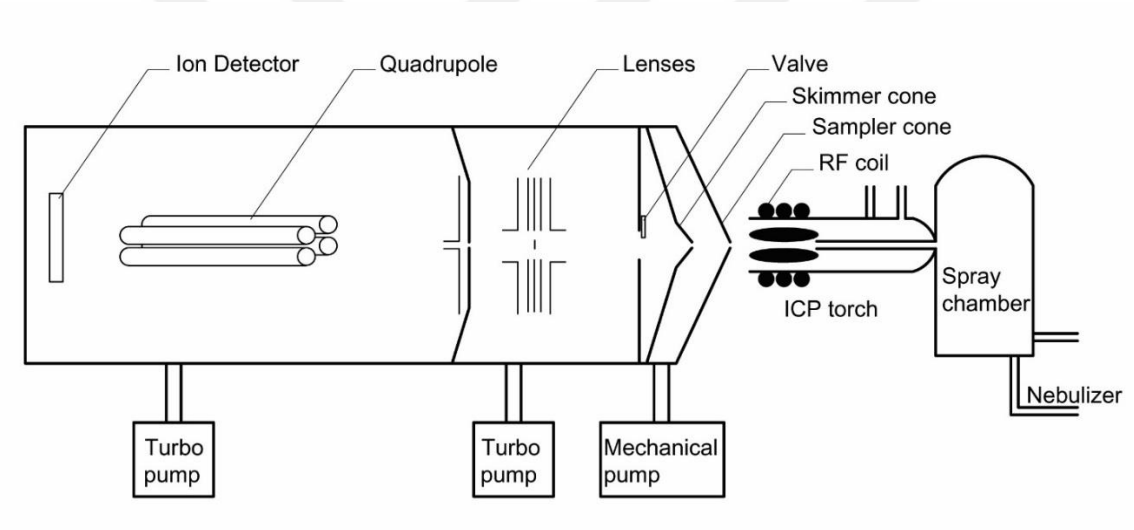

Figure 1.1. Schematic of Quadrupole-ICPMS.[177a]

Electron Multipliers (EM) is widely used in ICPMS and different designs are available. Its role is to amplify a weak current of ions from mass analyzer to higher currents at anode by using a series of secondary emission electrodes or dynodes. An ion striking the first dynode causes the emission of electrons. These emitted electrons from the surface are projected to the second dynode. This process repeats itself causing the emission of more and more electrons in the EM to produce a current by *cascading effect.* There are two types of EMs which are *discrete dynodes* and *continuous dynode.*[172,174]

[a] Adapted from Reference 177

In a discrete dynode EM, detector surface is constructed with a series of discrete dynodes (12 to 20 dynodes) connected by chain of resistors. The gain of this type detector depends on the voltage applied to the dynode string. On the other hand, continuous detector surface is used in continuous dynode design. Channeltron and microchannel plate are the type of continuous dynode EM. Channeltron is made from a lead-doped glass with a curved tube shape. Since the wall of tube has a uniform electric resistance, continuous accelerating field is produced when voltage is applied between two tips of the tube.[174] Achieved current gains are typically order of 10^5 to 10^7 depending on the age of detector for different types.[172]

1.9. Multi-Element Detection Capability of ICPMS with Transient Signals

Signals of different sample introduction techniques such as laser ablation, flow injection, ETV and sample separation devices like chromatography show time dependent transient peaks. To obtain higher signal to noise ratios (S/N) or to reduce overall analysis time transient signals become shorter and shorter. Short transient signals with few second duration or ultra-short transients of a few milliseconds require three challenging features from ICPMS. These are i) robust and stable plasma conditions during short time period, ii) fast data acquisition and iii) simultaneous detection of different masses or even full mass scans.[178] Unfortunately, first requirement cannot be provided since local and short term instabilities of plasma temperature have not been understood yet. Other parameters are related with the instrument and there have been many efforts on development of new instruments with improved properties on data acquisition. Among currently used four mass spectrometers which are, Quadrupole (QMS), Sector Field (SFMS), Multi collector (MCMS) and Time of Flight (TOFMS); only the last two is suitable for simultaneous determination with signals of less than few seconds duration.[178]

ETV coupled to ICPMS generates transient signals similar to those obtained from W-coil traps. Therefore, the studies in this area will also be presented in this section. ETV-ICPMS is used as the sample introduction technique for analysis of complex samples

with small sample volumes, 1-50 μL. Moreover, *temperature program* can be applied in ETV to separate analyte from matrix. It has been proved to be a very powerful method in terms of high sensitivity, multi-element capability and trace element determination in a wide variety of samples.[179,180] However, when quadrupole ICPMS is used, limited number of elements/isotopes up to eight are followed from one firing due transient nature of ETV signal. Transition signal is very fast with a duration of 1-2 s.[181]

Majority of studies have dealt with the simultaneous determination of 1-3 elements from the same tube firing. Limitation for the number of isotopes determined in a transient signal is seemed logical since quadrupole filter operates in a sequential mode.[182] In the early studies before 2000, actual limit was not clear. According to some researchers in order to avoid severe signal distortion, a maximum of 4-5, can be studied.[183] Other scientists indicated that it is possible to determine 5-8 elements during the same tube firing[181] while another group claimed that limit is 10 elements.[184] Unfortunately, none of these works presented experimental results to support their assumptions. In 2000, for the first time *Coedo et al*. reported the simultaneous determination of 10 elements using ETV-Quadrupole-ICPMS.[185]

Resano et al. studied on the maximum possible number of isotopes of Cd, Co and Ti that can be monitored during single firing using ETV-Quadrupole-ICPMS without losing the sensitivity.[182] To provide experimental data, effect of number of mass-to-charge ratios monitored (n_i), dwell time (t_d) and data processing mode either integration or counting on analyte signals were studied. It was concluded that as long as critical value of 3 or 4 points on the signal is obtained, it is possible to determine simultaneously 20 elements with 1.5-2.0 s peak width by ETV-Quadrupole-ICPMS without affecting precision, detection limit and sensitivity.[182]

Venable and coworkers performed two set of experiments with ETV-Q-ICPMS where 21 and 68 transient signals (different m/z) were monitored per ETV firing to validate the maximum number of masses that can be monitored with a good precision.[186] Various data collection times were examined, and it was found that 21 m/z values of 12 elements

can be monitored from a single firing of ETV. 40 points were totally obtained per each m/z value. Narrowest peak half-width was 0.5 s.[186]

It was shown that the use of low carrier gas flow rates[187], longer transport tubing[188] and Transient Extension (TEx) chamber[181] were broaden the ETV signal. In literature there are studies in which full mass scan was performed by using TOF mass analyzers with a very short transport tubing[189], TEx chamber with Quadrupole mass analyzer[181] and combination of Tex-TOF[190]. TEx chamber was designed to lengthen an ETV signal for obtaining a full mass scan (254 masses). TEx chamber is a simple flask with a mated joint which allow the ETV-generated aerosol to enter the chamber in a pulse and exit the chamber exponentially diluted. Duration of the transient signal extended from 2 s to 15 s or longer depending on the flask volume. In full mass scan mode nine masses were tested by using this chamber although approximately 20% decrease were observed in peak area values.[181] However, sensitivity was decreased due to sample loss between ETV and ICP as a result of broadening the signal.[186]

Broadening transient peak increases the risk of isobaric interferences. Isobaric interferences occur when equal mass isotopes of different elements present in the analyte solution. However, differences in vaporization temperatures of elements can be used to eliminate isobaric interferences. *Ertas and Holcombe* used differences in volatilization characteristic of elements to separate ^{64}Zn, ^{76}Se, ^{113}Cd and ^{116}Cd signals overlapping with ^{64}Ni, ^{76}Ge, ^{113}In, ^{116}Sn signals. In order to resolve ^{76}Ge/^{76}Se and ^{113}Cd/^{113}In isobar peaks approximately 35000 and 332000 mass resolving power is needed. Required resolution level was reached by combining thermal separation ability of ETV and TOF mass analyzer. Resolving power of the TOF used for this study was only 1500.[191]

When TOF mass analyzers are coupled to ICPs, it is possible to monitor all masses during a single tube firing. There is no spectral skewing problem since all masses are monitored at the same time. In addition, irreproducibility and signal fluctuations from plasma or sample introduction unit can be eliminated via rationing signals from all isotopes.[191] However, quadrupole coupled ICPMS are still widely used compared to

TOF coupled ICPMS. Only one mass at a time is followed using quadrupole mass analyzers and total number of points (N) which defines the peak shape of transient signal depends on four parameters. These are peak width (w), number of mass-to-charge ratios monitored (n_i), dwell time (t_d) and settling time (t_{st}).[182] *Dwell time* is defined as the time spent by quadrupole on a given ion mass during every sweep. *Settling time*[182] *or jump time*[186] is the duration for amplifier settling and stabilization of quadruple analyzer RF and DC voltages. Total number of points generating a signal is greatly influenced by both the n_i and t_d. Then, equation can be expressed as follows.[182]

$$N = \frac{w}{(t_d + t_{st})n_i}$$

According to this equation, as the dwell time increases number of points on the peak decreases. It is possible to increase the number of points on the peak by using the smallest dwell time possible; however this in turn will decrease the signal magnitude.[182] Therefore, selected dwell time should guarantee a sufficient number of points per peak and best detection limits.[192] In literature mostly 10 ms dwell time has been chosen for simultaneous determination of high numbers of elements such as ten by ETV-ICPMS.[185,193,194]

For more than one mass, monitoring system moves between masses and repetitive scans are done to obtain transient signals for each mass. *Scan time* (t_s) or *sweep time* is the time period required for one complete scan to obtain one point. Scan time includes dwell time (t_d), jump time (t_j) and fly back time (t_f). There is no jump time after the last monitored mass.[186] *Fly back time* is time period for the quadrupole settings to return to its initial values after monitoring the last mass.

Scan time, t_s, can be expressed as[186],

$$t_s = t_f + n_i t_d + (n_i - 1)t_j$$

This equation is valid when "*peak hopping*" mode is selected for data collection. In this mode quadrupole has been programmed to collect data one point per m/z per scan. When the equation is rearranged as shown in the following formula, it is easily seen that

increasing scan time will increase the number of masses followed since the contribution of fly back time to scan time is negligible.

$$n_m = (t_s - t_f + t_j) / (t_d + t_j)$$

Another term in signal collection is the *duty cycle*, (t_d/t_s), that is the fraction of time spent for a given mass. Duty cycle is equal to 1 if only one mass is followed. When number of masses increases time spent for a specific mass stays constant while scan time increases to get data for the other. Therefore, if multiple masses are to be monitored, $t_d/t_s < 1$ and causes worsening on the detection limits for the specific mass.[186]

1.10. Aim of the Study

The aim of this thesis study is to develop a novel sensitive analytical method for multi-element determination by using W-coil as both trap and vaporizer for hydride species and couple this system to ICPMS. Trapping provides preconcentration of the sample. Then, this method is applied for multi-element determination at ultra-trace level. To the best of our knowledge, this study is the first report on HG-W-Trap-ICPMS system in literature.

CHAPTER 2

EXPERIMENTAL

2.1. Reagents

All chemicals used for this study were analytical grade. Hydrochloric acid, HCl, was obtained from Merck (Darmstadt, Germany). 1000 mg/L Bi solution (High Purity, Charleston, SC, USA) in 2.0% (v/v) HNO_3 was used as stock solution. Standard solutions were prepared in 1.0 M HCl by diluting the stock solution with 18 MΩ.cm deionized water.

Since 4+ oxidation state of tellurium is favored for its hydride formation, 1000 mg/L Te stock solution was prepared from solid TeO_2 (Fisher Scientific, USA) in 10% (v/v) HCl with the help of ultrasonic water bath. All of the calibration standards were prepared in 2.0 M HCl solution.

Solid potassium antimony tartrate, $K(SbO)C_4H_4O_6$, (Sigma Aldrich, Steinheim, Germany) was used for the preparation of 1000 mg/L Sb stock solution in deionized water.

1000 mg/L Se(IV) stock solution was prepared by dissolving appropriate amount of sodium selenite, Na_2SeO_3 (Ventron, Karlsruhe, Germany) in deionized water. Acidity of the standard solution was provided by diluting the stock HCl solution (Merck, Darmstadt, Germany).

0.5% (w/v) $NaBH_4$ solution was prepared from solid $NaBH_4$ (Merck, Darmstadt, Germany) in 0.2% (w/v) NaOH (Sigma Aldrich, Steinheim, Germany).

In order to improve trapping efficiency of W-coil, 100 µL of 1000 mg/L Ir (High-Purity, Charleston, SC, USA) in 2.0% HCl , Pt (Inorganic Ventures, Christiansburg, VA, USA) and Rh (High-Purity, Charleston, SC, USA) in 10% HCl stock solutions were used for coating.

Accuracies of the methods for single and multiple element studies were controlled by using "NIST 1643e Trace Elements in Water" (NIST, Maryland, USA) and "NIST 1643f Trace Elements in Water" (NIST, Maryland, USA) solutions as Standard Reference Materials (SRM).

For hydride generation and W-coil experiments, Ar (99.9% pure) (Linde, Ankara, Turkey) and H_2 (99.9% pure) (Oksan, Ankara, Turkey) gasses were used.

2.2. Instrumentation and Experimental Setups

2.2.1. Instruments for General Purpose

In all experiments, 18 M Ω.cm deionized water from ELGA Purelab Option Q7 Water Purification System (High Wycombe, England) was used for preparation of the standard solutions.

For the preparation of 1000 mg/L Te stock solution solid TeO_2 was dissolved with the help of Elma S 40H ultrasonic water bath (New Jersey, USA).

A six-port injection valve with a 500 µL loop was used as flow injection system in nebulization and hydride generation parts of the study.

For hydride generation part, three peristaltic pumps were used to pump carrier acid solution, $NaBH_4$ solution and to drain waste solution from gas liquid separator. Two of the pumps with two-way channels were purchased from LongerPump-Shanghai, China while the rest has four channels from GILSON Minipuls 3, Middleton, USA.

In order to measure the flow rates of make-up Ar and H_2, two PTFE flowmeters (Cole Parmer Instrument Co., Illinois, USA) were used.

W-coil filament, which was obtained from a 15 V, 150 W projection lamp, Type 6550 (Philips, Aachen, Germany) was used as the trap. Coil was in conical shape in order to supply maximum cross-sectional area providing efficient trapping surface. Dimensions of filament were 4.0 mm x 3.0 mm x 1.0 mm. The coil temperature was manually controlled by a variable potential power supply (Variac) (Şimşek Laborteknik, Ankara, Turkey) connected to main electricity. 750 W transformer was connected between the variac and the tungsten coil. By using thermocouple and infrared thermometer Mirage, IRCON (Santa Cruz, USA), the temperature of the W-coil was measured. While thermocouple was used for the lower temperatures up to 700 ^{o}C, pyrometer was used to measure the temperatures above 1000 ^{o}C. For calibration of the pyrometer, graphite furnace of atomic absorption spectrometer (VARIAN GTA120, Walnut Creek, CA) was used.

XPS analysis for determination of species on W-coil was performed in Central Laboratory of the Middle East Technical University, Ankara, Turkey.

2.2.2. ICPMS with Nebulization System

Thermo X Series ICPMS instrument was used in this study (West Sussex, UK). The instrument was equipped with a borosilicate spray chamber-nebulizer system. In addition, flow injection system with a loop volume of 500 µL was used unless stated otherwise.

2.2.3. Hydride Generation System

Schematic representation of hydride generation (HG) system coupled to ICPMS is shown in Figure 2.1. HG system was connected directly to the inlet of ICP torch without using spray chamber and nebulizer system. ICP torch elbow was directly connected to a

10 cm long borosilicate glass tube which was further coupled to a 27 cm long tygoprene tubing extending to the exit part of gas liquid separator (GLS). Three peristaltic pumps were used for transporting of $NaBH_4$, analyte and waste solutions.

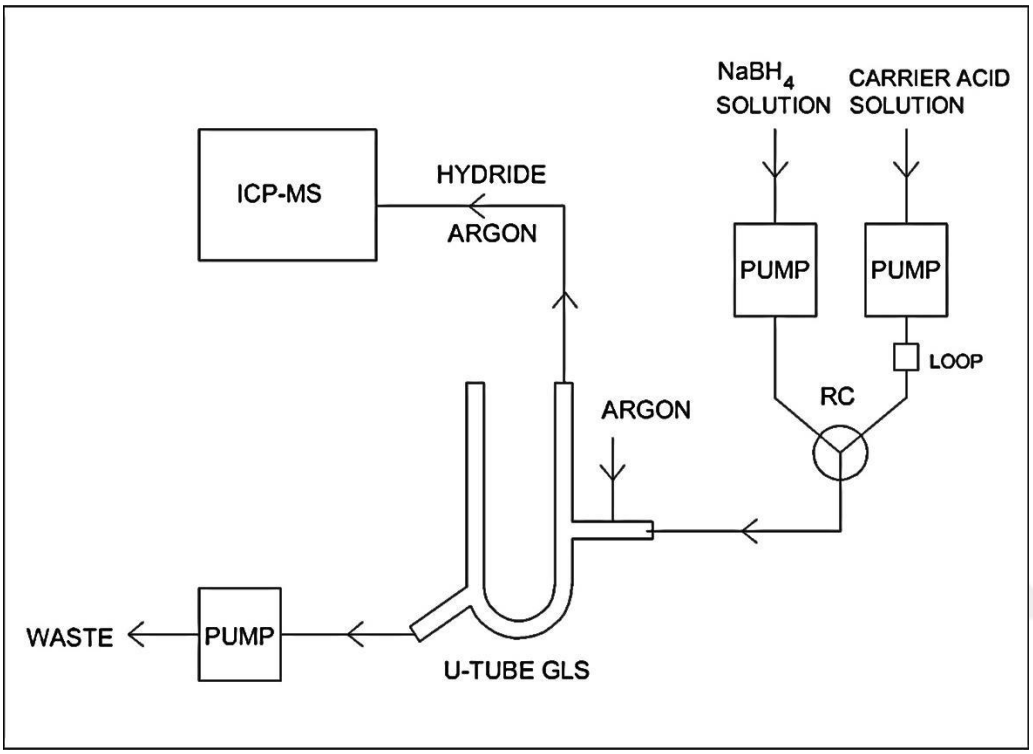

Figure 2.1. Schematic representation of HG-ICPMS system.

For the separation of bismuthine (BiH_3) and tellurium hydride (TeH_2) from liquid phase a U-tube shaped GLS and cylindrical type GLS were used; their schematic representations are given in Figure 2.2 and Figure 2.3, respectively.

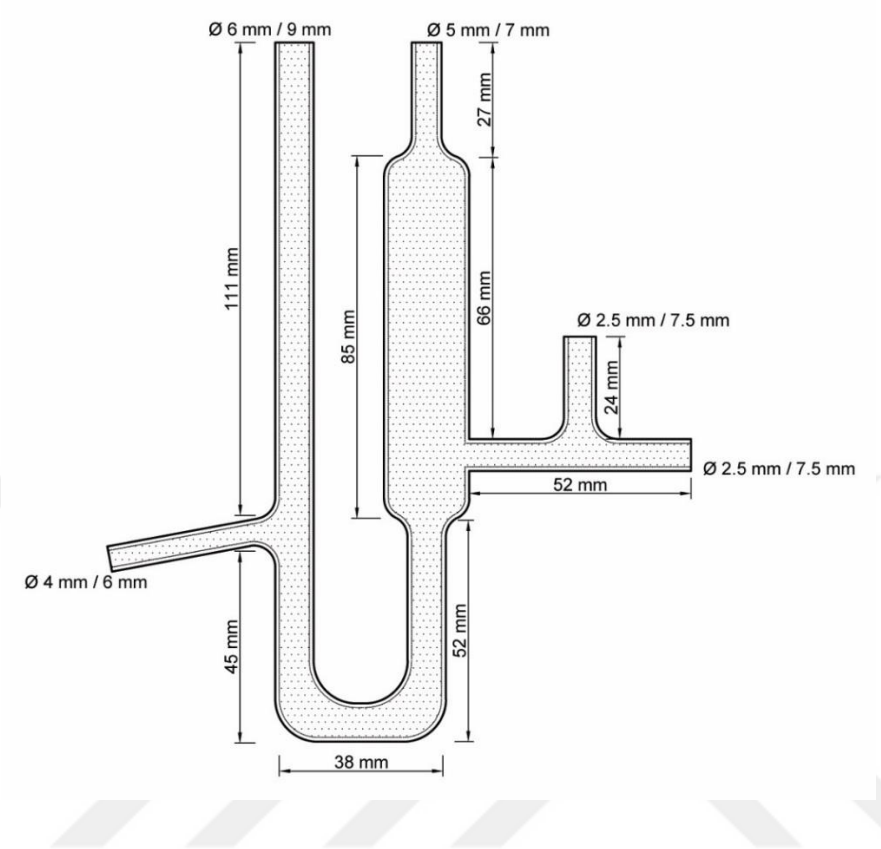

Figure 2.2. Schematic representation of U-Tube GLS.

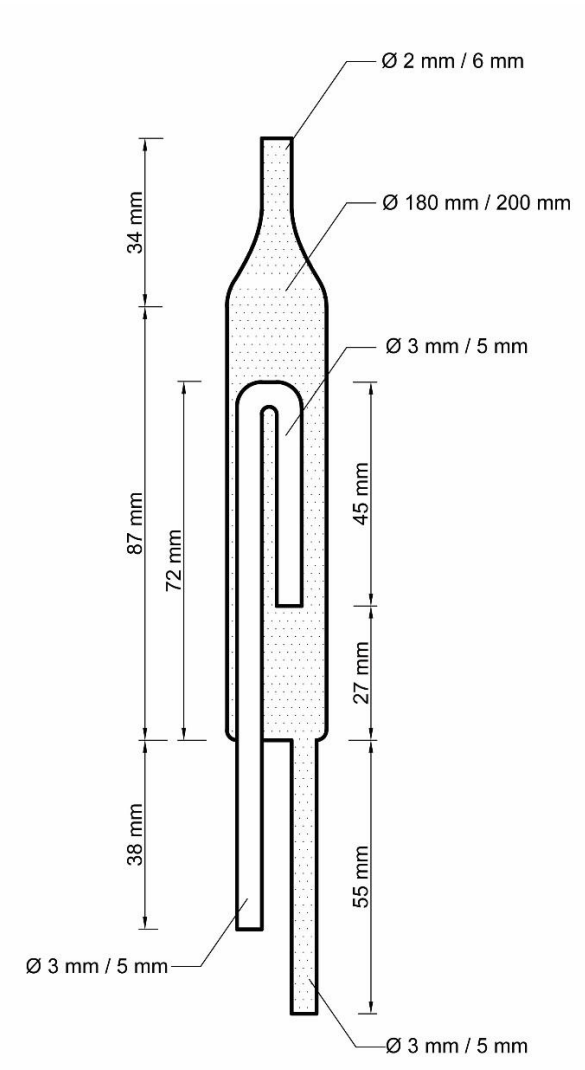

Figure 2.3. Schematic representation of cylindrical type GLS.

2.2.4. Hydride Generation W-trap ICPMS System

For this system, a glass tube apparatus containing W-coil was inserted between GLS and ICPMS; its design is shown in Figure 2.4. Produced hydride was transported with Ar flow from the right hand side entrance of the system as shown in Figure 2.4 a side arm constructed on the main tube was for the entrance of Ar gas. H_2 gas was introduced through the bottom glass connection that includes electrical apparatus for W-coil. The part that contains W-coil was inserted in the middle of the glass part as shown in Figure

2.4. W-coil configuration details are shown in Figure 2.5. W-coil was connected to the power supply for regulated heating. Two flowmeters were used for measuring the H_2 and make-up Ar flow rates.

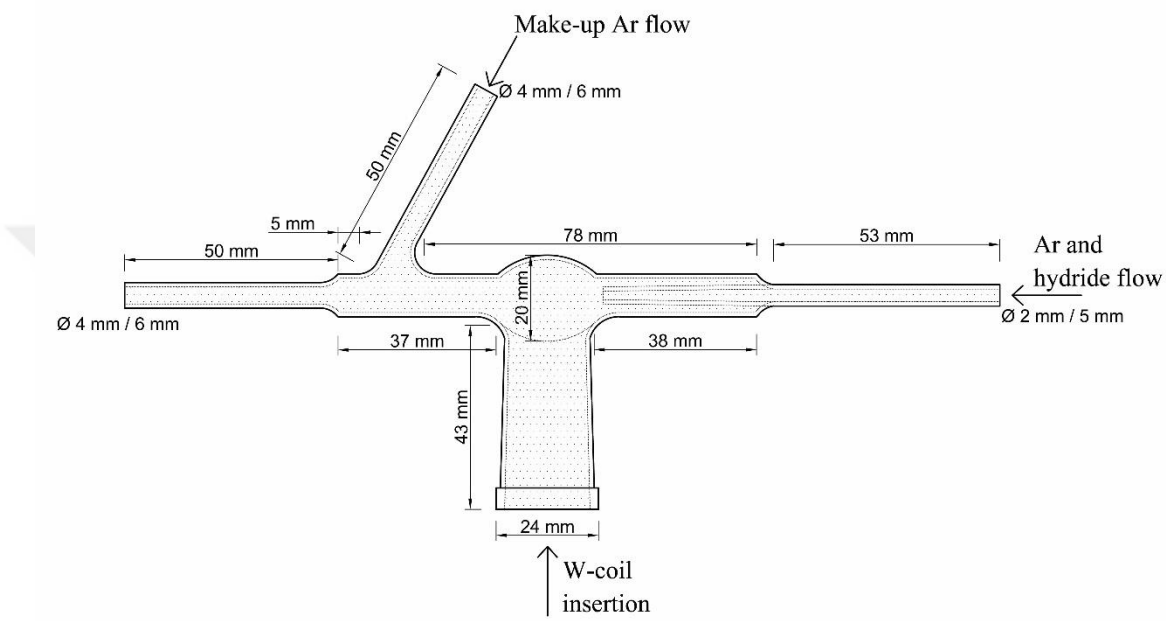

Figure 2.4. Schematic representation of glass tube for W-coil.

Figure 2.5. Picture of glass tube for W-coil and W-coil itself.

Length of the tygoprene tubing (I.D.: 4.8 mm, O.D.: 8 mm, Cole Parmer, Illinois, USA) between GLS outlet and glass part containing W-coil was 14.5 cm. 10.5 cm long tygoprene tubing was used between the glass tube containing W-coil and the glass part which was connected to torch elbow. Schematic representation of HG-W-Trap-ICPMS is given in Figure 2.6.

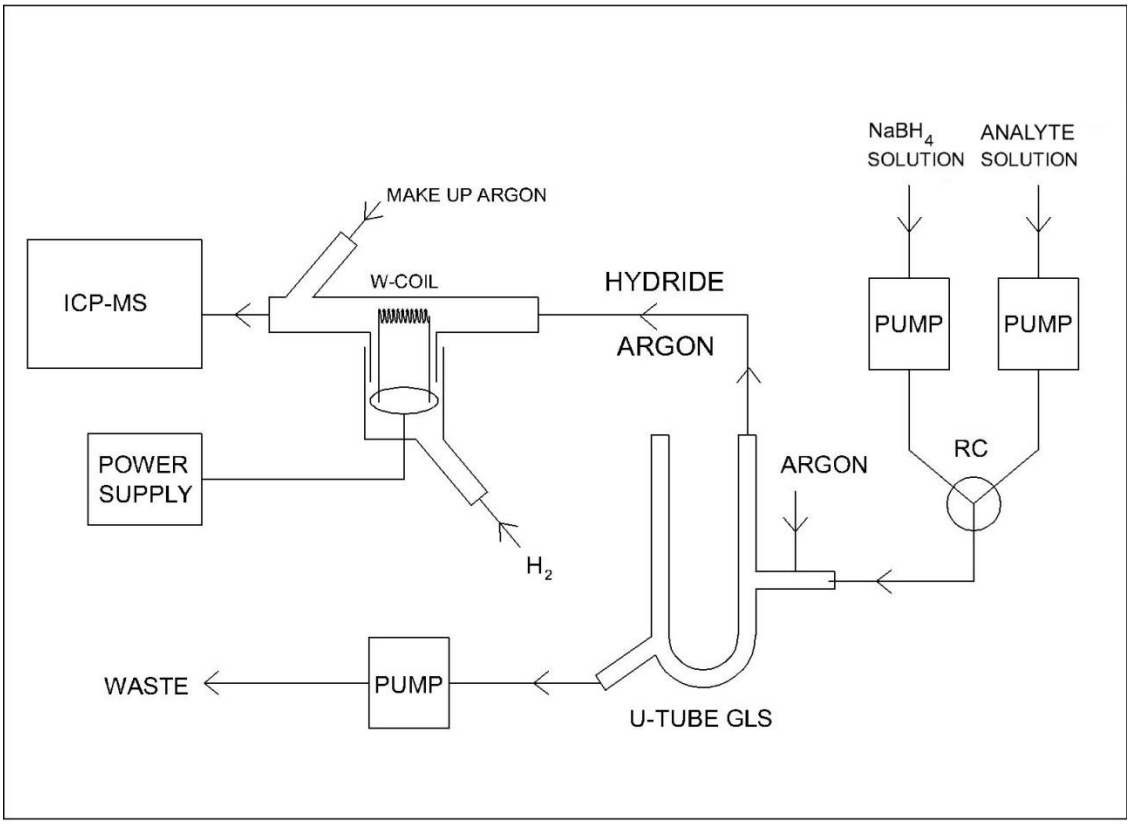

Figure 2.6. Schematic representation of HG-W-Trap-ICPMS system.

2.3. Procedures

In this study, conditions for ICPMS, hydride generation system and trap system were optimized to obtain best sensitivity. The procedural details for each system are given in the following sections.

2.3.1. ICPMS with Nebulization System

Flow injection system with a loop volume of 500 µL was used and the signals were recorded as peak height to provide direct comparison with the signals of HG and HG-W-Trap systems. Standard solutions of Bi and Te were prepared in 1.0 M and 2.0 M HCl, respectively by diluting the stock solution with 18 MΩ.cm deionized water. Concentration range of the Bi calibration standards were from 0.10 to 10.0 ng/mL. Te calibration standards were in the range of 0.25-25.0 ng/mL.

Dwell time was set to 10 ms for all parts of this study. It is worth to say that during this thesis study, operating conditions of ICPMS were varied not only for different elements monitored but also in case of developing methods. Moreover, after each replacement of the sampling and skimmer cones or torch, optimum values of sampling depth, vertical and horizontal position had to be changed. Optimum values of other parameters did not change drastically and set values were close to each other. A typical operating conditions for ICPMS in mixture study are given in Table 2.1.

"1643e Trace Elements in Water" SRM solution was used to check the accuracies of developed methods for Bi and Te determinations by using this system. Since Bi concentration is higher than Te concentration in SRM solution, SRM solution was diluted more for Bi case. While SRM was diluted 50-folds and prepared in 1.0 M HCl for Bi determination, 4-folds dilution was done for Te determination and acidity of the final solution was 2.0 M. In addition, standard addition technique was applied to obtain satisfactory results for Te in nebulization part.

Table 2.1. Operating Parameters of ICPMS.

Parameters	**Optimum Value**
Extraction lens voltage, V	-118
Lens 1 voltage, V	-4.1
Lens 2 voltage, V	-68.3
Focus lens voltage, V	11.6
1. diffraction aperture voltage, V	-38.4
2. diffraction aperture voltage, V	-140
Quadrupole voltage, V	-1.6
Hexapole voltage , V	0.8
Argon flow rate in nebulizer, L/min	0.9
Lens 3 voltage, V	-146
Horizontal position of torch	116
Vertical position of torch	45
3. Diffraction aperture voltage, V	-27
Argon flow rate to cool torch, L/min	13.0
Argon flow rate to produce plasma, L/min	0.8
Sampling depth	90
Forward power, Watt	1400

2.3.1.1. Isotopes Used in the Study

Bi element has one naturally occurring isotope at mass number 209. Although this isotope shows radioactive property with an experimental half-life of 1.9 x 10^{19} years[195] due to this very long half-life, it has classically been considered to be a "stable" isotope with a 100% abundance and often used in the scientific research, as in this study.

In case of Te, it has eight naturally occurring isotopes at mass numbers 120, 122, 123, 124, 125, 126, 128 and 130. Six of them are stable while the other two are found to be radioactive with very long half-lives. For ^{130}Te which has the highest abundance (34.5%), ^{130}Xe and ^{130}Ba interferences are mentioned. Since the calibration standard includes only Te element and also Argon gas used for plasma formation is free of Xe, ^{130}Te signal was used during the study except in SRM studies. Since both water SRMs contain Ba, instead of ^{130}Te, Ba interference free isotope of Te at mass 128 was used in the validation part.

There are two stable isotopes of Sb at mass numbers 121 and 123. Since ^{121}Sb has higher natural abundances (57.3%) and free of interference it was monitored in the study.

Lastly Se has six naturally occurring isotopes at masses 74, 76, 77, 78, 80 and 82. Among them one at mass number 82 shows radioactive character. Although ^{80}Se has the highest natural abundance (49.8 %) it is not preferred due to the possibility of Ar dimer interference. Instead, ^{78}Se with a 23.5% abundance was used for this study. Percent natural abundances of the stable isotopes and half-lives for radioactive ones are summarized in Table 2.2.

Table 2.2. Natural abundances and stabilities of isotopes used in this study[196]

Isotope	**Natural abundance, %**	**Stability**	**Half-life, $t_{1/2}$, y**
^{209}Bi	100	Radioactive	10^{19}
^{120}Te	0.091	Stable	-
^{122}Te	2.5	Stable	-
^{123}Te	0.89	Stable	-
^{124}Te	4.6	Stable	-
^{125}Te	7.0	Stable	-
^{126}Te	18.7	Stable	-
^{128}Te	31.7	Radioactive	1.5×10^{24}
^{130}Te	34.5	Radioactive	2.0×10^{21}
^{121}Sb	57.3	Stable	-
^{123}Sb	42.7	Stable	-
^{74}Se	0.87	Stable	-
^{76}Se	9.0	Stable	-
^{77}Se	7.6	Stable	-
^{78}Se	23.5	Stable	-
^{80}Se	49.8	Stable	-
^{82}Se	9.2	Radioactive	1.4×10^{20}

2.3.2. Hydride Generation System

Flow injection system with a loop volume of 500 µL was used in this part, too. Standard solutions of Bi and Te were prepared in 1.0 M and 2.0 M HCl, respectively by diluting the stock solution with 18 M Ω.cm deionized water. Concentration range of the Bi calibration standards were from 0.050 to 10.0 ng/mL while that of the Te calibration standards were 0.050-25.0 ng/mL. For Bi and Te binary mixture, acidity was adjusted to 2.0 M HCl to provide hydride formation of Te.

0.5% (w/v) $NaBH_4$ solution was used as a reducing agent in HG. It was prepared in 0.2% (w/v) NaOH which was used to stabilize $NaBH_4$ solution.

Hydride compounds produced in HG system were transported to the plasma using Ar as the carrier gas. Ar gas connection of the ICPMS nebulizer was used for supplying Ar to transport hydride species into plasma. Dwell time was 10 ms for both elements.

Five hydride forming parameters were optimized for determination of Bi and Te alone and also in mixture. Carrier solution was 1.0 M HCl solution for each element studied. 0.25 ng/mL Bi and 2.5 ng/mL Te standard solutions were used during optimization experiments. All the experimental parameters were optimized by changing one variable at a time while the others were kept constant. The optimum hydride generation conditions are summarized in Table 2.3.

Table 2.3. Optimum hydride generation conditions for Bi and Te

	Bi	**Te**
Carrier Ar flow rate, L/min	1.2	1.2
$NaBH_4$ flow rate, mL/min	1.1	1.1
Sample flow rate, mL/min	2.0	2.0
Concentration of $NaBH_4$, %(w/v)	0.5	0.5
Concentration of HCl, M	1.0	2.0

For multi-element study, optimum conditions of Te were used since no hydride formation occurs when acid concentration was below 2.0 M.

Accuracies of the methods for this system was checked by using "1643e Trace Elements in Water" SRM for both Bi and Te with direct calibration. SRM solution was diluted 50-folds and 10-folds for Bi and Te determinations, respectively. To match the acidity with calibration standards diluted SRM solution was prepared in 1.0 M HCl for Bi determination and in 2.0 M HCl for Te determination.

2.3.3. Hydride Generation W-trap ICPMS System

Lower concentrated standard solutions of Bi and Te were prepared for this part. Concentration range of the Bi calibration standards were from 0.010 to 10.0 ng/mL in 1.0 M HCl for HG-Ir-coated W-Trap-ICPMS system while Te calibration standards were in the range of 0.025-10.0 ng/mL in 2.0 M HCl for HG-Pt-coated W-Trap-ICPMS. Standards were prepared by diluting the stock solutions with 18 MΩ.cm deionized water. For Bi and Te binary mixture, solutions were prepared in 2.0 M HCl.

When the third element was Sb for multi-element study, a mixture solution of 2.0 ng/mL Sb, 0.25 ng/mL Bi and 1.0 ng/mL Te was prepared after suitable dilutions in 2.0 M HCl.

When Se was used as the third element for multi-element study, a mixture solution of 2.0 ng/mL Se, 0.25 ng/mL Bi and 1.0 ng/mL Te was prepared after suitable dilutions in 2.0 M HCl.

Experiments were carried out using the setup shown in Figure 2.6. W-coil as a trap was connected in between HG system and ICPMS. Wherever noted, coated W-coil was used as the trap. For each Ir, Pt or Rh coatings 20 µL of 1000 mg/L stock coating solution was pipetted on the coil and following heating program was employed in sequence: 179 ^{o}C for 60 s; 660 ^{o}C for 30 s; 1211 ^{o}C for 15 s and finally 1590 ^{o}C for three firings each with 2 seconds. This coating procedure was repeated 5 times. During the coating

process, H_2 and make-up Ar flows were continued and kept constant at optimized values.

HG-W-Trap-ICPMS system has two time stages. In the first one, called trapping or collection, while the W-coil is kept at an optimized temperature for a certain period, hydride is sent through the system. Continuous flow for analyte solution is used. At the end of this step, in the second step, the pumps are stopped, gas flows are continued and W-coil is heated rapidly to a higher temperature for revolatilization. The species released from W-coil are transported to plasma and the peak shaped signal is recorded. H_2 flow is used to protect W-coil from oxidation. Ar plasma is sensitive to fluctuations in the supply gas composition. Therefore, dilution of H_2 gas was needed to prevent the plasma from being extinguished. For this purpose additional make-up Ar gas was supplied to the plasma.

Optimum hydride generation parameters from the previous part were used throughout trapping study. During optimizations, 0.25 ng/mL Bi solution in 1.0 M HCl was used in the single element study while 0.5 ng/mL Bi and 2.5 ng/mL Te mixture solution was prepared for multi-element part. Effects of five parameters were evaluated for trapping system. Ir-coated W-coil was used for only Bi study while Pt-coated W-coil was selected through optimizations of Te. Optimum values of HG-W Trap system are given in Table 2.4 for Bi and Te elements.

Table 2.4. Optimum trapping system conditions for Bi and Te

	Bi	**Te**
H_2, mL/min	106	106
Make-up Ar, mL/min	125	125
Trapping T, ºC	179	585
Revolatilization T, ºC	1600	1600
Trapping period, s	60	60

Flow rates of protective H_2 and make-up Ar were not optimized for Te part specifically by considering that they do not depend on the elements. Optimum flow rates obtained from Bi part were used through the study. Only trapping temperature showed difference for Bi and Te. Lower one, namely 179 °C, was preferred in multi-element part to make contribution to the lifetime of the coil.

For method validation study of this novel system, “1643e Trace Elements in Water” SRM was used for only Bi determination part while “1643f Trace Elements in Water” SRM was used for only Te and binary mixture case. The reason of using different code of the same SRM was finishing of the former both in the laboratory and in market. Therefore, 1643e Trace Elements in Water SRM was diluted 200-folds for Bi determination. On the other hand, only Te and binary mixture cases, 20-folds dilution was applied to 1643f Trace Elements in Water SRM. Good results were obtained with direct calibration method for all cases in this part.

CHAPTER 3

RESULTS AND DISCUSSION

In the following sections, the results will be presented and discussed. The techniques of ICPMS, HG-ICPMS and finally HG-W-Trap-ICPMS will be applied; the last one is the main contribution of this thesis to literature. Comparison of these techniques will be presented. Firstly, Bi as a single element will be determined and this will be followed by Te determination. After these sections, the experiments involving multi-element studies will be given with the emphasis on Bi-Te mixture.

3.1. Determination of Bismuth by ICPMS

Starting point in this study was the determination of Bi by ICPMS. The application was continued by using HG-ICPMS and finally HG-W-Trap-ICPMS was used. In the following sections, comparison will be made between ICPMS, HG-ICPMS and HG-W-Trap-ICPMS systems using signal peak height for all cases.

3.1.1. Calibration Plot and Analytical Performance for Bi Determination by ICPMS

After optimization of the instrument parameters to get the best sensitivity, standard solutions of Bi were prepared in the range between 0.10 ng/mL and 10 ng/mL in 1.0 M HCl. Measurements were done by using flow injection system with a loop volume of 500 µL. Carrier solution was 1.0 M HCl solution. Up to 10 ng/mL, calibration plot was linear. Higher concentrations were not used due to memory effect problem. Calibration

plots of Bi for two concentration ranges using peak height values are given in Figure 3.1 and Figure 3.2.

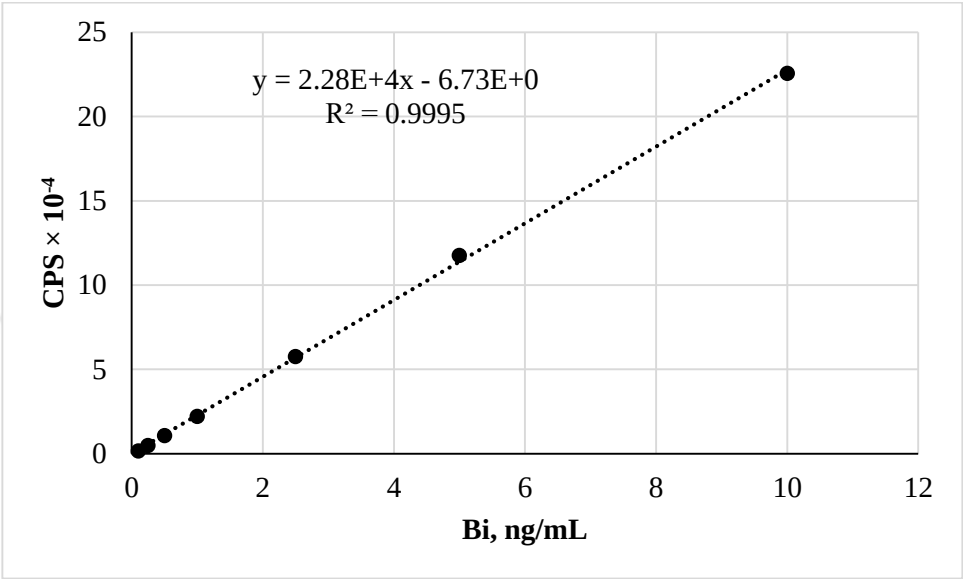

Figure 3.1. Calibration plot for Bi determination between 0.10 ng/mL and 10 ng/mL using ICPMS.

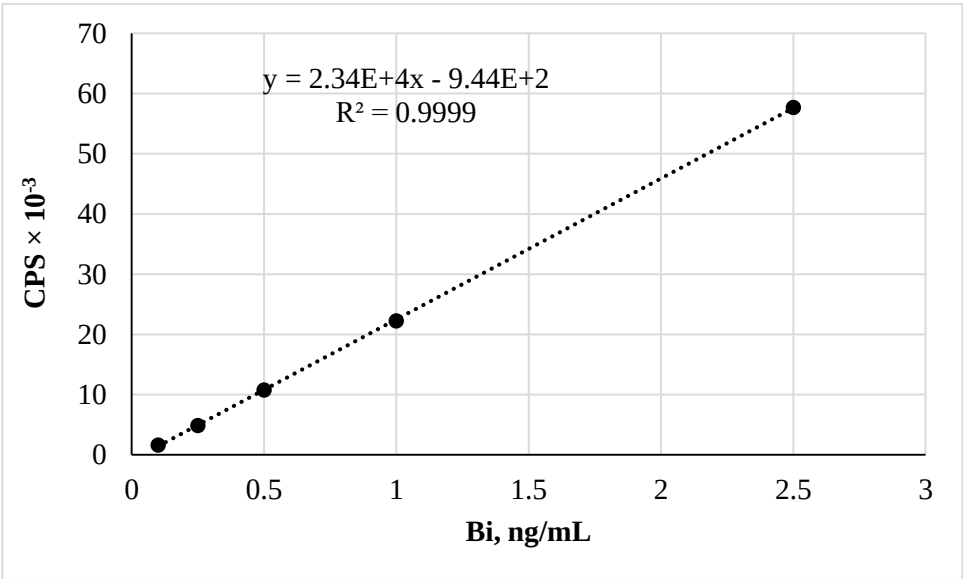

Figure 3.2. Calibration plot for Bi determination between 0.10 ng/mL and 2.5 ng/mL using ICPMS.

Signals of 1.0 M HCl as a blank solution and 0.10, 0.25 and 0.50 ng/L Bi standard solutions in 1.0 M HCl using flow injection system ICPMS are given in Figure 3.3. Average concentration of Bi in 1.0 M HCl solution was 0.05 ng/mL.

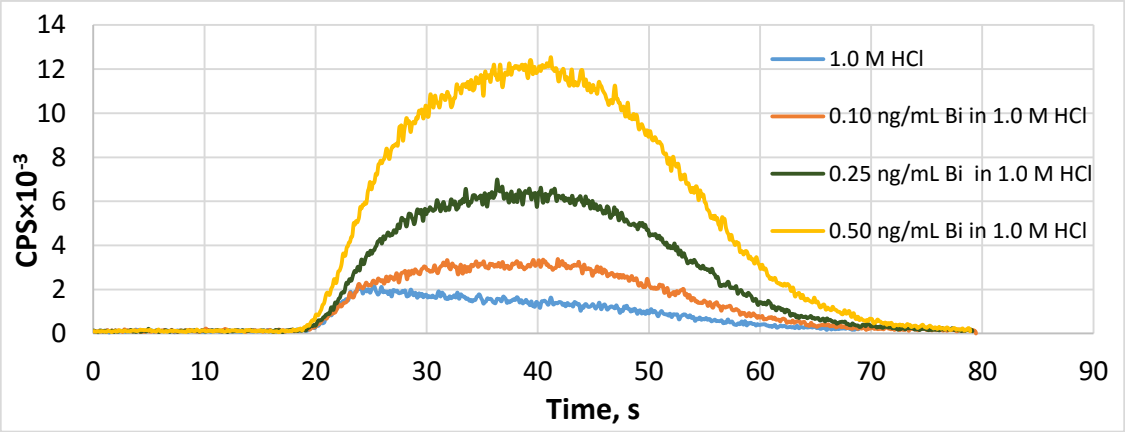

Figure 3.3. Flow injection signals of Bi solutions using ICPMS and a loop of 500 µL.

Limit of Detection (LOD), Limit of Quantification (LOQ) and % Relative Standard Deviation (%RSD) values of Bi using ICPMS were calculated using peak height measurements. They were calculated from 5 replicate measurements of smallest Bi concentration which is 0.10 ng/mL. Analytical figures of merit for Bi by ICPMS are given in Table 3.1.

Table 3.1. Analytical figures of merit for Bi by ICPMS.

	^{209}Bi, ng/mL
Limit of Detection, LOD, 3s/m (N=5)	0.021
Limit of Quantification, LOQ, 10s/m, (N=5)	0.069
Range	0.1-10
RSD,%	4.17

3.1.2. Accuracy Check for Bi Determination by ICPMS

Accuracy of the system was checked by using NIST 1643e Trace Elements in Water Standard Reference Material (SRM). SRM solution was diluted 50 times before the analysis. Peak area values were used for the calculations since peak areas from flow injection system were more easily calculated by using the software. However, for comparison of the signals from this part with transient signals of trap study, peak height measurements were also used. As it is seen from the Table 3.2, result was found in good agreement with certified value. Two separate check solutions were prepared and each was measured two times. Average of four measurements was found acceptable by applying t-test at 95% confidence level.

Table 3.2. Results of accuracy check for Bi determination by ICPMS.

SRM	**CertifiedValue, ng/mL**	**Found Value, ng/mL**
NIST 1643e Natural Water	14.09 ± 0.15	14.86 ± 0.53

3.2. Determination of Bismuth by HG-ICPMS

Second step in this study was the determination of Bi by HG-ICPMS system. After the system was set for hydride formation experiment, first aim for this part was to get signals with high S/N by adjusting the parameters roughly. At the very beginning hydride signals were very noisy. 1.0 M HCl as a blank, 0.25 ng/mL and 0.50 ng/mL Bi solutions in 1.0 M HCl were prepared to check the hydride-formation. Since HG of Bi was studied in our research group before, optimum parameters of the previous studies were used before starting the optimizations with this system. $NaBH_4$ concentration was 0.5% (w/v) in 0.2% NaOH.

Flow injection system was also used for this part. This helps to compare the nebulizer ICPMS and HG-ICPMS systems more accurately. In addition, consumption of the standard solutions was less with flow injection system. Carrier solution was 1.0 M HCl solution.

Although fluctuations were observed in plasma, it can resist extra H_2 gas produced from hydride formation reaction. When 0.5% (w/v) $NaBH_4$ and 1.0 M HCl were used limiting one was the concentration of $NaBH_4$. According to the hydride formation reaction below, 14 mL H_2 is generated per minute according to the hydride formation reaction. Calculations are given below.

$NaBH_4 + HCl + 3H_2O \rightarrow NaCl + H_3BO_3 + 4H_2$

0.5 % (w/v) $NaBH_4$ = 0.132 M

$NaBH_4 + HCl + 3H_2O \rightarrow NaCl + H_3BO_3 + 4H_2$

0.132 M 1.0 M

Limiting is $NaBH_4$

$NaBH_4$ flow rate: 1.1 mL/min

$1.1 \text{ mL/min} \times 0.132 \text{ mmol/mL} \times 10^{-3} \text{ mol/mmol} = 1.45 \times 10^{-4} \text{ mol/min}$

$NaBH_4 : H_2$

1 mol : 4 mol

$nH_2 = 1.45 \times 10^{-4} \times 4 = 5.81 \times 10^{-4} \text{ mol/min}$

P.V = n.R.T

$1 \text{ atm} \times V = (5.81 \times 10^{-4}) \text{mol/min} \times 0.082 \text{ atm.L/mol.K} \times 298 \text{ K}$

V = 14 mL/min

3.2.1. Optimizations for Bi Determination by HG-ICPMS

For the HG system 5 parameters, namely carrier Ar flow rate, $NaBH_4$ solution flow rate, carrier acid flow rate, concentration of $NaBH_4$ solution and concentration of HCl in analyte solution, were optimized to get high sensitivity. For this part, two different GLSs which are U-tube shaped and cylindrical shaped were used to get the best sensitivities from Bi signal. H_2 generated from the hydride generation reaction disturbs the plasma even its amount is small. Collected liquid in both arms of the U-tube GLS may balance the H_2 gas that reaches to the plasma. When U-tube GLS was used, plasma tolerates more to the H_2 gas disturbance. Therefore, U-tube was selected and used for the rest of the experiments. That's why only the optimization graphs for U-tube GLS were given in details. Peak area values were used for optimization studies. The optimum values were determined by flow injection method by injecting 500 µL of 0.25 ng/mL Bi.

3.2.1.1. Carrier Argon Flow Rate

Ar gas was used to carry the bismuthine into the plasma. Effect of carrier Ar flow on Bi signal was studied. Change in ^{209}Bi signal with respect to carrier Ar gas flow rate is given in Figure 3.4. For this optimization, 0.25 ng/mL Bi solution in 1.0 M HCl and 0.5% (w/v) $NaBH_4$ was used. Flow rates of carrier acid solution and $NaBH_4$ were 2.0 mL/min and 1.1 mL/min, respectively. Magnitude of the Bi signal decreases when the Ar flow rate is less or higher than 1.2 L/min. It is known that at lower carrier Ar flow rates, transport efficiency of hydride is low and the signal gets lower. Therefore, lower than 1.2 L/min flow rates, the transport efficiency is low and this resulted in lower Bi signal. Besides, Bi signal decreases also when Ar flow rate is higher than 1.2 L/min due to the dilution effect. In conclusion, flow rate of 1.2 L/min was selected as an optimum flow for the carrier gas.

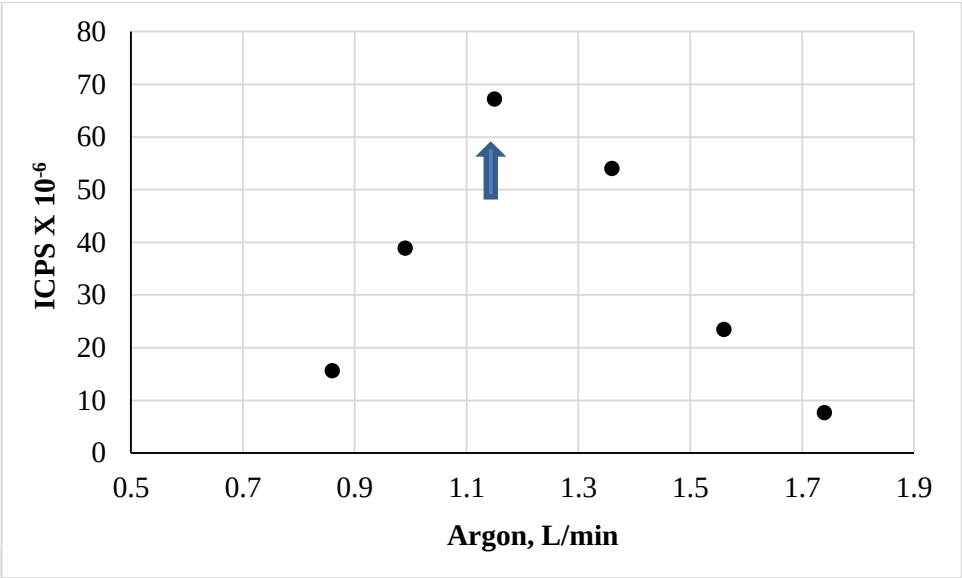

Figure 3.4. The optimization of carrier Ar flow rate for Bi determination by HG-ICPMS. 0.25 ng/mL Bi solution in 1.0 M HCl and 0.5% (w/v) $NaBH_4$ was used. Flow rates of carrier acid solution and $NaBH_4$ were 2.0 mL/min and 1.1 mL/min, respectively.

3.2.1.2. $NaBH_4$ Flow Rate

Second parameter to be optimized was the $NaBH_4$ flow rate. To provide continuous formation of bismuthine, flow rate of $NaBH_4$ is important. Change in ^{209}Bi signal with respect to $NaBH_4$ flow rate is given in Figure 3.5. Only $NaBH_4$ flow rate was varied for the determination of optimum flow rate while the other parameters were kept constant. 0.25 ng/mL Bi solution in 1.0 M HCl and 0.5% (w/v) $NaBH_4$ were used. For stabilization, the solutions of $NaBH_4$ were prepared in 0.2% NaOH. Flow rates of sample and carrier Ar were 2.0 mL/min and 1.2 L/min, respectively. When flow rate of $NaBH_4$ increases due to the increase in H_2 gas formation per minute besides bismuthine, plasma stability decreases and signal to noise ratio deteriorates. Therefore, 1.1 mL/min was selected as the optimum value for the rest of the study.

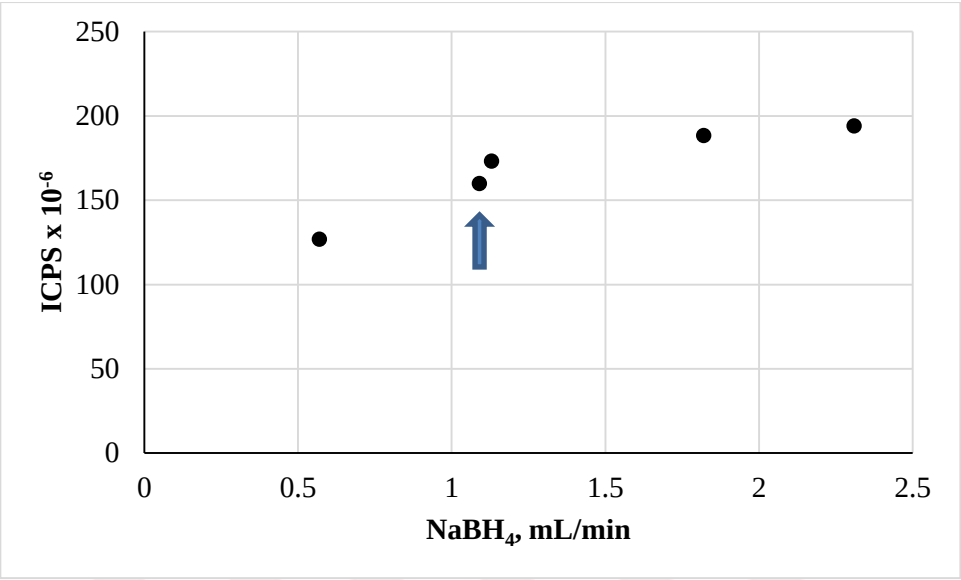

Figure 3.5. The optimization of $NaBH_4$ flow rate for Bi determination by HG-ICPMS. 0.25 ng/mL Bi solution in 1.0 M HCl and 0.5% (w/v) $NaBH_4$ were used. Flow rates of sample and carrier Ar were 2.0 mL/min and 1.2 L/min, respectively.

3.2.1.3.Carrier Acid Flow Rate

Effect of carrier acid flow rate was evaluated as a third parameter. Since flow injection system was used flow rate of carrier acid becomes important. The correlation between carrier acid flow rate and analytical signal was observed by varying the flow rate between 1.0-2.4 mL/min and the results are given in Figure 3.6. Maximum signal was obtained using 2.0 mL/min flow rate. For this optimization, 0.25 ng/mL Bi solution in 1.0 M HCl and 0.5% (w/v) $NaBH_4$ was used. Concentration of carrier HCl solution was 1.0 M. Flow rates of $NaBH_4$ and carrier Ar were 1.1 mL/min and 1.2 L/min, respectively.

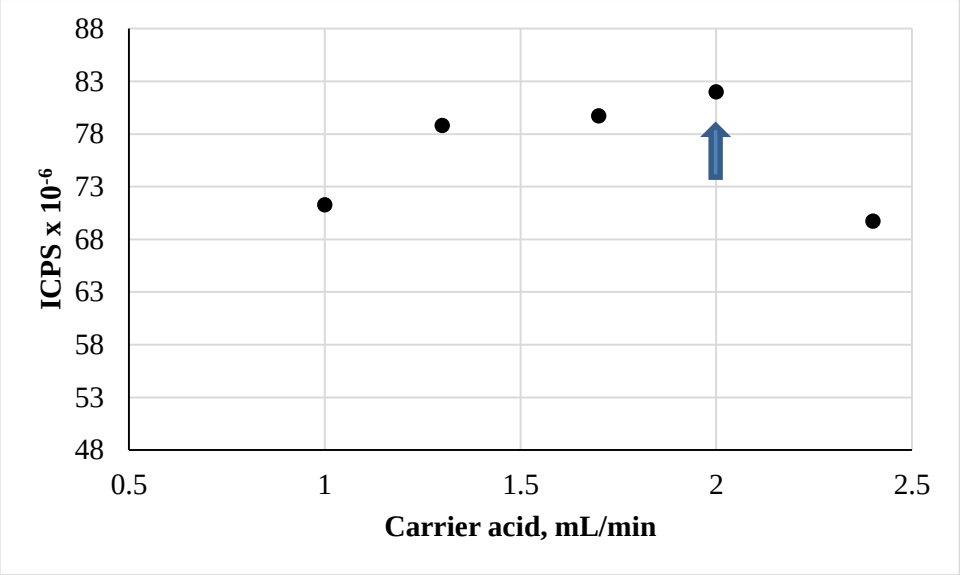

Figure 3.6. The optimization of carrier acid solution flow rate for Bi determination by HG-ICPMS. For this optimization, 0.25 ng/mL Bi solution in 1.0 M HCl and 0.5% (w/v) $NaBH_4$ was used. Concentration of carrier HCl solution was 1.0 M. Flow rates of $NaBH_4$ and carrier Ar were 1.1 mL/min and 1.2 L/min, respectively.

3.2.1.4. Concentration of $NaBH_4$

Like $NaBH_4$ flow rate, concentration of $NaBH_4$ is directly related with the H_2 formation and depending on the amount of formed H_2 plasma stability changes. Increase in H_2 formation causes the shutdown of the plasma. Therefore, the effect of $NaBH_4$ concentration on analytical signal and plasma stability was evaluated. For this optimization, 0.25 ng/mL Bi solution in 1.0 M HCl was used. Flow rates of $NaBH_4$, carrier acid solution and carrier Ar were 1.1 mL/min, 2.0 mL/min and 1.2 L/min, respectively. Four different $NaBH_4$ concentrations with 0.10, 0.25, 0.50 and 1.0% (w/v) were used to get best signals. Optimization graph of the $NaBH_4$ concentration is given in Figure 3.7. The signal increased gradually up to 1.0% (w/v) $NaBH_4$. 0.5% (w/v) was selected for the rest of the study as the optimum concentration. Although highest signal was obtained at 1.0% (w/v) $NaBH_4$, the signal was very noisy probably due to the formation of much more H_2 comparing other concentrations. In conclusion, for the rest of the study 0.5% (w/v) $NaBH_4$ was used.

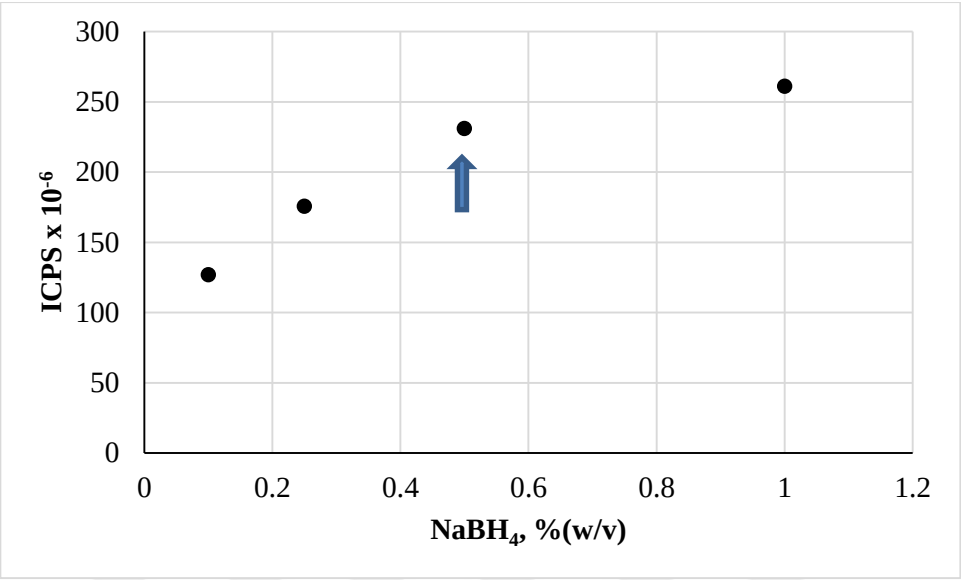

Figure 3.7. The optimization of $NaBH_4$ concentration for Bi determination by HG-ICPMS. Concentration of Bi was 0.25 ng/mL in 1.0 M HCl. Flow rates of $NaBH_4$, carrier acid solution and carrier Ar were 1.1 mL/min, 2.0 mL/min and 1.2 L/min, respectively.

3.2.1.5.Concentration of HCl in Analyte Solution

Last parameter to be optimized was concentration of HCl in analyte solution. Bi solutions were prepared in HCl solution to improve the hydride generation efficiency. Hydrolysis of THB is catalyzed by acid. The correlation between HCl concentration and analytical signal is given in Figure 3.8. As the acid concentration of the Bi solution increased, analytical signal increased in small amount. However, between 1.0 M HCl and 4.0 M HCl, there is no significant difference between the signal magnitudes. Thus, in order to use less chemical and produce less acid waste 1.0 M HCl was selected as an optimum concentration. Optimum values of other parameters which were studied up to this part were used during this study.

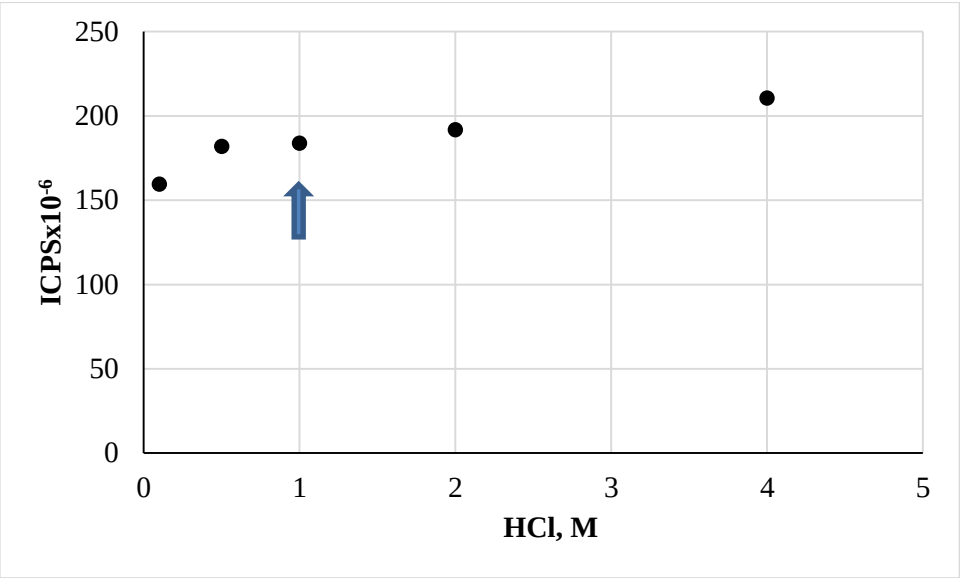

Figure 3.8. The optimization of HCl concentration for Bi determination by HG-ICPMS. 0.5% (w/v) $NaBH_4$ were used. Flow rates of $NaBH_4$, carrier acid solution and carrier Ar were 1.1 mL/min, 2.0 mL/min and 1.2 L/min, respectively.

Optimum values of five parameters for HG-ICPMS system using both U-tube and cylindrical GLS are listed in Table 3.3. Only the value for carrier Ar flow rate is different for these two GLSs.

Table 3.3. Optimum values of HG-ICPMS for Bi determination using U-Tube and Cylindrical GLSs.

	U-TUBE GLS	**CYLINDRICAL GLS**
Carrier Ar flow rate, L/min	*1.2*	*0.9*
$NaBH_4$ flow rate, mL/min	1.1	1.1
Sample flow rate, mL/min	2.0	2.0
Concentration of $NaBH_4$, %(w/v)	0.5	0.5
Concentration of HCl, M	1.0	1.0

3.2.2. Calibration Plot and Analytical Performance for Bi Determination by HG-ICPMS

Two calibration plots using peak heights for both GLS systems are given in Figure 3.9 and Figure 3.10, respectively. It was found that both of the plots were linear between the concentrations of 0.05 ng/mL and 10.0 ng/mL when the conditions used in Table 3.3. However, due to the memory effect problem higher concentrations were not studied above 10 ng/mL Bi concentration.

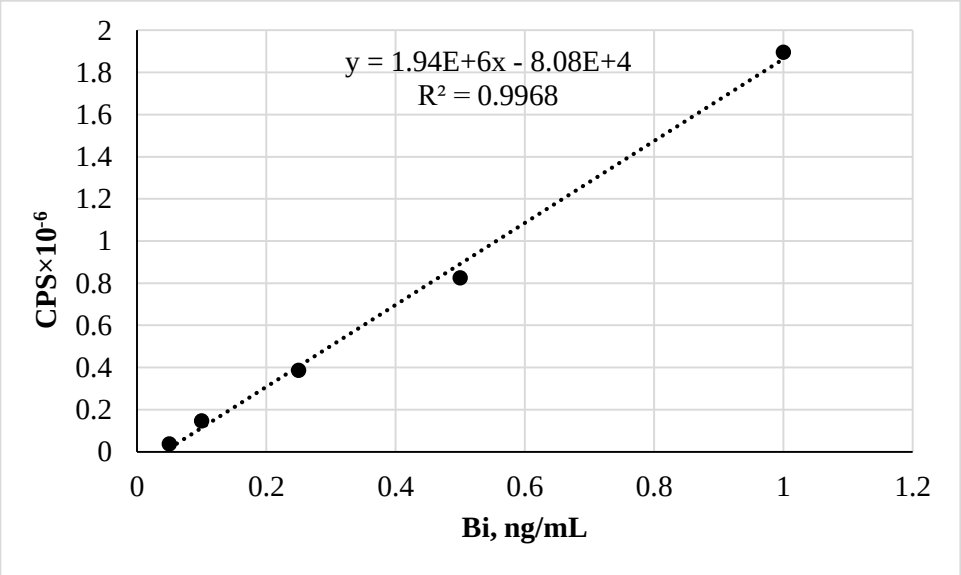

Figure 3.9. Calibration plot for Bi determination by using U-tube GLS and HG-ICPMS.

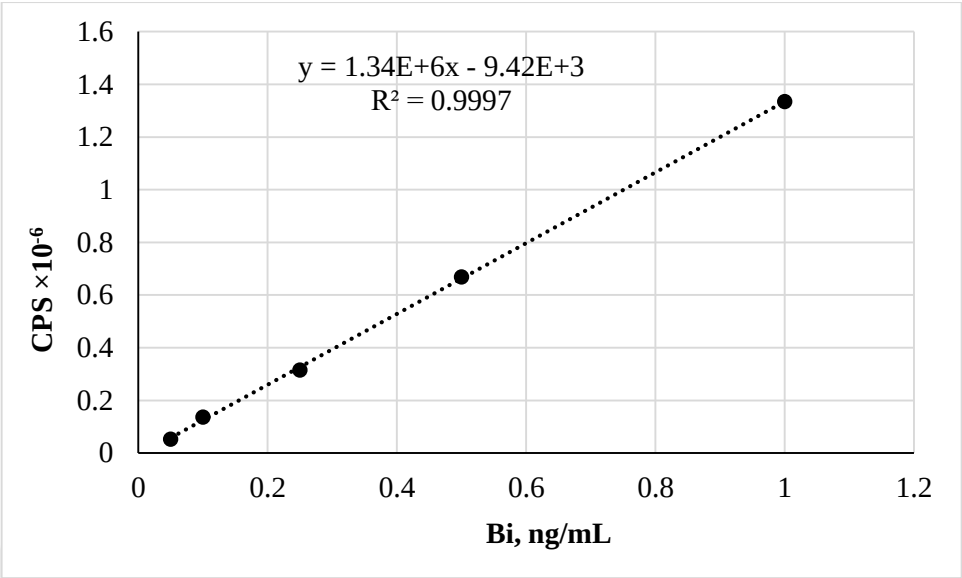

Figure 3.10. Calibration plot for Bi determination by using Cylindrical GLS and HG-ICPMS.

As seen from the calibration plots, slope sensitivity with U-tube GLS is 1.5 times higher than that of Cylindrical GLS. Additionally, the balance of liquid and gases due to the design of U-tube GLS compensate the noise resulted from H_2 generated from hydride which caused instability of the plasma. Therefore, U-tube GLS was used for the rest of the study.

Flow injection signals of blank, 0.05, 0.10 and 0.25 ng/mL Bi solutions in 1.0 M HCl obtained with U-tube GLS are given in Figure 3.11. Dwell time was 10 ms for this study.

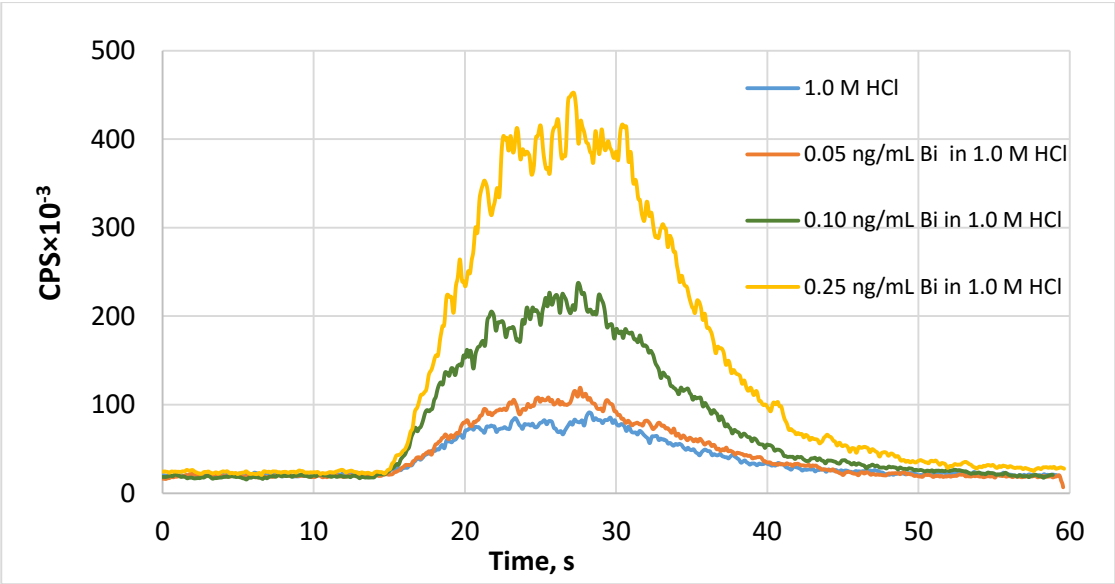

Figure 3.11. Flow injection signals of Bi by using U-tube GLS, HG-ICPMS and a loop of 500 µL.

Analytical figures of merit for Bi by HG-ICPMS are given in Table 3.4. Peak heights were used to calculate LOD and LOQ values. They were calculated from 5 replicate measurements of the smallest Bi concentration which was 0.05 ng/mL. Nebulization efficiency of ICPMS was calculated as 4.76% while transport efficiency of hydride is approximately 100%.[113,197] Slope of the calibration graph obtained from nebulization-ICPMS was 2.28×10^4 while it was 1.94×10^6 for HG-ICPMS. 85 fold enhancement in slopes was obtained as compared to nebulization system. %RSD value was calculated for lowest concentration similar to nebulization. Due to the higher noise obtained with HG system, %RSD value was worse than that of nebulization system.

Table 3.4. Analytical figures of merit for Bi determination by HG-ICPMS.

	^{209}Bi, ng/mL
LOD, (N=5)	0.010
LOQ, (N=5)	0.032
Range	0.050-10
%RSD	5.84

Some studies from literature are listed in Table 3.5 to compare the sensitivity of the HG-ICPMS study. The experimental parameters are not same for all the studies listed in this table. For example there are differences in the sensitivities of instruments. In some of the studies, blank signal was used to calculate LOD while lowest concentration was used for this study. More realistic RSD values were obtained when lowest concentration was used. Therefore, results found in this study are satisfactory.

Table 3.5. Comparison of LOD results with literature for Bi determination using HG-ICPMS.

Nebulization ICPMS, ng/mL	**Hydride Generation ICPMS, ng/mL**	**References**
0.021	0.010	*This work*
	0.030	*Chen et al., 2015* [47]
	0.002	*Fornieles et al., 2013* [48]
	0.002	*Zhang and Combs,1996* [96]
0.045	0.005	*Heitkemper and Caruso,1990* [50]

3.2.3. Accuracy Check for Bi Determination by HG-ICPMS

Accuracy of the system was checked by using NIST 1643e Natural Water Standard Reference Material. 50-fold dilution was applied to the original SRM solution and in final solution acid concentration was set to 1.0 M. Two replicates of SRM samples were

prepared and each was measured twice. Peak area measurements were used for the calculations. As it is seen from the Table 3.6, results were found in good agreement with certified value. Average of four measurements was found acceptable by applying t-test at 95% confidence level.

Table 3.6. Results of accuracy check for Bi determination by HG-ICPMS.

SRM	Certified, ng/mL	Found, ng/mL
NIST 1643e Natural Water	14.09 ± 0.15	14.50 ± 0.53

3.3. Determination of Bismuth by HG-W-Trap-ICPMS

After the study by HG-ICPMS, with the addition of W-coil to the system, trap studies were performed. By using a novel glass tube design that includes W-coil between Gas Liquid Separator and ICP-MS, produced bismuthine was collected on W-coil for 60 seconds. Collection/trapping on W-coil surface provides preconcentration of analyte species. H_2 gas was needed to protect W-coil from oxidation. Glass tube was placed on another glass part which includes electric connection for W-coil. In addition to H_2 gas entrance to the plasma, air diffusion from these glass connections causes the plasma instability. Therefore, long hours were spent to obtain stable plasma and to solve the problems at this part of the study.

When this system was connected to the ICPMS, during the ignition of plasma additional Ar (make-up Ar) was needed as shown in Figure 2.4. Ar gas flow continued throughout the experiment to prevent the entrance of air to the plasma and diluting the H_2 gas which causes the plasma instability.

3.3.1. Effect of Coating for Bi Determination

First experiments in trapping studies were performed with bare W-coil. The aim was to obtain repeatable and reproducible signals at the beginning and also to get familiar with W-trap system. However, uncoated coil was oxidized easily during optimization studies

and this situation prevents obtaining reproducible signals. Therefore, usage of coated W-coil was preferred during optimizations.

Coating of W-coil provides an improvement on trapping and releasing by modifying the surface. In other words, coating increases the trapping efficiency and prolongs the life-time of coil. [198, 162, 164, 15] During this study, coated W-coils were used up to 250 firings to eliminate the risk of decrease in trapping efficiency. After a while, coating material on the W-coil loses its property and cause a decrease in analytical performance.

In order to evaluate the effect of coating on trapping efficiency, Rhodium (Rh), Iridium (Ir) and Platinum (Pt) were used as coating materials for Bi. 0.25 ng/mL Bi in 1.0 M HCl solution was used for this part of the study. BiH_3 was collected for 30 s when flow rates of make-up Ar and H_2 were 125 and 106 mL/min, respectively. For each coating, average of 8 measurements was done. As it is seen from Table 3.7, among three types of coatings, trapping efficiency of Ir-coating was the best. Approximately 3 times increase in signal was obtained with this coating. Therefore, optimizations were done with Ir-coated W-coil. However, in the earlier studies of our research group uncoated W-coil was used for Bi determination.[15,163] After setting the optimum flow rate of H_2 to prevent W-coil from oxidation, reproducible results were obtained with bare coating in their studies.

Table 3.7. Effect of different coating materials for Bi determination by HG-W-Trap-ICPMS. Concentration of Bi was 0.25 ng/mL. Flow rates of make-up Ar and H_2 were 125 and 106 mL/min, respectively.

	Uncoated, N=8	**Rh-coated, N=8**	**Pt-coated, N=6**	**Ir-coated, N=8**
CPS, x±s	$(18.9 \pm 1.7) \times 10^5$	$(27.9 \pm 3.5) \times 10^5$	$(44.2 \pm 6.9) \times 10^5$	$(56.1 \pm 4.6) \times 10^5$
%RSD	8.96	12.5	15.6	8.13

3.3.2. Optimization for Bi Determination by HG-Ir coated-W Trap-ICPMS

For W-trap studies make-up Ar and H_2 flow rates, trapping and releasing temperatures and finally trapping period were optimized to get best S/N ratios. For optimization studies, 0.25 ng/mL Bi solution in 1.0 M HCl was used. Apart from trapping period optimization, trapping period was set to 30 seconds. Applied trapping and revolatilization temperatures were 179 and 1600 ^{o}C, respectively at the beginning of the optimization experiments.

3.3.2.1. H_2 Gas and Make-up Ar Flow Rate

H_2 is important for trap studies to protect W-coil from oxidation. However, presence of H_2 in the system disturbs the plasma and to enable plasma stability make-up Ar was directed to the plasma to sustain the stability of the plasma. The optimization graph of H_2 gas and make-up Ar flow rates are given in Figure 3.12 together. Below 75 mL/min H_2, W-coil started to oxidize quickly. Afterwards, in order to decrease the oxidation rate of W coil, flow rate was increased to 90 and then to 106 mL/min. Higher flow rates were not tried by considering the plasma stability. In addition, optimum value was 70 mL/min H_2 in *Cankur et. al*'s study.[15] For the optimization of H_2 flow rate, high flow rates of make-up Ar were used and it was seen that when flow rate of Ar was higher than 343 mL/min signal decreases sharply due to the dilution effect of bismuthine. Trend for H_2 was converse to make-up Ar. When H_2 flow rate was increased at fixed Ar flow rate, small increase was observed in signal magnitude. It can be concluded that up to critical value H_2 did not show dilution effect instead increases the transport of bismuthine to the plasma.

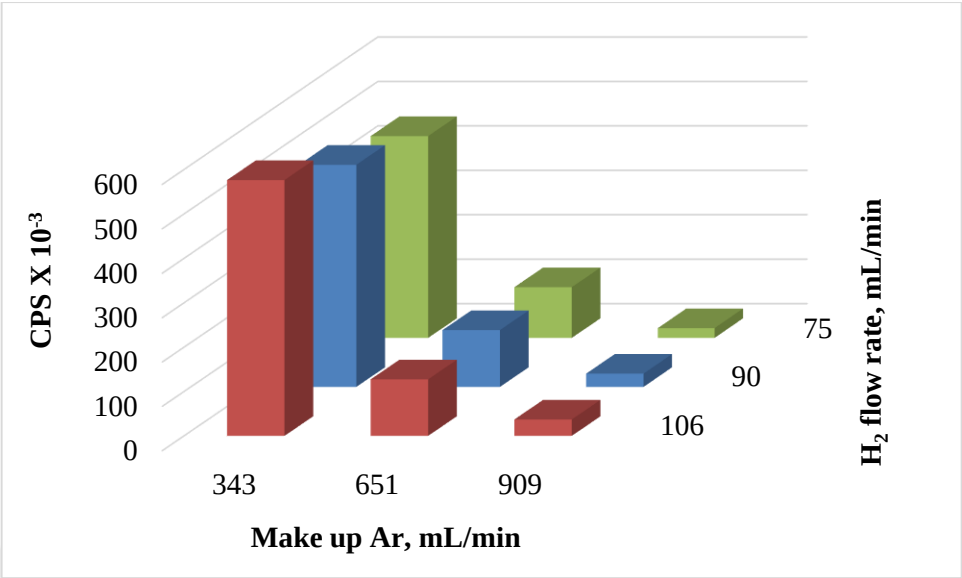

Figure 3.12. The optimization of make-up Ar and H_2 flow rates for Bi determination by HG-Ir coated-W Trap-ICPMS. Concentration of Bi was 0.25 ng/mL in 1.0 M HCl. Trapping and releasing temperatures were 179 and 1600 ºC, respectively.

As seen from Figure 3.12 when flow rate of make-up Ar is high low signals were obtained therefore lower flow rate for make-up gas were also was studied at optimized H_2 flow rate which was 106 mL/min. Tolerance of the plasma was changing when there was no make-up Ar. Sometime plasma resists the H_2 entrance without the help of Ar but another time it cannot resist and gone out. Optimization graph of make-up Ar flow rate is given in Figure 3.13. Flow rate of H_2 was fixed at 106 mL/min. When the make-up gas flow rate was 125 mL/min, maximum signal was obtained and the plasma was stable. Therefore, combination of 106 mL/min H_2 flow rate and 125 mL/min make-up Ar flow rate was selected as an optimum for trap study.

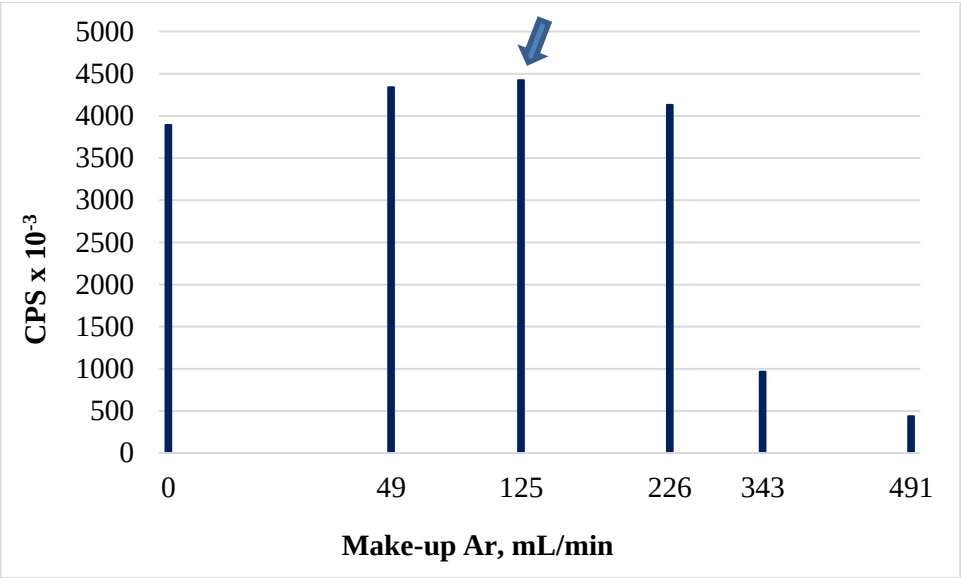

Figure 3.13. The optimization of make-up Ar flow rates for Bi determination by HG-Ir coated-W Trap-ICPMS. Concentration of Bi was 0.25 ng/mL in 1.0 M HCl. Trapping and releasing temperatures were 179 and 1600 ^{o}C, respectively. Flow rate of H_2 was 106 mL/min.

3.3.2.2. Trapping Temperature

To provide efficient trapping, optimization of applied temperature is important. Temperature of the W-coil at applied voltages was measured by using thermocouple. During temperature measurements H_2 and make-up Ar flows were on and system was not connected to plasma. 700 °C was the highest temperature that was measured with thermocouple in this study. Voltage vs. temperature relationship for thermocouple is given in Figure 3.14. Then, by using this relation optimization graph of trapping temperature was drawn and given in Figure 3.15. W-coil is heated by using the variac and temperature depends on the applied voltage. At low voltages, temperature was not sufficiently high for effective trapping. Although the signal increased up to 700 ^{o}C, 179 ^{o}C was selected as an optimum since at higher trapping temperatures lifetime of the coil decreases. In addition, when temperature was higher than 700 ^{o}C, high temperature causes volatilization of the trapped species. Therefore, signal decreases sharply. During this optimization, trapping period was 30 s, releasing temperature was 1600 ^{o}C and flow

rates of H_2 and make-up Ar were 106 and 125 mL/min, respectively. Revolatilization period was approximately 3 seconds and it is long enough to obtaining the transient signal.

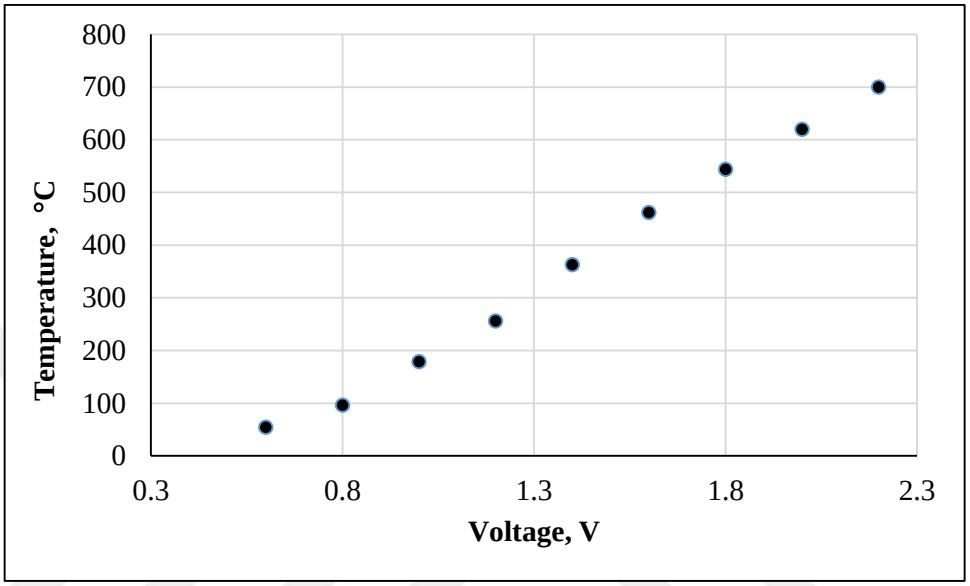

Figure 3.14. Temperature vs. voltage relationship using thermocouple.

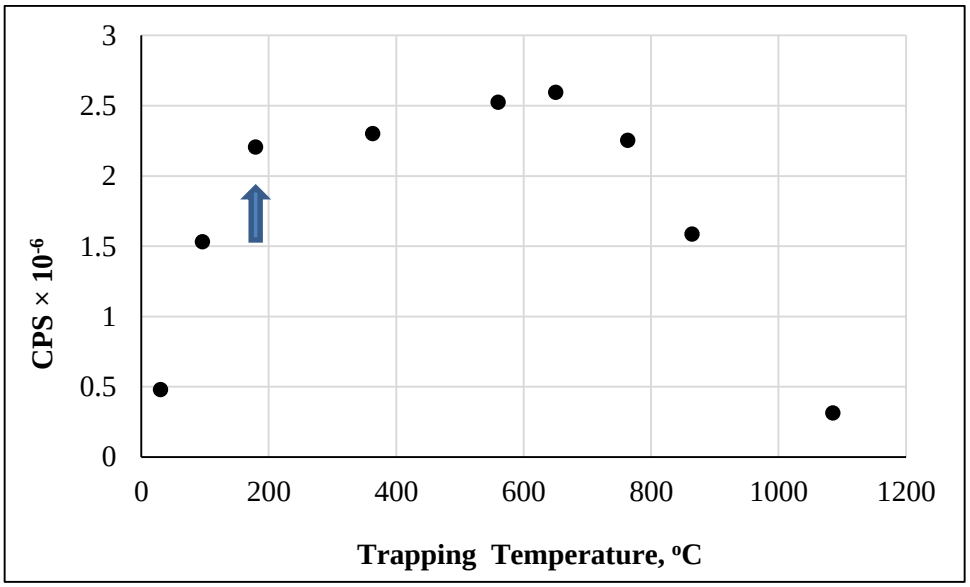

Figure 3.15. The optimization of trapping temperature for Bi determination by HG-Ir coated-W Trap-ICPMS. Concentration of Bi was 0.25 ng/mL in 1.0 M HCl. Releasing temperature was 1600 °C. Trapping period was 30 s. Flow rates of H_2 and make-up Ar were 106 mL/min and 125 mL/min, respectively.

Species on trap surface are not in hydride form. Their forms must have been chemically altered to enable trapping on the W-coil. *Kula and co-workers*[164] suggested that their analyte Se was trapped as selenium atoms. However, they did not prove their hypothesis with experiments. On the other hand, *Kratzer and Dedina*[170] mentioned that their trapped species were selenium oxide which was collected on quartz surface.

For this study Ir-coated W-coil on which Bi species were trapped was analyzed by X-Ray Photoelectron Spectroscopy (XPS). The aim was to check the presence of coating and trapped Bi. 50 ng/mL Bi solution in 1.0 M HCl was used for trapping. Trapping period was 1.0 min and trapping cycle was applied 10 times to trap enough Bi species on the surface for XPS measurement. Flow rate of analyte solution and $NaBH_4$ were 2.0 mL/min and 1.1 mL/min, respectively. Flow rates of H_2 and make-up Ar were 106 mL/min and 125 mL/min, respectively. Spectrum of XPS is given in Figure 3.16. As it is seen from the spectrum, main peaks belong to O, C, W, Ir, N and Bi. This spectrum is satisfactory to prove that W-coil could be coated well with the proposal coating procedure. In addition, Bi analyte species can be trapped on coated W-coil at 179 ^{o}C. The source of the W peaks was coil itself while that of O, N and C peaks was the air and also water vapor on the coil. With the XPS measurements, the chemical form of trapped species can also be determined. However, in order to find a satisfactory answer about chemical form of species scanned region should be restricted and reference species must also be analyzed.

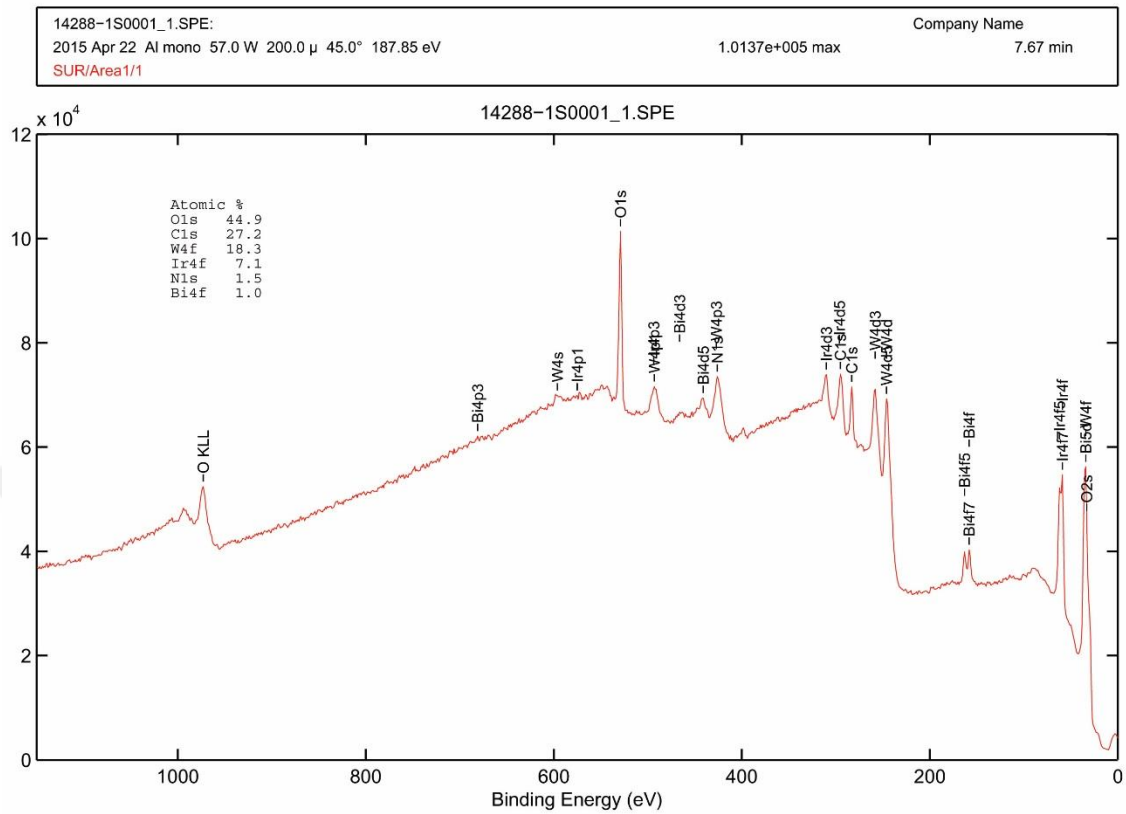

Figure 3.16. XPS spectrum of Ir-coated W-coil with trapped Bi species.

3.3.2.3. Revolatilization Temperature

After trapping of the bismuthine on W-coil effectively, all trapped species should be volatilized at once for sharper signals. Similar to the trapping studies, for revolatilization step power supply was used but this time higher voltages were set for revolatilization. Higher the voltage means higher the temperature of the coil. Unfortunately thermocouple was not suitable for measurement of higher temperatures so pyrometer was used for the calibration of voltage to temperature. To check the accuracy of the results, pyrometer was calibrated using graphite furnace AAS. Working range was from 900 ^{o}C to 1700 ^{o}C. Applied voltage vs. temperature relationship for pyrometer is given in Figure 3.17. At low temperatures, shapes of the signals were broad and smaller in magnitude. When temperature was increased from 1418 ^{o}C to 1590 ^{o}C, signals became

sharper and signal peak height increased significantly. Therefore, 1590 ^{o}C was selected as the optimum value. It is expected that with an increase in revolatilization temperature, signal increases up to a point where maximum revolatilization efficiency is reached and then signal is expected to stay constant with further increase in temperature. However, the results exhibited somehow a different trend. When 1850 ^{o}C was applied, a decrease in signal magnitude was observed. The reason of this situation can be the deterioration of coating materials. Peak shapes of the signals, which were obtained at 1590 ^{o}C and 1850 ^{o}C, were evaluated and no significant difference was observed. The correlation between revolatilization temperature and analytical signal was observed by varying the temperature between 1240 ^{o}C and 1850 ^{o}C and the results are given in Figure 3.18. During this optimization, trapping time was 30 s, trapping temperature was set to 179 ^{o}C and flow rates of H_2 and make-up Ar were 106 and 125 mL/min, respectively.

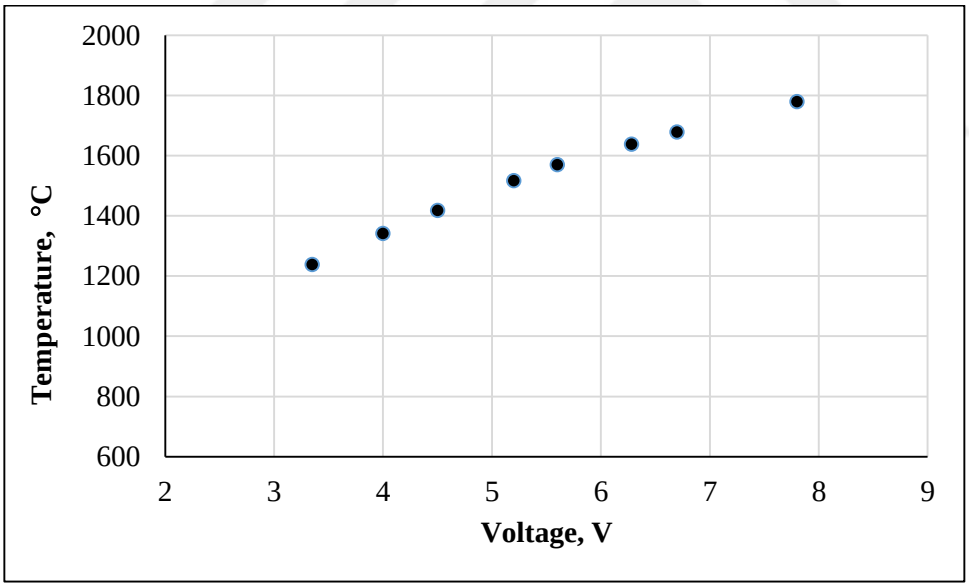

Figure 3.17. Temperature vs.voltage relationship for pyrometer using ETAAS.

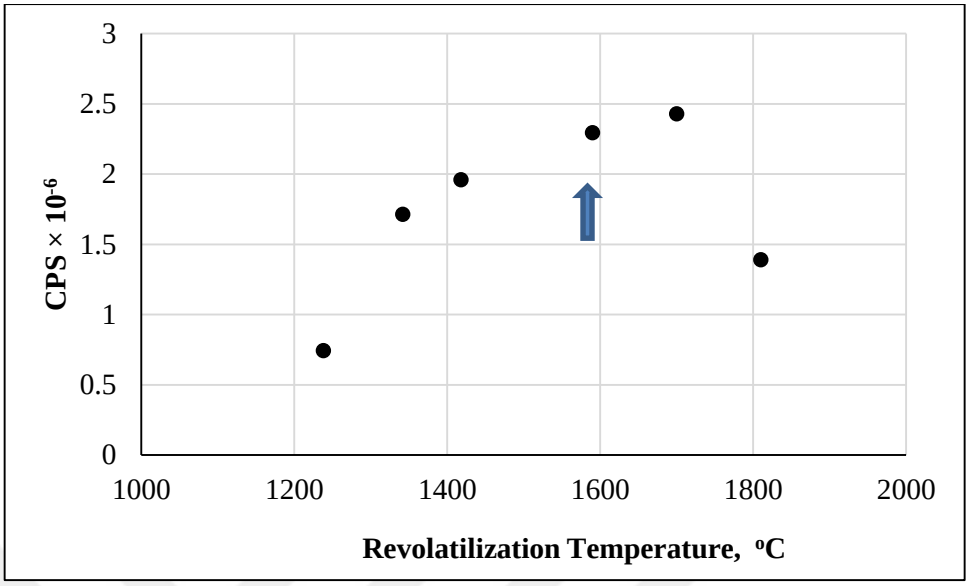

Figure 3.18. The optimization of revolatilization temperature for Bi determination by HG-Ir coated-W Trap-ICPMS. Concentration of Bi was 0.25 ng/mL in 1.0 M HCl. Trapping temperature was 179 ºC. Trapping period was 30 s. Flow rates of H_2 and make-up Ar were 106 mL/min and 125 mL/min, respectively.

Nature of revolatilized Bi species was proposed as either molecular or short-lived atomic form by *Cankur and coworkers.*[15] They reached to this conclusion since they did not obtain any signal when silica T-tube was not heated in their study.

3.3.2.4. Trapping Period

Last parameter to be optimized was the trapping period for W-coil trap study. Optimization graph for trapping period is given in Figure 3.19. Trapping period is directly related with the signal magnitude. It means longer the trapping period, bigger the signal due to an increase in trapped analyte species up to some limit since increase in blank signal and/or trapping of interfering species prevent further development in signals. 15 s was the shortest time period tried for this optimization. From 15 s to 180 s there was a linear increase in the signals. In terms of time efficiency of whole analysis 60 seconds were chosen as an optimum trapping period.

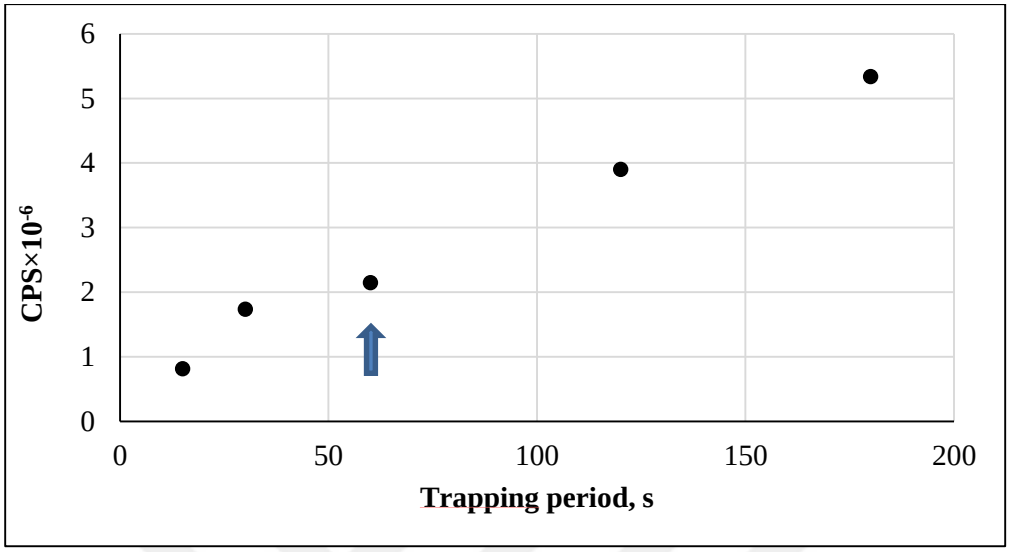

Figure 3.19. The optimization of trapping period for Bi determination by HG-Ir coated-W Trap-ICPMS. Concentration of Bi was 0.25 ng/mL in 1.0 M HCl. Trapping and revolatilization temperatures were 179 ºC and 1600 ºC, respectively. Flow rates of H_2 and make-up Ar were 106 mL/min and 125 mL/min, respectively**.**

Optimum values were selected not only obtaining a sensitive system but also to keep the performance of the HG-W-Trap-ICPMS system in good condition. It means at optimum conditions there must not be the risk of plasma extinguishing. Optimum values are summarized in Table 3.8.

Table 3.8. Optimum values for Bi determination by HG-Ir-Coated-W Trap-ICPMS system.

H_2, mL/min	106
Make-up Ar, mL/min	125
Trapping T, ºC	179
Revolatilization T, ºC	1590
Trapping Period, s	60

3.3.3. Calibration Plot and Analytical Performance for Bi Determination by HG-W-Trap-ICPMS

By using the optimum values, calibration plots of Bi using HG-W-Trap-ICPMS system were drawn for Ir-coated and uncoated W-coil. The measurements were based on peak height of the analytical signal. The calibration plots which were obtained for Bi standard solutions ranging from 0.010 ng/mL to 0.50 ng/mL are given in Figure 3.20 and Figure 3.21 for uncoated and Ir-coated W-coil systems, respectively. The plots are linear ranged from 0.010 ng/mL to 10.0 ng/mL Bi concentrations for both systems. As it is seen from the plots, slope of Ir-coated W-coil system was better 1.4times than slope of uncoated W system. In the study from *Cankur and co-workers*,[15] linear range was up to 0.50 ng/mL for trap study by AAS while range was linear up to 10.0 ng/mL in this study by ICPMS. As expected, linear range of the ICPMS is wider than that of AAS.

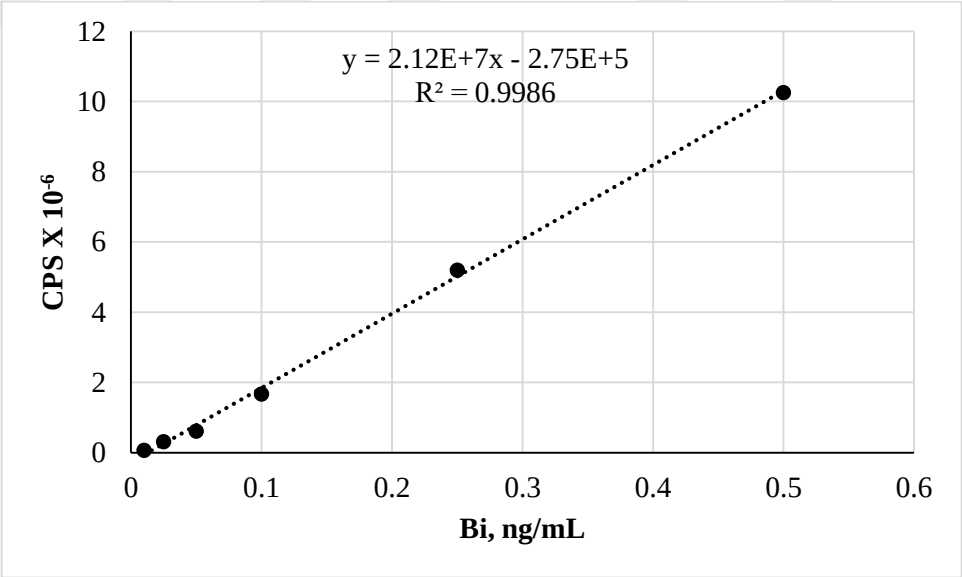

Figure 3.20. Calibration plot for Bi determination by HG-uncoated-W Trap-ICPMS.

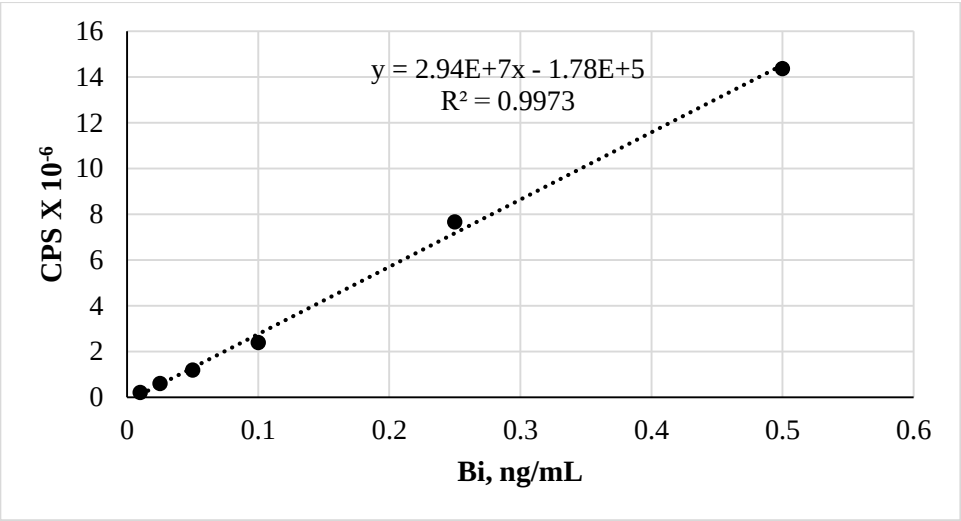

Figure 3.21. Calibration plot for Bi determination by HG-Ir coated-W Trap-ICPMS.

LOD, LOQ and %RSD values of this novel system were calculated for Ir-coated and un-coated W-coil systems, separately. Peak height values were used. For this W-coil system, analytical performance was calculated by using 0.01 ng/mL Bi concentration. For reliable comparison, same conditions were used when coil was replaced with the other one. Analytical performances of the uncoated and Ir-coated W-coil systems are given in Table 3.9. Slopes of the calibration graphs and analytical performances show that Ir-coating helped to increase the sensitivity of the system. More importantly, by coating reproducibility of the system increased.

Table 3.9. Analytical figures of merit for Bi determination by HG-Uncoated-W Trap-ICPMS and HG-Ir coated-W Trap–ICPMS.

	Uncoated, ng/mL	**Ir-coated, ng/mL**
LOD, (N=8)	0.0034	0.0027
LOQ, (N=8)	0.011	0.0090
Range	0.010-10.0	0.010-10.0
%RSD	7.7	6.3

In order to evaluate results of this study comparison was made with the studies in literature. Since there are no studies used W trap coupled to ICPMS, the results obtained in this study are compared with HG-W-Trap studies performed by using AAS and AFS. Results of the comparisons are given in Table 3.10. Improvements were calculated considering E_t and E_v term which were introduced by *Ataman*.[150] E refers to Enhancement factor (ratio of characteristic concentrations), Et= E/(minutes of sampling), min^{-1} and Ev= E/(milliliters of sample), mL^{-1}. These terms are better for comparison because different time periods or different volumes are used for different studies. Since AAS is not as sensitive as ICPMS, LOD values for HG systems using AAS are approximately 45 times higher than that of ICPMS. Hence, W-Trap system coupled to AAS and AFS causes large enhancement in sensitivity. In addition, with and without trap systems of HG were compared, *Cankur and co-workers*[15] obtained 137 folds enhancement while in this study enhancement was only 3.3 folds. The reason of this big difference was the good fixation of the W-coil to the quartz tube. They fixed and sealed the coil from the outside by using a temperature resistant alumina based powder material. Al_2O_3 powder was mixed with sodium silicate solution to form viscous slurry. This slurry was used and then quartz tube with W-coil was dried at room temperature for at least 2 days. This provides perfect isolation which is required good trapping-volatilization performance. However, enhancements for this study are comparable to the other works if coupled systems performances are considered.

Table 3.10. Comparison of the results for Bi determination by HG-Ir coated-W Trap–ICPMS with literature.

Method	Coating Material	Without Trap LOD, ng/L	With Trap LOD, ng/L	E	E_t, min^{-1}	E_v, mL^{-1}	Reference
HG-ICPMS	Ir	10	3	3.3	3.3	1.7	*This work*
HG-AFS	Ir	90	4	23	11	1.9	*Liu et al. 2008*[156]
HG-AAS	uncoated	470	25	19	19	2.4	*Kula et al. 2009*[163]
HG-AAS	uncoated	410	3	137	46	7.6	*Cankur et al. 2002*[15]

3.3.4. Accuracy Check for Bi Determination by HG-Ir coated-W Trap-ICPMS

To check the accuracy of the HG-Ir coated-W Trap-ICPMS system, "1643e Trace Elements in Water SRM was used. The SRM was diluted 200 times and in the final solution acid concentration was 1.0 M HCl. Similar to the previous SRM studies, direct calibration method was used. Two SRM samples were prepared and each was measured four times. Results which were found in good agreement with the certified value are given in Table 3.11. Average of eight measurements was found acceptable by applying t-test at 95% confidence level.

Table 3.11. Results of accuracy check for Bi determination by HG-Ir-coated-W Trap-ICPMS.

SRM	Certified, ng/mL	Found, ng/mL
NIST 1643e Natural Water	14.09 ± 0.15	12.87 ± 1.60

Four different methods were tried stepwise to get a very sensitive system for Bi determination. With the addition of HG system, trapping and coating parts, sensitivity of bare ICPMS increased approximately one order of magnitude. LOD, %RSD and signals of lowest concentration and also slopes of calibration graphs for four methods by using peak height measurements are summarized in Table 3.12.

Table 3.12. Analytical figures of merits for Bi determination by the four methods.

	Lowest Conc, ng/mL	**x±s, CPS**	**%RSD**	**LOD, ng/L**	**Slope**
ICPMS	0.1	$(3.85 \pm 0.16) \times 10^3$	4.17	21	0.02×10^6
HG-ICPMS	0.05	$(10.5 \pm 0.61) \times 10^4$	5.84	9.5	1.9×10^6
HG-W-trap-ICPMS (60 s)	0.01	$(32.0 \pm 2.45) \times 10^4$	7.68	3.4	21×10^6
HG-Ir-coated-W-trap-ICPMS (60 s)	0.01	$(43.6 \pm 2.75) \times 10^4$	6.30	2.7	29×10^6

Transport efficiencies of nebulization and HG which are approximately 5% and 100%, respectively. By considering this information, nearly 20 times enhancement is expected using HG system. However, for this system about 2 times improvement was obtained when HG system was used. There are two reasons of this situation. First, plasma composition changes when HG system was coupled to ICPMS. H_2 gas which is the side product of hydride formation reaction affects the plasma composition. Therefore plasma conditions are different than those in nebulization. To check this situation, $^+Ar_2$ (Ar-dimer) signals was monitored for both systems. It was observed that Ar-dimer signal was affected differently for nebulization and HG systems for the same concentration of solution. Signal for HG case was 2 times higher than that for nebulization. In *Heitkemper and Caruso's*[50] work, for four different elements, which were Bi, As, Se and Te, maximum 9 times improvement in LOD were obtained when HG system was

coupled to ICPMS. Second reason is that nebulization and HG systems were not studied for the same plasma conditions. In other words, an analytical performance of the HG system was evaluated in different day and may be with different optimum parameters of the ICPMS.

3.3.5. Trapping Efficiency Calculations for Bi Determination

For trap studies, trapping efficiency of the W-coil is important and has to be calculated. Trapping efficiency depends on the H_2 and make-up Ar flow rates, trapping temperature, coating and collection period. For this part of the study, 0.25 ng/mL Bi standard solution was used. Bismuthine was trapped on Ir-coated W-Coil for 30 seconds. Continuous signals before trapping and during trapping period are seen in Figure 3.22. Voltage was turned on to start trapping at 30th second of the analysis. When trap starts the signal decreases compared to without trap conditions since analyte species are trapped on the surface of the coil and this decreases the concentration of the Bi species in plasma. This in turn decreases the signal intensity at trapping experimental conditions. At the end of trapping period, transient signals obtained by applying high releasing temperature. Trapping temperature was 179 ^{o}C, releasing temperature was 1600 ^{o}C and flow rates of H_2 and make-up Ar were 106 and 125 mL/min, respectively.

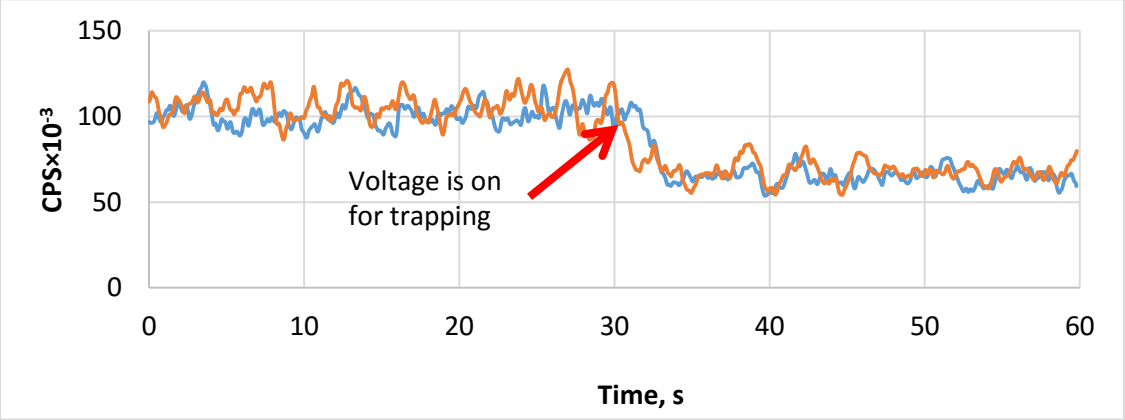

Figure 3.22. Continuous signals of 0.25 ng/mL Bi before and during trapping period by HG-Ir coated–W Trap-ICPMS. Trapping temperature was 179 ^{o}C. Trapping period was 30 s. Flow rates of H_2 and make-up Ar were 106 and 125 mL/min, respectively.

Trapping efficiency was calculated in two ways. For the first way, counts per second (cps) values before and during trapping were used. The extent of the decrease in cps for continuous signal to cps before trapping gives the efficiency of the trapping. By this way trapping efficiency of Bi with Ir-coated W-coil was found as 40% for 30 s collection.

Trapping Efficiency, % = (cps difference between trapping and hydride / cps for hydride) x 100

This estimation was different than that was proposed by *Liu and coworkers's*.[156] In their calculations they do not use the signal difference before and during trapping and also they care the periods of continuous and trapping signals. Equation is given below. Signal intensity of trapped analyte (S_t) per trapping time and that of conventional hydride generation (S_c) per sampling time. Trapping efficiency of Bi was found as 73% by using this equation.

Trapping Efficiency, % = $[(S_t/t_{trapping}) / (S_c/t_{sampling})] \times 100$

The other way was the calculation of *operational trapping efficiency*. It was calculated by taking the ratio of peak area of transient signal to the area of the continuous HG signal before trapping.

Operational Trapping Effic, % = (peak area of transient signal/peak area of hydride signal) x 100

Contrary to first one, conditions for the two signals compared are very different. Pumps were stopped during revolatilization step while they were on during trapping cycle. The transient signal was recorded while there is a rapid gas expansion since W-coil was heated to a high temperature. In the mentioned conditions operational trapping efficiency was calculated as 29% for 30 s trapping period. Transient signals for duplicate analysis are given in Figure 3.23.

As expected, in the second calculation, the efficiency was found to be lower. In the first method only trapping efficiency has been calculated. The losses of analyte on inner

surfaces and degree of recovery from W-coil surface are not reflected in the calculations. On the other hand, in the second method all of these effects were included and an overall efficiency was found. Naturally the second figure turned out to be lower.

At the end of trapping period, pumps were stopped and variac voltage was adjusted manually. That's why small shifts in time were observed for transient signals.

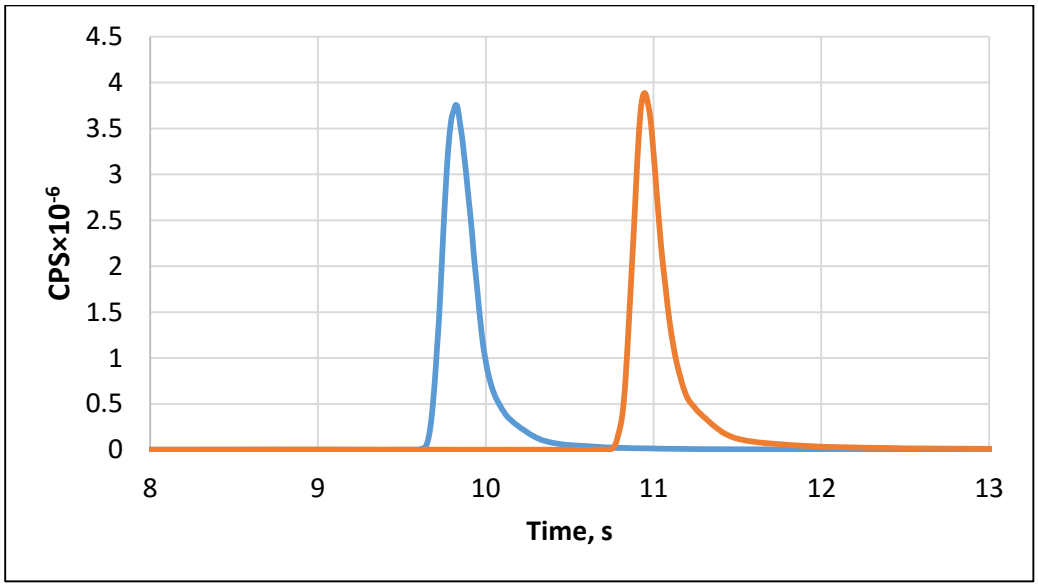

Figure 3.23. Transient signals of 0.25 ng/mL Bi by HG-Ir coated–W Trap-ICPMS. Releasing temperature was 1600 ºC. Flow rates of H_2 and make-up Ar were 106 and 125 mL/min, respectively.

3.3.6. Dwell Time and Smoothing Studies for Bi Determination

"Dwell time" term is specific to ICPMS and depending on the selected dwell time signal quality differs. Number of points per peak obtained are influenced by number of m/z monitored and dwell time. If dwell time increases at fixed scan time, the number of points defines the peak decreases. When the number of points on the peak decreases, the uncertainty will increase. On the other hand, if dwell time is very small, this will deteriorate the sensitivity. Therefore, for optimum dwell time value, 10, 20, 50 and 100 ms dwell times were set and results were discussed as follows. This study was

performed after Te determination experiment. For this study, Pt-coated coil was used in order to compare the effect of dwell time on the signal shapes of Bi and Te. Flow rate of H_2 and make-up Ar was 106 mL/min and 125 mL/min, respectively. Concentration of the Bi solution was 0.50 ng/mL during this study. "Peak hopping" mode of the instrument was used during this study. Signals of 0.50 ng/mL Bi solution when dwell time was set to 10 ms, 20 ms, 50 ms and 100 ms are given in Figure 3.24, respectively.

Transient signals were drawn by using OriginPro 8 program. For Bi, the peak width at half maximum is about 0.2 s. When dwell time was increased from 10 ms to 100 ms, there was no change on peak width however signal magnitude decreased gradually as seen from Figure 3.24. Therefore, 10 ms was selected as an optimum dwell time to keep the sensitivity at maximum value. Similarly, in literature mostly 10 ms dwell time has been chosen for simultaneous determination of high number of elements by ETV-ICPMS.[185,193,194]

Smoothing is applied to the signals in order to remove the noise. However, a criterion in smoothing process is not to lose the original magnitude of the signal. Signal magnitude is important for transient signals since peak height values are used for LOD, LOQ etc. There are different smoothing methods that work differently depending on the nature of the signal and the noise contained in signal. Among them "*Adjacent-Averaging*" method was selected for smoothing process in OriginPro 8 program. With a signal that contains normally distributed noise; adjacent-averaging is good choice for removing the background noise. In this method, average of user specified number of data points around each point in data is replaced with original data. 10 points and 20 points smoothing were applied to the signals obtained for dwell time studies and results were compared to signals without smoothing. When dwell time was longer, smoothing affected the signal shape and magnitude drastically as shown in Figure 3.24. With this type of smoothing process not only signal magnitude decreased but also peak became wider. This can be explained by moving box approach used for smoothing process. Therefore, in order to use real points, smoothing was not preferred for this study. Smoothed signals of 0.5 ng/mL Bi solution are given in Figure 3.24 when four different

dwell times were used. In conclusion, 10 ms dwell time and no smoothing were used for Bi determination in trap studies.

If smoothing is necessary, again it is clear that 10 ms dwell time is the best choice. Because signal magnitude is affected less at this value.

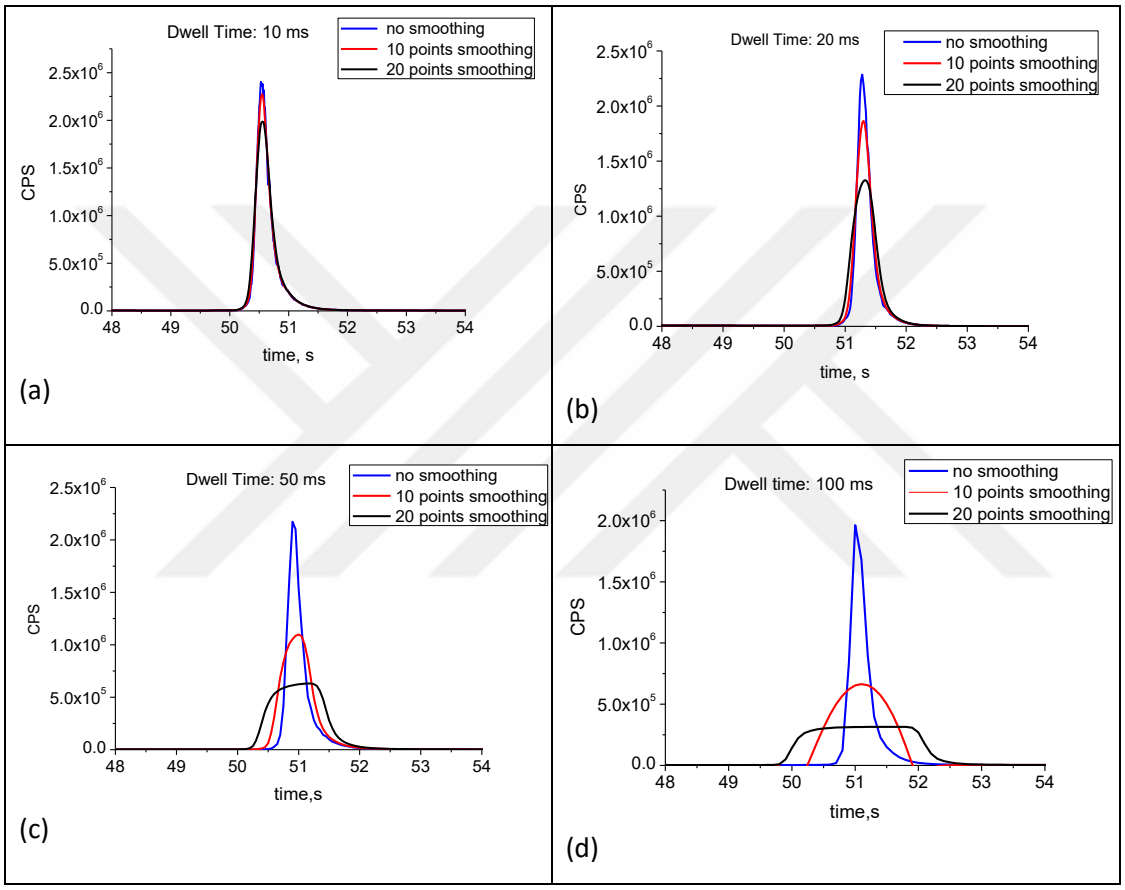

Figure 3.24. Transient signals of 0.50 ng/mL Bi by HG-Pt coated–W Trap-ICPMS when dwell time is (a) 10 ms, (b) 20 ms, (c) 50 ms, (d) 100 ms and smoothing process is applied.

3.4. Determination of Tellurium by ICPMS

After sensitive novel method was developed for Bi by HG-W-Trap-ICPMS, possibility of multi-element determination was evaluated with this system. Tellurium (Te) was selected as a second element since hydride formation conditions are similar to that of Bi, there is no risk of interference from Cl^- ion used to acidify analyte solution unlike in

Arsenic (As) case.[199] In addition, Te is a toxic element even at lower concentrations so sensitive method is necessary to determine Te at trace levels. When first trial results of multi-element study was promising, experiments were also performed for determination of Te alone to compare with multi-element study.

Similar to Bi, determination of Te was done by nebulization system first to compare with HG-ICPMS and HG-W-Trap-ICPMS studies.

3.4.1. Calibration Plot and Analytical Performance for Te Determination by ICPMS

Optimizations of instrumental parameters were done to get the best sensitivities. Then, calibration solutions of Te were prepared in the range between 0.25 ng/mL and 25 ng/mL in 2.0 M HCl solution. Flow injection system with a loop volume of 500 µL was used as in Bi studies. 1.0 M HCl solution was used as a carrier solution. Concentrations higher than 25 ng/mL were not prepared for this study since range from 0.25 ng/mL to 25 ng/mL was wide enough with two orders of magnitude. Calibration plot was linear up to 25 ng/mL and given in Figure 3.25.

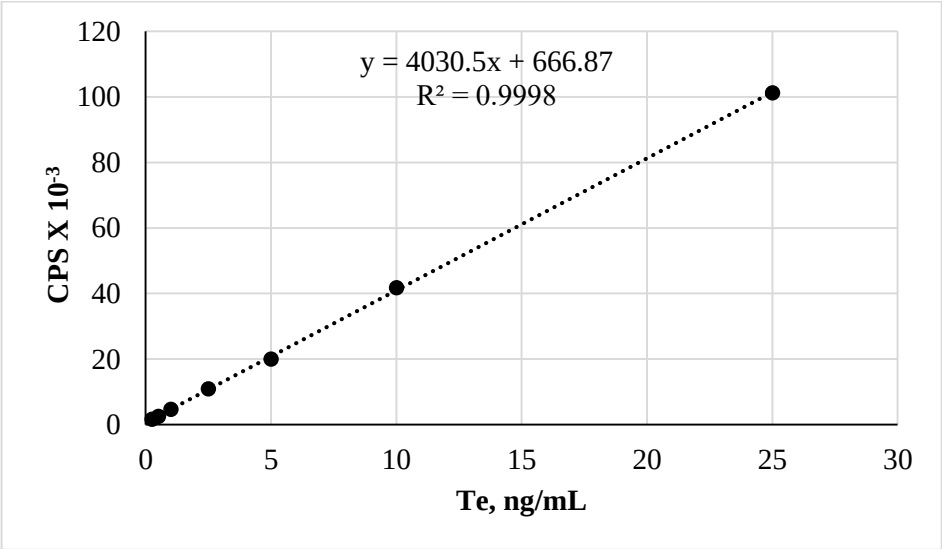

Figure 3.25. Calibration plot for Te determination by ICPMS.

Calibration plot by using the lower concentrations of Te solutions are given in Figure 3.26. Peak height values were used for each system.

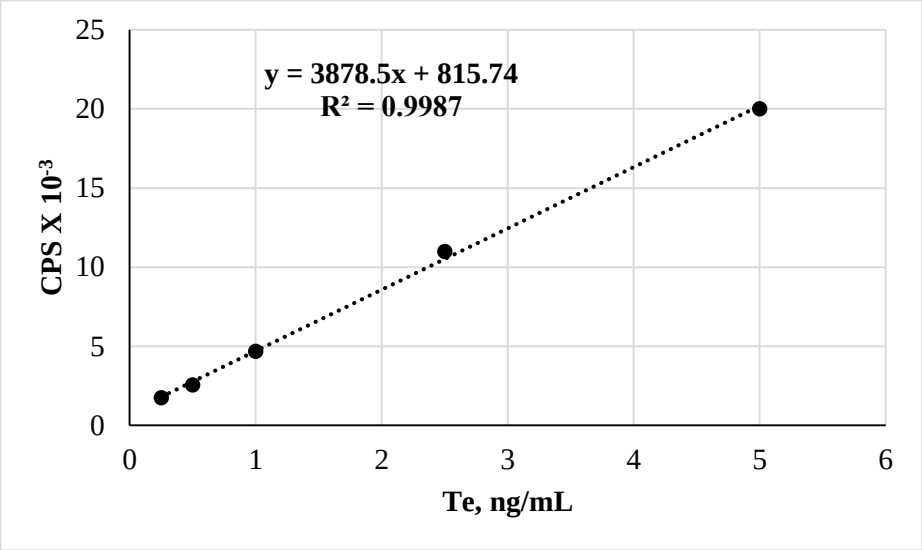

Figure 3.26. Calibration plot for Te determination between 0.25 ng/mL and 5.0 ng/mL using ICPMS.

Te has eight naturally occurring isotopes (Table 2.2). At mass number 125 there is no other stable isotopes from other elements which can interfere but the natural abundance of ^{125}Te is only 7.1%. On the other hand, natural abundance of ^{130}Te is 34.5%. Possible interference of ^{130}Xe, which is found in Ar gas as an impurity, was checked on ^{130}Te by comparing the Te signals with and without ^{129}Xe correction at the same plasma condition. At mass 129 there is no other stable isotope except ^{129}Xe which has 26.4% abundance. PlasmaLab software uses an equation to correct interferences using mathematical algorithms. Correction equation for ^{130}Te is $^{130}Te^{+} = {}^{130}M^{+} - 0.15431 \times {}^{129}Xe^{+}$. In this equation 0.15431 is the ratio of percent natural abundances for ^{130}Xe to ^{129}Xe (4.1/26.4). Magnitude of ^{130}Xe signal is calculated by using this ratio together with signal corresponding to ^{129}Xe and then by subtracting the value obtained from the 130 mass signal ($^{130}M^{+}$) which corresponds to interference-free magnitude of ^{130}Te signal. Comparisons of the corrected and uncorrected magnitudes of ^{130}Te signals showed no significant difference. Therefore, as no interference was observed, ^{130}Te was monitored

for method development parts of this study contrary to the studies mentioning ^{130}Xe interference even when ultra-pure argon was used.[76,91] *Yang et al.* evaluated the $^{130}Te/^{125}Te$ ratio for solutions when there was no Te and Te concentration increased in the solution. They observed that when there was no Te, ratio was higher due to the ^{130}Xe interference. As Te concentration increased, $^{130}Te/^{125}Te$ ratio came close to that of natural abundances. It is worth to mention that Sector-Field-ICPMS, which is more sensitive than Quadrupole-ICPMS, was used in *Yang et al.'s* study.[76] However, in our study the interference from Xe was insignificant.

LOD, LOQ and %RSD values of Te for ICPMS system were calculated by using peak height measurements. They were calculated from 8 replicate measurements of smallest Te concentration which was 0.25 ng/mL. Analytical figures of merit for Te by ICPMS are given in Table 3.13.

Table 3.13. Analytical figures of merit for Te determination by ICPMS

	^{130}Te, ng/mL
LOD, (N=8)	0.029
LOQ, (N=8)	0.097
Range	0.25-25
%RSD	2.3

3.4.2. Accuracy Check for Te Determination by ICPMS

To check the accuracy of the system, "1643e Trace Elements in Water" SRM was used. 4 fold dilution was applied and in the final solution concentration of HCl was 2.0 M. When ^{130}Te isotope was used for the calculations, results were found higher than the certified value. The possible reason was the interference from Barium (^{130}Ba with natural abundance of 0.106%) since SRM includes Ba with 545 fold higher concentration than Bi. Therefore, isotope of Te at mass 128 was used. By direct

calibration results were found smaller than the certified value. Therefore, standard addition technique was applied and results were found in good agreement with the certified value. Peak area values were used for this part since evaluating the peak area value of flow injection signal was easier by using the software program of the instrument. Standard addition plot of ^{128}Te for SRM study by ICPMS is given in Figure 3.27.

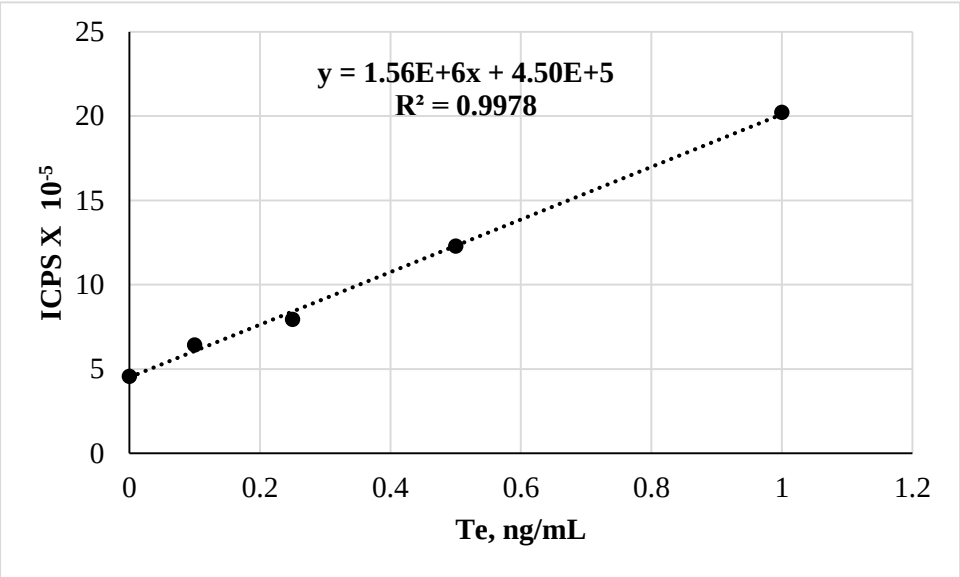

Figure 3.27. Standard addition plot of ^{128}Te for SRM study by ICPMS.

For SRM study, two replicates of SRM samples were prepared and each sample was measured three times. Average of six data was found acceptable with respect to certified value according to 99% confidence level of t-test. Results of the SRM study are given in Table 3.14.

Table 3.14. Results of accuracy check for Te determination by ICPMS**.**

SRM	Certified Value , ng/mL	Found Value, ng/mL
NIST 1643e Natural Water	1.09 ± 0.11	1.20 ± 0.08

3.5. Determination of Tellurium by HG-ICPMS

For Te determination directly moved to the HG part after nebulization-ICPMS study. Hydride forming conditions have to be optimized for this part. Standard solutions of Te were diluted from 1000 mg/L Te stock solution. Flow injection system was also used for this part with a loop volume of 500 µL. Carrier solution was 1.0 M HCl solution. U-tube GLS was used for the separation of tellurium hydride. The length of the tubing used was same with that of Bi experiments. ^{130}Te was monitored throughout this part of the study.

3.5.1. Optimizations for Te Determination by HG-ICPMS

For this part and also HG-W-Trap-ICPMS part of Te determination, optimization experiments were not performed using only Te solution. It means optimum values of Te found in multi-element study were used. For Bi, optimum values of hydride condition for single element study were same with that of multi-element part. Therefore, by considering the results of Bi experiments, optimum values of mixture experiment were used in this part. For optimization of hydride parameters, mixture solution with 2.5 ng/mL Te and 0.25 ng/mL Bi were used. Actually there are 5 parameters to be optimized in HG part namely carrier Ar flow rate, $NaBH_4$ solution flow rate, carrier acid flow rate, concentration of $NaBH_4$ solution and concentration of HCl solution. However, carrier Ar flow rate was not optimized since it is not related with the hydride forming efficiency of Te. But it affects the hydride signal by changing the transportation of formed hydride to the plasma. Optimum value of carrier Ar flow rate which was obtained for Bi was used for this part and also in mixture study. Aim was not to change the sensitivity of Bi in negative way by keeping mostly the optimum values of Bi for mixture study. Optimization graphs for both Te and Bi by using mixture solution was given in the following multi-element determination part. In brief, only optimum acid concentration was significantly different for Te compared to Bi. Concentrations below 2.0 M, no tellurium hydride formed. Hence, solutions of Te were prepared in 2.0 M acid solution. Optimum values of five parameters to get reasonably best signals for Te by HG-ICPMS system are listed in Table 3.15.

Table 3.15. Optimum values of HG parameters for Te determination by HG-ICPMS system.

	^{130}Te
Carrier Ar flow rate, L/min	1.2
$NaBH_4$ flow rate, mL/min	1.1
Sample flow rate, mL/min	2.0
Concentration of $NaBH_4$, %(w/v)	0.5
Concentration of HCl, M	2.0

3.5.2. Calibration Plot and Analytical Performance for Te Determination by HG-ICPMS

After optimizing the hydride forming parameters for Te, calibration plot was drawn for Te by using the calibration standards that include only Te. Calibration graph was linear for the concentration range 0.050-25.0 ng/mL. Plots for whole range and for lower concentrations are given in Figure 3.28 and Figure 3.29, respectively.

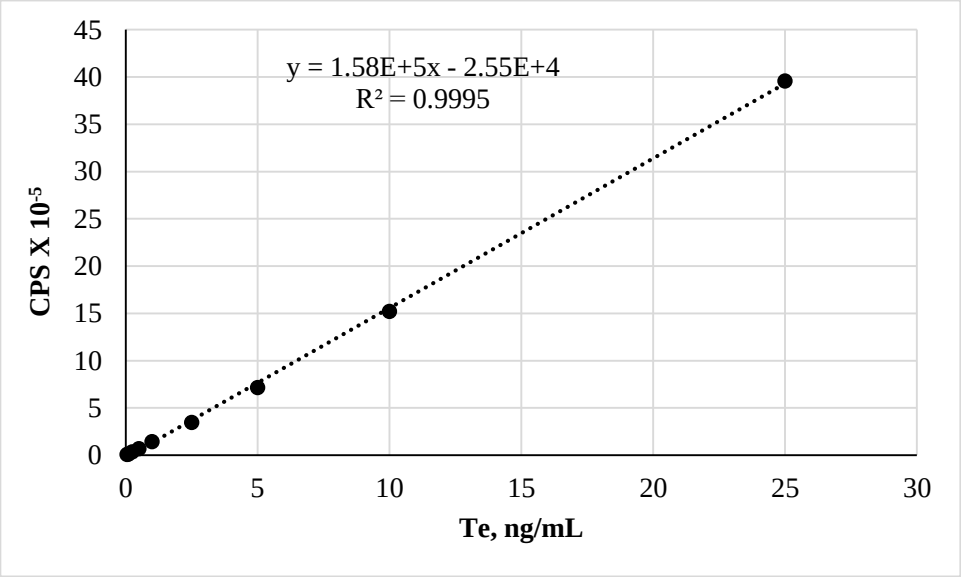

Figure 3.28. Calibration plot for ^{130}Te between 0.050 ng/mL and 25.0 ng/mL.by HG-ICPMS.

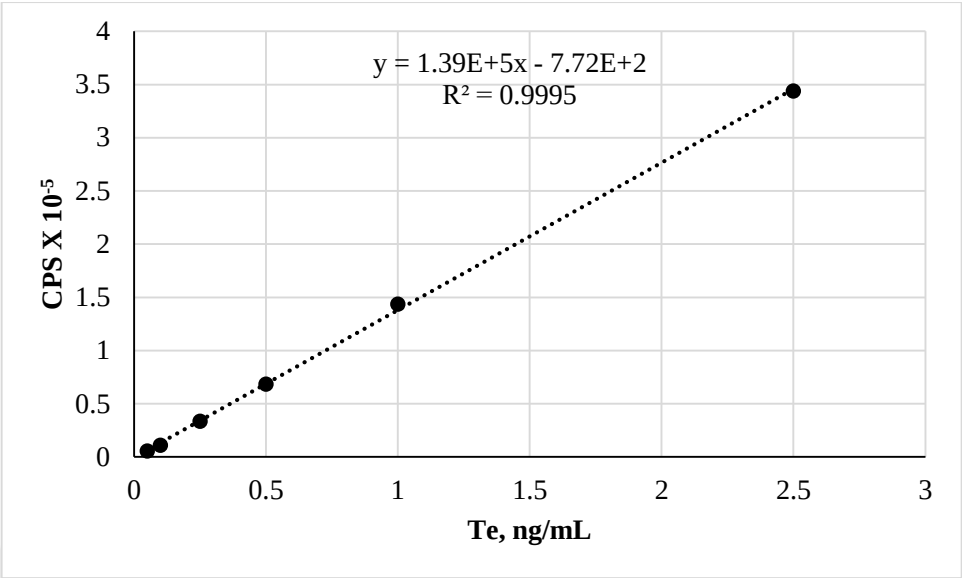

Figure 3.29. Calibration plot for ^{130}Te between 0.050 ng/mL and 2.5 ng/mL by HG-ICPMS.

Analytical performances of the HG-ICPMS system for Te were calculated from nine replicates of lowest concentration which was 0.050 ng/mL. Reproducibility of the HG system was worse than that of nebulization due to the noise resulted from the pulsed formation of hydride. Analytical performances of the HG-ICPMS system for Te are given in Table 3.16.

Table 3.16. Analytical figures of merit for Te determination by HG-ICPMS**.**

	^{130}Te, ng/mL
LOD, (N=9)	0.012
LOQ, (N=9)	0.039
Range	0.050-25
%RSD	6.5

The limit of detection of this study is compared with the literature and the LOD values are given in Table 3.17. Since in different studies different isotopes of Te especially isotope at mass 125 were used by considering the possible interferences, it is not straightforward to compare the results of this study with the literature. Therefore, while comparing these studies, one should consider the differences between the isotopic abundance of Te isotopes. However, there is not much study that used ^{130}Te and results by other isotopes also included in Table 3.17. Not only isotopes used but also conditions of each study were different. When compared to *Heitkemper and Caruso*'s[50] work that used the same isotope with this study, sensitivity was found approximately 3 times better in this study.

Table 3.17. Comparison of results for Te determination by HG-ICPMS with literature.

	HG-ICPMS LOD, ng/mL	**References**
^{130}Te	0.012	*This work*
^{130}Te	0.034	*Heitkemper and Caruso, 1990*[50]
^{128}Te	0.027	*Chen et al., 2000*[95]
^{125}Te	0.006	*Zhang and Combs,1996* [96]
^{125}Te	0.003	*Yang et al, 2013*[76]
^{128}Te	0.007	*Hu, 2006*[91]

3.5.3. Accuracy Check for Te Determination by HG-ICPMS

To check the accuracy of HG-ICPMS system, '1643e Trace Elements in Water' SRM was used, too. 10 fold dilution was applied to minimize the possible interference effects and concentration of HCl was 2.0 M in the final solution. Since Ba does not form hydride, no effect was observed in this system unlike to nebulization system. By direct calibration technique, very close result to certified one was found. ^{130}Te was monitored for this part. Two replicates of SRM samples were prepared and duplicate and triplicate measurements of each were done. Average of five measurements was found acceptable by applying t-test at 99% confidence level. Results are given in Table 3.18.

Table 3.18. Results of accuracy check for Te determination by HG-ICPMS

SRM	Certified, ng/mL	Found, ng/mL
NIST 1643e Natural Water	1.09 ± 0.11	0.95± 0.09

3.6. Determination of Tellurium by HG-W-Trap-ICPMS

Third system to check the sensitivity of the Te was HG-W-Trap ICPMS. Both for Bi and Te no such a system studied in literature. Same glass tube between Gas Liquid Separator and ICP-MS that includes W-coil was used for Te determination. Since the optimization parameters such as flow rate of H_2, make-up Ar and trapping period are not specific to element, optimum values that obtained in Bi part were used. Remaining two parameters which are trapping and revolatilization temperatures were not optimized for only Te. Optimum values which were found in multi-element determination part were used. Tellurium hydride was collected on W-coil for 30 seconds similar to Bi part in optimization experiments.

3.6.1. Effect of Coating for Te Determination

Effect of coating on trapping efficiency was evaluated for Te determination similar to the study for Bi. Ir, Pt and Rh metal solutions were used as coating materials. Coating procedure was same with Bi. Detailed procedure is given in experimental part. 0.50 ng/mL Te standard solution was used for this part of the study. TeH_2 was collected for 30 s when flow rates of make-up Ar and H_2 were 125 and 106 mL/min, respectively. For each coating, average of 7 measurements was done. As it is seen from Table 3.19, Pt-coating gave the best signal enhancement compared to uncoated W coil.

Table 3.19. Effect of different coating materials for Te by HG-W-Trap-ICPMS. Concentration of Te was 0.5 ng/mL. Flow rates of make-up Ar and H_2 were 125 and 106 mL/min, respectively.

	Uncoated, N=5	**Rh-coated, N=7**	**Pt-coated, N=7**	**Ir-coated, N=6**
CPS, x±s	$(1.85 \pm 0.133) \times 10^4$	$(11.0 \pm 1.3) \times 10^4$	$(20.9 \pm 1.1) \times 10^4$	$(6.09 \pm 0.30) \times 10^4$
%RSD	6.89	11.8	5.44	4.88

The coating materials used in this study caused more signal enhancement compared to that obtained in Bi studies as seen from Table 3.7 and Table 3.19. It is clearly seen that coating material is necessary for Te determination to develop more sensitive system. With Pt-coating magnitude of trap signal increases approximately 10 times compared with bare W-coil in Te case. As a result, Pt-coated W-coil was used for Te determination studies.

3.6.2. Optimizations for Te Determination by HG-Pt coated-W Trap-ICPMS

Ideally five parameters have to be optimized for W-trap studies. Among them no need to optimize three parameters which are make-up Ar flow rate, H_2 flow rates and trapping period because they are not specific to element and optimum values obtained in Bi part can be used. As trapping period increases, trapping efficiency increases up to the maximum limit. Make-up Ar flow is needed to protect the plasma stability so its optimum value should not be changed. Moreover, H_2 is used to protect W-coil from oxidation and its optimum value should be same to provide long lifetime of coil. Trapping and revolatilization temperatures were optimized but mixture solution of 2.5 ng/mL Te and 0.50 ng/mL Bi were used for this purpose. Therefore, optimization graphs can be attained in multi-element determination part. Optimum values of five parameters to get reasonably better signals for Te by HG-Pt coated-W Trap-ICPMS system are

listed in Table 3.20. Luckily, optimum values of Bi and Te were very similar to each other.

Table 3.20. Optimum values for Te by HG-Pt Coated-W Trap-ICPMS system

H_2, mL/min	106
Make-up Ar, mL/min	125
Trapping T, ºC	585
Revolatilization T, ºC	1600
Trapping Period, s	60

3.6.3. Calibration Plot and Analytical Performance for Te Determination by HG-Pt coated-W Trap-ICPMS

By using the optimum values, calibration plot of Te for HG-Pt-coated-W Trap-ICPMS system was drawn. Peak heights of the analytical signals were used both for calibration plot and calculations of analytical performances. Concentrations of the calibration standards ranged from 0.025 to 10.0 ng/mL and solutions included only Te. Two calibration plots based on two different concentration ranges are given in Figure 3.30 and Figure 3.31, respectively.

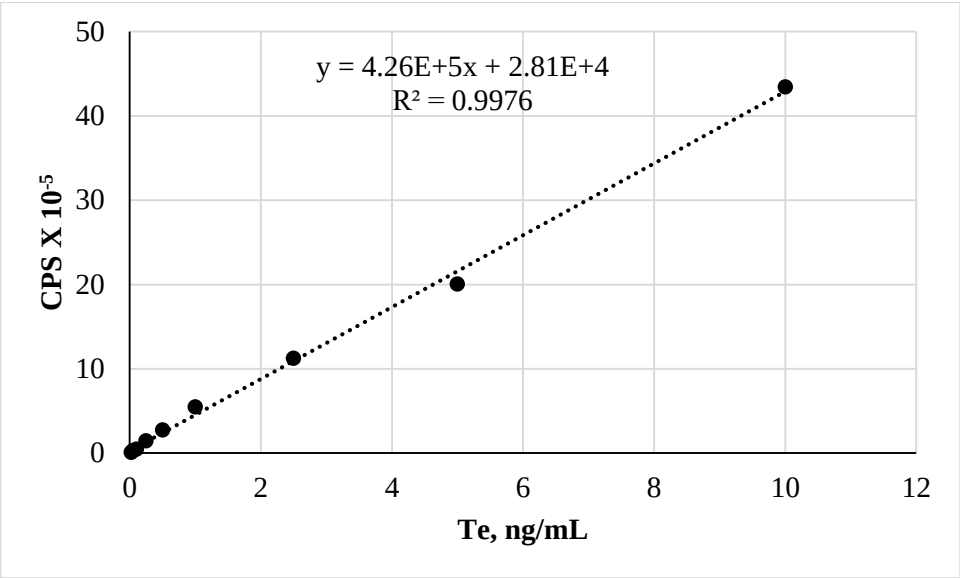

Figure 3.30. Calibration plot of ^{130}Te between 0.025 ng/mL and 10.0 ng/mL by HG-Pt coated-W Trap-ICPMS**.**

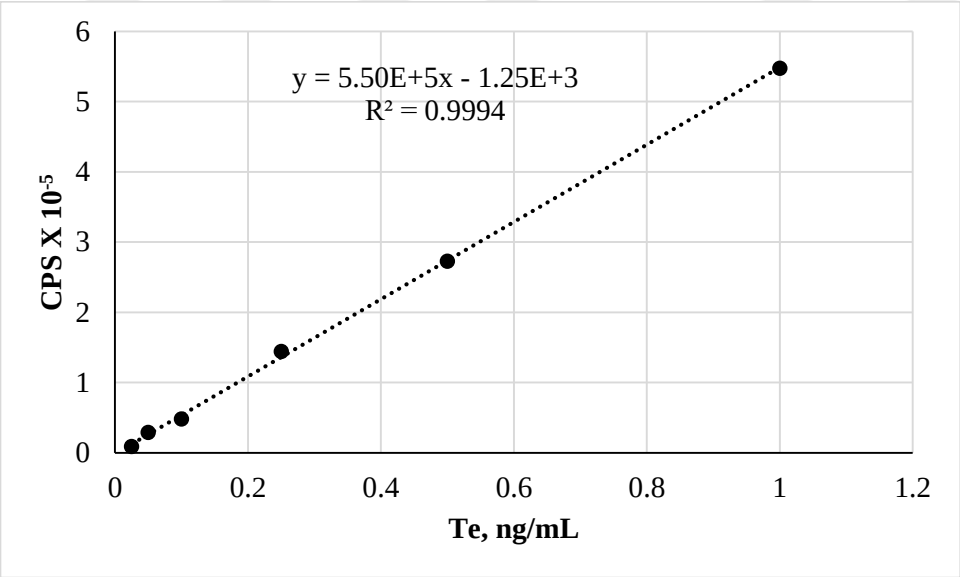

Figure 3.31. Calibration plot of ^{130}Te between 0.025 ng/mL and 1.0 ng/mL by HG-Pt coated-W Trap-ICPMS.

LOD, LOQ and %RSD values obtained from nine measurements of lowest concentration (0.025 ng/mL) are given in Table 3.21.

Table 3.21. Analytical figures of merit for Te determination by HG-Pt-coated-W Trap-ICPMS.

	^{130}Te, ng/mL
LOD, (N=9)	0.006
LOQ, (N=9)	0.019
Range	0.025-10
%RSD	4.4

Sensitivity of this study was compared with the studies in literature. As it was mentioned HG-W-trap study that uses ICPMS as a detector was done first in this thesis study. Therefore, direct comparison is not possible. HG-W-Trap studies performed by using AAS as a detector and even graphite furnace studies were used for comparison of the analytical results. Improvements were calculated considering E_t and E_v term similar to Bi part. E was calculated by taking the ratios of LOD's. More convenient comparisons can be made by using these terms since different trapping periods or different volumes were used for different studies. Results of the comparisons are given in Table 3.22. Although sensitivity of Te obtained with this proposed method was 13 times better than that of Xi et al.'s[165] study, trapping performance of their system was 14 times more efficient than this study. Moreover, when compared with the study by *Yildirim and co-workers*[109] trapping efficiency of this system was found worse.

Table 3.22. Comparison of the results for Te by HG-Pt coated-W Trap–ICPMS with literature.

Method	**Coating Material**	**Without Trap LOD, ng/L**	**With Trap LOD, ng/L**	**E**	**E_t, min^{-1}**	**E_v, mL^{-1}**	**Reference**
HG-ICPMS	Pt	12	6	2.0	2.0	1.0	*This work*
HG-AAS	Pt	2200	80	28	28	18	*Xi et al. 2010*[165]
HG-ETAAS	Ru	190	2.2	86	29	9.0	*Yildirim et al., 2012*[109]

3.6.4. Accuracy Check for Te Determination by HG-Pt coated-W Trap-ICPMS

Accuracy of the system was checked by using the "1643f Trace Elements in Water" SRM. Stock SRM solutions were diluted 20 fold. Dilution as much as possible is favored since possible interferents are also diluted. In the final solution HCl concentration was 2.0 M. Similar to the previous SRM studies two replicates of SRM solutions were prepared. Satisfactory results were obtained from four measurements by direct calibration technique and using the isotope of Te at mass 130. Confidence of the results was checked by applying t-test at 95% level. Obtained result for SRM study is given in Table 3.23.

Table 3.23. Result of accuracy check for Te determination by HG-Pt coated-W Trap-ICPMS.

SRM	Certified, ng/mL	Found, ng/mL
NIST 1643f Natural Water	0.98 ± 0.01	0.87 ± 0.09

A novel method was developed for Te determination stepwise by coupling of various sample introduction techniques to the plasma. HG system helped to increase the number of species introduced to the plasma while W-coil provide preconcentration of the analyte species to increase the sensitivity and also to separate the analyte from the matrix. LOD, %RSD and signals of the lowest concentration and also slopes of calibration graphs for three methods by using peak height measurements are summarized in Table 3.24.

Improvement in sensitivity of HG-Pt coated-W Trap-ICPMS was consistent compared to the HG-ICPMS system when slopes of calibration graphs and LOD values were evaluated. Approximately 3 times enhancement was obtained from both. However, it seemed that there was a conflict between the enhancement factor of LOD and slopes when ICPMS and HG-ICPMS systems were considered. Reason of this significant difference can be explained by considering standard deviation values. LOD calculation

involves standard deviation value of the lowest concentrated signal (for this study) and there was more than 10 fold difference between the standard deviation values for lowest concentrations for ICPMS and HG-ICPMS. Therefore, lowest concentrations and x±s values are also given in Table 3.24.

Table 3.24. Analytical figures of merits for ^{130}Te by three methods**.**

	Lowest Conc, ng/mL	**x±s, CPS**	**%RSD**	**LOD, ng/L**	**Slope**
ICPMS	0.25	$(17.4 \pm 0.39) \times 10^2$	2.25	29	0.4×10^4
HG-ICPMS	0.050	$(83.2 \pm 5.39) \times 10^2$	6.48	12	16×10^4
HG-Pt coated-W-trap-ICPMS (60 s)	0.025	$(23.8 \pm 1.04) \times 10^3$	4.37	6	55×10^4

3.6.5. Trapping Efficiency Calculations for Te

Trapping efficiency of the W-coil is important since sensitivity enhancement of the developed method depends directly on that for trap part. In addition, flow rates of H_2 and make-up Ar, trapping voltage and collection period are the key parameters that affect trapping efficiency. For this part of the study, 2.5 ng/mL Te standard solution was used. Tellurium hydride was trapped on Pt-coated W-Trap for 30 seconds. For efficiency calculations both peak height and peak area values of the continuous signals are required. Duplicate continuous signals for trapping experiments are given in Figure 3.32. As it is understood from the signal difference voltage turned on to start trapping after 30 seconds pass from the beginning. At the end of trapping period, transient signals obtained by applying higher revolatilization temperatures. Trapping temperature was 179 ^{o}C, revolatilization temperature was 1600 ^{o}C and flow rates of H_2 and make-up Ar were 106 and 125 mL/min, respectively during this experiment.

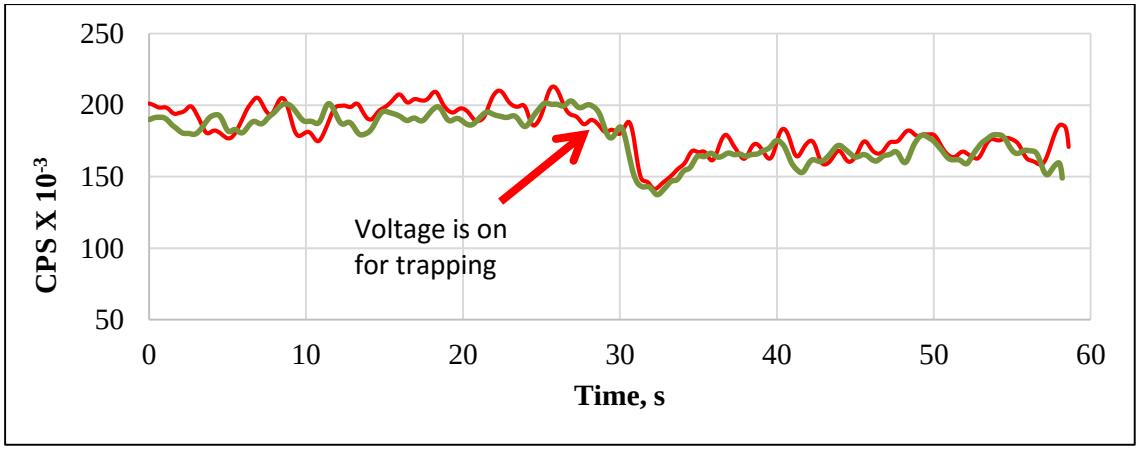

Figure 3.32. Continuous ^{130}Te signals of two replicates of 2.5 ng/mL Te solution before and during trapping period by HG-Pt coated–W Trap-ICPMS. Trapping temperature was 179 ^{o}C. Trapping period was 30 s. Flow rates of H_2 and make-up Ar were 106 and 125 mL/min, respectively.

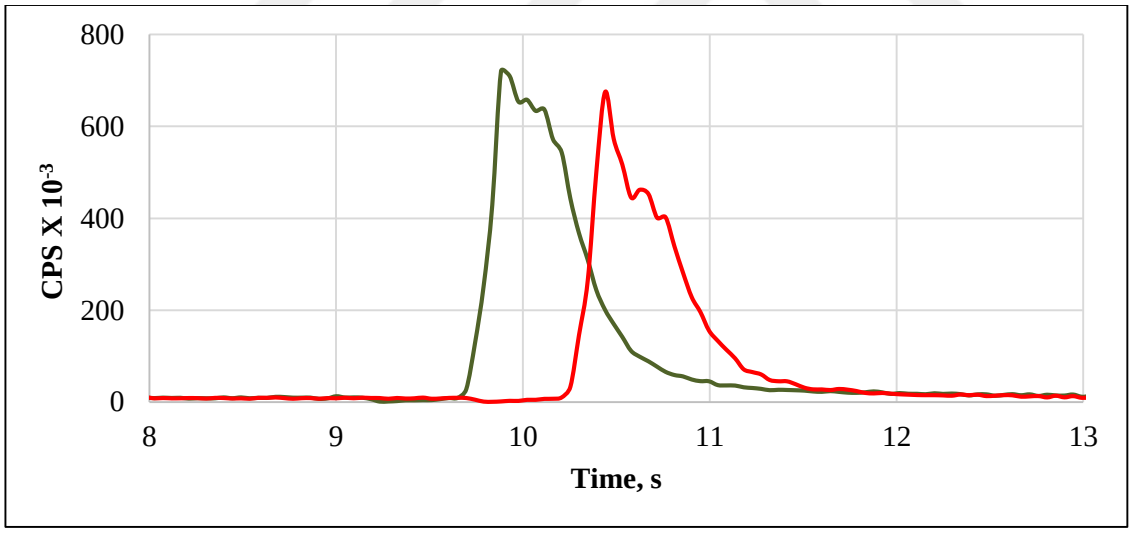

Figure 3.33. Transient signals of 2.5 ng/mL ^{130}Te by HG-Pt coated–W Trap-ICPMS. Revolatilization temperature was 1600 ^{o}C. Flow rates of H_2 and make-up Ar were 106 and 125 mL/min, respectively.

Information about trapping efficiency calculations was given before for Bi determination (Section 3.3.5). Similar calculations were done for Te case and trapping efficiency using the cps of the ^{130}Te signal before and during trapping was found as 15% for 30 seconds

collection. On the other hand, operational trapping efficiency was calculated as 10% for 30 seconds trapping period. Make-up Ar and H_2 flows were on and flow rates were same for both trapping and revolatilization stages. Therefore, trapping efficiency of Bi is better than trapping efficiency of the Te using the same trapping conditions. Transient signals of ^{130}Te for duplicate analysis are given in Figure 3.33. Comparing to the transient signals of Bi, peaks of Te were a bit broader.

3.7. Multi-Element Studies by HG-W-Trap-ICPMS

This part can be mentioned as the second main part of this thesis study. In the first main part, HG-W-Trap-ICPMS system was used to study only one element at a time and for this second part aim was to show the multi-element capability of ICPMS in W-trap studies. Te was chosen as a second element since hydride forming conditions are close to Bi, it does not have serious interference problems by ICPMS and also detection at lower levels is required due to its toxic character.

3.7.1. Simultaneous Determination of Bi and Te in Mixture by HG-ICPMS

For this multi-element study first HG-ICPMS parameters were optimized to find the best conditions for both Bi and Te. Before trap part, HG-ICPMS study was needed since first step was to develop a sensitive method for hydride part. Bi and Te elements were monitored at masses 209 and 130, respectively during this study. The point in this multi-element study by HG-ICPMS was to find optimum hydride forming conditions that match well for both elements.

3.7.1.1. Optimizations for Simultaneous Determination of Bi and Te in Mixture by HG-ICPMS

A solution of 2.5 ng/mL Te and 0.25 ng/mL Bi was used in this part. Two elements were monitored simultaneously during optimization study. Flow injection system with a loop volume of 500 µL was used. Carrier Ar flow rate was not optimized since it is not

specific to the hydride forming element. Optimum value which was obtained for Bi was used for this part. Four parameters, which were $NaBH_4$ solution flow rate, carrier acid flow rate, concentration of $NaBH_4$ solution and concentration of HCl solution, were optimized to get high sensitivities for two elements. U-Tube GLS was used. By chance, except from acid concentration, optimum values of other four parameters were found same for both Bi and Te. Peak area measurements were used for optimization part. Except analytical performance calculations of nebulization-ICPMS, for HG-ICPMS and whole parts of trap studies, peak area measurements were used. The reason was that evaluating of the peak area was easier by software of the instrument.

3.7.1.1.1. $NaBH_4$ Flow Rate for Simultaneous Determination of Bi and Te in Mixture

Formation of bismuthine and tellurium hydride continuously depends on the flow rate of $NaBH_4$. During this experiment only $NaBH_4$ flow rate was varied for the determination of optimum flow rate while the other parameters were kept constant. For this optimization, 2.5 ng/mL Te and 0.25 ng/mL Bi in 4.0 M HCl and 0.5% (w/v) $NaBH_4$ were used. Solutions were prepared in 4.0 M at the beginning of the Te experiments. This concentration was the optimum value of the study which was performed by our research group[109] by using the optimum values of 2.0 mL/min and 1.2 L/min for sample and carrier Ar flow rates, respectively. Concentration of carrier HCl solution was 1.0 M. Optimization graphs for Bi and Te are given in Figure 3.34 and Figure 3.35, respectively. With an increase in flow rate of $NaBH_4$, formation of H_2 gas from the hydride reaction becomes rapidly, filled the GLS faster and causes plasma instability. This situation was also not related with the hydride forming element itself. Therefore, 1.1 mL/min was selected as the optimum value for both Bi and Te and this value was used for the rest of the study.

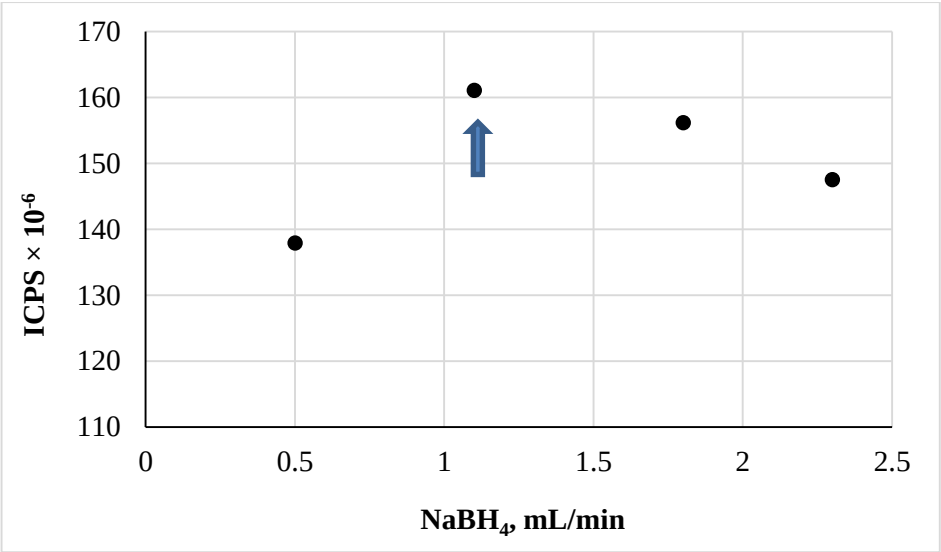

Figure 3.34. The optimization of $NaBH_4$ flow rate for ^{209}Bi in mixture solution by HG system. 0.25 ng/mL Bi and 2.5 ng/mL Te solution in 4.0 M HCl and 0.5% (w/v) $NaBH_4$ was used. Flow rates of carrier Ar and HCl solution were 1.2 L/min and 2.0 mL/min, respectively.

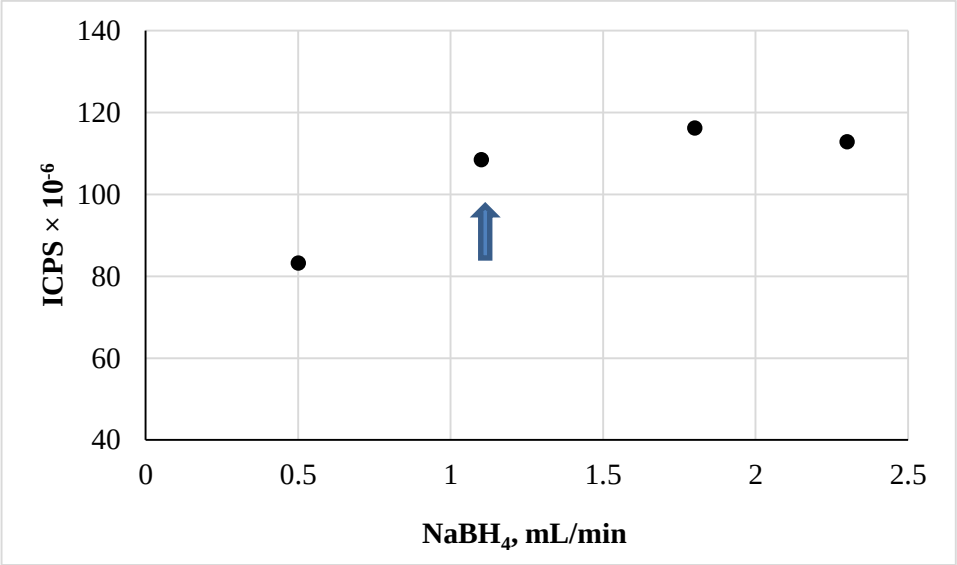

Figure 3.35. The optimization of $NaBH_4$ flow rate for ^{130}Te in mixture solution by HG system. 0.25 ng/mL Bi and 2.5 ng/mL Te solution in 4.0 M HCl and 0.5% (w/v) $NaBH_4$ was used. Flow rates of carrier Ar and HCl solution were 1.2 L/min and 2.0 mL/min, respectively.

3.7.1.1.2. Carrier Acid Flow Rate for Simultaneous Determination of Bi and Te in Mixture

Flow rate of sample solution is important for HG studies. The effect of carrier acid flow rate on analytical signals of Bi and Te can be seen in Figure 3.36 and Figure 3.37, respectively. 2.5 ng/mL Te and 0.25 ng/mL Bi in 4.0 M HCl and 0.5% (w/v) $NaBH_4$ were used. Concentration of carrier HCl solution was 1.0 M. Flow rates of $NaBH_4$ and carrier Ar were 1.1 mL/min and 1.2 L/min, respectively. Value that gave maximum signal was chosen for Te and this value was suitable for Bi since there was no significant difference between the analytical signals obtained between 1.3 mL/min and 2.0 mL/min flow rates. Therefore, 2.0 mL/min was selected as an optimum value. In addition, shapes of the signals became broader at low flow rates and analysis time increased. This was another reason of not choosing lower flow rates.

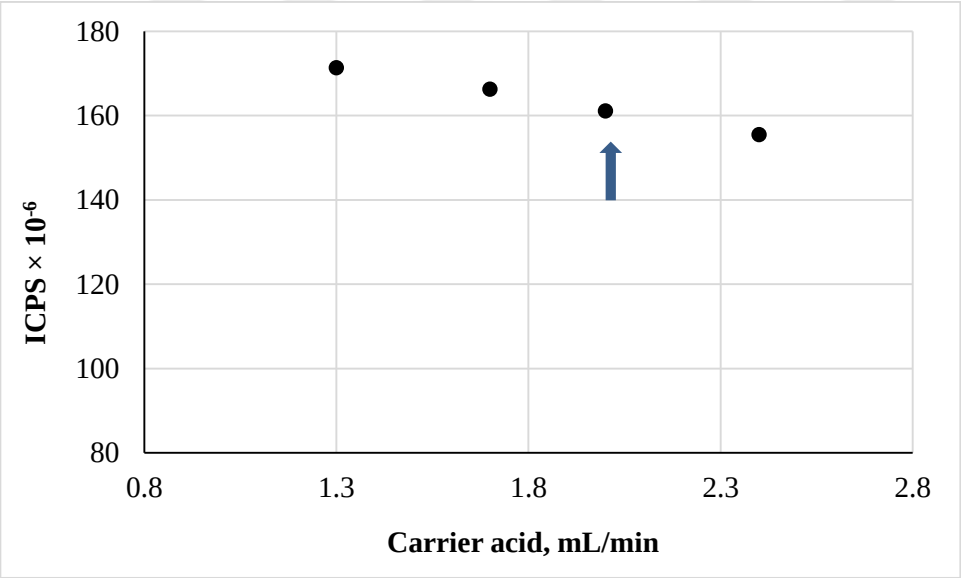

Figure 3.36. The optimization of carrier acid flow rate for ^{209}Bi in mixture solution by HG system. 0.25 ng/mL Bi and 2.5 ng/mL Te solution in 4.0 M HCl and 0.5% (w/v) $NaBH_4$ was used. Flow rates of carrier Ar and $NaBH_4$ solution were 1.2 L/min and 1.1 mL/min, respectively.

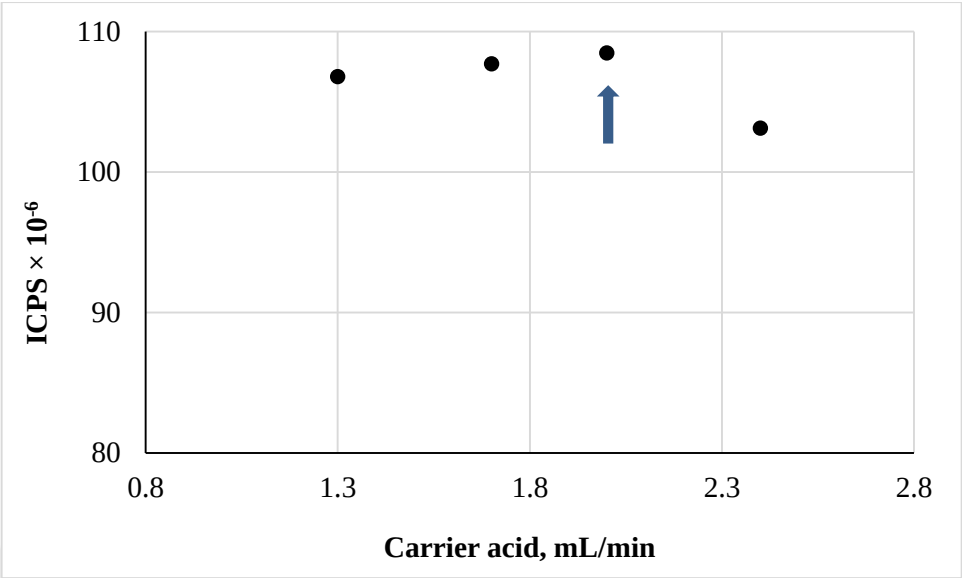

Figure 3.37. The optimization of carrier acid flow rate for ^{130}Te in mixture solution by HG system. 0.25 ng/mL Bi and 2.5 ng/mL Te solution in 4.0 M HCl and 0.5% (w/v) $NaBH_4$ was used. Flow rates of carrier Ar and $NaBH_4$ solution were 1.2 L/min and 1.1 mL/min, respectively.

3.7.1.1.3. Concentration of $NaBH_4$ for Simultaneous Determination of Bi and Te in Mixture

Concentration of $NaBH_4$ shows very similar effect with its flow rate. With an increase in both cases, H_2 formation increases, too. Then plasma stability affected and it extinguishes eventually. 2.5 ng/mL Te and 0.25 ng/mL Bi in 4.0 M HCl and 0.5% (w/v) $NaBH_4$ were used. Flow rates of $NaBH_4$, carrier acid solution and carrier Ar were 1.1 mL/min, 2.0 mL/min and 1.2 L/min, respectively. Correlations between $NaBH_4$ concentrations and analytical signals were studied and results are given in Figure 3.38 and Figure 3.39 for Bi and Te, respectively. 0.5% (w/v) was selected as the optimum value by considering the stability of the plasma for both Bi and Te.

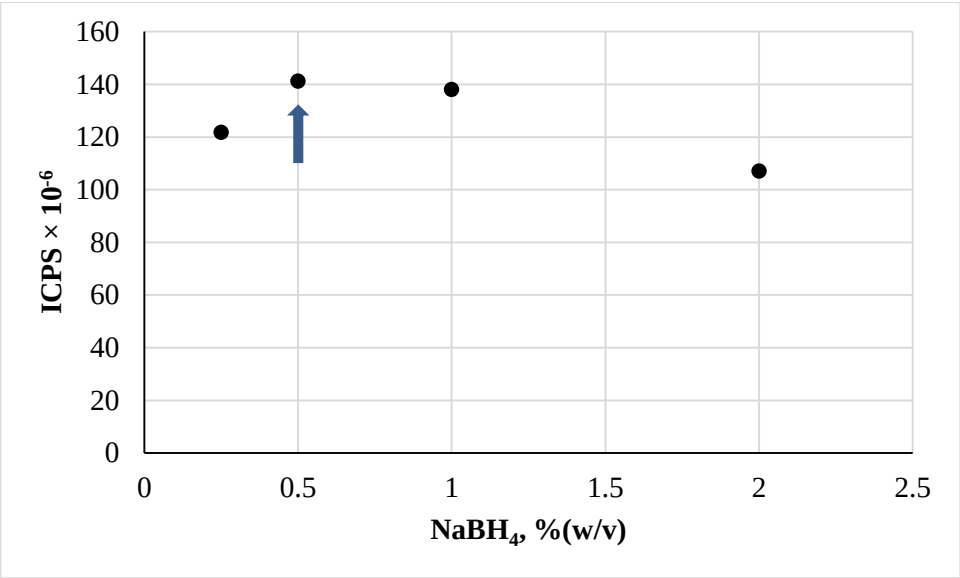

Figure 3.38. The optimization of $NaBH_4$ concentration for ^{209}Bi in mixture by HG system. 0.25 ng/mL Bi and 2.5 ng/mL Te solution in 4.0 M HCl was used. Flow rates of carrier Ar, $NaBH_4$ and carrier acid solution were 1.2 L/min, 1.1 mL/min and 2.0 mL/min, respectively.

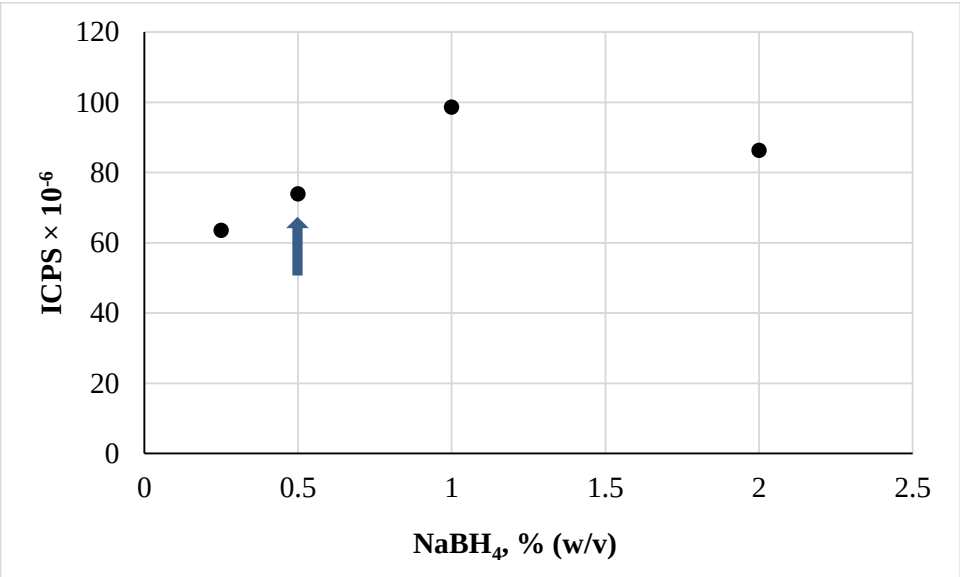

Figure 3.39. The optimization of $NaBH_4$ concentration for ^{130}Te in mixture by HG system. 0.25 ng/mL Bi and 2.5 ng/mL Te solution in 4.0 M HCl was used. Flow rates of carrier Ar, $NaBH_4$ and carrier acid solution were 1.2 L/min, 1.1 mL/min and 2.0 mL/min, respectively.

3.7.1.1.4. Concentration of HCl in Analyte Solution for Simultaneous Determination of Bi and Te in Mixture

Acid concentration of analyte solution plays an important role in HG since hydride generation efficiency is directly related with the acidity of the solution. Therefore, concentration of HCl in analyte solution has to be optimized. For this optimization 2.5 ng/mL Te and 0.25 ng/mL Bi mix solutions were prepared in different concentrations of HCl. Optimum values of other parameters which were studied up to this part were used during this optimization. 1.0 M HCl solution was used as a carrier solution. Optimization graphs to see the effect of acid content on analytical signals for Bi and Te are given in Figure 3.40 and Figure 3.41, respectively. HCl concentrations below 2.0 M, no tellurium hydride was formed since no signal was measured. When 4.0 M acid was used, analytical signal increased as it was expected. On the other hand, bismuthine formation was possible at lower acid contents. Hence, to make tellurium hydride formation possible at highest sensitivity, 2.0 M acid content was selected as an optimum for the preparation of mixture solutions.

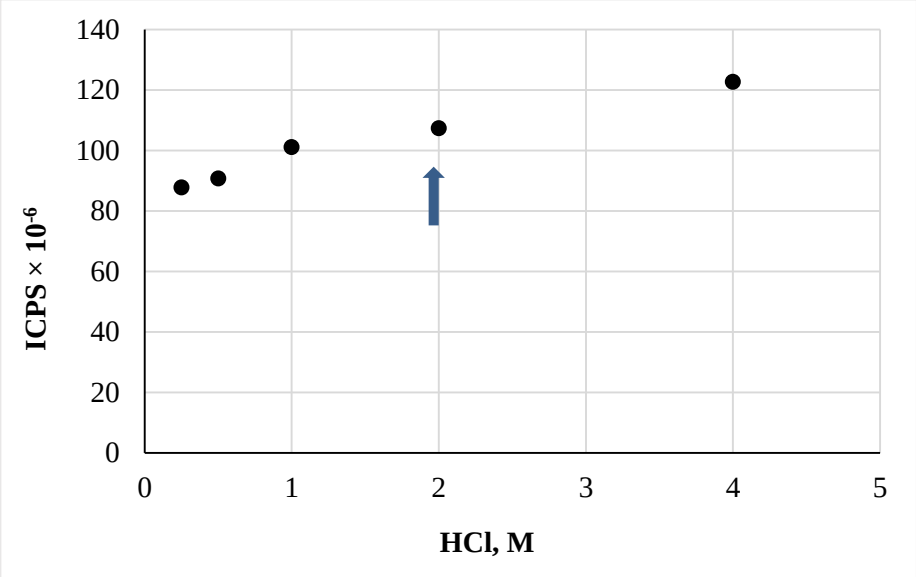

Figure 3.40. The optimization of HCl concentration for ^{209}Bi in mixture by HG system. 0.25 ng/mL Bi and 2.5 ng/mL Te solution and 0.5% (w/v) $NaBH_4$ was used. Flow rates of carrier Ar, $NaBH_4$ and carrier acid solution were 1.2 L/min, 1.1 mL/min and 2.0 mL/min, respectively.

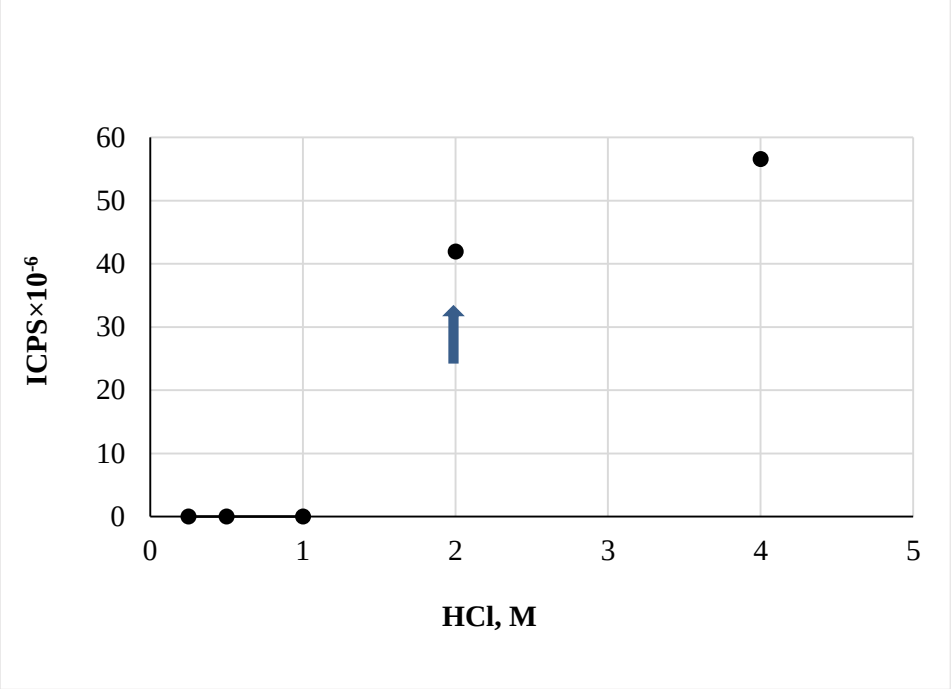

Figure 3.41. The optimization of HCl concentration for ^{130}Te in mixture by HG system. 0.25 ng/mL Bi and 2.5 ng/mL Te solution and 0.5% (w/v) $NaBH_4$ was used. Flow rates of carrier Ar, $NaBH_4$ and carrier acid solution were 1.2 L/min, 1.1 mL/min and 2.0 mL/min, respectively.

Apart from acid concentration, optimum values of other HG parameters were found same for Te and Bi. For the selection of optimum acid content leveling was done based on Te signals. Optimum values of five parameters to get reasonably best signals for multi-element determination of Bi and Te by HG-ICPMS system are listed in Table 3.25 below.

Table 3.25. Optimum values of HG parameters for simultaneous determination of Bi and Te in mixture by HG-ICPMS.

	^{209}Bi & ^{130}Te
Carrier Ar flow rate, L/min	1.2
$NaBH_4$ flow rate, mL/min	1.1
Sample flow rate, mL/min	2.0
Concentration of $NaBH_4$, %(w/v)	0.5
Concentration of HCl, M	2.0

3.7.1.2. Calibration Plots and Analytical Performances for simultaneous determination of Bi and Te in mixture by HG-ICPMS

By setting the optimum values after optimization step, calibration graph was drawn for both Bi and Te. Calibration plots are given in Figure 3.42 and Figure 3.43 for Bi and Te in mixture, respectively. It was very good to see that second element; Te did not decrease the sensitivity of the Bi. This result was expected since hydride forming conditions for Bi did not change much. For Te case similar sensitivity was obtained compared to single element study. Therefore, simultaneous measurement of Bi and Te can be done by HG-ICPMS without affecting the sensitivities negatively.

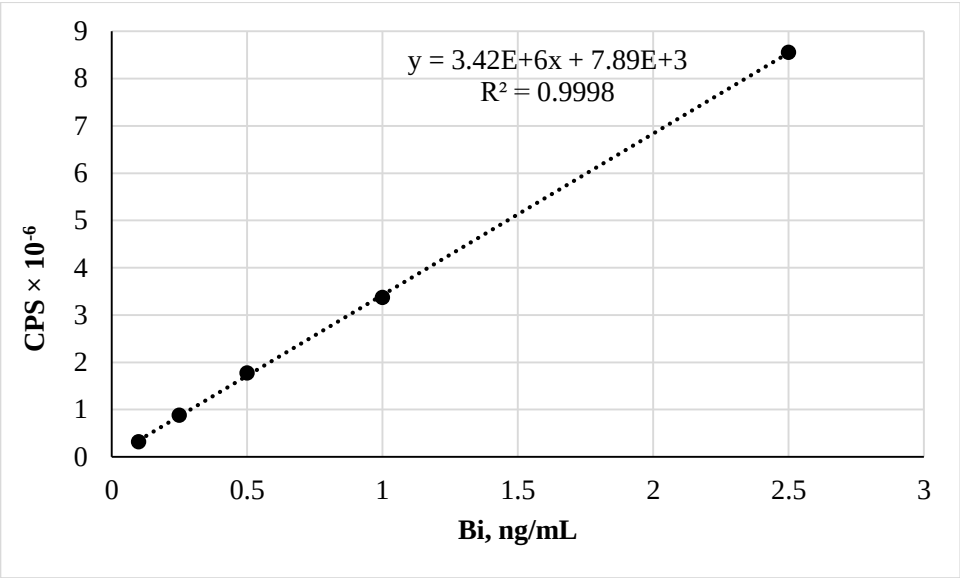

Figure 3.42. Calibration plot for ^{209}Bi in mixture by HG-ICPMS system.

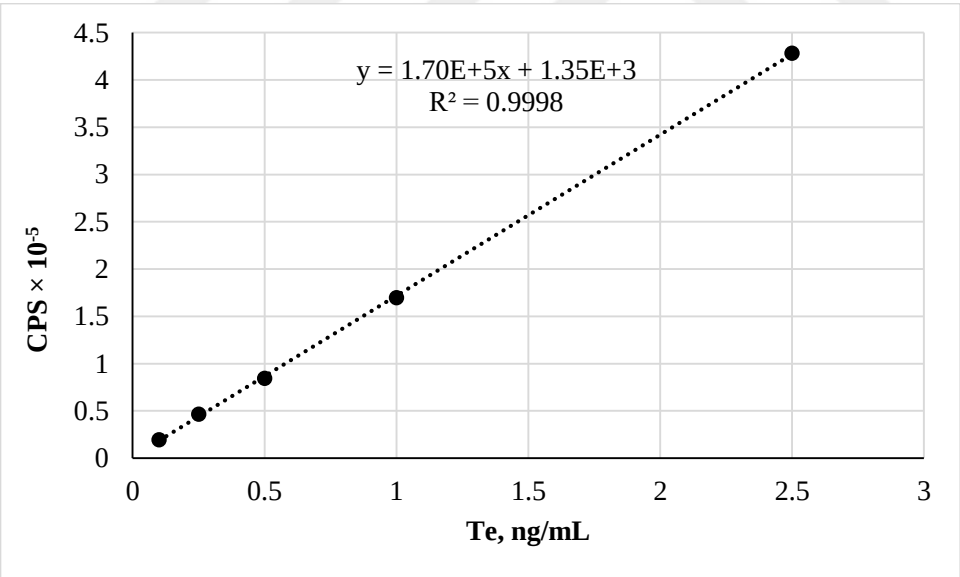

Figure 3.43. Calibration plot for ^{130}Te in mixture by HG-ICPMS system.

LOD and LOQ values were calculated for Bi and Te in mixture by HG-ICPMS system. Peak height measurements were used for accurate comparison of analytical performance of this system with that of trap system. Analytical performances were calculated from

eight replicate measurements of smallest concentration which was 0.1 ng/mL for both elements. Analytical figures of merit for two elements by HG-ICPMS are given in Table 3.26.

Table 3.26. Analytical figures of merit for simultaneous determination of ^{209}Bi and ^{130}Te in mixture by HG-ICPMS.

	^{209}Bi, ng/mL	**^{130}Te, ng/mL**
LOD, (N=8)	0.009	0.019
LOQ, (N=8)	0.031	0.064
Range	0.10-10	0.10-10
%RSD	3.2	5.6

In order to compare the sensitivities of the Bi and Te elements for single and binary mixture studies, LOD values and slopes of the calibration graphs are given in Table 3.27. As it is seen, values are very close to each other. It means, without losing the sensitivities multi-element study of these two elements can be performed.

Table 3.27. Analytical figures of merits for Bi and Te in single and multi-element studies by HG-ICPMS.

	LOD, ng/L	**Slope**
^{209}Bi		
HG-ICPMS (single)	9.5	1.90×10^{6}
HG-ICPMS (in mixture)	9	3.42×10^{6}
^{130}Te		
HG-ICPMS (single)	12	1.60×10^{5}
HG-ICPMS (in mixture)	19	1.70×10^{5}

3.7.2. Simultaneous Determination of Bi and Te in Mixture by HG-Pt Coated-W Trap-ICPMS

For this part of the multi-element study, first thing was to decide which coating is the best for mixture of Bi and Te. Coating materials showed different trend for Te comparing to Bi. Pt-coating increased the trapping efficiency more for Te and approximately 10-fold increase in signals obtained compared to uncoated coil. In case of Bi, there was no significant difference between the signals of Ir-coating and Pt-coating although Ir was a bit better. Therefore, for multi-element study, Pt-coating was selected since positive effect of Pt-coating was more pronounced for Te while there was not much difference between the effects of Ir and Pt coatings for Bi.

3.7.2.1. Optimizations for Simultaneous Determination of Bi and Te in Mixture by HG-Pt Coated-W Trap-ICPMS

Optimizations were done by using Pt-coated W-coil. For this part of the study H_2 and make-up Ar flow rates were not optimized. Roles of them are to prevent oxidation and enable plasma stability, respectively. Trapping and revolatilization temperatures were optimized to select a common value for both Te and Bi. 60 seconds trapping period was selected as an optimum value in the Bi determination part of this thesis study. Hence, for this part optimization of this parameter was not done. However, during optimization of temperatures, trapping period was 30 seconds. 0.5 ng/mL Bi and 2.5 ng/mL Te mixture solution was prepared for optimizations.

3.7.2.1.1. Trapping Temperature

Trapping temperature was optimized before releasing temperature. More detailed scan was done by using eleven different values for optimum trapping temperature. Optimum temperatures to get maximum signals were not same for Bi and Te. While 179 ^{o}C was best for Bi, 585 ^{o}C was good for Te. By considering the coil lifetime and observing that the difference between the signals at 179 ^{o}C and 585 ^{o}C were not significant; even two

times increase could not be obtained; 179 ºC was selected as an optimum value for mixture study. The effect of trapping temperature on analytical signals of Bi and Te can be seen in Figure 3.44 and Figure 3.45, respectively.

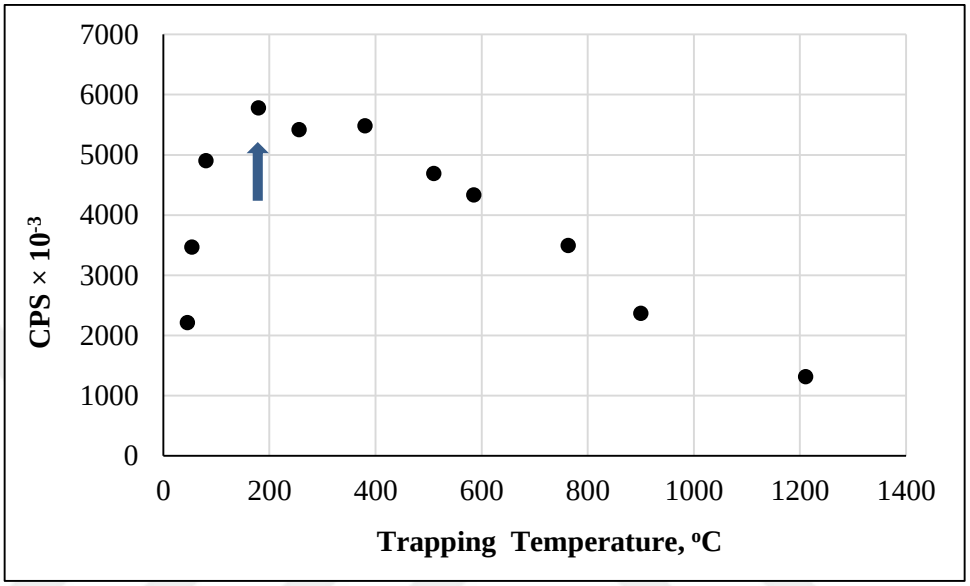

Figure 3.44. The optimization of trapping temperature for ^{209}Bi in mixture by HG-Pt coated-W Trap-ICPMS. Concentrations of Bi and Te were 0.25 ng/mL and 2.5 ng/mL in 2.0 M HCl. Revolatilization temperature was 1600 ºC. Trapping period was 30 s. Flow rates of H_2 and make-up Ar were 106 mL/min and 125 mL/min, respectively.

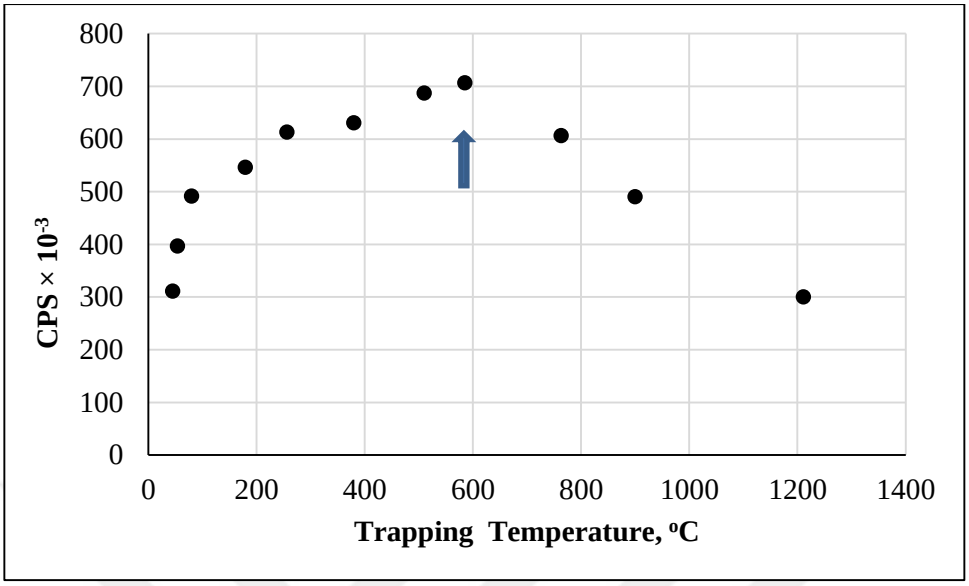

Figure 3.45. The optimization of trapping temperature for ^{130}Te in mixture by HG-Pt coated-W Trap-ICPMS. Concentrations of Bi and Te were 0.25 ng/mL and 2.5 ng/mL in 2.0 M HCl. Revolatilization temperature was 1600 ºC. Trapping period was 30 s. Flow rates of H_2 and make-up Ar were 106 mL/min and 125 mL/min, respectively.

3.7.2.1.2. Revolatilization Temperature

After fixing the trapping temperature as 179 ºC, revolatilization temperature optimization was done. Applied voltage is directly related with temperature. With increase in temperature volatilization chance of all the trapped species increase. However, small decrease was observed at higher temperatures for both Te and Bi. It can be resulted from the change for coating properties on coil. Therefore, 1600 ºC was selected as an optimum value for revolatilization. At this temperature sharper transient signals obtained for both elements. Optimization graphs are given in Figure 3.46 and Figure 3.47 for Bi and Te, respectively.

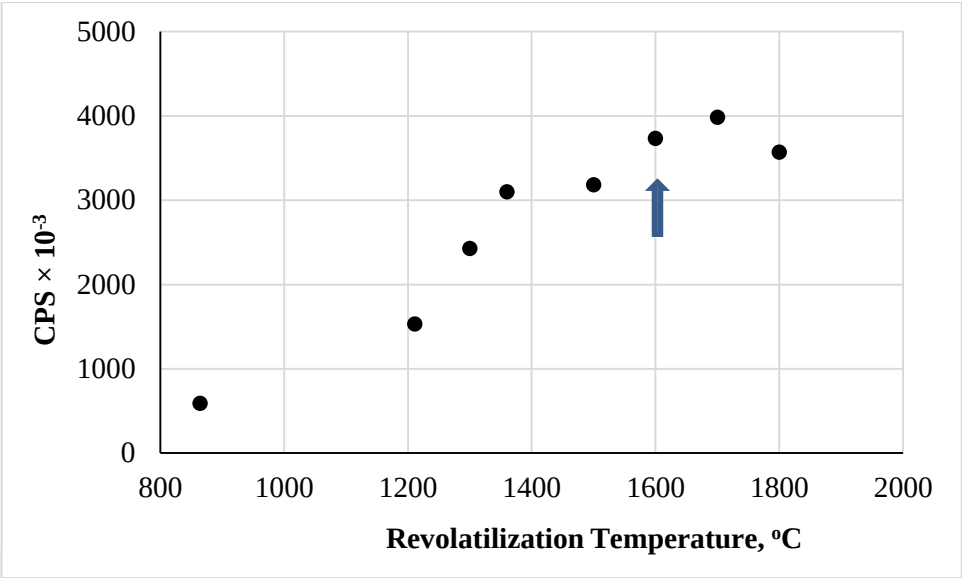

Figure 3.46. Optimization of revolatilization temperature for ^{209}Bi in mixture by HG-Pt coated-W Trap-ICPMS. Concentrations of Bi and Te were 0.25 ng/mL and 2.5 ng/mL in 2.0 M HCl. Trapping temperature was 179 ºC. Trapping period was 30 s. Flow rates of H_2 and make-up Ar were 106 mL/min and 125 mL/min, respectively.

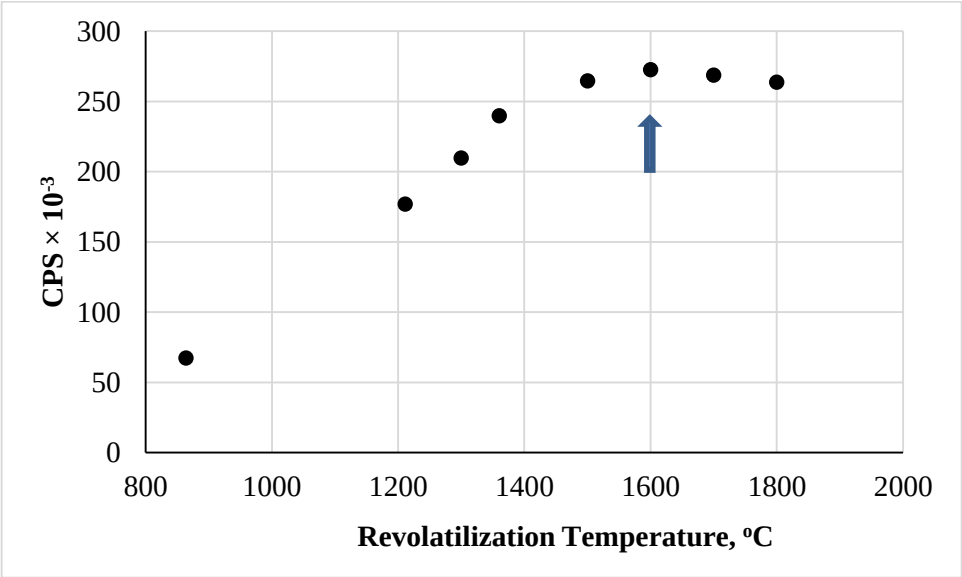

Figure 3.47. Optimization of revolatilization temperature for ^{130}Te in mixture by HG-Pt coated-W Trap-ICPMS. Concentrations of Bi and Te were 0.25 ng/mL and 2.5 ng/mL in 2.0 M HCl. Trapping temperature was 179 ºC. Trapping period was 30 s. Flow rates of H_2 and make-up Ar were 106 mL/min and 125 mL/min, respectively.

Optimum values of trap system for multi-element study are listed in Table 3.28. For decision of the best value for both, a criterion was not only signal magnitude. Conditions which provide continuation of the experiment without any problem were selected for some parts.

Table 3.28. Optimum values of HG-Pt coated-W Trap-ICPMS system for simultaneous determination of Te and Bi

H_2, mL/min	106
Make-up Ar, mL/min	125
Trapping T, ºC	179
Revolatilization T, ºC	1600
Trapping Period, s	60

3.7.2.2.Calibration Plots and Analytical Performances for Simultaneous Determination of Bi and Te in Mixture by HG-Pt coated-W Trap-ICPMS

After optimization step, calibration graphs were drawn for both elements by using HG-Pt coated-W Trap-ICPMS system. Both Te and Bi were studied in the range of 0.025-10.0 ng/mL. Ranges of calibration plots for both elements were linear over 2 to 4 orders of magnitude. Calibration plots for larger range and also lower concentrations by using peak height measurements are given in Figure 3.48 and Figure 3.49 for Bi in mixture. Similarly, wide range and small range of calibration standards were used for calibration plots of Te in mixture and graphs are given in Figure 3.50 and Figure 3.51, respectively.

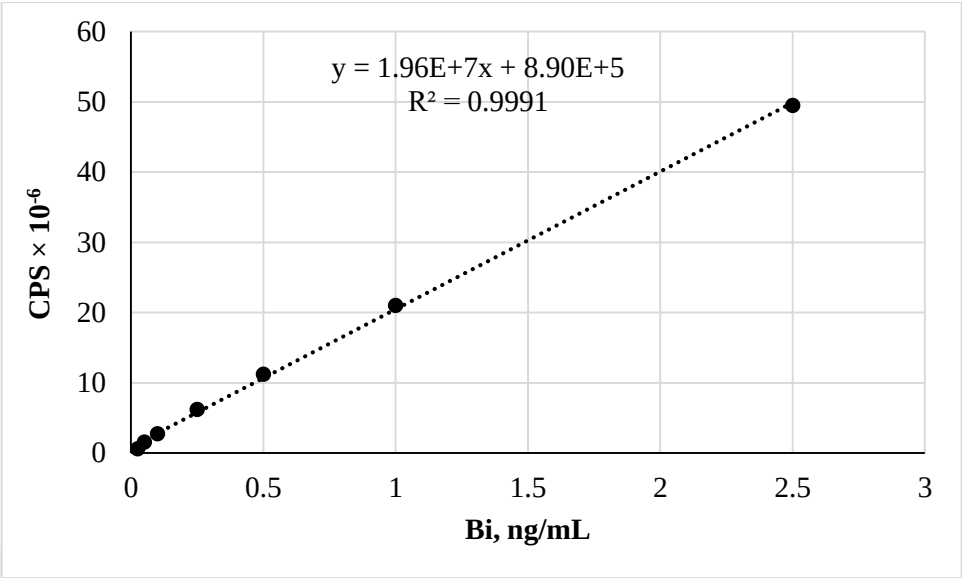

Figure 3.48. Calibration plot for ^{209}Bi in Bi-Te mixture between 0.025 ng/mL and 2.5 ng/mL by HG-Pt coated-W Trap-ICPMS.

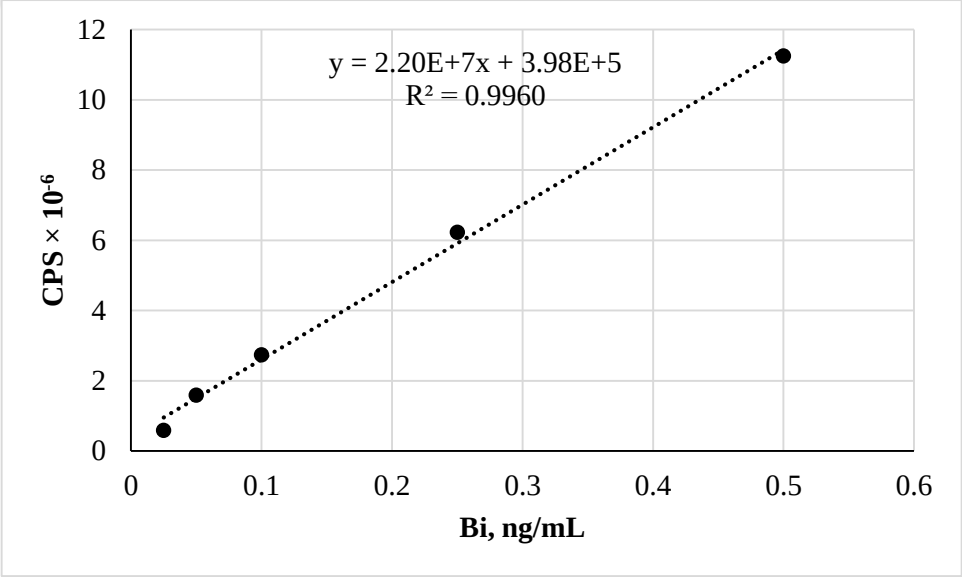

Figure 3.49. Calibration plot for ^{209}Bi in Bi-Te mixture between 0.025 ng/mL and 0.50 ng/mL by HG-Pt coated-W Trap-ICPMS.

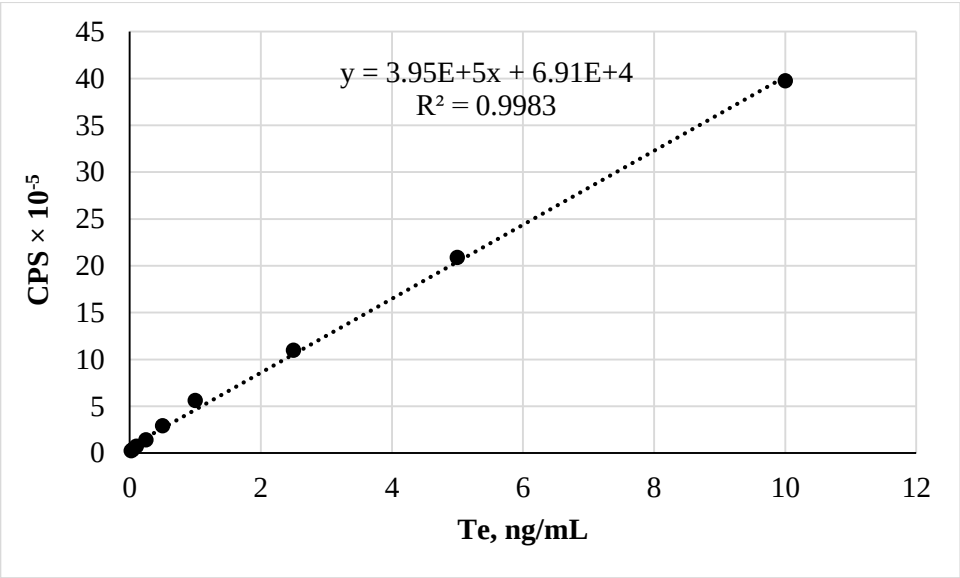

Figure 3.50. Calibration plot for ^{130}Te in Bi-Te mixture between 0.025 ng/mL and 10.0 ng/mL by HG-Pt coated-W Trap-ICPMS.

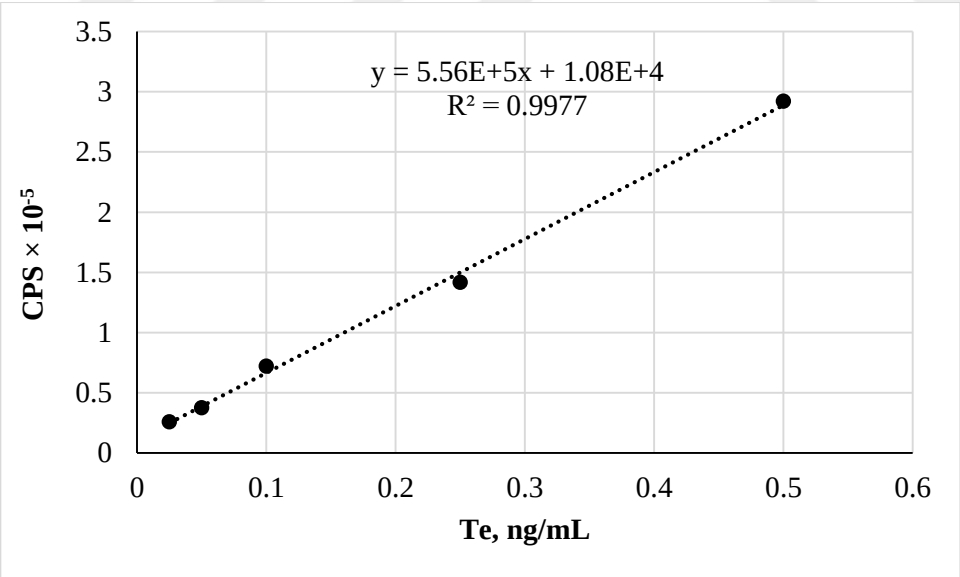

Figure 3.51. Calibration plot for ^{130}Te in Bi-Te mixture between 0.025 ng/mL and 0.5 ng/mL by HG-Pt coated-W Trap-ICPMS.

LOD, LOQ and %RSD values of both Te and Bi in mixture for Pt-coated W-Trap system were calculated by using peak height measurements. They were calculated from eight replicate measurements of smallest concentration which is 0.025 ng/mL for both Te and Bi. Analytical figures of merit for Bi and Te in mixture by HG-Pt Coated-W Trap-ICPMS are given in Table 3.29.

Table 3.29. Analytical figures of merit for simultaneous determination of ^{209}Bi and ^{130}Te in mixture by HG-Pt coated-W Trap-ICPMS.

	^{209}Bi, ng/mL	**^{130}Te, ng/mL**
LOD, (N=8)	0.009	0.007
LOQ, (N=8)	0.028	0.024
Range	0.025-10.0	0.025-10.0
%RSD	7.8	5.2

Results were found satisfactory for both elements. When analytical performances were compared for single and multi-element studies, it was clearly seen that sensitivities were not affected much in multi-element study if slopes of the calibration graphs were taken into consideration. It can be concluded that for the proposed working conditions, there was no serious interference effect of Bi and Te on each other's to affect the sensitivities much. However, it is worth to say that success of this multi-element study could be related with the selected elements. Moreover, it was possible to make ultra-trace multi-element determination by HG-W-Trap-ICPMS system. Analytical performances of Bi and Te in single and multi-element studies by HG-W-Trap-ICPMS are listed in Table 3.30 below with respect to LOD and slopes of calibration plots.

Table 3.30. Analytical figures of merits for Bi and Te in single and multi-element studies by HG-Pt Coated-W Trap-ICPMS.

	LOD, ng/L	Slope
^{209}Bi		
HG-Ir coated-W-trap-ICPMS (single)	2.7	2.94×10^{7}
HG-Pt coated-W-trap-ICPMS (in mixture)	8.5	2.20×10^{7}
^{130}Te		
HG-Pt coated-W-trap-ICPMS (single)	6	5.50×10^{5}
HG-Pt coated-W-trap-ICPMS (in mixture)	7.2	5.56×10^{5}

3.7.2.3.Accuracy Check for Simultaneous Determination of Bi and Te in Mixture by HG-Pt Coated-W Trap-ICPMS

Multi-element determination study by HG-Pt Coated-W Trap-ICPMS was the most crucial part of this thesis study. So, it was necessary to check the accuracy of this novel system. Since "1643e Trace Elements in Water" SRM was finished "1643f Trace Elements in Water" SRM was used in this part. Stock SRM was diluted 20 folds in two replicates. Concentration of HCl was 2.0 M in the final solution. Each replicate was measured three times. By direct calibration technique results of both elements were found acceptable by applying t-test at 95% confidence level. Measurements were done at mass 130 for Te. Results of SRM study are given in Table 3.31.

Table 3.31. Results of accuracy check for ^{209}Bi and ^{130}Te in Bi-Te mixture by HG-Pt coated-W Trap-ICPMS.

SRM NIST 1643f Natural Water	**^{209}Bi**	**^{130}Te**
Certified, ng/mL	12.62 ± 0.11	0.98 ± 0.01
Found, ng/mL	11.66 ± 0.91	1.03 ± 0.17

3.7.3. Dwell Time Studies for Two Masses

Studies on dwell time were performed for Bi part as a single mass work. As it was mentioned in the introduction part, number of points per peak is influenced by number of m/z monitored and dwell time. For a fixed analysis time and dwell time when numbers of monitored masses increase number of points per peak decreases. The reason is that the time spent for a specific mass decreases when other mass(es) are added for monitoring. There is another relation between the dwell time and number of points per peak for same number of masses monitored. In this case, number of points per peak decreases with the increase in dwell time. Longer the time spent for each point for a fixed analysis time, less the number of points obtained. In this part these relations were observed experimentally. Two masses, which were Bi and Te in mixture, were studied. Experiments were done by HG-Pt coated-W Trap-ICPMS system and in the same conditions of single mass study to obtain a sound comparison. Smoothing process was not applied in this part since it was not suggested according to the study in Bi part. Concentrations of the Bi and Te in mixture solution were 0.50 ng/mL and 2.5 ng/mL, respectively for this study. During the study, flow rate of H_2 was 106 mL/min while that of make-up Ar was 125 mL/min. In addition, "Peak hopping" mode of the instrument was used. Effect of dwell time on number of points per peak was evaluated only for Bi element when single mass and two masses were monitored. A very similar trend was obtained for Te. Transient signals of 0.50 ng/mL Bi alone and in mixture solution are given in Figure 3.52, Figure 3.53, Figure 3.54 and Figure 3.55, when dwell time was set to 10 ms, 20 ms, 50 ms and 100 ms, respectively.

Transient signals were redrawn by using Microsoft Office Excel program to see the points on peaks. When dwell time was increased from 10 ms to 100 ms, number of points per peak decreased for both signals obtained by single mass and two masses studies. Furthermore, number of points per peak decreased approximately to half when extra mass was monitored for the same dwell time. Therefore, poorer %RSD values are expected with an increase in the number of monitored masses. For multi-element studies

the best choice is to select small dwell times. For this case, 10 ms was the best among the others. In conclusion, dwell time was set as 10 ms also for multi-element part.

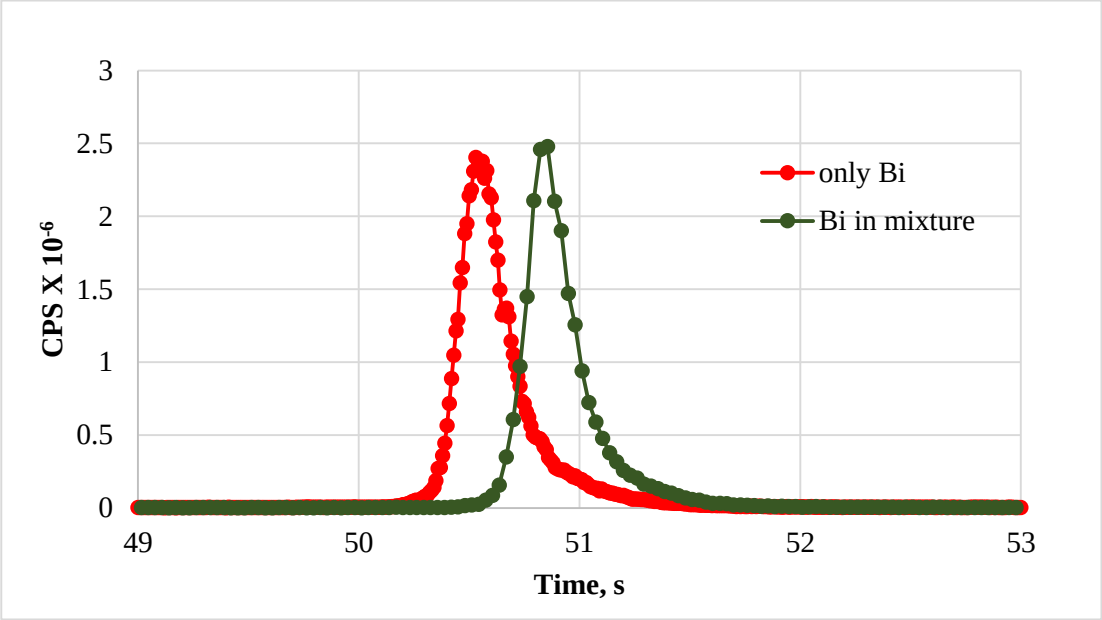

Figure 3.52. Transient signals of 0.50 ng/mL Bi alone and in binary mixture by HG-Pt coated–W Trap-ICPMS when dwell time is 10 ms.

Number of points per 2 seconds for Bi alone case: 200

Number of points per 2 seconds for binary mixture case: 65

Number of points per peak was calculated by taking the ratio of time interval between the starting and ending of the transient signal to the time spent for each datum. Time spent for each datum was 0.01 s for single mass study while 0.031 s for two elements study when dwell time was 10 ms. Time values were obtained from the numerical data windows of instrument's software program.

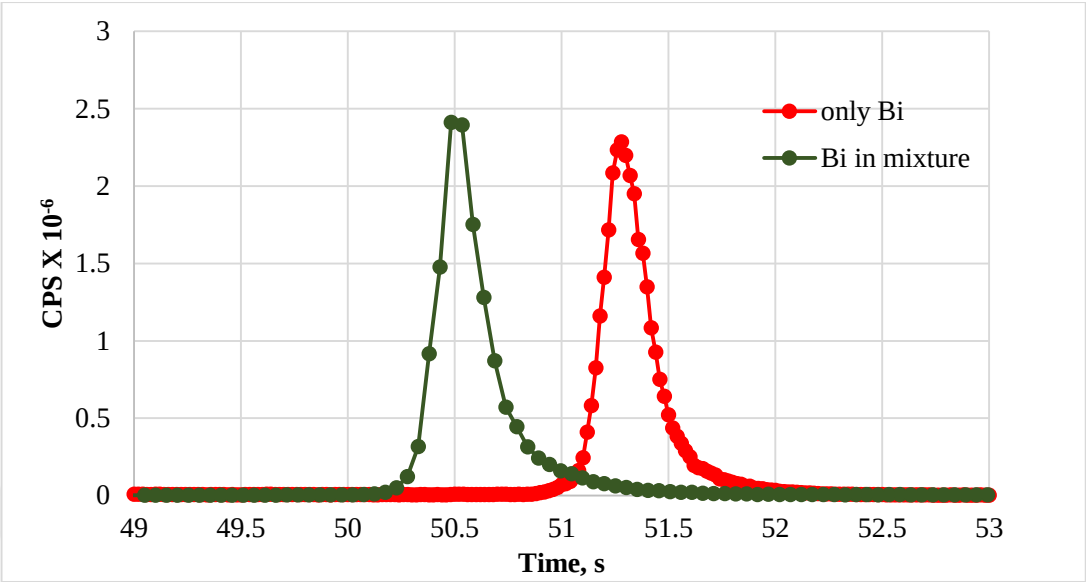

Figure 3.53. Transient signals of 0.50 ng/mL Bi alone and in binary mixture by HG-Pt coated–W Trap-ICPMS when dwell time is 20 ms.

Number of points per 2 seconds for Bi alone case: 100

Number of points per 2 seconds for binary mixture case: 39

Time spent for each data was 0.02 s for single mass study while 0.051 s for two elements study when dwell time was 20 ms.

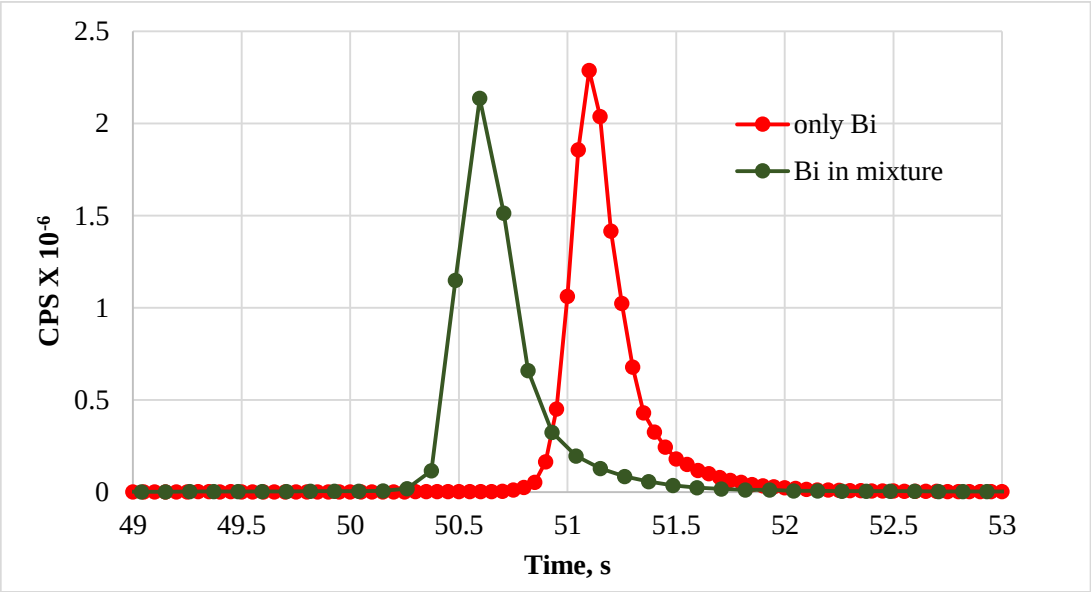

Figure 3.54. Transient signals of 0.50 ng/mL Bi alone and in binary mixture by HG-Pt coated–W Trap-ICPMS when dwell time is 50 ms.

Number of points per 2 seconds for Bi alone case: 40

Number of points per 2 seconds for binary mixture case: 18

Time spent for each data was 0.05 s for single mass study while 0.11 s for two elements study when dwell time was 50 ms.

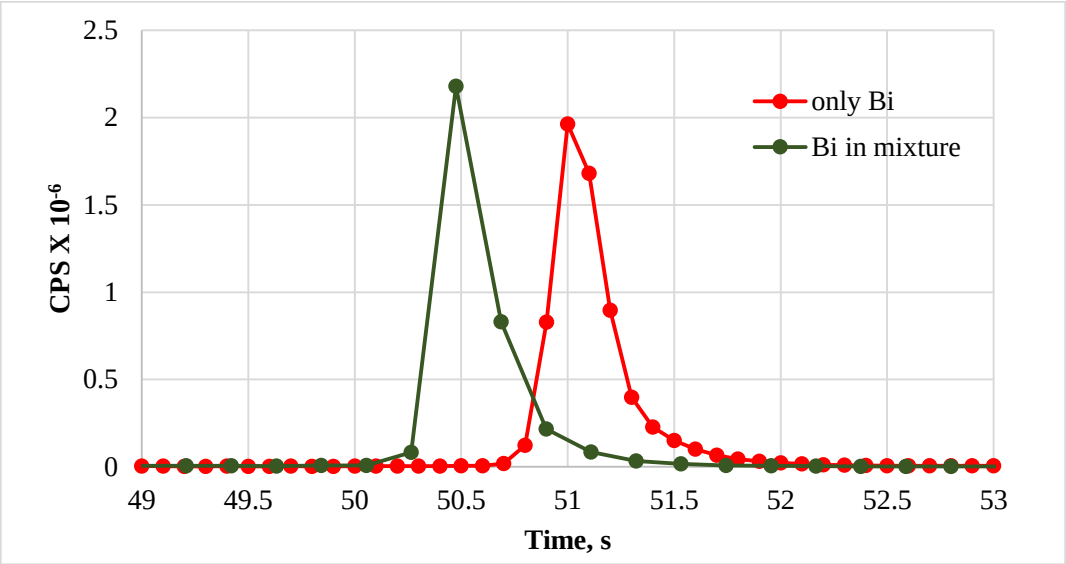

Figure 3.55. Transient signals of 0.50 ng/mL Bi alone and in binary mixture by HG-Pt coated–W Trap-ICPMS when dwell time is 100 ms.

Number of points per 2 seconds for Bi alone case: 20

Number of points per 2 seconds for binary mixture case: 10

Time spent for each data was 0.1 s for single mass study while 0.21 s for two elements study when dwell time was 100 ms.

As a conclusion, scan number decreases for multi mass study compared to single mass study in the specified analysis time. In addition, extra jump delays decrease the number of points per peak. From multi element studies, fly back and jump times were calculated by using the sweep times acquired from the instruments software. It is assumed that fly back and jump times differ depending on instrument and mass intervals. For example, for four different masses at 125, 128, 130 and 209 sweep time was 54 ms. On the other

hand, again for four masses but this time at 75, 111, 112 and 114 scan time was 49 ms for the same dwell time. As a last example for another set of four masses at 206, 207, 208 and 209 sweep time was found as 46 ms. Dwell time was fixed for all examples. These three examples verified that as the mass difference between monitored masses increases, jump time and also fly back time also increase. Other conclusion derived from above examples was fly back time also depends on mass intervals of monitored elements. When monitored masses are very close to each other, both jump time and fly back time decrease.

Jump time and fly back time were calculated roughly by using the mass range from 116 to 209. The scan times of two, three, four and six different masses in this range were taken into consideration for calculations. These calculations were specific to instrument that was used during this study. Therefore, in the light of above information fly back time was 9 ms and average jump time was approximately 2 ms when monitored masses were in the interval of 116 and 209. This range involves the masses of Te and Bi elements.

When dwell time is increased from 10 ms to 100 ms, slight decrease in signal height was observed. On the other hand, signal magnitude did not change in binary mixture study for same dwell time. One transient signal of Bi is given for each single and binary mixture study. However, during this part of the study five or six measurements were done. To reach more conclusive results, average counts and %RSD of the 0.50 ng/mL Bi for single and binary mixture study were summarized at different dwell times in Table 3.32. It is concluded that for both single and multi-element studies it is advised to use low dwell times in order not to lose the real magnitude of the signal.

Table 3.32. Effect of dwell time on signal magnitude.

Dwell time, ms		N	Average CPS	%RSD
10	Only Bi	6	$(2.49 \pm 0.14) \times 10^6$	5.45
	Bi in binary mixture	6	$(2.60 \pm 0.11) \times 10^6$	4.11
20	Only Bi	6	$(2.23 \pm 0.15) \times 10^6$	6.58
	Bi in binary mixture	5	$(2.49 \pm 0.07) \times 10^6$	2.82
50	Only Bi	5	$(2.16 \pm 0.10) \times 10^6$	4.81
	Bi in binary mixture	5	$(2.26 \pm 0.18) \times 10^6$	8.17
100	Only Bi	5	$(1.86 \pm 0.16) \times 10^6$	8.69
	Bi in binary mixture	5	$(2.03 \pm 0.15) \times 10^6$	7.46

3.7.4. Studies on Simultaneous Determination of Three Elements in Mixture by HG-W-Trap-ICPMS

By using the developed novel method, multi-element study was applied for the determination of two elements. Experiments proved that it was possible to study two elements simultaneously by HG-W-Trap-ICPMS system. It was questioned that how many elements can be determined simultaneously without problems with this developed method. Therefore, next and the last part in this thesis was determination of three elements in mixture solution. Criteria for choosing the third element were the similarity on hydride forming conditions and boiling points with Bi and Te. In addition, possibility of interferences between elements should be minimum.

Hydride formation conditions of Pb are very different than that of Bi and Te. For As, there is a risk of isobaric interference from $^{75}ArCl^+$ with ICPMS due to HCl usage as an acid source in Bi and Te study. Fortunately, Sb and also Se are suitable for simultaneous multi-element determinations together with Bi and Te elements. In a broad acid concentration range hydrides of both elements can be formed.[113]Furthermore, boiling points of Sb and Se are 1750 ºC and 685 ºC, respectively while that of Bi is 1560 ºC and

Te is 990 ºC. Difference in boiling points is preferred for multi-element study in order to avoid interferences during volatilization step from the trap surface. However, transient signals are very fast signals with a half width of only 0.2 s. Only the top of the peaks can be separated even there was an approximately 550 ºC difference between boiling points of Bi and Te elements. Since boiling point of Te is lower than that of Bi, when power supply was turned on, the needed temperature was reached first by volatilizing Te. Transient signals for 0.25 ng/mL Bi and 1.0 ng/mL Te in mixture by HG-Pt coated-W Trap-ICPMS that illustrates the above situation are given in Figure 3.56.

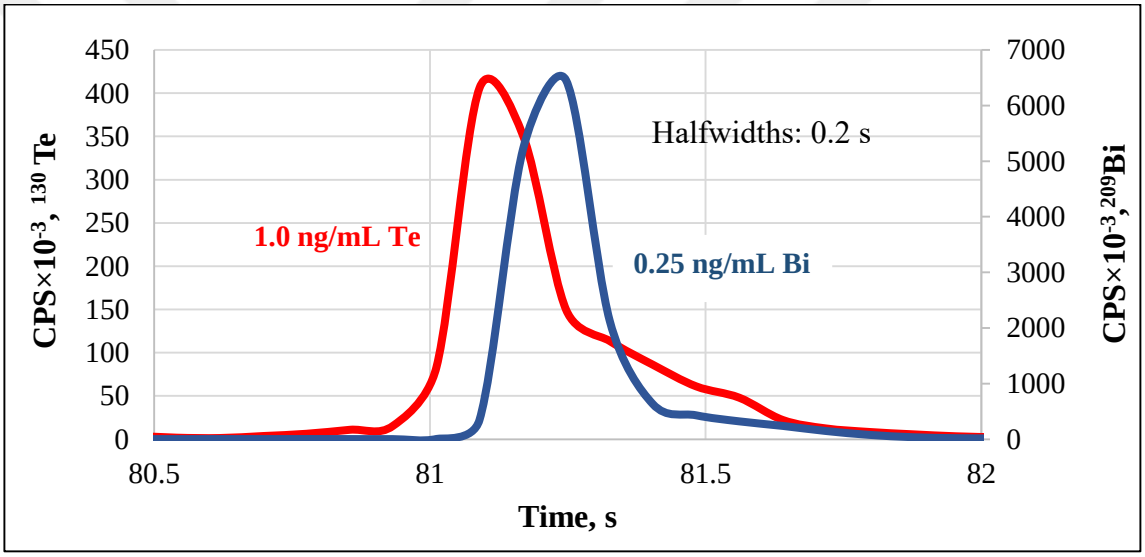

Figure 3.56. Transient signals of 0.25 ng/mL ^{209}Bi and 1.0 ng/mL ^{130}Te in Bi-Te mixture by HG-Pt coated–W Trap-ICPMS.

In addition, Sb has more tolerance to interferences compare to As and Se. Presence of Bi causes depression effect on As signals while effect is less for Sb and Se elements. For Sb, interference effect was observed when concentrations of Bi and Te were 100 mg/L. These results were obtained from HG studies.[113] Last criteria for this thesis study was, concentration of third candidate in SRM solution which was used in previous studies. Higher concentration in original stock was preferred to enable dilution process. By this way interference effects from other elements are also diluted.

As a conclusion, Sb and Se were the best candidates as a third element. By limiting the coating materials experiments were performed to see whether it was possible to obtain signals of Sb and Se in mixture solutions. Only two coatings were used which were Pt coating and Ir coating. Pt coating was the best for two-element study while Ir coating was the best for Bi determination. Therefore, selection of these two coatings was meaningful. Two separate mixture solutions were prepared. One included 0.25 ng/mL Bi, 1.0 ng/mL Te and 2.0 ng/mL Sb in 2.0 M HCl whereas other contained 0.25 ng/mL Bi, 1.0 ng/mL Te and 2.0 ng/mL Se in 2.0 M HCl. Mixture solutions were analyzed by using Pt and Ir coated W-coils separately for the same plasma and hydride forming conditions. Optimum values of hydride forming parameters and trap conditions obtained for Bi and Te mixture study were used for this part as given in Table 3.25 and Table 3.28.

Continuous hydride and transient signals of 2.0 M HCl as a blank and Sb, Se, Te and Bi elements in mixture are given for Pt and Ir-coated W coils in following figures. Two replicate signals of each analyte are shown in all figures. For Bi and Te, while one of the signals was obtained from Bi-Te-Sb mixture the other was derived from Bi-Te-Se mixture. Sb and Se were monitored at masses 121 and 78, respectively. There is no other mass to interfere at 121. For Se, mass at 78 is better with high natural abundance (23.78%) and very low possibility of ^{78}Kr (0.35%) interference. If Se is selected as a third element, more detailed study can be made on isotope selection. Signals of blank and 2.0 ng/mL Sb, 2.0 ng/mL Se, 1.0 ng/mL Te and 0.25 ng/mL Bi in two different mixtures by HG-Pt coated–W Trap-ICPMS system are given in Figure 3.57, Figure 3.58, Figure 3.59 and Figure 3.60, respectively.

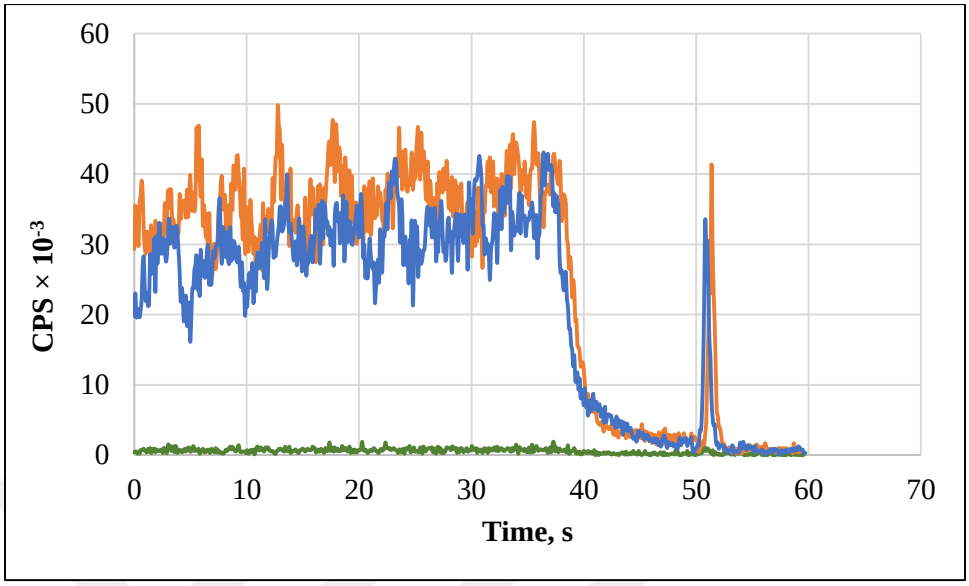

Figure 3.57. Hydride and transient signals of blank and 2.0 ng/mL ^{121}Sb in Bi-Te-Sb mixture by HG-Pt coated–W Trap-ICPMS.

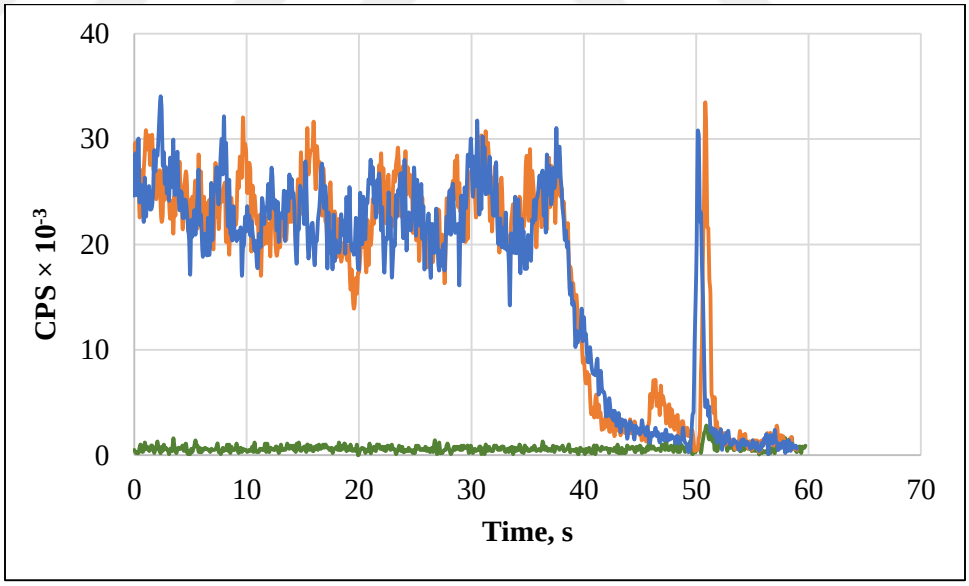

Figure 3.58. Hydride and transient signals of blank and 2.0 ng/mL ^{78}Se in Bi-Te-Se mixture by HG-Pt coated–W Trap-ICPMS.

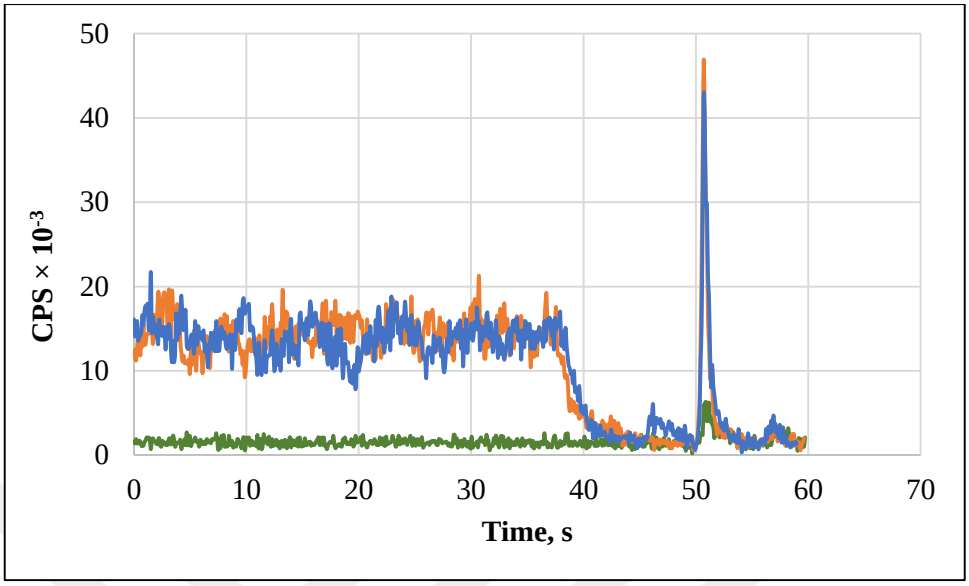

Figure 3.59. Hydride and transient signals of blank and 1.0 ng/mL ^{130}Te in Bi-Te-Se/Sb mixture by HG-Pt coated–W Trap-ICPMS.

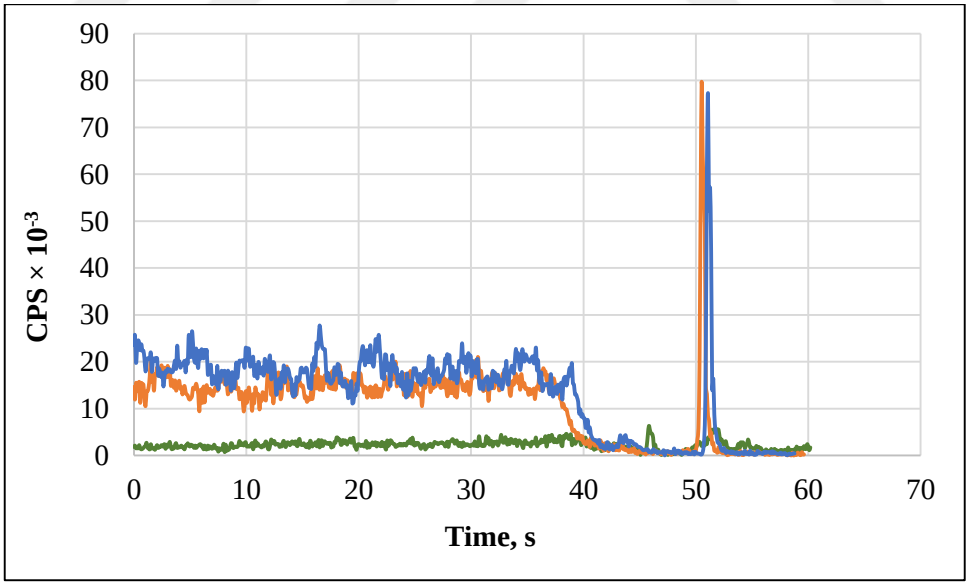

Figure 3.60. Hydride and transient signals of blank and 0.25 ng/mL ^{209}Bi in Bi-Te-Se/Sb mixture by HG-Pt coated–W Trap-ICPMS.

Signals of blank and 2.0 ng/mL Sb, 2.0 ng/mL Se, 1.0 ng/mL Te and 0.25 ng/mL Bi in two different mixtures by HG-Ir coated–W Trap-ICPMS system are given in Figure 3.61, Figure 3.62, Figure 3.63 andFigure 3.64, respectively.

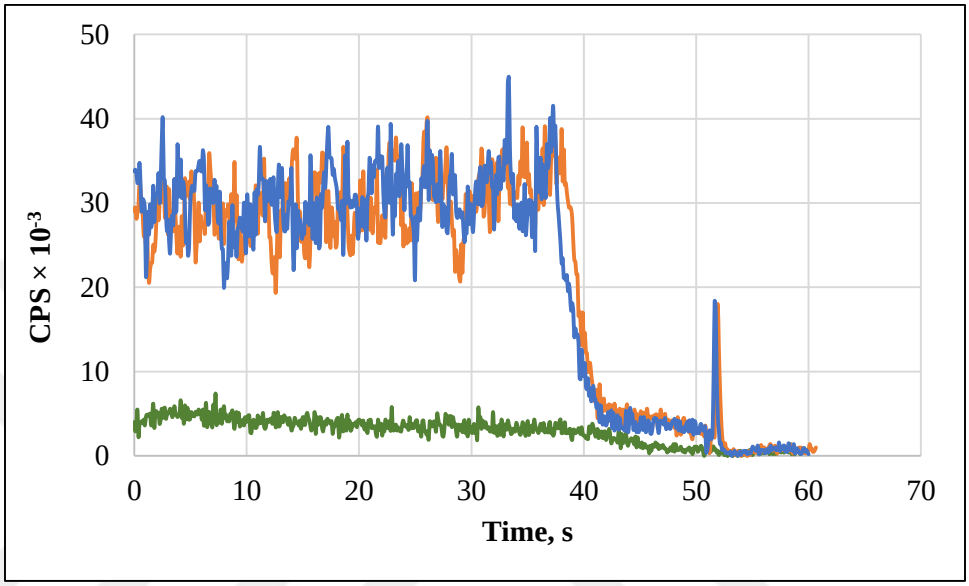

Figure 3.61. Hydride and transient signals of blank and 2.0 ng/mL ^{121}Sb in Bi-Te-Sb mixture by HG-Ir coated–W Trap-ICPMS.

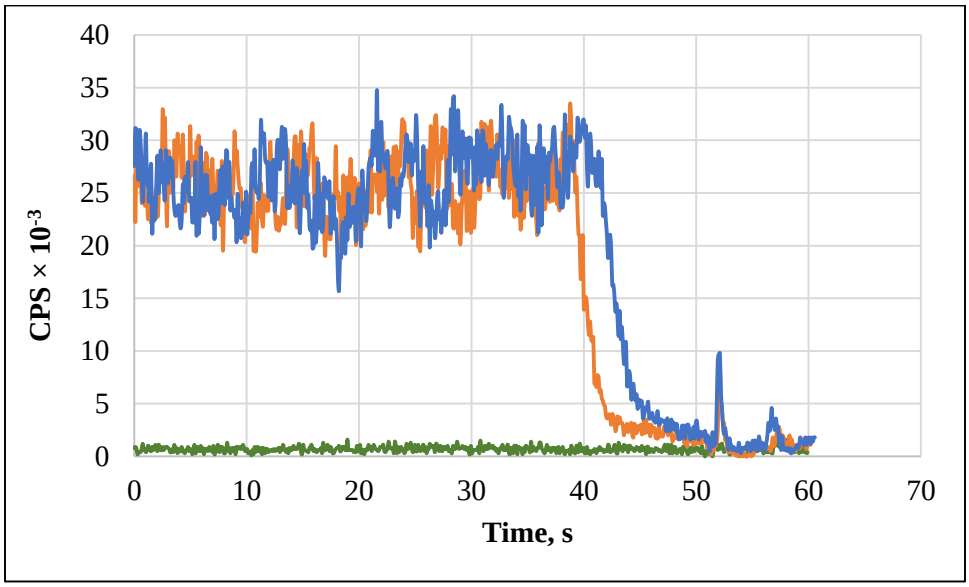

Figure 3.62. Hydride and transient signals of blank and 2.0 ng/mL ^{78}Se in Bi-Te-Se mixture by HG-Ir coated–W Trap-ICPMS.

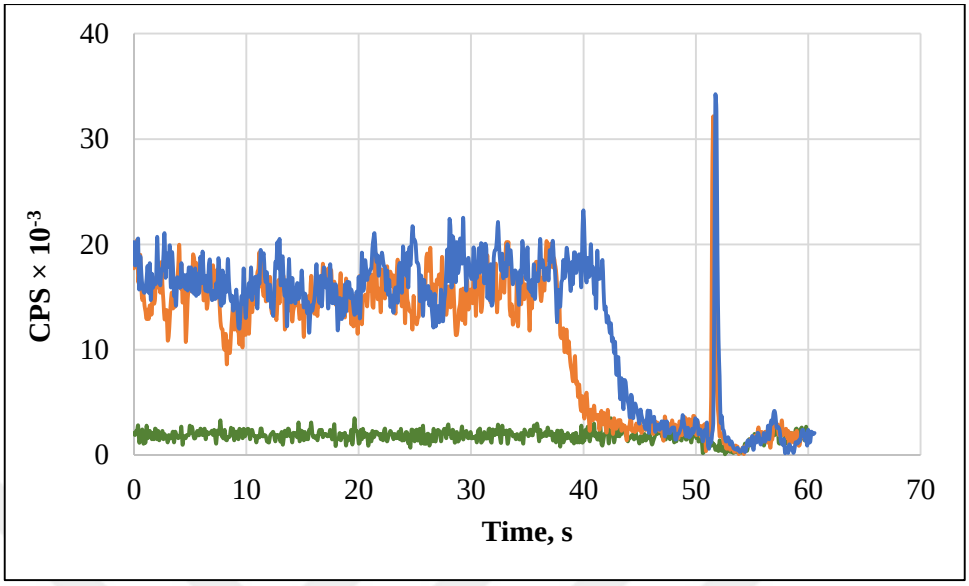

Figure 3.63. Hydride and transient signals of blank and 1.0 ng/mL ^{130}Te in Bi-Te-Se/Sb mixture by HG-Ir coated–W Trap-ICPMS.

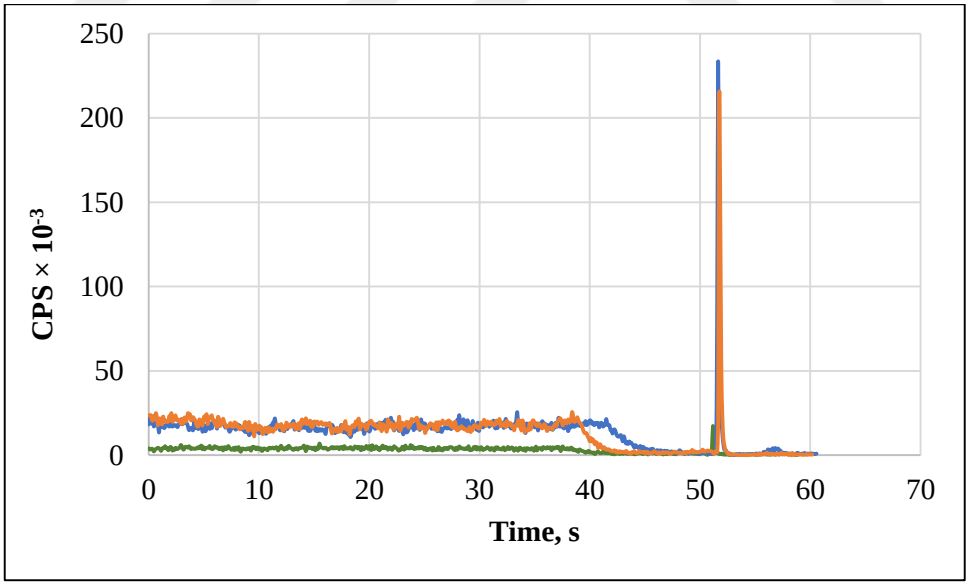

Figure 3.64. Hydride and transient signals of blank and 0.25 ng/mL ^{209}Bi in Bi-Te-Se/Sb mixture by HG-Ir coated–W Trap-ICPMS.

It was concluded from the signals that for the same hydride forming conditions, trap conditions and concentration both Sb and Se gave higher signals with Pt-coated W-coil

system. Performances of Pt and Ir-coated W-coils were good and it was proven from the signals of Te and Bi. As it was found in previous experiments trap signal of Te was higher when Pt-coated W-coil was used. On the other hand, Bi signal was higher when analyte trapped on Ir-coated coil as it was expected. Therefore, for three elements study, Pt-coated W-coil should be preferred if same trap conditions are used which was obtained previously.

Again for the optimum values obtained up to now and using Pt-coated W-coil, trap signal of Sb was a bit better than that belongs to Se. Of course by changing the hydride forming conditions and trapping conditions, more sensitive results could be acquired for both Sb and Se. However, changes in sensitivities of Bi and Te elements in mixture of three elements are inevitable for new conditions. In addition, different coating materials can be tried to check the trapping efficiencies of Sb and Se. There are two different choices for three elements study. One is choosing the third element first then finding optimum conditions and coating for three elements. Second is evaluating the coating materials first for both candidates and two main elements in detail and then select the third elements.

Moreover, in three elements study, since number of monitored masses increases number of points per peak decreases for each mass. Therefore, worse %RSD values are the probable consequence of three elements study.

CHAPTER 4

CONCLUSIONS

In this study a novel analytical method was developed for the simultaneous multi-element determination of Bi and Te by HG-Pt coated-W Trap-ICPMS. In addition, it was proven that it is feasible to determine three elements (Bi, Te and Sb or Se) simultaneously using the developed method. Two systems coupled to ICPMS provided sub ng/L level determination. HG system increased the sensitivity of the method by improving the transport efficiency of analyte aerosols nearly to 100%. Sensitivity was further increased when W-coil trap system was coupled to HG-ICPMS system. By trapping of the analyte on W-coil, preconcentration was achieved. Moreover, coating of the W-coil with solutions of some transition metals such as Ir, Pt and Rh, which have the high boiling points, helped to improve the sensitivity of trap system even further by changing the trapping efficiency positively. Another advantage of coating is to prolong the lifetime of W-coil.

For this novel method, one of the most critical issue was to maintain the plasma stability when trap system was connected in between HG system and ICPMS. Trap system consists of a glass manifold with connections to ICP torch on one end and to GLS on other end; addition connections are available for insertion of W-coil and make-up Ar. Another glass part that includes the W-coil and its electrical connections, can be easily inserted to or separated from the main trap manifold. Therefore, replacement of W-coil could be conveniently performed. These connections caused problems of leaks with air diffusion to the whole system. If the diffused air is not sucked out from the system before plasma was on or there was any air diffusion in the course of the experiment the

problems were encountered with plasma. In addition, H_2 gas entrance to the plasma, which was used for prevention of oxidation on W-coil surface, could also cause the plasma instability. In addition, it should be remembered that hydrogen gas is also produced in reaction between HCl and $NaBH_4$ for hydride production. In order to understand and solve the problems associated with this system, long hours were spent. Therefore, H_2 gas flow rate and absence of air in the system were the key parameters to overcome plasma instability.

Not only the H_2 gas flow rate but also make-up Ar flow rate was related with the plasma stability. Make-up Ar was needed to stabilize the plasma since it dilutes H_2 gas. Consequently, there was a relation between the flow rates of H_2 and make-up Ar. Reference was the H_2 flow rate. In order to make sure that W-coil is not oxidized, sufficiently high flow rate of H_2 was used by also considering the minimum dilution of the hydride species. Then, depending on the H_2 flow rate, optimum make-up Ar flow rate was set. Higher the H_2 flow rate, higher make-up Ar flow was required to enable the proper dilution of H_2 gas. Unfortunately, as flow rate of make-up Ar increases due to dilution effect of volatile analyte species lower signals were obtained. This was an undesired situation; therefore optimizations of flow rates for these two gases were very important.

This novel method was developed step by step and using one element at a time starting with Bi. The first step was determination of Bi by ICPMS using nebulization as sample introduction technique. For this part, optimizations of ICPMS parameters were completed to get the best sensitivity. Flow injection system with a loop volume of 500 µL was used. After optimizations, LOD of system was found 21.0 ng/L with a %RSD of 4.17 using the lowest concentration of Bi. Calibration range was from 0.10 to 10 ng/mL. Since Bi has only one natural isotope at mass 209, ^{209}Bi was monitored during this thesis study.

In the second stage, HG system was coupled to ICPMS. Two GLSs with different designs were tried for this part to separate formed hydride species and directly sent them

to ICPMS. One of them was U-Tube shaped and the other one was cylindrical. Optimizations for HG-ICPMS were done by using both GLSs. The effects of carrier Ar flow rate, $NaBH_4$ solution flow rate, carrier acid flow rate, concentration of $NaBH_4$ solution and concentration of HCl in Bi solution were checked on Bi signals. Except carrier Ar flow rate optimum values of other parameters were same for both GLSs. U-tube GLS was used for this study due to two reasons. First reason was signals obtained with U-tube GLS were higher in magnitude. Second and more important reason was its larger volume that compensates the chemical noise resulted from generated H_2. Unfortunately, plasma was very sensitive to fluctuations in gas flows even a small volume of H_2 was produced. Flow injection system with a loop volume of 500 µL was also used in this part. LOD and %RSD of this system was 9.5 ng/L and 5.84, respectively using the lowest concentration of Bi in its range which was 0.050 ng/mL. Enhancement was found to be better when comparison was done in slopes of calibration graphs. 85 fold enhancement was obtained as compared to nebulization system. Due to H_2 gas formation, noise in the system increased and %RSD became poorer.

For the last step, W-coil trap system was added in between HG system and ICPMS. This novel system was called HG-W-Trap-ICPMS. Volatile Bi species introduced from HG were trapped on W-coil. Trap parameters, which were H_2 gas flow rate, make-up Ar flow rate, trapping temperature, revolatilization temperature and trapping period, were optimized not only to get reasonably high signals but also to provide sustainability of the plasma/system. In addition, effect of coatings was evaluated. Among Ir, Pt and Rh metal coatings, Ir gave the best trapping efficiency for Bi determination. Then, in order to check the effect of coating on reproducibility and magnitude of the trap signals both uncoated and Ir-coated W-coils were used. At optimum values for hydride and trap systems, LOD and %RSD of uncoated-W-coil system were found to be 3.4 ng/L and 7.68, respectively. On the other hand, LOD was 2.7 ng/L while %RSD was 6.30 for Ir-coated-W-coil system. The lowest concentration of Bi in the range, which was 0.010 ng/mL, was used for calculations of analytical performances for both systems. As it was shown from %RSD values, coating improved the reproducibility. Peak height values were used for each step of this study for calculation of analytical performances.

Since HG-W-Trap-ICPMS method developed in this study was the first one in literature at present, direct comparison of found results was not possible. However, there are studies in literature with W-coil using AAS or AFS as a detector. These works were used for comparison.

In trap studies, collected volume or collection period was the critical point that affects sensitivity of the system directly. For different studies in literature, different volumes or periods were used. Therefore, to make meaningful calculations of enhancements, E_v and E_t terms were used. For this study, with 60 seconds collection period and 2.0 mL/min flow rate of sample solution E_t and E_v was found as 3.3 and 1.7, respectively for Bi. Ratio of LOD values for HG and HG-trap systems was used for calculation of enhancement values.

After HG-W-Trap-ICPMS method was developed successfully for the determination of Bi, multi-element determination was studied as a second main part in this thesis. Initial multi-element study was done by using two elements, Bi and Te. Common optimum values of HG and trap parameters were found for both elements in mixture after optimizations. Acid content of analyte solution was critical for Te; therefore mixture solution was prepared in 2.0 M HCl. In addition to HG-W-Trap-ICPMS method, analytical performances of Bi and Te in mixture were studied by HG-ICPMS. Pt-coated-W-coil was used for mixture since significantly higher signals obtained for Te when coil was coated with Pt. On the other hand, difference on signal magnitude obtained from Ir and Pt-coated W coil systems was small for Bi. As a conclusion, Pt-coated W-coil was preferred for mixture study and analytical performances were found to be satisfactory for both elements. When slopes of calibration graphs were compared for one and two masses studies, results were found very close for both Bi and Te. However, LOD values became marginally higher in the mixture study. This situation was probable since a higher of monitored masses was handled. In addition, optimum conditions for single and two elements studies were different although the deterioration was not too much. Interference effects of Bi and Te on each other has also been considered. ^{130}Te was

monitored during the method development experiments. Isobaric interference of Xe, which can be present in Ar gas, was checked on ^{130}Te and no significant effect was found. LOD values for ^{209}Bi and ^{130}Te in mixture were 9.0 ng/L and 7.0 ng/L, respectively.

In order to compare the sensitivities of Te in mixture and single element studies, single mass study for ^{130}Te was performed by both HG-ICPMS and HG-Pt-coated-W-coil-ICPMS. For the former, LOD and %RSD were calculated as 12 ng/L and 6.5, respectively using the lowest concentration of Te in the range which was 0.050 ng/mL. Sensitivities of Bi and Te were very close by HG-ICPMS. Similar to Bi determination, flow injection system with a loop volume of 500 µL was used.

For determination of Te alone by HG-Pt-coated-W-coil-ICPMS method, analytical performances were calculated by using the optimum values. LOD of this system was found as 6.0 ng/L using the lowest concentration of Te in range which was 0.025 ng/mL. Enhancement factor with respect to HG-ICPMS system was 2.0. With 60 seconds collection period and 2.0 mL/min flow rate of sample solution E_t and E_v were found to be 2.0 min^{-1} and 1.0 mL^{-1}, respectively.

Trapping efficiency was the critical part in trap studies. For both Bi and Te, trapping efficiencies were calculated in two ways. For 30 seconds trapping period on Ir-coated-W-coil, average trapping efficiency of Bi was calculated as 35% using two different ways. On the other hand, trapping efficiency of Te was performed on Pt-coated-W-coil. Trapping efficiency of Te was calculated as 13% for 30 seconds trapping period.

Importance of dwell time and smoothing of the signal were also evaluated in this study. Experiments were done in trap part by monitoring the signals in single and two masses studies. When the dwell time was increased, number of points per peak decreased and this situation affected the RSD value negatively. Furthermore, number of points per peak declined if number of monitored m/z values increased for a fixed dwell time. Therefore, small dwell time was preferred especially for multi-element studies. Dwell time was 10

ms in all parts of this study. Smoothing helps to obtain a signal with less noise. However, both magnitude and shape of the signal changed when degree of smoothing was increased. Magnitude of the signal decreased and peak became broad. It was concluded that smoothing was not useful in the case handled here where sharp transient signals with halfwidth of 0.2 s were obtained.

Accuracy of all parts was checked by using "NIST 1643e Trace Elements in Water" and "NIST 1643f Trace Elements in Water" SRM solutions. Results were found in good agreement with certified ones by using direct calibration technique for ^{209}Bi in all parts. However, for Te, standard addition technique was needed in ICPMS and HG-Pt coated-W Trap-ICPMS parts. In addition, isotope of ^{128}Te was monitored in standard addition technique to eliminate interferences. SRM includes Ba which has an isotope at mass 130. Although natural abundance of ^{130}Ba is very small, risk of interference was eliminated by monitoring the ^{128}Te.

Last part in this study was to check the possibility of three elements determination simultaneously by HG-W-Trap-ICPMS. Sb and Se were the candidates as a third element. By using the optimum values of hydride and trap systems for Bi-Te mixture study, experiments were done by HG-Pt coated-W Trap-ICPMS. Two mixture solutions were prepared separately. While one included Sb besides Bi and Te, the other contained Se, Bi and Te. It was concluded that determination of three elements simultaneously was feasible by the developed method in this study. Of course, detailed experiments must be performed to obtain optimum values for three elements and then analytical performances could be calculated.

In conclusion, a novel analytical method, which was called HG-W-Trap-ICPMS, was developed and multi-element determination at ultra-trace level was performed successfully by the developed method in this thesis.

REFERENCES

1. Lagrone, C. B., Bismuth (Bi) Salem Press Encyclopedia of Science, January, 2015.

2. Das, A. K.; Chakraborty, R.; Cervera, M. L.; de la Guardia, M., Analytical techniques for the determination of bismuth in solid environmental samples. *Trac-Trends in Analytical Chemistry* **2006,** *25* (6), 599-608.

3. Ivanova, J.; Djingova, R.; Korhammer, S.; Markert, B., On the microwave digestion of soils and sediments for determination of lanthanides and some toxic and essential elements by inductively coupled plasma source mass spectrometry. *Talanta* **2001,** *54* (4), 567-574.

4. Hall, G. E. M.; Pelchat, J. C., Analysis of geological materials for bismuth, antimony, selenium and tellurium by continuous flow hydride generation inductively coupled plasma mass spectrometry .1. Mutual hydride interferences. *Journal of Analytical Atomic Spectrometry* **1997,** *12* (1), 97-102.

5. Moscoso-Perez, C.; Moreda-Pineiro, J.; Lopez-Mahia, P.; Muniategui-Lorenzo, S.; Fernandez-Fernandez, E.; Prada-Rodriguez, D., Bismuth determination in environmental samples by hydride generation-electrothermal atomic absorption spectrometry. *Talanta* **2003,** *61* (5), 633-642.

6. Krishna, M. V. B.; Arunachalam, J., Ultrasound-assisted extraction procedure for the fast estimation of major, minor and trace elements in lichen and mussel samples by ICP-MS and ICP-AES. *Analytica Chimica Acta* **2004,** *522* (2), 179-187.

7. Messerschmidt, J.; VonBohlen, A.; Alt, F.; Klockenkamper, R., Determination of arsenic and bismuth in biological materials by total reflection X-ray fluorescence after

separation and collection of their hydrides. *Journal of Analytical Atomic Spectrometry* **1997,** *12* (11), 1251-1254.

8. Korhammer, S.; Herzig, R.; Schramel, P.; Kumpulainen, J.; Markert, B.; Muntau, H.; Quevauviller, P., The preparation of a cabbage reference material for environmental monitoring and food analysis. *Accreditation and Quality Assurance* **2000,** *5* (6), 238-242.

9. Gundersen, V.; Bechmann, I. E.; Behrens, A.; Sturup, S., Comparative investigation of concentrations of major and trace elements in organic and conventional Danish agricultural crops. 1. Onions (Allium cepa Hysam) and peas (Pisum sativum Ping Pong). *Journal of Agricultural and Food Chemistry* **2000,** *48* (12), 6094-6102.

10. Cava-Montesinos, P.; Cervera, M. L.; Pastor, A.; de la Guardia, M., Room temperature acid sonication ICP-MS multielemental analysis of milk. *Analytica Chimica Acta* **2005,** *531* (1), 111-123.

11. Gonzalez-Weller, D.; Rubio, C.; Gutierrez, A. J.; Gonzalez, G. L.; Mesa, J. M. C.; Girones, C. R.; Ojeda, A. B.; Hardisson, A., Dietary intake of barium, bismuth, chromium, lithium, and strontium in a Spanish population (Canary Islands, Spain). *Food and Chemical Toxicology* **2013,** *62*, 856-868.

12. Burguera, J. L.; Burguera, M.; Rivas, C.; Rondon, C.; Carrero, P.; Gallignani, M., Determination of bismuth in biological samples using on-line flow-injection microwave-assisted mineralization and precipitation/dissolution for electrothermal atomic absorption spectrometry. *Talanta* **1999,** *48* (4), 885-893.

13. Taylor, D. M.; Williams, D. R., *Trace Element Medicine and Chelation Therapy*. The royal society of chemisty: Cambridge, 1995.

14. Cadore, S.; dos Anjos, A. P.; Baccan, N., Determination of bismuth in urine and prescription medicines using atomic absorption with an on-line hydride generation system. *Analyst* **1998,** *123* (8), 1717-1719.

15. Cankur, O.; Ertas, N.; Ataman, O. Y., Determination of bismuth using on-line preconcentration by trapping on resistively heated W coil and hydride generation atomic absorption spectrometry. *Journal of Analytical Atomic Spectrometry* **2002,** *17* (6), 603-609.

16. Merian, E.; Clarkson, T. W., *Bismuth in: Metals and Their Compounds in the Environment*. VCH: Weinheim, 1991.

17. Pamphlett, R.; Stoltenberg, M.; Rungby, J.; Danscher, G., Uptake of bismuth in motor neurons of mice after single oral doses of bismuth compounds. *Neurotoxicology and Teratology* **2000,** *22* (4), 559-563.

18. Madrakian, T.; Afkhami, A.; Esmaeili, A., Spectrophotometric determination of bismuth in water samples after preconcentration of its thiourea-bromide ternary complex on activated carbon. *Talanta* **2003,** *60* (4), 831-838.

19. Kolekar, G. B.; Lokhande, T. N.; Bhosale, P. N.; Anuse, M. A., Extraction, separation and spectrophotometric determination of bismuth(III) using 1(4 '-bromophenyl) 4,4,6-trimethyl (1H,4H)-pyrimidine-2-thiol. *Analytical Letters* **1998,** *31* (13), 2241-2254.

20. Dean, S. U.; Tscherwonyi, P. J.; Riley, W. J., Elimination of Matrix Effects in Electrothermal Atomic-Absorption Spectrophotometric Determinations of Bismuth in Serum and Urine. *Clinical Chemistry* **1992,** *38* (1), 119-122.

21. Lin, R. J.; Pan, J. M., Direct spectrophotometric determination of bismuth in pharmaceutical products using a flow-injection system. *Indian Journal of Chemistry Section a-Inorganic Bio-Inorganic Physical Theoretical & Analytical Chemistry* **2000,** *39* (6), 676-678.

22. Zhu, Z. C.; Zheng, J. H.; Chi, S. L.; Lin, C. R., A sensitive spectrophotometric method for the determination of bismuth with ethyl violet and nitroso-R salt. *Chinese Journal of Analytical Chemistry* **1999,** *27* (9), 1116-1116.

23. Kilinc, E.; Bakirdere, S.; Aydin, F.; Ataman, O. Y., Sensitive determination of bismuth by flame atomic absorption spectrometry using atom trapping in a slotted quartz tube and revolatilization with organic solvent pulse. *Spectrochimica Acta Part B-Atomic Spectroscopy* **2012,** *73*, 84-88.

24. Fayazi, M.; Afzali, D.; Mostafavi, A., Pre-concentration procedure using dispersive liquid-liquid microextraction for the determination of bismuth by flame atomic absorption spectrometry. *Journal of Analytical Atomic Spectrometry* **2011,** *26* (10), 2064-2068.

25. Burguera, M.; Burguera, J. L.; Rondon, C.; Garcia, M. I.; de Pena, Y. P.; Villasmil, L. M., Determination of bismuth in biological tissues by electrothermal atomic absorption spectrometry using platinum and tartaric acid as chemical modifier. *Journal of Analytical Atomic Spectrometry* **2001,** *16* (10), 1190-1195.

26. Chamsaz, M.; Arbab-Zavar, M. H.; Riazi, M. M.; Takjoo, R., Determination of Bismuth by Electrothermal Atomic Absorption Spectrometry using Single Drop Micro Extraction in Real Samples. *Asian Journal of Chemistry* **2011,** *23* (6), 2441-2444.

27. Shemirani, F.; Baghdadi, M.; Ramezani, M.; Jamali, M. R., Determination of ultra trace amounts of bismuth in biological and water samples by electrothermal atomic absorption spectrometry (ET-AAS) after cloud point extraction. *Analytica Chimica Acta* **2005,** *534* (1), 163-169.

28. Sun, M.; Wu, Q., Determination of trace bismuth in human serum by cloud point extraction coupled flow injection inductively coupled plasma optical emission spectrometry. *Journal of Hazardous Materials* **2011,** *192* (3), 935-939.

29. Itagaki, T.; Ashino, T.; Takada, K.; Wagatsuma, K., Determination of Trace Amounts of Arsenic, Bismuth, Antimony and Tin in Low Alloy Steel by Inductively Coupled Plasma Optical Emission Spectrometry after Separation by Co-Precipitation with Manganese (IV) Oxide. *Bunseki Kagaku* **2010,** *59* (1), 43-50.

30. El-Shahawi, M. S.; Al-Sibaai, A. A.; Bashammakh, A. S.; Alwael, H.; Al-Saidi, H. M., Ion pairing based polyurethane foam sorbent packed column combined with inductively coupled plasma-optical emission spectrometry for sensitive determination and chemical speciation of bismuth(III & V) in water. *Journal of Industrial and Engineering Chemistry* **2015,** *28*, 377-383.

31. Li, H. Y.; Keohane, B. M.; Sun, H. Z.; Sadler, P. J., Determination of bismuth in serum and urine by direct injection nebulization inductively coupled plasma mass spectrometry. *Journal of Analytical Atomic Spectrometry* **1997,** *12* (10), 1111-1114.

32. Jia, X.; Han, Y.; Liu, X.; Duan, T.; Chen, H., Dispersive liquid-liquid microextraction combined with flow injection inductively coupled plasma mass spectrometry for simultaneous determination of cadmium, lead and bismuth in water samples. *Microchimica Acta* **2010,** *171* (1-2), 49-56.

33. Norisuye, K.; Sohrin, Y., Determination of bismuth in open ocean waters by inductively coupled plasma sector-field mass spectrometry after chelating resin column preconcentration. *Analytica Chimica Acta* **2012,** *727*, 71-77.

34. Schramel, P.; Wendler, I.; Angerer, J., The determination of metals (antimony, bismuth, lead, cadmium, mercury, palladium, platinum, tellurium, thallium, tin and tungsten) in urine samples by inductively coupled plasma-mass spectrometry. *International Archives of Occupational and Environmental Health* **1997,** *69* (3), 219-223.

35. Kobayashi, J.; Terada, H.; Sugiyama, H.; Matsukawa, T.; Chiba, M.; Yokoyama, K., Determination of Bismuth in Environmental Samples by ICP-MS and Basic Examination of Cell Toxicity for Their Compounds. *Bunseki Kagaku* **2011,** *60* (4), 357-362.

36. Wan, A. T.; Froomes, P., Determination of Bismuth in Biological Materials by Atomic Absorption Spectrometry with Hydride Generation. *Atomic Spectroscopy* **1991,** *12* (3), 77-80.

37. Li, Z. X.; Guo, Y. A., Simultaneous determination of trace arsenic, antimony, bismuth and selenium in biological samples by hydride generation-four-channel atomic fluorescence spectrometry. *Talanta* **2005,** *65* (5), 1318-1325.

38. Cava-Montesintos, P.; Cervera, M. L.; Pastor, A.; De La Guardia, M., Determination of ultratrace bismuth in milk samples by atomic fluorescence spectrometry. *Journal of Aoac International* **2003,** *86* (4), 815-822.

39. Guo, S.; Ji, Z.; Feng, B.; Bian, J., Simultaneous Determination of Trace Antimony and Bismuth in Jilin Ginseng with Microwave Digestion Hydride Generation Atomic Fluorescence Spectrometry. *Chemical Engineering and Material Properties Ii* **2012,** *549*, 188-192.

40. Wang, F.; Zhang, G., Simultaneous Quantitative Analysis of Arsenic, Bismuth, Selenium, and Tellurium in Soil Samples Using Multi-channel Hydride-Generation Atomic Fluorescence Spectrometry. *Applied Spectroscopy* **2011,** *65* (3), 315-319.

41. Zhang, N.; Fu, N.; Fang, Z.; Feng, Y.; Ke, L., Simultaneous multi-channel hydride generation atomic fluorescence spectrometry determination of arsenic, bismuth, tellurium and selenium in tea leaves. *Food Chemistry* **2011,** *124* (3), 1185-1188.

42. Wu, H.; Du, B.; Fang, C., Flow injection on-line preconcentration coupled with hydride generation atomic fluorescence Spectrometry for ultra-trace amounts of bismuth determination in biological and environmental water samples. *Analytical Letters* **2007,** *40* (14), 2772-2782.

43. Matos Reyes, M. N.; Cervera, M. L.; de la Guardia, M., Determination of total Sb, Se, Te, and Bi and evaluation of their inorganic species in garlic by hydride-generation-atomic-fluorescence spectrometry. *Analytical and Bioanalytical Chemistry* **2009,** *394* (6), 1557-1562.

44. Afonso, D. D.; Baytak, S.; Arslan, Z., Simultaneous generation of hydrides of bismuth, lead and tin in the presence of ferricyanide and application to determination in

biominerals by ICP-AES. *Journal of Analytical Atomic Spectrometry* **2010,** *25* (5), 726-729.

45. Rigby, C.; Brindle, I. D., Determination of arsenic, antimony, bismuth, germanium, tin, selenium and tellurium in 30% zinc sulfate solution by hydride generation inductively coupled plasma atomic emission spectrometry. *Journal of Analytical Atomic Spectrometry* **1999,** *14* (2), 253-258.

46. Kilinc, E.; Aydin, F., Optimization of Continuous Flow Hydride Generation Inductively Coupled Plasma Optical Emission Spectrometry for Sensitivity Improvement of Bismuth. *Analytical Letters* **2012,** *45* (17), 2623-2636.

47. Chen, W.-N.; Jiang, S.-J.; Chen, Y.-L.; Sahayam, A. C., Slurry sampling flow injection chemical vapor generation inductively coupled plasma mass spectrometry for the determination of trace Ge, As, Cd, Sb, Hg and Bi in cosmetic lotions. *Analytica Chimica Acta* **2015,** *860*, 8-14.

48. Calvo Fornieles, A.; Garcia de Torres, A.; Vereda Alonso, E. I.; Cano Pavon, J. M., Determination of antimony, bismuth and tin in natural waters by flow injection solid phase extraction coupled with online hydride generation inductively coupled plasma mass spectrometry. *Journal of Analytical Atomic Spectrometry* **2013,** *28* (3), 364-372.

49. Hall, G. E. M.; MacLaurin, A. I.; Pelchat, J. C.; Gauthier, G., Comparison of the techniques of atomic absorption spectrometry and inductively coupled plasma mass spectrometry in the determination of Bi, Se and Te by hydride generation. *Chemical Geology* **1997,** *137* (1-2), 79-89.

50. Heitkemper, D. T.; Caruso, J. A., Continuous Hydride Generation for Simultaneous Multielement Detection With Inductively Coupled Plasma Mass Spectrometry. *Applied Spectroscopy* **1990,** *44* (2), 228-234.

51. Xiong, C.; Hu, B., Headspace trapping of the hydrides on a Pd(II)-coated graphite adsorptive bar as a microextraction method for ETV-ICP-MS determination of Se, Te and Bi in seawater and human hair samples. *Talanta* **2010,** *81* (1-2), 578-585.

52. Yun, Y.; Cui, F.; Geng, S.; Jin, J., Determination of bismuth in pharmaceutical products using phosphoric acid as molecular probe by resonance light scattering. *Luminescence* **2012,** *27* (5), 352-356.

53. Gadhari, N. S.; Sanghavi, B. J.; Karna, S. P.; Srivastava, A. K., Potentiometric stripping analysis of bismuth based on carbon paste electrode modified with cryptand 2.2.1 and multiwalled carbon nanotubes. *Electrochimica Acta* **2010,** *56* (2), 627-635.

54. Wang, E.; Sun, W.; Yang, Y., Potentiometric Stripping Analysis With a Thin-Film Gold Electrode for Determination of Copper, Bismuth, Antimony and Lead *Analytical Chemistry* **1984,** *56* (11), 1903-1906.

55. Eskilsson, H.; Jagner, D., Potentiometric Stripping Analysis for Bismuth (III) in sea-water. *Analytica Chimica Acta* **1982,** *138* (JUN), 27-33.

56. Tanaka, T.; Taguchi, S.; Ota, Y.; Katano, K.; Hirabayashi, R., Sensitive Determination of Bismuth in Iron and Steel by Stripping Voltammetry after Extraction of the Matrix. *Tetsu to Hagane-Journal of the Iron and Steel Institute of Japan* **2011,** *97* (2), 85-89.

57. Ashkenani, H.; Taher, M. A., Application of a new ion-imprinted polymer for solid-phase extraction of bismuth from various samples and its determination by ETAAS. *International Journal of Environmental Analytical Chemistry* **2013,** *93* (11), 1132-1145.

58. Shakerian, F.; Shabani, A. M. H.; Dadfarnia, S.; Avanji, M. K., Hydride generation atomic absorption spectrometric determination of bismuth after separation and preconcentration with modified alumina. *Journal of Separation Science* **2015,** *38* (4), 677-682.

59. Kratzer, J.; Bousek, J.; Sturgeon, R. E.; Mester, Z.; Dedina, J., Determination of Bismuth by Dielectric Barrier Discharge Atomic Absorption Spectrometry Coupled with Hydride Generation: Method Optimization and Evaluation of Analytical Performance. *Analytical Chemistry* **2014,** *86* (19), 9620-9625.

60. Park, C. J., Determination of Bi impurity in lead stock standard solutions by hydride-generation inductively coupled plasma mass spectrometry. *Bulletin of the Korean Chemical Society* **2004,** *25* (2), 233-236.

61. Cui, F.; Wang, L.; Cui, Y., Determination of bismuth in pharmaceutical products using methyltriphenylphosphonium bromide as a molecular probe by resonance light scattering technique. *Journal of Pharmaceutical and Biomedical Analysis* **2007,** *43* (3), 1033-1038.

62. Fathirad, F.; Afzali, D.; Mostafavi, A.; Shamspur, T.; Fozooni, S., Fabrication of a new carbon paste electrode modified with multi-walled carbon nanotube for stripping voltammetric determination of bismuth(III). *Electrochimica Acta* **2013,** *103*, 206-210.

63. Guo, H. S.; Li, Y. H.; Xiao, P. F.; He, N. Y., Determination of trace amount of bismuth(III) by adsorptive anodic stripping voltammetry at carbon paste electrode. *Analytica Chimica Acta* **2005,** *534* (1), 143-147.

64. Yamini, Y.; Chaloosi, M.; Ebrahimzadeh, H., Solid phase extraction and graphite furnace atomic absorption spectrometric determination of ultra trace amounts of bismuth in water samples. *Talanta* **2002,** *56* (4), 797-803.

65. Ribeiro, A. S.; Arruda, M. A. Z.; Cadore, S., Determination of bismuth in metallurgical materials using a quartz tube atomizer with tungsten coil and flow injection-hydride-generation atomic absorption spectrometry. *Spectrochimica Acta Part B-Atomic Spectroscopy* **2002,** *57* (12), 2113-2120.

66. Matusiewicz, H.; Sturgeon, R. E., Atomic spectrometric detection of hydride forming elements following in situ trapping within a graphite furnace. *Spectrochimica Acta Part B-Atomic Spectroscopy* **1996,** *51* (4), 377-397.

67. Thompson, M.; Pahlavanpour, B.; Walton, S. J., Simultaneous Determination of Trace Concentrations of Arsenic, Antimony, Bismuth, Selenium and Tellurium in Aqueous Solution by Introduction of Gaseous Hydrides into an Inductively Coupled

Plasma Source for Emission Spectrometry 1.Preliminary Studies. *Analyst* **1978,** *103* (1227), 568-579.

68. Secrest, R., Tellurium (Te). Salem Press Encyclopedia of Science, January, 2015.

69. Glover, J.; Vouk, V.; L., i. F.; Nordberg, G. F.; Vouk, V. B. E., *Tellurium, in Handbook on the Toxicology of Metals*. Elsevier: Amsterdam, 1979.

70. *Sadeh, T.*; *in : Patai, S. E., The chemistry of Organic Selenium and Tellurium Compounds*. Wiley: Chichester, 1987; Vol. 2.

71. D'Ulivo, A., Determination of selenium and tellurium in environmental samples. *Analyst* **1997,** *122* (12), 117R-144R.

72. Ba, L. A.; Doering, M.; Jamier, V.; Jacob, C., Tellurium: an element with great biological potency and potential. *Organic & Biomolecular Chemistry* **2010,** *8* (19), 4203-4216.

73. Asami, T. *Metal Pollution in Japanese Soils (in Japanese)*; Heiwa Kogyo Co., Ltd.: Tokyo, Japan, 2010; p 447.

74. Merian, E.; Anke, M.; Ihnat, M.; Stoeppler, M., *Elements and their Compounds in the Environment*. Wiley-VCH Verlag: Weinheim, 2004.

75. Ha, J.; Sun, H. W.; Sun, J. M.; Zhang, D. Q.; Yang, L. L., Determination of tellurium in urine by hydride generation atomic absorption spectrometry with derivative signal processing. *Analytica Chimica Acta* **2001,** *448* (1-2), 145-149.

76. Yang, G.; Zheng, J.; Tagami, K.; Uchida, S., Rapid and sensitive determination of tellurium in soil and plant samples by sector-field inductively coupled plasma mass spectrometry. *Talanta* **2013,** *116*, 181-187.

77. Groth, D. H.; Stetler, L.; Mackay, G., *Effects and Dose Response Relationships of Toxic Metals*. Elsevier: Amsterdam, 1976.

78. Karlson, U.; Frankenberger, W. T., *Metal Ions in Biological Systems*. Marcel Dekker: New York, 1993.

79. Jiang, X.; Gan, W.; Han, S.; He, Y., Determination of Te in soldering tin using continuous flowing electrochemical hydride generation atomic fluorescence spectrometry. *Spectrochimica Acta Part B-Atomic Spectroscopy* **2008,** *63* (6), 710-713.

80. Emsley, J., *The Elements of Murder*. Oxford University Press: Oxford, UK, 2005.

81. Oda, S.; Arikawa, Y., Determination of tellurium in coal samples by means of graphite furnace atomic absorption spectrometry after coprecipitation with iron(III) hydroxide. *Bunseki Kagaku* **2005,** *54* (11), 1033-1037.

82. Feng, X. J.; Fu, B., Determination of arsenic, antimony, selenium, tellurium and bismuth in nickel metal by hydride generation atomic fluorescence spectrometry. *Analytica Chimica Acta* **1998,** *371* (1), 109-113.

83. Kujirai, O.; Kobayashi, T.; Ide, K.; Sudo, E., Determination of Traces of Tellurium in Heat-Resisting Alloys by Graphite-Furnace Atomic Absorption Spectrometry After Coprecipitation with Arsenic. *Talanta* **1982,** *29* (1), 27-30.

84. Niskavaara, H.; Kontas, E., Reductive Coprecipitation As a Separation Method for the determination of Gold, Palladium, Platinum, Rhodium, Silver, Selenium and Tellurium in Geological Samples by Graphite-Furnace Atomic Absorption Spectrometry. *Analytica Chimica Acta* **1990,** *231* (2), 273-282.

85. Pedro, J.; Stripekis, J.; Bonivardi, A.; Tudino, M., Determination of tellurium at ultra-race levels in drinking water by on-line solid phase extraction coupled to graphite furnace atomic absorption spectrometer. *Spectrochimica Acta Part B-Atomic Spectroscopy* **2008,** *63* (1), 86-91.

86. Ghasemi, E.; Najafi, N. M.; Raofie, F.; Ghassempour, A., Simultaneous speciation and preconcentration of ultra traces of inorganic tellurium and selenium in environmental samples by hollow fiber liquid phase microextraction prior to

electrothermal atomic absorption spectroscopy determination. *Journal of Hazardous Materials* **2010,** *181* (1-3), 491-496.

87. Tsalev, D. L.; Dulivo, A.; Lampugnani, L.; DiMarco, M.; Zamboni, R., Thermally stabilized iridium on an integrated, carbide-coated platform as a permanent modifier for hydride-forming elements in electrothermal atomic absorption spectrometry .2. Hydride generation and collection, and behaviour of some organoelement species. *Journal of Analytical Atomic Spectrometry* **1996,** *11* (10), 979-988.

88. Yildiz, H. B.; Ertas, N.; Ataman, O. Y., Oxidation state related evaluation of tellurium determination by flame AAS. *Fresenius Environmental Bulletin* **2008,** *17* (7B), 911-914.

89. Cerutti, S.; Kaplan, M.; Moyano, S.; Gasquez, J. A.; Martinez, L. D., Determination of tellurium by ETAAS with preconcentration by coprecipitation with lanthanum hydroxide. *Atomic Spectroscopy* **2005,** *26* (3), 125-129.

90. Kaplan, M.; Cerutti, S.; Moyano, S.; Olsina, R. A.; Martinez, L. D.; Gasquez, J. A., On-line preconcentration system by coprecipitation with lanthanum hydroxide using packed-bed filter for the determination of tellurium in water by ICP-OES with USN. *Instrumentation Science & Technology* **2004,** *32* (4), 423-431.

91. Hu, Z.; Gao, S.; Guenther, D.; Hu, S.; Liu, X.; Yuan, H., Direct determination of tellurium in geological samples by inductively coupled plasma mass spectrometry using ethanol as a matrix modifier. *Applied Spectroscopy* **2006,** *60* (7), 781-785.

92. Kaplan, M. M.; Cerutti, S.; Salonia, J. A.; Gasquez, J. A.; Martinez, L. D., Preconcentration and determination of tellurium in garlic samples by hydride generation atomic absorption spectrometry. *Journal of Aoac International* **2005,** *88* (4), 1242-1246.

93. Rodenas-Torralba, E.; Morales-Rubio, A.; de la Guardia, M., Multicommutation hydride generation atomic fluorescence determination of inorganic tellurium species in milk. *Food Chemistry* **2005,** *91* (1), 181-189.

94. Grotti, M.; Lagomarsino, C.; Frache, R., Multivariate study in chemical vapor generation for simultaneous determination of arsenic, antimony, bismuth, germanium, tin, selenium, tellurium and mercury by inductively coupled plasma optical emission spectrometry. *Journal of Analytical Atomic Spectrometry* **2005,** *20* (12), 1365-1373.

95. Chen, Y. L.; Jiang, S. J., Determination of tellurium in a nickel-based alloy by flow injection vapor generation inductively coupled plasma mass spectrometry. *Journal of Analytical Atomic Spectrometry* **2000,** *15* (12), 1578-1582.

96. Zhang, L. S.; Combs, S. M., Using the installed spray chamber as a gas-liquid separator for the determination of germanium, arsenic, selenium, tin, antimony, tellurium and bismuth by hydride generation inductively coupled plasma mass spectrometry. *Journal of Analytical Atomic Spectrometry* **1996,** *11* (11), 1043-1048.

97. Luo, L.; Tang, Y.; Xi, M.; Li, W.; Lv, Y.; Xu, K., Hydride generation induced chemiluminescence for the determination of tellurium (IV). *Microchemical Journal* **2011,** *98* (1), 51-55.

98. Kumar, A.; Sharma, P.; Chandel, L. K.; Kalal, B. L., Synergistic extraction and spectrophotometric determination of palladium(II), iron(III), and tellurium(IV) at trace level by newly synthesized p- 4-(3,5-dimethylisoxazolyl)azophenylazo calix(4)arene. *Journal of Inclusion Phenomena and Macrocyclic Chemistry* **2008,** *61* (3-4), 335-342.

99. Suvardhan, K.; Krishna, P. M.; Puttaiah, E. T.; Chiranjeevi, P., Spectrophotometric determination of tellurium(IV) in environmental and telluride film samples. *Journal of Analytical Chemistry* **2007,** *62* (11), 1032-1039.

100. Zong, P.; Nagaosa, Y., Cathodic Stripping Voltammetric Determination of Tellurium(IV) with in situ Plated Bismuth-Film Electrode. *Analytical Letters* **2009,** *42* (13), 1997-2010.

101. Yang, H. Y.; Sun, I. W., Cathodic stripping voltammetric determination of tellurium(IV) in chloride media using a Tosflex/8-quinolinol mercury film electrode. *Electroanalysis* **1999,** *11* (3), 195-200.

102. Ferri, T.; Rossi, S.; Sangiorgio, P., Simultaneous determination of the speciation of selenium and tellurium in geological matrices by use of an iron(III)-modified chelating resin and cathodic stripping voltammetry. *Analytica Chimica Acta* **1998,** *361* (1-2), 113-123.

103. Brainina, K. Z.; Chernysheva, A. V.; Stozhko, N. Y., Determination of Tellurium in Natural Waters by Stripping Voltammetry. *Industrial Laboratory* **1984,** *50* (4), 315-318.

104. Mesko, M. F.; Pozebon, D.; Flores, E. M. M.; Dressler, V. L., Determination of tellurium in lead and lead alloy using flow injection-hydride generation atomic absorption spectrometry. *Analytica Chimica Acta* **2004,** *517* (1-2), 195-200.

105. Grotti, M.; Mazzucotelli, A., Electrothermal Atomic Absorption Spectrometric Determination of Ultratrace Amounts of Tellurium Using a Palladium Coated LVOV Platform After Separation and Concentration by Hydride Generation and Liquid Anion-Exchange. *Journal of Analytical Atomic Spectrometry* **1995,** *10* (4), 325-327.

106. Cava-Montesinos, P.; Cervera, M. L.; Pastor, A.; de la Guardia, M., Hydride generation atomic fluorescence spectrometric determination of ultratraces of selenium and tellurium in cow milk. *Analytica Chimica Acta* **2003,** *481* (2), 291-300.

107. Reyes, M. N. M.; Cervera, M. L.; de la Guardia, M., Determination of Inorganic Species of Sb and Te Cereals by Hydride Generation Atomic Fluorescence Spectrometry. *Journal of the Brazilian Chemical Society* **2011,** *22* (2), 197-203.

108. Korez, A.; Eroglu, A. E.; Volkan, M.; Ataman, O. Y., Speciation and preconcentration of inorganic tellurium from waters using a mercaptosilica microcolumn and determination by hydride generation atomic absorption spectrometry. *Journal of Analytical Atomic Spectrometry* **2000,** *15* (12), 1599-1605.

109. Yildirim, E.; Akay, P.; Arslan, Y.; Bakirdere, S.; Ataman, O. Y., Tellurium speciation analysis using hydride generation in situ trapping electrothermal atomic

absorption spectrometry and ruthenium or palladium modified graphite tubes. *Talanta* **2012,** *102*, 59-67.

110. Kuo, C.-Y.; Jiang, S.-J., Determination of selenium and tellurium compounds in biological samples by ion chromatography dynamic reaction cell inductively coupled plasma mass spectrometry. *Journal of Chromatography A* **2008,** *1181* (1-2), 60-66.

111. Deng, J. Q.; He, P. X.; Chen, X. M., A Study of Anodic Stripping Voltammetry of Trace Tellurium on Gold Film Electrode. *Acta Chimica Sinica* **1980,** *38* (6), 529-534.

112. Wang, J.; Lu, J. M., Adsorptive Stripping Voltammetric Determination of Trace Tellurium in the Presence of Oxine. *Electroanalysis* **1994,** *6* (5-6), 405-408.

113. Dedina, J.; Tsalev, D. L., *Hydride Generation Atomic Absorption Spectrometry*. John Wiley & Sons: England, 1995.

114. D'Ulivo, A., Mechanisms of chemical generation of volatile hydrides for trace element determination (IUPAC Technical Report) (c) 2011 IUPAC. *Spectrochimica Acta Part B-Atomic Spectroscopy* **2012,** *69*, 67-68.

115. Matusiewicz, H.; Sturgeon, R. E., Chemical Vapor Generation with Slurry Sampling: A Review of Applications to Atomic and Mass Spectrometry. *Applied Spectroscopy Reviews* **2012,** *47* (1), 41-82.

116. Kumar, A. R.; Riyazuddin, P., Non-chromatographic hydride generation atomic spectrometric techniques for the speciation analysis of arsenic, antimony, selenium, and tellurium in water samples - a review. *International Journal of Environmental Analytical Chemistry* **2007,** *87* (7), 469-500.

117. Holak, W., Gas Sampling Technique for Arsenic Determination by Atomic Absorption Spectrophotometry. *Analytical Chemistry* **1969,** *41* (12), 1712-&.

118. Braman, R. S., Membrane Probe Spectral Emission Type Detection System for Mercury in Water. *Analytical Chemistry* **1971,** *43* (11), 1462-&.

119. Braman, R. S.; Foreback, C. C.; Justen, L. L., Direct Volatilization Spectral Emission Type Detection System for Nanogram Amounts of Arsenic and Antimony. *Analytical Chemistry* **1972,** *44* (13), 2195-&.

120. Robbins, W. B.; Caruso, J. A., Development of Hydride Generation Methods for Atomic Spectroscopic Analysis. *Analytical Chemistry* **1979,** *51* (8), A889-&.

121. Laborda, F.; Bolea, E.; Baranguan, M. T.; Castillo, J. R., Hydride generation in analytical chemistry and nascent hydrogen: when is it going to be over? *Spectrochimica Acta Part B-Atomic Spectroscopy* **2002,** *57* (4), 797-802.

122. D'Ulivo, A., Chemical vapor generation by tetrahydroborate(III) and other borane complexes in aqueous media - A critical discussion of fundamental processes and mechanisms involved in reagent decomposition and hydride formation. *Spectrochimica Acta Part B-Atomic Spectroscopy* **2004,** *59* (6), 793-825.

123. D'Ulivo, A.; Mester, Z.; Sturgeon, R. E., The mechanism of formation of volatile hydrides by tetrahydroborate(III) derivatization: A mass spectrometric study performed with deuterium labeled reagents. *Spectrochimica Acta Part B-Atomic Spectroscopy* **2005,** *60* (4), 423-438.

124. Narsito; Agterdenbos, J.; Santosa, S. J., Study of Processes in the Hydride Generation Atomic Absorption Spectrometry of Antimony, Arsenic and Selenium. *Analytica Chimica Acta* **1990,** *237* (1), 189-199.

125. Agterdenbos, J.; Bax, D., A study on the Generation of Hydrogen Selenide and Decomposition of Tetrahydroborate in Hydride Generation Atomic Absorption Spectrometry. *Analytica Chimica Acta* **1986,** *188*, 127-135.

126. Kumar, A. R.; Riyazuddin, P., Chemical interferences in hydride-generation atomic spectrometry. *Trac-Trends in Analytical Chemistry* **2010,** *29* (2), 166-176.

127. Pohl, P.; Zyrnicki, W., On the transport of some metals into inductively coupled plasma during hydride generation process. *Analytica Chimica Acta* **2001,** *429* (1), 135-143.

128. Dedina, J., Atomization of volatile compounds for atomic absorption and atomic fluorescence spectrometry: On the way towards the ideal atomizer. *Spectrochimica Acta Part B-Atomic Spectroscopy* **2007,** *62* (9), 846-872.

129. Farias, S.; Rodriguez, R. E.; Ledesma, A.; Batistoni, D. A.; Smichowski, P., Assessment of acid media effects on the determination of tin by hydride generation-inductively coupled plasma atomic emission spectrometry. *Microchemical Journal* **2002,** *73* (1-2), 79-88.

130. Smichowski, P.; Marrero, J., Comparative study to evaluate the effect of different acids on the determination of germanium by hydride generation inductively coupled plasma atomic emission spectrometry. *Analytica Chimica Acta* **1998,** *376* (3), 283-291.

131. Welz, B.; Schubertjacobs, M., Mechanisms of Transition Metal Interferences in Hydride Generation Atomic Absorption Spectrometry 4. Influence of Acid and Tetrahydroborate Concentrations on Interferences in Arsenic and Selenium Determinations. *Journal of Analytical Atomic Spectrometry* **1986,** *1* (1), 23-27.

132. Pohl, P.; Zyrnicki, W., Study of chemical and spectral interferences in the simultaneous determination of As, Bi, Sb, Se and Sn by hydride generation inductively coupled plasma atomic emission spectrometry. *Analytica Chimica Acta* **2002,** *468* (1), 71-79.

133. Schmidt, C.; Bahadir, M., Determination of Arsenic in the Presence of High Copper Concentrations Using Flow Injection Analysis Hydride Atomic Absorption Spectrometry. *Fresenius Journal of Analytical Chemistry* **1993,** *346* (6-9), 683-685.

134. Chen, H. W.; Brindle, I. D.; Le, X. C., Prereduction of Arsenic (V) to Arsenic (III), Enhancement of the Signal and Reduction of Interferences by L-Cysteine in the Determination of Arsenic by Hydride Generation. *Analytical Chemistry* **1992,** *64* (6), 667-672.

135. Brindle, I. D.; Le, X. C., Reduction of Interferences in the determination of Germanium by Hydride Generation and Atomic Emission Spectrometry. *Analytica Chimica Acta* **1990,** *229* (2), 239-247.

136. Kirkbright, G. F.; Taddia, M., Application of Masking Agents in Minimizing Interferences from Some Metal Ions in Determination of Arsenic by Atomic Absorption Spectrometry with Hydride Generation Technique. *Analytica Chimica Acta* **1978,** *100* (SEP), 145-150.

137. D'Ulivo, A.; Gianfranceschi, L.; Lampugnani, L.; Zamboni, R., Masking agents in the determination of selenium by hydride generation technique. *Spectrochimica Acta Part B-Atomic Spectroscopy* **2002,** *57* (12), 2081-2094.

138. Anderson, R. K.; Thompson, M.; Culbard, E., Selective Reduction of Arsenic Species by Continuous Hydride Generation 1. Reaction Media. *Analyst* **1986,** *111* (10), 1143-1152.

139. Risnes, A.; Lund, W., Comparison of systems for eliminating interferences in the determination of arsenic and antimony by hydride generation inductively coupled plasma atomic emission spectrometry. *Journal of Analytical Atomic Spectrometry* **1996,** *11* (10), 943-948.

140. Xing, Z.; Wang, J.; Zhang, S.; Zhang, X., Determination of bismuth in solid samples by hydride generation atomic fluorescence spectrometry with a dielectric barrier discharge atomizer. *Talanta* **2009,** *80* (1), 139-142.

141. Moscoso-Perez, C.; Moreda-Pineiro, J.; Lopez-Mahia, P.; Muniategui-Lorenzo, S.; Fernandez-Fernandez, E.; Prada-Rodriguez, D., Hydride generation atomic fluorescence spectrometric determination of As, Bi, Sb, Se(IV) and Te(IV) in aqua regia extracts from atmospheric particulate matter using multivariate optimization. *Analytica Chimica Acta* **2004,** *526* (2), 185-192.

142. Moscoso-Perez, C.; Moreda-Pineiro, J.; Lopez-Mahia, P.; Muniategui-Lorenzo, S.; Fernandez-Fernandez, E.; Prada-Rodriguez, D., As, Bi, Se(IV), and Te(IV)

determination in acid extracts of raw materials and by-products from coal-fired power plants by hydride generation-atomic fluorescence spectrometry. *Atomic Spectroscopy* **2004,** *25* (5), 211-216.

143. Pohl, P., Hydride generation - recent advances in atomic emission spectrometry. *Trac-Trends in Analytical Chemistry* **2004,** *23* (2), 87-101.

144. Thompson, M.; Pahlavanpour, B.; Walton, S. J.; Kirkbright, G. F., Simultaneous Determination of Trace Concentrations of Arsenic, Antimony, Bismuth, Selenium and Tellurium in Aqueous Solution by Introduction of Gaseous Hydrides into an Inductively Coupled Plasma Source for Emission Spectrometry 2.Interference Studies. *Analyst* **1978,** *103* (1228), 705-713.

145. Wolnik, K. A.; Fricke, F. L.; Hahn, M. H.; Caruso, J. A., Sample Introduction System for Simultaneous Determination of Volatile Elemental Hydrides and Other Elements in Foods by Inductively Coupled Argon Plasma Emission Spectrometry. *Analytical Chemistry* **1981,** *53* (7), 1030-1035.

146. Huang, B. L.; Zhang, Z. Y.; Zeng, X. J., A new Nebulizer Hydride Generator System for Simultaneous Multielement Inductively Coupled Plasma Atomic Emission Spectrometry. *Spectrochimica Acta Part B-Atomic Spectroscopy* **1987,** *42* (1-2), 129-137.

147. Welna, M.; Zyrnicki, W., Influence of chemical vapor generation conditions on spectroscopic and analytical characteristics of a hyphenated CVG-ICP system. *Journal of Analytical Atomic Spectrometry* **2009,** *24* (6), 832-836.

148. Welna, M.; Zyrnicki, W., Investigation of Simultaneous Generation of Arsenic, Bismuth and Antimony Hydrides Using Inductively Coupled Plasma Optical Emission Spectrometry. *Analytical Letters* **2011,** *44* (5), 942-953.

149. Date, A. R.; Gray, A. L., Progress in Plasma Source Mass Spectrometry. *Spectrochimica Acta Part B-Atomic Spectroscopy* **1983,** *38* (1-2), 29-37.

150. Ataman, O. Y., Vapor generation and atom traps: Atomic absorption spectrometry at the ng/L level. *Spectrochimica Acta Part B-Atomic Spectroscopy* **2008,** *63* (8), 825-834.

151. de Souza, S. S.; Santos, D., Jr.; Kxug, F. J.; Barbosa, F., Jr., Exploiting in situ hydride trapping in tungsten coil atomizer for Se and As determination in biological and water samples. *Talanta* **2007,** *73* (3), 451-457.

152. Barth, P.; Hauptkorn, S.; Krivan, V., Improved slurry sampling electrothermal vaporization system using a tungsten coil for inductively coupled plasma atomic emission spectrometry. *Journal of Analytical Atomic Spectrometry* **1997,** *12* (12), 1351-1358.

153. Guo, X. M.; Guo, X. W., Determination of ultra-trace amounts of selenium by continuous flow hydride generation AFS and AAS with collection on gold wire. *Journal of Analytical Atomic Spectrometry* **2001,** *16* (12), 1414-1418.

154. Korkmaz, D. K.; Ertas, N.; Ataman, O. Y., A novel silica trap for lead determination by hydride generation atomic absorption spectrometry. *Spectrochimica Acta Part B-Atomic Spectroscopy* **2002,** *57* (3), 571-580.

155. Docekal, B.; Gucer, S.; Selecka, A., Trapping of hydride forming elements within miniature electrothermal devices: part 1. Investigation of collection of arsenic and selenium hydrides on a molybdenum foil strip. *Spectrochimica Acta Part B-Atomic Spectroscopy* **2004,** *59* (4), 487-495.

156. Liu, R.; Wu, P.; Xu, K.; Lv, Y.; Hou, X., Highly sensitive and interference-free determination of bismuth in environmental samples by electrothermal vaporization atomic fluorescence spectrometry after hydride trapping on iridium-coated tungsten coil. *Spectrochimica Acta Part B-Atomic Spectroscopy* **2008,** *63* (6), 704-709.

157. Williams, M.; Piepmeie.Eh, Commerical Tungsten Filament Atomizer for Analytical Atomic Spectrometry. *Analytical Chemistry* **1972,** *44* (7), 1342-&.

158. Hou, X. D.; Yang, Z.; Jones, B. T., Determination of selenium by tungsten coil atomic absorption spectrometry using iridium as a permanent chemical modifier. *Spectrochimica Acta Part B-Atomic Spectroscopy* **2001,** *56* (2), 203-214.

159. Salido, A.; Jones, B. T., Simultaneous determination of Cu, Cd and Pb in drinking-water using W-coil AAS. *Talanta* **1999,** *50* (3), 649-659.

160. Wagner, K. A.; Levine, K. E.; Jones, B. T., A simple, low cost, multielement atomic absorption spectrometer with a tungsten coil atomizer. *Spectrochimica Acta Part B-Atomic Spectroscopy* **1998,** *53* (11), 1507-1516.

161. Parsons, P. J.; Qiao, H. C.; Aldous, K. M.; Mills, E.; Slavin, W., A low-cost tungsten filament atomizer for measuring lead in blood by atomic absorption spectrometry. *Spectrochimica Acta Part B-Atomic Spectroscopy* **1995,** *50* (12), 1475-1480.

162. Barbosa, F.; de Souza, S. S.; Krug, F. J., In situ trapping of selenium hydride in rhodium-coated tungsten coil electrothermal atomic absorption spectrometry. *Journal of Analytical Atomic Spectrometry* **2002,** *17* (4), 382-388.

163. Kula, I.; Arslan, Y.; Bakirdere, S.; Titretir, S.; Kenduezler, E.; Ataman, O. Y., Determination and interference studies of bismuth by tungsten trap hydride generation atomic absorption spectrometry. *Talanta* **2009,** *80* (1), 127-132.

164. Kula, I.; Arslan, Y.; Bakirdere, S.; Ataman, O. Y., A novel analytical system involving hydride generation and gold-coated W-coil trapping atomic absorption spectrometry for selenium determination at ng l(-1) level. *Spectrochimica Acta Part B-Atomic Spectroscopy* **2008,** *63* (8), 856-860.

165. Xi, M.; Liu, R.; Wu, P.; Xu, K.; Hou, X.; Lv, Y., Atomic absorption spectrometric determination of trace tellurium after hydride trapping on platinum-coated tungsten coil. *Microchemical Journal* **2010,** *95* (2), 320-325.

166. Alp, O.; Ertas, N., Determination of tin by in situ trapping of stannane on a resistively heated iridium treated tungsten coil surface and interference studies. *Talanta* **2010,** *81* (1-2), 516-520.

167. Cankur, O.; Ataman, O. Y., Chemical vapor generation of Cd and on-line preconcentration on a resistively heated W-coil prior to determination by atomic absorption spectrometry using an unheated quartz absorption cell. *Journal of Analytical Atomic Spectrometry* **2007,** *22* (7), 791-799.

168. Titretir, S.; Kenduezler, E.; Arslan, Y.; Kula, I.; Bakirdere, S.; Ataman, O. Y., Determination of antimony by using tungsten trap atomic absorption spectrometry. *Spectrochimica Acta Part B-Atomic Spectroscopy* **2008,** *63* (8), 875-879.

169. Chen, P.; Deng, Y.; Guo, K.; Jiang, X.; Zheng, C.; Hou, X., Flow injection hydride generation for on-atomizer trapping: Highly sensitive determination of cadmium by tungsten coil atomic absorption spectrometry. *Microchemical Journal* **2014,** *112*, 7-12.

170. Kratzer, J.; Dedina, J., Arsine and selenium hydride trapping in a novel quartz device for atomic-absorption spectrometry. *Analytical and Bioanalytical Chemistry* **2007,** *388* (4), 793-800.

171. Kratzer, J.; Dedina, J., In situ trapping of bismuthine in externally heated quartz tube atomizers for atomic absorption spectrometry. *Journal of Analytical Atomic Spectrometry* **2006,** *21* (2), 208-210.

172. Downard, K., *Mass Spectrometry: a foundation course*. Royal Society of Chemistry: Cambridge, 2004.

173. Ekman, R.; Silberring, J.; Westman-Brinkmalm, A.; Kraj, A., *Mass Spectrometry: instrumentation, interpretation and applications*. John Wiley & Sons: 2009.

174. Hoffmann, E.; Stroobant, V., *Mass Spectrometry: Principles and Applications*. Wiley: Chichester, England, 2007.

175. Thomas, R., *Practical Guide to ICP-MS*. M. Dekker: New York, 2004.

176. Barker, J., *Mass Spectrometry*. Wiley: New York, 1998.

177. http://web.natur.cuni.cz/ugmnz/icplab/icpm1.html; 2005 [Last accessed on 11.10.2015].

178. Tanner, M.; Guenther, D., Short transient signals, a challenge for inductively coupled plasma mass spectrometry, a review. *Analytica Chimica Acta* **2009,** *633* (1), 19-28.

179. Resano, M.; Verstraete, M.; Vanhaecke, F.; Moens, L.; van Alphen, A.; Denoyer, E. R., Simultaneous determination of Co, Mn, P and Ti in PET samples by solid sampling electrothermal vaporization ICP-MS. *Journal of Analytical Atomic Spectrometry* **2000,** *15* (4), 389-395.

180. Ertas, G.; Holcombe, J. A., Determination of absolute transport efficiencies of Be, Cd, In, Pb and Bi for electrothermal vaporization sample introduction into an inductively coupled plasma using an in-line electrostatic precipitator. *Spectrochimica Acta Part B-Atomic Spectroscopy* **2003,** *58* (9), 1597-1612.

181. Langer, D.; Holcombe, J. A., Simple transient extension chamber to permit full mass scans with electrothermal vaporization inductively coupled plasma mass spectrometry. *Applied Spectroscopy* **1999,** *53* (10), 1244-1250.

182. Resano, M.; Verstraete, M.; Vanhaecke, F.; Moens, L., Evaluation of the multi-element capabilities of electrothermal vaporization quadrupole-based ICP mass spectrometry. *Journal of Analytical Atomic Spectrometry* **2001,** *16* (9), 1018-1027.

183. Yu, L. J.; Koirtyohann, S. R.; Rueppel, M. L.; Skipor, A. K.; Jacobs, J. J., Simultaneous determination of aluminium, titanium and vanadium in serum by electrothermal vaporization-inductively coupled plasma mass spectrometry. *Journal of Analytical Atomic Spectrometry* **1997,** *12* (1), 69-74.

184. Moor, C.; Boll, P.; Wiget, S., Determination of impurities in micro-amounts of silver alloys by electrothermal vaporization inductively coupled plasma mass spectrometry (ETV-ICP-MS) after in-situ-digestion in the graphite furnace. *Fresenius Journal of Analytical Chemistry* **1997,** *359* (4-5), 404-406.

185. Coedo, A. G.; Dorado, T.; Padilla, I.; Maibusch, R.; Kuss, H. M., Slurry sampling electrothermal vaporization inductively coupled plasma mass spectrometry for steelmaking flue dust analysis. *Spectrochimica Acta Part B-Atomic Spectroscopy* **2000,** *55* (2), 185-196.

186. Venable, J. D.; Langer, D.; Holcombe, J. A., Optimizing the multielement analysis capabilities of an ICP quadrupole mass spectrometer using electrothermal vaporization sample introduction. *Analytical Chemistry* **2002,** *74* (15), 3744-3753.

187. Sparks, C. M.; Holcombe, J.; Pinkston, T. L., Particle Size Distribution of Sample Transported from an Electrothermal Vaporizer to an Inductively Coupled Plasma Mass Spectrometer. *Spectrochimica Acta Part B-Atomic Spectroscopy* **1993,** *48* (13), 1607-1615.

188. Venable, J.; Holcombe, J. A., Peak broadening from an electrothermal vaporization sample introduction source into an inductively coupled plasma. *Spectrochimica Acta Part B-Atomic Spectroscopy* **2001,** *56* (8), 1431-1440.

189. Mahoney, P. P.; Ray, S. J.; Li, G. Q.; Hieftje, G. M., Preliminary investigation of electrothermal vaporization sample introduction for inductively coupled plasma time-of-flight mass spectrometry. *Analytical Chemistry* **1999,** *71* (7), 1378-1383.

190. Ertas, G.; Holcombe, J. A., Use of a simple transient extension chamber with ETV-ICPMS: quantitative analysis and matrix effects. *Journal of Analytical Atomic Spectrometry* **2003,** *18* (8), 878-883.

191. Ertas, G.; Holcombe, J. A., Optimization of ETV-ICP(TOF)MS and transient signal profiles for reducing isobaric interferences. *Journal of Analytical Atomic Spectrometry* **2005,** *20* (8), 687-695.

192. Laborda, F.; Medrano, J.; Castillo, J. R., Data acquisition of transient signals in inductively coupled plasma mass spectrometry. *Analytica Chimica Acta* **2000,** *407* (1-2), 301-309.

193. Sturgeon, R. E.; Willie, S. N.; Zheng, J.; Kudo, A.; Gregoire, D. C., Determination of Ultratrace levels of Heavy Metals in Arctic Snow by Electrothermal Vaporization Inductively Coupled Plasma Mass Spectrometry. *Journal of Analytical Atomic Spectrometry* **1993,** *8* (8), 1053-1058.

194. Byrne, J. P.; Chapple, G., Direct determination of trace metals in seawater by electrothermal vaporization ICP-MS with Pd-HNO3 modifier. *Atomic Spectroscopy* **1998,** *19* (4), 116-120.

195. de Marcillac, P.; Coron, N.; Dambier, G.; Leblanc, J.; Moalic, J. P., Experimental detection of alpha-particles from the radioactive decay of natural bismuth. *Nature* **2003,** *422* (6934), 876-878.

196. Lederer, C. M.; Shirley, V. S., *Table of Isotopes*. 7 ed.; Wiley & Sons: USA, 1978.

197. Cullen, W. R.; Reimer, K. J., Arsenic speciation in the environment. *Chemical Reviews* **1989,** *89* (4), 713-764.

198. Docekal, B.; Marek, P., Investigation of in situ trapping of selenium and arsenic hydrides within a tungsten tube atomiser. *Journal of Analytical Atomic Spectrometry* **2001,** *16* (8), 831-837.

199. Gao, Y.; Sturgeon, R. E.; Mester, Z.; Hou, X.; Yang, L., Multivariate optimization of photochemical vapor generation for direct determination of arsenic in seawater by inductively coupled plasma mass spectrometry. *Analytica Chimica Acta* **2015,** *901*, 34-40.

CURRICULUM VITAE

Selin BORA

PERSONAL INFORMATION

Date of birth:	06.03.1984
Address:	Mustafa Kemal Mahallesi 2148. Sokak No:3/56 Çankaya, Ankara
Telephone:	0536 370 1355
e-mail:	selinodt@yahoo.com, selin.bora@tubitak.gov.tr

EDUCATION

Ph.D.	Chemistry, METU, Ankara CGPA: 3.57 /4.00 Jan. 2010- Jan. 2016 Thesis Title: "Use of Tungsten Coil in Plasma Spectrometry" *Supervisor:* Prof. Dr. O. Yavuz Ataman
M.S.	Chemistry, METU, Ankara CGPA: 3.86 /4.00 Sept. 2007-Jan. 2010 Thesis Title: "Determination of Boron in Biological Fluids by ICP-OES & ICP-MS" *Supervisor:* Prof. Dr. O. Yavuz Ataman
B.S. Major	Chemistry, METU, Ankara CGPA: 3.15 /4.00 Sept. 2002-June 2007 Research Project Title: "Development of a Sensitive Analytical Method for Lead Determination by Using Titanium Coated Slotted Quartz Trap (SQT) – FAAS"
B.S. Minor	Food Engineering- Food Science, METU, Ankara CGPA: 2.44 /4.00 Sept. 2004-June 2007
High School	Eskişehir Anatolian High School, Eskişehir Mathematics-Science Branch

SCHOLARSHIP

2015-2010	2211-TUBITAK Scholarship for Graduate Students (PhD program)
2008-2009	2211-TUBITAK Scholarship for Graduate Students (MS program)
2004-2007	TUBITAK Scholarship for Undergraduate Students, *Natural Science Scholarship*

EMPLOYMENT HISTORY

2009 Oct.- present	Teaching Assistant in Analytical Chemistry Laboratory, Chemistry Department, METU. Gravimetric Analysis, Titration Methods, Spectrometry.

Experience on Flame Atomic Absorption Spectrometry (FAAS), Ultraviolet-Visible Spectrometry (UV-VIS), Refractometry, Polarimetry, Fourier Transform Infrared Spectrometry (FTIR), Inductively Coupled Plasma-Optical Emission Spectrometry

(ICPOES), Inductively Coupled Plasma-Mass Spectrometry (ICPMS), High Pressure Liquid Chromatography (HPLC), Gas Chromatography (GC), X-Ray Fluorescence Spectrometry (XRF).

2006 June-July Summer practice at Novagenix Bioanalytical Drug R&D Center, Ankara
Bioequivalence studies of drugs are performed by using HPLC, HPLC-MS and HPLC/MS-MS instruments.

2005 July-Aug. Summer Practice at Paşabahçe Glass Factory, Eskişehir
Production Department- Laboratory, Analysis of daily glass products

PUBLISHED PAPERS

1. "Chapter 9: Speciation of Arsenic in Soil, Sediment and Environmental Samples", *Selin Bora*, Işıl Aydın, Ersin Kılınç, Fırat Aydın, *Speciation Studies in Soil, Sediment and Environmental Samples*, Dr. Sezgin Bakirdere, CRC Press, Taylor and Francis Group, 2014.

2. S. Bakırdere, *S. Bora*, E. G. Bakırdere, F. Aydın, Y. Arslan, O. T. Komesli, I. Aydın, E. Yıldırım, "Aflatoxin Species: Their Health Effects and Determination Methods in Different Foodstuffs", *Central Europian Journal of Chemistry*, 10 (3), 2012, 675-685.

PROJECTS

1. "Kronik Bor Etkisinde Kalan ve Kalmayan Kadınlarda HPV Sıklığı ile Genotiplerinin Karşılaştırılması" TÜBİTAK 111S177, 2011-2014 – Researcher.

2. "Bora Maruz Kalan Bireylerdeki Transkripsiyon Faktörlerinin Gen Ekspresyon Profilinin RT-PCR Array ile Araştırılması" Celal Bayar University BAP Project, Project No 2009-026, 2010-2013 – Researcher.

3. "Doğal Yolla Alınan Bor Mineralinin Erkeklerde Prostat Büyüklüğü, Benign Prostat Hiperplazisi ve Alt Üriner Sistem Semptomlarına Etkisinin Topluma Dayalı Bir Çalışma ile Araştırılması" BOREN 2008-Ç0164 – Researcher.

CONFERENCE PRESENTATIONS

1. O.Yavuz Ataman, *Selin Bora*, Gülay Ertaş, Anılcan Yılmaz, "Tungsten Coil Traps Meet ICPMS and a Short Review BBCAC History", 7th Black Sea Basin Conference on Analytical Chemistry, 10-15 September 2015, Golden Sands, Bulgaria.

2. O.Yavuz Ataman, *Selin Bora*, Gülay Ertaş, "ICPOES ve ICPMS: Plazma Spektrometri ve Girişimleri", XIV. Ulusal Spektroskopi Kongresi, 29-31 Mayıs 2015, Elazığ, Türkiye.

3. *Selin Bora*, Gülay Ertaş, O. Yavuz Ataman, "Spectral and Non-Spectral Interference Effects of ^{12}C on $^{10}B^+$, $^{11}B^+$ and $^{9}Be^+$ Signals in ICP-MS", 9th Aegean Analytical Chemistry Days, 29 September- 3 October 2014, Chios, Greece.

4. Pınar Mercan, *Selin Bora*, O. Yavuz Ataman, "Rodyum Kaplı Tungsten Sarmal Atom Tuzaklı ve Hidrür Oluşturmalı Atomik Absorpsiyon Spektrometrisi ile Bizmut Tayini", 7. National Analytical Chemistry Congress, 1-5 Eylül 2014, Kahramanmaraş, Turkey.

5. *S. Bora*, M. O. Oral, M. Aydın, E. Yurdanur, S. Bilikmen, O. Y. Ataman, "Comparison of ICP-OES, XRF and LIBS Techniques for Determination of Tin in Metal Containers", 8th Agean Analytical Chemistry Days, 16-20 September 2012, Urla, İzmir, Turkey.

6. *Selin Bora*, N. İlkem Evcimen, Sezgin Bakırdere, O. Yavuz Ataman, "ICP-MS ile Güvenilir Bor Tayini için Örneklerden Karbon Uzaklaştırma Çalışmaları" XII. National Spectroscopy Congress, 18-22 May 2011, Side, Antalya, Turkey.

7. *S. Bora*, S. Bakırdere, O. Y. Ataman, "Boron Determination in Human Blood by ICP-MS", 7th Aegean Analytical Chemistry Days, 29 September- 3 October 2010, Lesvos, Greece.

8. E. Yıldırım, *S. Bora*, Y. Arslan, S. Bakırdere, O. Yavuz Ataman, "Hava Filtresi Örneklerinde ICP-OES ile Bor Tayini", 5. National Analytical Chemistry Congress, 21-25 June 2010, Erzurum, Turkey.

9. M. Aydın, E. Özdemir, Ş. Özcan, *S. Bora*, Y. Arslan, S. Bakırdere, O. Yavuz Ataman, "Semen Örneklerinde ICP-MS ile Bor Tayini", 5. National Analytical Chemistry Congress, 21-25 June 2010, Erzurum, Turkey.

10. T. Müezzinoğlu, M. Korkmaz, İ. Celen, O. Y. Ataman, *Selin Bora*, S. Bakırdere, M. Lekili, S. Keskin, "Bor Elementinin Erkeklerde Prostat Büyüklüğü ve Alt Üriner Sistem Semptomlarına Etkisi", XI. National Spectroscopy Congress, 23-26 June 2009, Ankara, Turkey. (Excellent poster award)

11. S. Ataman, G. Karaman, *S. Bora*, P. Akay, Y. Arslan, S. Bakırdere, M. Korkmaz, O. Y.Ataman, "Idrar Orneklerinde ICP-OES ile Bor Tayini", XI. National Spectroscopy Congress, 23-26 June 2009, Ankara, Turkey.

12. G. Karaman, A. Atakol, *S. Bora*, N. Njie, E. Yıldırım, S. Bakırdere, O. Y.Ataman, "Gıda Örneklerinde ICPMS ile Bor Tayini", XI. National Spectroscopy Congress, 23-26 June 2009, Ankara, Turkey.

13. *S. Bora*, S. Bakırdere, O. Y. Ataman, "Titanyum Kaplanmış Yarıklı Kuvars Tüp Atom Tuzağı-Alevli AAS ile ng/mL Düzeyinde Kurşun Tayini", 4. National Analytical Chemistry Congress, 25-27 June 2008, Elazığ, Turkey.

14. *Selin Bora*, without presentation, X. National Spectroscopy Congress, 4-7 July 2007, Urla, İzmir, Turkey.

RESEARCH INTERESTS

Developing sensitive analytical methods by applying different techniques: Atom Traps, Hydride Generation, Electrothermal Atomization, ICP-OES, ICP-MS, HPLC-ICPMS, Speciation

LANGUAGES

- English – Advanced in reading and writing, fluent in speaking
- German – Beginner level

COMPUTER SKILLS

- MS Office applications
- Internet Tools